RH-TRU Payload Appendices

Revision 1
February 2011

This page intentionally left blank to facilitate duplex printing.

TABLE OF CONTENTS

This page intentionally left blank.

1.0   INTRODUCTION

This document, the RH-TRU Payload Appendices, accompanies the Remote-Handled Transuranic Waste Authorized Methods for Payload Control (RH-TRAMPAC) and is provided as supplemental information pertaining to issues related to the transportation of remote-handled transuranic (RH-TRU) waste in the RH-TRU 72-B packaging. The RH-TRAMPAC contains all information, including requirements and methods of compliance, required for the qualification of a payload for transport in the RH-TRU 72-B packaging. The methodology and logic for the requirements are provided in this document, along with previously performed assessments and evaluations.

The information contained in this document is separated into specific sections, as follows:

- Gas Generation Methodology (Section 2.0)

- Assessment Methods (Section 3.0)

- Supporting Evaluations (Section 4.0)

- Payload Container Design Basis Evaluations (Section 5.0).

This document supports the RH-TRU 72-B SAR, as well as the RH-TRAMPAC document.

This page intentionally left blank

APPENDIX 2.1

RADIOLYTIC G VALUES FOR WASTE MATERIALS

This page intentionally left blank.

Table of Contents

List of Tables

List of Tables (Concluded)

Figures

Attachments

A   Chemical Properties and Commercial Uses of Organic Materials
B   Absorption of Alpha Decay Energy Inside Particles of PuO_2

Glossary

adsorption
The adhesion in an extremely thin layer of molecules (such as gases, solutes, or liquids) to the surfaces of solid bodies or liquids with which they are in contact.

absorbed dose
The amount of energy absorbed from the radiation field per unit of mass of irradiated material.

activation energy
The energy, in excess over the ground state, that must be added to an atomic or molecular system to allow a particular process to take place.

adiabatic
Any change or process resulting in no heat loss or gain.

alcohol
A class of organic compounds derived from hydrocarbons, containing the hydroxyl group OH (general formula ROH). Phenols, a subgroup of alcohols, are derived from aromatic hydrocarbons.

aldehyde
Compounds of the general formula RCHO, where R is any aliphatic or aromatic group and the oxygen is attached via a double bond to the carbon chain.

aliphatic
Any of a class of organic compounds characterized by straight or branched chain structures. Aliphatic compounds may contain single, double, and/or triple carbon-carbon bonds.

alkane
Any of a class of aliphatic hydrocarbon compounds characterized by single carbon-carbon bonds.

alkene
Any of a class of unsaturated aliphatic hydrocarbon compounds characterized by at least one double carbon-carbon bond.

alkyd
A thermoplastic or thermoset synthetic resin used especially for protective coatings.

alkyl
An aliphatic hydrocarbon group that may be derived from an alkane by dropping one hydrogen from the formula, such as "methyl" (CH_3).

alkyne
Any of a class of organic compounds containing at least one triple carbon-carbon bond.

alpha particle | A massive, positively charged particle (He^{++}) emitted by certain radioactive materials; particle energy depends on the parent material, and penetrating ability is limited.

amine | Any of a class of organic compounds that can be considered to be derived from ammonia by replacement of one or more hydrogen atoms with alkyl or aryl groups.

anaerobic | In the absence of oxygen.

antioxidant | An inhibitor, such as ascorbic acid, effective in preventing replacement of other elements by molecular oxygen.

aqueous solution | A solution that contains water as the dominant solvent.

aromatic | Any of a class of organic compounds characterized by closed ring structure and resonance stabilized (shifting/shared) unsaturation.

Arrhenius Equation | An equation relating the rate constant of a chemical reaction and the temperature at which the reaction is taking place:

$$k = A \exp(-E/RT)$$

where A is a constant, k the rate constant, T the temperature in degrees Kelvin, R the gas constant, and E the activation energy of the reaction.

aryl | A compound whose molecules have the ring structure characterized by benzene; that is, six carbon atoms condensed into a planar ring.

beta particle | A particle emitted by certain radioactive materials. A negatively charged beta particle has the characteristics of an electron; a positively charged beta particle is called a positron.

bond dissociation energy | The required energy for complete separation of two atoms within a molecule.

carbonyl compound | A compound containing the carbonyl group, (C=O), such as aldehydes, carboxylic acids, esters, etc.

carboxyl | A univalent group (-COOH) typical of organic acids.

cellulosic | Any of the derivatives of cellulose, such as cellulose acetate.

chain reaction

A reaction that involves a series of steps, each of which generates a reactive substance that brings about the next step.

chemical reaction rate

The speed at which a change occurs when a substance (or substances) is (are) changed into one or more new substances.

contact-handled

Radioactively contaminated materials having a container surface dose rate of no more than 200 mrem/hr, which may be handled manually.

crosslink

A chemical bond formed between separate polymer elements; crosslinking may be intermolecular (between molecules) or intramolecular (between parts of the same molecule).

Curie

The basic unit of radioactivity; equal to 3.7×10^{10} disintegrations per second.

depolymerization

The decomposition of macromolecular compounds into relatively simple compounds.

diffusion

The spontaneous movement and scattering of atomic and molecular particles of liquids, gases, and solids.

diluent

An inert substance added to a material so that the concentration per unit volume of the material is decreased.

dose

See "absorbed dose."

dose rate

The rate at which energy is deposited in a material.

dose rate effect

An effect depending on the rate at which a material is irradiated.

elastomer

A natural or synthetic rubber that stretches to at least twice its original length and retracts rapidly to near its original length when released.

emulsifier

A surface-active agent (like a soap) that promotes the formation and stabilization of a solid-in-liquid or liquid-in-liquid suspension.

Envirostone®

A licensed (U. S. Gypsum) gypsum-based process used for the solidification of organic and low pH aqueous sludges.

ester

A compound formed from the bonding of an alcohol (including phenols) with an organic acid or organic acid derivative by the elimination of water.

ether   A compound formed by attaching two groups to an oxygen atom, of the form R-O-R'.

excitation   The process by which energy is supplied to electrons, atoms, or radicals, usually rendering them chemically more reactive.

free radical   An atom or group of atoms having at least one unpaired electron not involved in bond formation. Free radicals are highly reactive.

gamma rays   Electromagnetic radiation (photons) emitted from the nucleus of certain radioactive materials; gamma rays are more penetrating than particle radiation of comparable energy.

Gray (Gy)   The SI recommended unit of absorbed dose that represents an absorption by a specified material of 1×10^4 ergs/gram; 1 Gray = 100 rads.

G value   The number of molecules, radicals, crosslinks, etc., of a specified type formed or consumed per 100 electron volts (eV) of energy absorbed by a system; this value is also used to specify the number of reactions that occur per 100 eV absorbed.

half-life   The time required for a quantity of a specific radionuclide to decay to one-half of its original amount.

halogenated compound   A compound that contains a member of the halogen family (for example, fluorine, chlorine, bromine).

halogenation   A chemical process or reaction in which a halogen atom (F, Cl, Br, I, At) is introduced into a substance.

hydrocarbon   One of a very large group of chemical compounds composed only of carbon and hydrogen.

hydrolysis   Decomposition or alteration of a chemical substance by water. In aqueous solutions of electrolytes, the reaction of cations with water to produce a weak base or of anions with water to produce a weak acid.

inelastic collision   An encounter in which the total kinetic energy of the colliding particles is lower after the collision than before it.

inhibitor   A substance that slows down or stops a reaction.

ion	An electrically charged atom, radical, or molecule resulting from the addition or removal of electrons by any of a number of possible processes.
ionization	The process of ion formation.
ionizing radiation	Particles or photons that have sufficient energy to produce ionization directly by their passage through a substance.
irradiation	Exposure to radiation.
isomer	One of two or more chemical substances having the same elementary percentage composition and molecular weight but differing in structure and, therefore, usually differing in properties.
isotactic	Refers to crystalline polymers in which groups in the asymmetric carbon atoms have the same (rather than random) configuration in relation to the main chain.
ketone	Any of a class of organic compounds characterized by the presence of the carbonyl group, C=O, attached to two alkyl groups.
LET (Linear Energy Transfer)	The radiation energy lost per unit length of path through a material, usually expressed in kilo-electron volts (keV) per micron of path (or eV/nm). A higher value of LET indicates more effective ionization of the absorber.
monomer	A simple molecule that is a repeating structural unit within a polymer. It is capable of combining with a number of like or unlike molecules to form a polymer.
neutron	An uncharged elementary particle present in the nucleus of every atom heavier than hydrogen; neutrons are released during fission.
nitration	Introduction of an NO_3^- group into an organic compound.
olefin	An alkene.
organic acid	A chemical compound with one or more carboxyl radicals (-COOH) in its structure.
outgas	The release of adsorbed or occluded gases or water vapor, usually as the result of heating or differences in vapor pressure.
oxidation	A chemical reaction in which a compound or radical loses electrons.

paraffin   An alkane.

permeation   The movement of atoms, molecules, or ions into or through a
                        porous or permeable substance (such as a membrane).

pi orbital   A region in a molecule, formed by the overlap of atomic orbitals,
                        in which there is a high probability of finding a "p" or "d" electron;
                        two atomic p or d orbitals overlapping at right angles to the axis
                        between the atoms' nuclei form a pi orbital with electron regions
                        above and below the axis.

polyamide   The product of polymerization of an amino acid or the
                        condensation of a polyamine with a polycarboxylic acid.

polymer   Any of a class of organic compounds characterized by repeating
                        structural units (monomers).

polymerization   The process of bonding two or more monomers to produce a
                        polymer.

rad   The traditional unit of absorbed radiation dose representing the
                        absorption by a specified material of 100 ergs per gram of that
                        material; 1 rad = 1.0E-2 Gray; 1 rad = 6.24E13 eV/g.

radiation   The emission and propagation of energy through matter or space;
                        also, the energy so propagated; the term has been extended to
                        particles, as well as electromagnetic radiation.

radical   A molecular fragment having one or more unpaired electrons (e.g.,
                        $^-$H or $^-$CH$_3$). It may be charged or uncharged.

radical scavenger   A substance that readily combines with a radical.

radiolysis   Alteration of materials caused by irradiation.

range   The distance a given ionizing particle can penetrate into a given
                        material before its energy drops to the point that the particle no
                        longer ionizes the material.

repeat unit   See "monomer."

resin   Any of a class of solid or semisolid organic products of natural or
                        synthetic origin with no definite melting point, generally of high
                        molecular weight; most resins are polymers.

saturated hydrocarbon   A carbon-hydrogen compound containing no double or triple bonds.

saturated vapor pressure   The vapor pressure of a substance at its boiling point.

scission   The process by which chemical bonds are broken; also, the number of bonds broken by the process. Usually refers to breaks in the backbone of a polymer macromolecule.

spur   A small group of excited and ionized species associated with the track caused by passage of ionizing radiation. Consists of the molecules ionized directly, radicals, and secondary ionizations produced by electrons released in the primary ionization. A spur usually forms a side track from the path of the particle or ray.

steric hindrance   The prevention or retardation of chemical reaction caused by geometrical restrictions of neighboring groups on the same molecule.

synergistic effect   The effect on a material of two or more stresses applied simultaneously that is greater in magnitude than that resulting from the same stresses applied separately.

track   The path of gamma rays, x-rays, or charged particles through matter.

TRU nuclide   A nuclide with an atomic number greater than that of uranium (92). All transuranic nuclides are produced artificially and are radioactive.

TRU waste   Waste materials contaminated with alpha-emitting TRU nuclides with half-lives >20 years, in concentration >100 nCi/g of waste at the time of assay.

unsaturated hydrocarbon   One of a class of hydrocarbons that have at least one double or triple carbon-carbon bond. Such compounds are different from aromatic hydrocarbons.

vapor   A gas that exists at a temperature below the critical temperature and that can be liquefied by compression without lowering its temperature.

viscous   Having relatively high resistance to flow.

x-rays   Penetrating electromagnetic radiation, usually generated by decelerating high-velocity electrons through collision with a solid body or by inner-shell electron transitions for atoms with atomic number greater than 10.

Acronyms and Abbreviations

CH-TRU (wastes)	contact-handled transuranic wastes
e	accelerated electrons
E_a	activation energy
EPRI	Electric Power Research Institute
F	fraction of energy absorbed
FDA	Food and Drug Administration
HC	hydrocarbon
HDPE	high-density polyethylene
INEEL	Idaho National Engineering and Environmental Laboratory
LANL	Los Alamos National Laboratory
LDPE	low-density polyethylene
LET	linear energy transfer
ORNL	Oak Ridge National Laboratory
PET	polyethylene terephthalate
PMMA	polymethyl methacrylate
PTFE	polytetrafluoroethylene (Teflon)
PVC	polyvinyl chloride
RFETS	Rocky Flats Environmental Technology Site
SAR	Safety Analysis Report
SRS	Savannah River Site

Chemical Notation

$CaCl_2$	calcium chloride
CaO	calcium oxide
Ca	calcium
C-C	carbon-carbon bond
C-Cl	carbon-chlorine bond
CCl_3F	trichlorofluoromethane
CCl_4	carbon tetrachloride
C-F	carbon-fluorine bond
CF_4	carbon tetrafluoride
C_4H_8	butene
C_4H_{10}	butane
C-H	carbon-hydrogen bond
$CHCl_3$	chloroform
CH_3	methyl group
CH_4	methane
Cl_2	chlorine
Cm-244	curium isotope with atomic mass of 244
CO	carbon monoxide
CO_2	carbon dioxide
C_3H_6	cyclopropane or propylene
C_3H_8	propane
C_2H_2	acetylene (or ethyne)
C_2H_4	ethylene (or ethene)
C_2H_6	ethane
Fe_2O_3	iron (III) oxide (ferric oxide)
HCl	hydrogen chloride
He^{++}	doubly charged helium ion. An alpha particle.
H_2	Hydrogen
KCl	potassium chloride
$MgCl_2$	magnesium chloride
MgO	magnesium oxide
NaCl	sodium chloride
Na_2O	sodium oxide
OH	hydroxyl group
O_2	oxygen
Po	polonium
Pu-238	plutonium isotope with atomic mass of 238
Pu-239	plutonium isotope with atomic mass of 239
$Pu(NO_3)_x$	plutonium nitrate
PuO_2	plutonium dioxide
R, R'	any alkyl or aromatic group
SiO_2	silicon dioxide
SO_2	sulfur dioxide
Z	atomic number
Zn	zinc

G Value Notation

Notation	Interpretation - G Value for
$G(C_2)$	all hydrocarbons with two carbon atoms
$G(C_3)$	all hydrocarbons with three carbon atoms
$G(C_4)$	all hydrocarbons with four carbon atoms
$G(CH_4)$	methane
$G(C_2H_6)$	ethane
$G(H_2)$	hydrogen
$G(S)$	scission
$G(gas)$	all gas generated
$G(water\ vapor)$	water vapor
$G(X)$	crosslinking

Executive Summary

This appendix presents radiolytic G values for solids, liquids, vapors, and gases obtained from the technical literature. Experimental data are evaluated, and applicable maximum G values are determined for use in calculations of flammable gas concentration and total pressure for transport of contact-handled transuranic (CH-TRU) wastes. G values for organic solids are related to G values for structurally-related liquids. It is demonstrated that G values (for hydrogen and other flammable gases) for organic materials can be ranked according to the functional groups that determine most other chemical properties. This relationship allows G values for other organic solids to be estimated. Maximum G values obtained from laboratory-scale experiments are compared to effective G values measured for actual drums of CH-TRU wastes. This analysis is applicable to remote-handled (RH) TRU waste forms as well, given the similar physical and chemical nature of the waste. In addition, the date derived in this appendix include radiolysis experiments from alpha, beta, and gamma emissions. For materials that are commonly present in the CH-TRU wastes, polyethylene has the highest value of $G(H_2)$ of 4.0. The maximum $G(H_2)$ value for water is 1.6.

This appendix is not meant to be a comprehensive summary of all radiolysis experiments that have measured gas generation. Instead, the literature has been searched for typical and upper bound G values, and for general characteristics that allow extrapolation to other materials for which no radiolysis experiments have been reported. Where possible, data obtained by various authors are discussed and compared. When authors disagree, an effort has been made to determine which data are valid and the reasons for the differences.

Factors affecting gas generation from the reactions of alpha, beta, neutron, or gamma radiation with matter are discussed. These factors include the linear energy transfer (LET) and range of the incident radiation; irradiation environment, including temperature, pressure, and gases present; absorbed dose and dose rate; specific composition of the material; and particle size and distribution of radioactive contaminants.

The controlling factor in the behavior of materials under irradiation, as under most other environmental influences, is the chemical structure. Chemical bonds are not broken randomly even though the excitation energy may exceed the bond dissociation energy. Energy may be transferred from the location on a molecule where it is absorbed to another chemical bond that is broken. Additives to improve physical or aging properties may affect changes produced by radiation.

For this reason, radiolysis can be discussed in terms of functional groups as can other chemical reactions. The functional group is the atom or group of atoms that defines the structure of a particular family of organic compounds, and, at the same time, determines their properties. A particular set of properties can be associated with a particular group wherever it is found.

G values for a given material may depend on the type of radiation absorbed by the material (LET effect). For several liquids, such as cyclohexane, benzene, water, and acetone, alpha radiolysis experiments yield higher G values than gamma radiolysis experiments. Similar effects may also occur in solids, such as polymers, but very few experiments have been conducted to determine

LET effects in gas generation in solids. This is possibly due to the difficulty in measuring the absorbed dose in alpha radiolysis, where self-absorption of some of the alpha radiation emitted from particulate contamination occurs. G values measured using nonalpha radiation are the best data available for many materials. These data are included in establishing maximum G values in a best faith effort to establish upper bound gas generation calculations for CH-TRU wastes.

Liquids that have G values for flammable gas greater than 4.0 are saturated hydrocarbons, alcohols, ethers, ketones, and organic acids. Liquids that have G values for flammable gases less than 4.0 include unsaturated hydrocarbons, aromatic hydrocarbons, water, esters, halogenated hydrocarbons, aromatic halides, and commercial lubricant oils. G values for liquid organic nitrogen compounds are low for those having aromatic characteristics or C-N triple bonds.

Common plastics and papers are composed of one or more base polymers and additives designed to increase flexibility, stability, or other properties. Organic functional groups found in common polymers include saturated C-C bonds, unsaturated C-C bonds, and alcohol, ether, and ester groups. Aromatic characteristics (resonant structures containing carbon and hydrogen or carbon and nitrogen atoms) greatly increase the stability of many polymers, and are commonly found in additives.

Saturated hydrocarbons produce hydrogen as the principal radiolysis gas. Small amounts of other hydrocarbons are formed. The maximum $G(H_2)$ value is 4.0 for polyethylene.

Polymers having ether functional groups generate gases that contain oxygen, even when irradiated in a vacuum. G values for cellulose and urea formaldehyde have been shown to be strongly dependent on the absorbed dose. For absorbed doses greater than 10 Mrad, the maximum value of $G(H_2)$ is 3.2 for cellulose. One of the polymers in this family (polyoxymethylene) generates other flammable gases that cause the G(flam gas) value to exceed 4.1, and another (polyvinyl formal) has a measured G(gas) that is 1.4 times the G(gas) value for polyethylene. For this reason, polyoxymethylene and polyvinyl formal are permitted in CH-TRU wastes only in trace amounts.

Polymers containing chlorine are stabilized to reduce the catalytic effect of HCl generated by radiolysis or thermal degradation. The strong effect of the plasticizers and stabilizers on the radiolysis of PVC is demonstrated by the differences in the composition of the radiolysis gas, which vary from 85% H_2 to 83% HCl to 70% CO_2, depending on the specific polymer formulation and whether oxygen is present.

Radiolysis of adsorbed or absorbed liquids indicates that the sorbing medium can either be inert to radiation or can transfer energy to the sorbed liquid. Unless experimental data demonstrate that the binding medium is radiolytically inert (e.g., vermiculite), all of the radiation energy should be assumed to interact with the sorbed liquid. Nitrates present in solidified aqueous wastes significantly reduce $G(H_2)$ from the value for water, while increasing $G(O_2)$.

Very low G values have been observed from irradiation of water present as the hydrate in crystals. Water in the hydrates appears to exhibit the property of an "energy sink."

Gas generation experiments conducted on actual CH-TRU wastes are summarized. Typically, several different contaminated materials were present inside a given waste container. The results are presented in terms of effective G values that include the effects of the different materials and self-absorption of some alpha decay energy by particulate contamination.

On the whole, the effective hydrogen G values for actual CH-TRU wastes are much lower than the maximum hydrogen G values for the waste forms that would be estimated based on the worst-case material. Similar results would be expected for RH-TRU waste forms. For drums of combustible wastes, the maximum $G(H_2)$ value determined in controlled experiments was 2.1 versus a possible value of 4.0 based on laboratory experiments. For drums of sludge, the maximum $G(H_2)$ value measured was 0.3 versus a possible value of 1.6 based on laboratory experiments. No explanation currently exists for high $G(H_2)$ values calculated from experiments conducted on solidified organic waste forms.

Gas pressure and composition data for retrieved drums of stored wastes are also discussed. Calculated G values for sealed retrieved drums provide only lower limits, because of uncertainties in the rates at which gases can permeate through the drum gaskets or diffuse through gaps between the gasket and the sealing surfaces. Typically, only the drum head space was sampled, and the concentrations of generated gases could have been higher inside the rigid liner and waste bags. Most of the lower limit G values were very low.

This page intentionally left blank.

2.1   Radiolytic G Values for Waste Materials

2.1.1   Introduction

The purpose of this appendix is to establish maximum G values from the technical literature for production of gas (particularly hydrogen) from the radiolysis of materials in remote-handled transuranic (RH-TRU) wastes. These maximum G values are used in calculations of flammable gas concentrations and total pressure in safety analyses for transport of the wastes. A similar analysis of experimental data was performed for establishing bouding G values for waste materials in contact-handled (CH) TRU wastes. RH-TRU waste forms are similar to CH-TRU wastes in physical and chemical form (solid or solidified materials with similar waste constituents), and G values in actual waste containers are expected to be smaller than the bounding G values. In Section 2.1.6, the maximum G values obtained from laboratory-scale experiments are compared to G values calculated from gas generation experiments conducted on drums of actual CH-TRU wastes. The maximum G values typically are much larger than those obtained from actual wastes at room temperature.

This appendix reports radiolysis data (including temperature dependence) for many types of materials, including the chemical families of organic compounds that are liquids (e.g., alcohols, aldehydes, and ketones); organic solvents; water; polymers; and commercial plastics, cellulosics, and rubbers. Inorganic materials and commercial plastics, cellulosics, and rubbers are the major constituents in CH-TRU wastes and packaging materials. Liquids may be major constituents (> 10 wt%) of solidified liquid wastes or minor or trace (< 1 wt%) constituents when they are absorbed on paper tissues or used as plasticizers in plastics and rubbers. For solid materials for which the G values are unknown, related organic solids or liquids are used to estimate bounding values. In order to provide a thorough discussion of this subject, G values are reported for some materials that are not known to be present in the CH-TRU wastes.

This appendix is not meant to be a comprehensive summary of all radiolysis experiments that have measured gas generation. Instead, the literature has been searched for typical and upper bound G values, and for general characteristics that allow extrapolation to other materials for which no radiolysis experiments have been reported. Where possible, data obtained by various authors are discussed and compared. When authors disagree, an effort has been made to determine which data are valid and the reasons for the differences. For example, discrepant data in the case of PVC appear to be largely caused by variations in material composition and not by experimental error.

Radiolysis data used in this appendix result from irradiation of materials by gamma, alpha, or other particles; accelerated electrons; or x-rays. Chemists and materials scientists for many years have used gamma radiolysis as a tool to explore the stability of materials. As a result, many more materials have been studied by gamma than by alpha radiolysis. Many alpha radiolysis experiments were performed during the 1970s at the Los Alamos National Laboratory (LANL), the Savannah River Site (SRS), and the Rocky Flats Environmental Technology Site (RFETS) to measure radiolytic gas generation from common materials that appear in CH-TRU wastes [see Molecke (1979[1]) and Blauvelt (1986[2]) for discussions of these experiments]. Some of these data have been reanalyzed in this report, and different conclusions are now drawn from these data.

---

[1] Molecke 1979. M. A. Molecke, "Gas Generation from Transuranic Waste Degradation: Data Summary and Interpretation," Sandia National Laboratories, SAND79-1245, December 1979.

G values for a given material may depend on the type of radiation absorbed by the material (known as an LET effect). For several liquids, such as cyclohexane, benzene, water, and acetone, alpha radiolysis experiments yield higher G values than gamma radiolysis experiments. Similar effects may also occur in solids, such as polymers, but very few experiments have been conducted to determine LET effects in gas generation in solids. This is possibly due to the difficulty in measuring the absorbed dose in alpha radiolysis, where self-absorption of some of the alpha radiation emitted from particulate contamination occurs. G values measured using nonalpha radiation are the best data available for many materials. These data are included in establishing maximum G values in a best-faith effort to establish upper bound gas generation calculations for CH-TRU wastes.

Section 2.1.2 of this document introduces basic concepts of radiation chemistry and factors that affect radiolytic gas generation or consumption. This forms the basis for discussions of the experimental data on radiolysis of liquids and vapors in Section 2.1.3, the radiolysis of polymers in Section 2.1.4, and the radiolysis of non-polymer solids in Section 2.1.5. Section 2.1.6 compares the laboratory G values measured for specific materials with rates of gas generation measured for actual drums of CH-TRU wastes. Attachment A describes the families of organic liquids and polymers, and shows the structures of many common polymers. Attachment B calculates the fraction of alpha decay energy escaping from a particle of PuO_2 as a function of particle radius. A glossary is provided that includes acronyms, abbreviations, chemical notation, and G value notation.

Major reviews of the radiation chemistry literature, such as An Introduction to Radiation Chemistry by J.W.T. Spinks; The Radiation Chemistry of Macromolecules edited by M. Dole; and Radiation Effects on Organic Materials edited by R.O. Bolt and J.G. Carroll, have been used extensively. When these references are cited, the original reports were not reviewed by this author.

2.1.2 Radiation Chemistry

Radiation chemistry is the study of the chemical effects produced in a system by the absorption of ionizing radiation. Included in this definition are the chemical effects produced by radiation (alpha and beta particles and gamma rays) and by electromagnetic radiation of short wavelength (x-rays). Photochemistry, on the other hand, deals with reactions of excited species unaccompanied by ionization.

This chapter discusses the factors affecting gas generation from the reactions of alpha, beta, gamma, or neutron radiation with matter. These factors include linear energy transfer (LET) and range of the incident radiation; irradiation environment including temperature, pressure, and atmosphere present; absorbed dose and dose rate; specific composition of the irradiated material; and particle size and distribution of radioactive contaminants.

---

[2] Blauvelt 1986. R. K. Blauvelt and R. J. Janowiecki, "General Strategy for Evaluating the Radiolytic Gas Generation Potential in Newly-Generated CH-TRU Waste," Monsanto Research Corporation, Mound Laboratory, MLM-MU-86-61-0013, January 1986.

2.1.2.1 Reactions of Radiation with Matter

The discussion that follows is based primarily on Spinks (1976[3]).

Absorption of energy from ionizing radiation results in the formation of tracks of excited and ionized species in matter. The incident radiation is not selective and may react with electrons of any atom or molecule lying along its track. Free radicals are produced by the dissociation of excited molecules and by ion reactions in or near the tracks of ionizing particles. Free radicals have one or more unpaired electrons available to form chemical bonds, but free radicals are generally uncharged. These free radicals are often more important in the chemical reactions that follow than are the primary species. Back reactions can combine two radicals to form a stable molecule. Radicals that do not undergo radical-radical reactions in the tracks diffuse into the bulk of the material and generally react there. Some of the more reactive radicals are H^+, ^-OH, Cl^+, and $^-CH_3$. Stable radicals include NO, NO_2, and O_2. Nitric oxide and nitrogen dioxide both have a single unpaired electron. Oxygen has a triplet ground state and behaves in radical reactions as a diradical.[3] Oxygen readily reacts with other free radicals and, if it is present, will almost invariably affect the radiation-induced reactions. Free radicals can also be produced by other processes, such as thermal degradation.

The species produced by ionizing radiation will, in general, be the same in a particular material regardless of the type or energy of the ionizing radiation. All ionizing radiation will, therefore, give rise to qualitatively similar chemical effects. With respect to gas generation, different types of ionizing radiation will generally produce the same gas species, though possibly in different amounts.

Alpha particles consist of two protons and two neutrons and, therefore, are the same as the nuclei of helium atoms and have a double positive charge. On passing through matter, alpha particles lose energy principally by inelastic collisions with electrons lying in their paths, leading to excitation and ionization (if the energy transmitted is high enough) of the atoms and molecules to which those electrons belong. Electrons liberated in the process also interact with other atoms and molecules of the material. An alpha particle loses only a small fraction of its energy per collision. As a consequence, alpha particles slow down gradually as the result of a large number of small energy losses and travel in a nearly straight path. The energy of an alpha particle decreases as the distance traveled increases. Because each of the alpha particles from a given radionuclide has the same initial energy, each will have about the same range in a given material. Alpha particles can also be produced in situ in a material by combining it with a compound of boron or lithium and irradiating the mixture with slow neutrons. Some radiolysis experiments have used this technique for producing alpha particles.

Beta particles are fast electrons emitted by radioactive nuclei. In contrast to alpha particles, the beta particles from a particular radioactive element are not all emitted with the same energy.[3] Instead, the energies range from zero up to a maximum value that is characteristic of the element. On passing through matter, beta particles lose energy predominantly through inelastic collisions

---

[3] Spinks 1976. J. W. T. Spinks and R. J. Woods, <u>An Introduction to Radiation Chemistry</u>, John Wiley & Sons, New York, 1976.

with electrons, in a similar manner to alpha particles. However, because the beta particle and the electron with which it collides have the same mass, the beta particle can lose up to half of its energy in a single collision and may be deflected through a large angle. As a result, even beta particles that start with the same energy may come to rest at widely separated points.

Gamma rays are electromagnetic radiation with wavelengths in the region of 3E-9 to 3E-11 cm. The gamma rays emitted by radionuclides are monoenergetic, but each decay may be to one of a small number of discrete energies. Low-energy gamma rays tend to lose most of their energy through a single interaction with an electron (the photoelectric effect). The entire energy is transferred to a single electron, which is then ejected from the atom. Photoelectric interactions are most probable for high-atomic-number materials and for low gamma energies. A fraction of the incident gamma rays is completely absorbed by the material, but the remainder are transmitted through the material with up to their full initial energy. For example, the number of low-energy-gamma photons transmitted through a sheet of absorbing material decreases exponentially as the thickness of the absorber increases.

For low-atomic-number materials and for gamma energies between 1 and 5 MeV in high-atomic-number materials, the Compton effect predominates. In the Compton effect, a gamma ray interacts with an electron, which may be loosely bound or free, so that the electron is accelerated and the gamma ray deflected with reduced energy. For example, Compton interactions in water predominate for gamma rays with energy from about 30 keV to 20 MeV.

Neutrons are uncharged nuclear particles with a mass of one mass unit (Spinks 1976[3]). Because they are uncharged, neutrons do not produce ionization directly in matter. However, the products of neutron interactions can produce ionization and give rise to radiation-induced chemical changes. The main ionizing species are protons or heavier positive ions, and the chemical effects of neutron irradiation are similar to those produced by beams of these positively charged particles.

2.1.2.2 Energy Transfer

Sometimes energy absorbed at one location on a large molecule appears to damage a more susceptible site elsewhere on the molecule. Thus, one type of bond may be broken more frequently than would be calculated from the statistical distribution of electrons.[4] Another way of looking at this phenomenon is to compare the likelihood of a recombination reaction when a given kind of bond is broken. For example, by comparing the C-C and C-H bond energies in hydrocarbon polymers, one would think that cleavage of the main polymer chain is more probable than the splitting off of the hydrogen atoms. However, during irradiation of most polymers, processes caused by the cleavage of the C-H bonds predominate. A model used to explain this apparent contradiction is that simultaneous cleavages of the C-C and C-H bonds occur. In the case of polymers that primarily crosslink, a considerable fraction of the broken C-C

---

[4] O'Donnell 1970. J. H. O'Donnell and D. F. Sangster, Principles of Radiation Chemistry, American Elsevier Publishing Company, Inc., New York, 1970.

bonds recombine, and as a result, the C-H bond cleavage processes predominate. In degradable polymers, a rapid recombination of the split ends of the chain is sterically hindered[5].

The concept of energy transfer from the location on a molecule where energy is absorbed to the chemical bond that is broken is a key concept for understanding the effects of radiolysis. The major products of radiolysis are influenced by molecular structure[6]. Chemical bonds are not broken randomly even though the excitation energy may exceed the bond dissociation energy.

For this reason, radiolysis can be discussed in terms of functional groups as can other chemical reactions. The functional group is the atom or group of atoms that defines the structure of a particular family of organic compounds, and, at the same time, determines their properties[7]. A particular set of properties can be associated with a particular group wherever it is found. Functional groups in macromolecules also determine their chemical reactions. Sections 2.1.3 and 2.1.4 contain more detailed discussions of the functional groups.

Certain structures, such as aromatic rings (e.g., a benzene ring), seem to absorb ionizing energy and dissipate it as heat in the form of molecular vibrations. In this way, systems containing these structures undergo less decomposition than would be expected.[4]

When a homogeneous mixture of two compounds is irradiated, the yields of the different products often are generally directly proportional to the yields from the pure components and their relative proportions (by electron density) in the mixture. This behavior is found when each component degrades independently of another. However, some components of a mixture may transfer absorbed energy to other components. In a two-component mixture, the second component may be decomposed more readily, and the result is a higher product yield. On the other hand, if the second component is less readily decomposed, as with an aromatic compound, there may be correspondingly less decomposition and a lower product yield.[4]

During gamma irradiation of polymers filled with finely dispersed metals, the absorbed energy can distribute itself nonuniformly between the two components of the system. In rubbers containing heavy metals ($Z \geq 40$) in a free state or in the form of chemical compounds, the rate of radiation cross-linking has been observed to double. The energy absorbed by the polymeric component increases because of secondary electrons generated by gamma interactions with the metal.[5] This effect is not expected to be significant for surface alpha irradiation of leaded rubber gloves because the lead is dispersed throughout the rubber material.

---

[5] Makhlis 1975. F. A. Makhlis, Radiation Physics and Chemistry of Polymers, John Wiley & Sons, New York, 1975, translated from the Russian.

[6] Hall 1963. K. L. Hall, et al., "Radiation Chemistry of Pure Compounds," in Radiation Effects on Organic Materials, Academic Press, New York, 1963, eds. R. O. Bolt and J. G. Carroll.

[7] Morrison 1973. R. T. Morrison and R. N. Boyd, Organic Chemistry, Allyn and Bacon, Inc., Boston, 1973, 3rd edition.

2.1.2.3 Factors Affecting the Rate of Radiolytic Gas Generation (or Consumption) from a Material

The rate of radiolytic gas generation (or consumption) from a material depends on: (1) the G value for gas production (or consumption) for the given material and type of radiation, (2) the energy emitted from radioactive decay, and (3) the fraction of emitted energy absorbed by the material (F). G values also appear in the radiation chemistry literature for other products, such as the number of crosslinks or scissions, or the production of a non-gas substance. A G value may be positive (as in the generation of hydrogen or carbon dioxide) or negative (as in the depletion of oxygen). F depends on the nature of the emitted energy and the materials being irradiated. In the case of short-range radiation. F also will depend on the spatial distribution of radioactivity, especially when several different materials are present, such as in wastes.

The rate of radiolytic gas generation (n) in moles per second from a material is given by:

$$n = W \times \Sigma_i(F_i \times G_i) \times C$$

where

W = total decay heat (watts),

F_i = fraction of energy emitted that is of radiation type i and is absorbed by the material (range 0 to 1),

G_i = number of molecules of gas produced (or consumed) per 100 eV of energy absorbed from radiation type i, and

C = conversion constant

= (1 joule/W-sec) x (1E7 erg/joule) x (1 eV/1.6E-12 erg)
    x (1 g-mole/6.02E23 molecules)

= 1.04E-5 (g-mole)(eV)/(molecule)(W-s)

= 1.04E-7 (g-mole)(100 eV)/(molecule)(W-s).

2.1.2.3.1 Factors Affecting the G Value

A number of factors influence the G value measured in an experiment. They include LET of the radiation, temperature, pressure, atmosphere in which irradiation occurs, total absorbed dose, dose rate, and specific composition of the material.

2.1.2.3.1.1 <u>Linear Energy Transfer (LET) Effect</u>

Differences in G values for a material when irradiated by different types of radiation are ascribed to differences in the ways in which energy is lost in matter. Linear energy transfer (LET) is the linear rate of energy loss by an ionizing particle traveling through a material. An average LET

value is calculated by dividing the initial energy of a particle by its range in the material. Expressions that reflect the changing density of active species in particle tracks, such as specific ionization and LET, are useful in evaluating the overall chemical effect. Track effects of this sort have been thought to be more important in the case of liquids or solids, where the active species are hindered from moving apart by the proximity of other molecules, than in gases, where species can move apart with relative ease. In gases, the different types of radiation do not give the different yields of products that may be found in liquids or solids.[3]

The linear energy transfer from alpha particles to irradiated materials follows the Bragg curve, which rises sharply from low energies to reach a peak at about 1 MeV, then falls off gradually at higher alpha particle energies. This behavior leads to an "end of track" effect, with higher LET than at the beginning of the track.[8] Table 2.1-1 lists average LET values for irradiation of water.

Table 2.1-1 — Average Values of LET in Water Irradiated with Various Types of Radiation

Radiation	Average LET (eV/nm)
Co-60 γ-rays	0.2
2-MeV electrons	0.2
200-kV x-rays	1.7
H-3 ß-rays	4.7
50-kV x-rays	6.3
10 MeV H-1	8.3
10 MeV He-4	92
5.3 MeV α-particles (Po-210)	136
3 MeV He-4	180
65.7-MeV N-14 ions	553

Refs.: Spinks 1976[3], Chapter 2 and Table 8.19.

Radiation-chemistry studies on LET effects in low-molecular-weight compounds have shown that the molecular product yields increase with increasing LET. Molecular products are generated in the spurs, before the reactive species can diffuse into the bulk of the system.[9] The result is that $G(H_2)$ appears to increase with increasing LET, at least in liquids such as benzene, acetone, cyclohexane, and water (see Section 2.1.3 for details). These effects could also occur in solids. Unfortunately, similar experiments have not been uncovered in the radiation chemistry literature that measure G values of a solid material using different LET radiation at the same absorbed dose.

A characteristic feature of radiation with high LET is the sharp decrease in the effectiveness of protective additives (such as antioxidants) in the material being irradiated, particularly those that react with free radicals. The reason for this is the intense reactions of the radicals in the track.[5]

---

[8] Cember 1978. H. Cember, <u>Introduction to Health Physics</u>, Pergamon Press, New York, 1978.

[9] Schnabel 1981. W. Schnabel, <u>Polymer Degradation--Principles and Practical Applications</u>, Macmillan Publishing Company, Inc., New York, 1981.

2.1.2.3.1.2 **Temperature**

Chemical reaction rates depend on temperature. The rate constant (k) of a chemical reaction can be expressed by: $k = A \exp(-B/T)$ where T is the absolute temperature, and A and B are constants. The equation can be written in the form $k = A \exp(-E_a/RT)$, generally known as the Arrhenius law. E_a is an activation energy, which will have different values for different chemical reactions. R is the ideal gas constant (1.99 cal/g-mole-K), and temperatures are in Kelvin. This law holds for elementary reactions but does not necessarily hold for successive reactions that may have different E_as.[3] Also, the E_a can change when the reactions change, as at the melting point for crystalline materials.

In an Arrhenius plot, the log of the reaction rate versus the reciprocal temperature (degrees Kelvin), ln k vs. 1/T, has a slope equal to $-E_a/R$. Arrhenius plots of G values versus 1/T for several materials are shown in Chapiro 1962[10] and Jellinek 1978[11].

The activation energy (E_a) for G values for gas generation from most materials appears to be less than or equal to 3 kcal/g-mole, giving a weak temperature dependence compared to many other chemical reactions. E_a for PVC is about 3 kcal/g-mole, and E_a for polyethylene is about 0.8 kcal/g-mole (see Section 2.1.4.1.1). Alpha radiolysis data for cellulosics are consistent with an E_a of 1-2 kcal/g-mole [12,13] (see Section 2.1.4.3.1). The temperature dependence of $G(H_2)$ in liquid n-hexane and neopentane corresponds to an activation energy of about 3 kcal/g-mole.[14]

The relationship between the rate constants k_2 and k_1 at two different temperatures T_2 and T_1 is given by:

$$\ln (k_2/k_1) = (E_a/R)[(T_2-T_1)/(T_2 \times T_1)]$$

For example, if the activation energy for gas produced by a material is equal to 1 kcal/g-mole, then the ratio of the G(gas) value at 55°C to the G(gas) value at 25°C would be:

$$G(55\,°C)/G(25\,°C) = \exp \{(1E3/1.99)[(328\ K - 298\ K)/(328\ K \times 298\ K)]\}$$

$$= \exp \{(5.03E2)[30/(328)(298)]\}$$

---

[10] Chapiro 1962. A. Chapiro, <u>Radiation Chemistry of Polymeric Systems</u>, Interscience Publishers, New York, 1962.

[11] Jellinek 1978. H. H. G. Jellinek, <u>Aspects of Degradation and Stabilization of Polymers</u>, Elsevier Scientific Publishing Company, New York, 1978.

[12] Kosiewicz 1981. S. T. Kosiewicz, "Gas Generation from Organic Transuranic Wastes. I. Alpha Radiolysis at Atmospheric Pressure," <u>Nuclear Technology 54</u>, pp. 92-99, 1981.

[13] Zerwekh 1979. A. Zerwekh, "Gas Generation from Radiolytic Attack of TRU-Contaminated Hydrogeneous Waste," Los Alamos National Laboratory, LA-7674-MS, June 1979.

[14] Bolt 1963. R. O. Bolt and J. G. Carroll, <u>Radiation Effects on Organic Materials</u>, Academic Press, New York, 1963.

$$= \exp (0.154)$$

$$= 1.17.$$

At -29 °C, the ratio $G(-29\ °C)/G(25\ °C)$ would be 0.69 for E_a = 1 kcal/g-mole. An activation energy of E_a = 3 kcal/g-mole, considered as the maximum value of E_a for materials present in the CH-TRU wastes, results in the following:

$$G(55\ °C)/G(25\ °C)\ =\ \exp (3\ x\ 0.154) = \exp (0.462)$$

$$= 1.59.$$

For most polymers then, the radiolytic gas generation rate at 55°C should be no greater than approximately 1.6 times the gas generation rate at room temperature (25°C).

Rates and product yields from radiation-induced chemical reactions in many polymers are influenced by molecular mobility.[9, 15] This explains why increases in temperature, leading to phase transitions or allowing specific intramolecular motions (such as rotations of side groups), frequently influence the G values. Increasing the temperature generally reduces the probability of radical recombinations[9] and increases the diffusion rates of gas molecules, such as H_2.

For polymers containing crystalline areas, the molecular mobility increases drastically above the crystalline melting temperature, with consequent changes radiation chemical yields.[11] For example, an abrupt increase in the activation energy occurs for both G(X) (crosslinking between polymer molecules) and G(S) (scission - breaking of the polymer molecule backbone) near the melting temperature. Large changes in the ratio G(X)/G(S) are often observed at higher temperatures, which suggests changes in reaction mechanisms. For example, a ten-fold increase in G(S) is observed in radiolysis of polystyrene when the temperature is increased from 30 to 150°C.[15]

There is no general correlation between thermal stability and radiation resistance. For instance, irradiated polytetrafluoroethylene (Teflon[R]) readily undergoes main-chain scission while polysiloxanes are efficiently crosslinked, although both polymers are heat resistant.[9] At elevated temperatures, radiation may accelerate the usual thermal degradation reactions because thermal initiation characterized by a high activation energy (about 20 to 80 kcal/g-mole[16]) is replaced by radiation initiation, which has a much lower activation energy.[5] The threshold temperature for thermal degradation can be decreased significantly if the material is irradiated before (or during) heating.

---

[15] Jellinek 1983. H. H. G. Jellinek, ed., <u>Degradation and Stabilization of Polymers</u>, Vol. 1, Elsevier, New York, 1983.

[16] Madorsky 1964. S. L. Madorsky, <u>Thermal Degradation of Organic Polymers</u>, Interscience Publishers, John Wiley & Sons, New York, 1964.

2.1.2.3.1.3 **Pressure**

Pressure up to 50 psig may slightly lower G values as a result of back reactions. Experiments conducted in a vacuum measure more of the gas generated than do experiments conducted at ambient pressure, in which some of the gases can remain dissolved in the material being irradiated.

The decrease in segmental motions in polybutadiene with increasing pressure led to a corresponding decrease in G values for chain scission in polybutadiene[17] and an increase in G values for crosslinking.

2.1.2.3.1.4 **Atmosphere in Which Irradiation Occurs**

Measured total gas G values depend on the atmosphere in which the irradiation occurs, especially whether or not any oxygen is present. In most polymers, oxygen retards or completely eliminates formation of a cross-linked network. Even polymers that otherwise would crosslink will degrade in the presence of oxygen.[5] Radiation-induced oxidation initially consumes dissolved oxygen that has diffused into the material from the surrounding oxygen-containing atmosphere.[5] The efficiency of radiolytic oxidation of polymers under otherwise equal conditions depends on the dose rate and on other factors determining the rate at which oxygen can permeate the sample (e.g., oxygen pressure, sample thickness, oxygen solubility and ability to penetrate through the material, irradiation temperature, and polymer phase state).[5]

Organic solvents can change the net effect of radiolysis by permeating the material and reacting chemically. Reactions of trapped radicals may occur with chemically active molecules (such as oxygen or solvents) that have diffused into the sample after irradiation ceases.[5] These effects are most pronounced in materials that have been irradiated in the absence of oxygen. Intense degradation of polymers that have been pre-irradiated in the absence of oxygen has been observed when the polymers are exposed to oxygen.[5]

Most G values are measured in a vacuum, in air, or in pure oxygen. In the vacuum experiments, a larger amount of evolved gas may be measured because gas molecules will be pulled out of the materials rather than remain dissolved in the materials. A few experiments have been conducted in atmospheres different from air or pure oxygen, such as oxygen plus carbon tetrachloride, chloroform vapor, or nitrous oxide; or air saturated with water vapor. (The results of these experiments are discussed in later chapters.)

Various thermal, chemical, and radiolytic oxidation processes occur in the CH-TRU waste materials, the packaging materials, and the waste containers themselves. Eventually, these processes could deplete the oxygen inside the transport package cavity.

The gases that could be present inside the transport package include the following: (1) ambient air; (2) nitrogen, argon, or helium used to inert the cavity; (3) nitrogen plus hydrogen and carbon dioxide, with trace amounts of carbon monoxide, oxygen, and methane; (4) any of the above plus

---

[17] Sasuga 1975. T. Sasuga and M. Takehisa, "Effect of High Pressure on Radiation-Induced Cross-Linking of Synthetic Rubbers," J. Macromol, Sci.-Phys. B11, pp. 389-401, 1975.

vapor from absorbed water or other liquids. These liquids may include various oils and solvents. For example, some of the solvents that could be present in the wastes include: 1,1,1-trichloroethane, carbon tetrachloride, 1,1,2-trichloro-1,2,2 trifluoroethane (Freon), methylene chloride, methanol, xylene, and butanol.

2.1.2.3.1.5 <u>Total Absorbed Dose</u>

As irradiation of a material proceeds, the end products of radiolysis (called primary products) may increase to such a concentration in the material that they are irradiated or react with some of the free radicals or other species to form secondary products. It follows that the G value (slope of the yield of a product versus dose curve) may decrease as the absorbed dose increases (assuming that the products are more stable under irradiation than the parent material), and the concentration of the product may ultimately reach a steady-state limit.[4] Many of the common plastics contain saturated carbon-carbon bonds. Radiolysis of these materials results in release of hydrogen and an increase in unsaturation. Unsaturated hydrocarbon liquids have much lower $G(H_2)$ values than do related saturated hydrocarbon liquids. Therefore, the degraded material in the plastics should be more stable than the parent material with respect to gas formation, leading to lower $G(H_2)$ values with absorbed dose. Eventually, all of the available hydrogen will have been released from the material. The decrease in G values with absorbed dose has also been called a "matrix-depletion" effect. To avoid this complication, G values are often expressed as initial G values or as the G values extrapolated to zero absorbed dose.

On the other hand, radiolysis of plastics where additives are used to acheive stabilty, such as PVC, could result in higher G values with increasing absorbed dose as the additives are consumed.

Absorbed dose effects can disappear at higher temperatures. For example, for irradiation of crystalline polyethylene at 25°C, the value of $G(H_2)$ decreased from about 3.7 to 3.2 as the absorbed dose increased from near zero to 15 Mrad (0.15 MGy).[18] For the same sample, irradiated at 120°C, virtually no change in $G(H_2)$ with increasing radiation dose was reported.

Several reports discuss absorbed dose effects for alpha radiolysis. For Cm-244 irradiation of paper tissue, Bibler observed a decrease in G(gas) from an initial value of 1.9 to about 0.8 after 17 days.[19] Zerwekh's data show decreases in G(gas) values by about 50% in 250 days of irradiation from Pu-238.[13]

For alpha irradiation, the absorbed dose for waste materials is applicable only to the mass of the waste reached by the alpha particles. The range of alpha particles in low density materials for $4 < E < 8$ MeV is given by (see Section 2.1.2.3.2.1):

Range(cm) = [1.24 x E(MeV) - 2.62] x [1.2E-3 g/cm^3/(density of material)].

---

[18] Mandelkern 1972. L. Mandelkern, "Radiation Chemistry of Linear Polyethylene," in <u>The Radiation Chemistry of Macromolecules</u>, Vol. I, Academic Press, New York, 1972, ed. M. Dole.

[19] Bibler 1976. N. E. Bibler, "Radiolytic Gas Production During Long-Term Storage of Nuclear Wastes," E. I. DuPont de Nemours and Company, Savannah River Laboratory, DP-MS-76-51, American Chemical Society Meeting (preprint), October 27-29, 1976.

The density of plastics and paper is approximately 1 g/cm^3. The range of a 5.14 MeV alpha particle (Pu-239 alpha) in plastics or paper would be 4.6E-3 cm, while the range of 5.59 MeV alpha particle (Pu-238 alpha) would be 5.2E-3 cm.

The alpha particle track is cylindrical, with 90% of the ions present within a diameter of 1E-2 microns. The remaining 10% are recoil electrons with sufficient energy to produce their own ionization(s). Such ions are present out to about 0.2 microns from the center of the track.[20]

The volume of material most affected by an alpha particle can, therefore, be approximated by a cylinder of diameter 1E^{-6} cm and length equal to the range of the alpha particle. For 5.59-MeV alpha particles, the estimated volume of irradiated material is 4.1E-15 cm^3. For 5.14-MeV alpha particles, the estimated volume of irradiated material is 3.6E-15 cm^3. The corresponding dose absorbed by that material from one alpha particle is given by:

$$Dose(rad) = \frac{Decay\,energy(eV) \times 1rad \Big/ \big[6.24E13 \quad eV\big/g \big]}{Volume\left(cm^3\right) \times density\left(g\big/cm^3\right)}$$

Therefore, the dose absorbed by material irradiated by a Pu-238 or Pu-239 alpha particle is 22-23 Mrad. With time, the particle tracks will begin to overlap, and the dose absorbed by the material will increase. For a given particle size of PuO$_2$, for example, absorbed dose effects should be observed much more quickly during Pu-238 irradiation, which produces a factor of about 200 times the disintegrations per second of Pu-239 irradiation.

Several conclusions may be reached from this discussion:

(1)   The gas-generation rates from materials irradiated to absorbed doses much less than 22 Mrad are expected to be greater than expected for alpha radiolysis of these materials in CH-TRU wastes.

(2)   A particle of Pu-238 oxide will have an activity over 200 times the activity of the same size Pu-239 oxide particle. Absorbed dose effects should occur much sooner with Pu-238 contamination than with Pu-239 contamination.

(3)   G values measured using Pu-238 contamination should be extrapolated to initial G values before the results are applied to Pu-239 contamination to minimize the difference in absorbed dose effects.

2.1.2.3.1.6 Dose Rate

Some radicals are fairly stable and may build up to quite high concentrations. Under these conditions they may react with other radicals, rather than with the material being irradiated. If

---

[20] NAS 1976. National Academy of Sciences, "Health Effects of Alpha-Emitting Particles in the Respiratory Tract," EPA 520/4-76-013, October 1976.

this occurs, the G values may exhibit a nonlinear dependence on the dose rate. For example, a radiation-initiated chain reaction can result in a G value for products that is inversely proportional to the square root of the dose rate.[4] In a number of experiments, however, the G values for molecular gas products for specific materials were independent of dose rate for the ranges studied [e.g., Bibler 1976[19], Chapiro 1962[10] (p. 415)].

Some apparent dose rate effects are caused by an increase in the material's temperature. Since the major portion of the absorbed radiation energy is converted to heat, at high dose rates the rate of heat release to the environment can be insufficient, resulting in an increase in temperature. Many chemical reactions have activation energies in the range of 20-50 kcal/mole. Consequently, it is feasible that at high absorbed dose rates (i.e., at high localized material temperatures), reaction pathways different from those occurring at low dose rates may dominate.[9]

Gillen and co-workers have documented evidence of physical and chemical dose-rate effects in gamma radiolysis of polymers in oxygen-containing environments as part of their efforts to perform accelerated aging simulations. Much of this work is summarized in Bonzon (1986)[21].

Physical dose-rate effects appear to be a common occurrence for gamma radiation aging of polymeric materials. Evidence for dose-rate effects was observed for polyolefins and ethylene-propylene rubber, while no noticeable dose-rate effects were noted for a chloroprene rubber, silicone, and two chlorosulfonated polyethylene materials. The dose-rate effects ranged from insignificant to very large, depending on such factors as polymer type, aging conditions, sample geometry, and the degradation parameter being monitored. (Change in tensile elongation was commonly used in these studies to detect radiation damage.) More mechanical degradation was produced for a given total dose as the dose rate was lowered. Diffusion-limited oxidation processes were shown to be the cause of such effects. When the oxidation processes in a material use up dissolved oxygen faster than it can be replenished from the atmosphere surrounding the material (through diffusion), a heavily oxidized layer of material is formed near the sample surfaces, and oxygen depletion occurs in the sample interior. As the dose rate is reduced, oxidation of the sample increases due to the longer times available for the diffusion processes.

Oxidation-controlled dose-rate effects are less likely to occur for alpha irradiation of polymers from surface contamination. In order for the reactions to be dose-rate independent, oxygen must diffuse only to a depth equal to the range of the alpha particles. Physical dose-rate effects are minimized in gamma irradiation experiments by using thin films.[21]

---

[21] Bonzon 1986. L. L. Bonzon, et al., "Status Report on Equipment Qualification Issues -- Research and Resolution," Sandia National Laboratories, NUREG/CR-4301, SAND85-1309, November 1986.

Other chemical dose-rate effects were observed in the interactions between radiation and thermal degradation. Deterioration in polyethylene and polyvinyl chloride cable materials was found in the containment building of the Savannah River nuclear reactor.[22] The degradation in material properties was much higher than expected for the maximum dose [2 Mrad (0.02 MGy)] experienced by the cable materials at the relatively low operating temperature of 43°C. Experiments performed to model this behavior showed that the most severe mechanical degradation was found when irradiation occurred at elevated temperature. The observed degradation was much greater than the sum of the damage caused by separate exposure to radiation and to the elevated temperature. This effect was also attributed to an oxidation mechanism, in which peroxides initially formed by the radiation are then thermally decomposed.

Chemical dose-rate effects caused by synergistic behavior of radiation and elevated temperature would also occur for alpha irradiation when oxygen is present. The magnitude of these effects could be reduced by removing any remaining oxygen before the irradiated materials are heated.

2.1.2.3.1.7 Specific Material Composition

Many of the radiolysis experiments reported in the radiation chemistry literature were performed to examine the chemical reactions occurring in the pure material. However, commercial plastics differ from the pure polymers because they contain large fractions of various additives, such as stabilizers and plasticizers. These materials can significantly influence the amount and species of gases generated by thermal degradation and radiolysis. See Attachment A of this appendix and Section 2.1.4 for more detailed discussions.

2.1.2.3.1.8 Extreme Upper Bound Estimate for Gas Generation G Values in Most Organic Liquids and Polymers

For most materials, bond dissociation energies can be used to estimate an extreme upper bound to the number of gas molecules produced by radiolysis per unit energy absorbed. Dissociation energies of chemical bonds in common polymers range from about 65 kcal/g-mol (C-Cl) to 108 kcal/g-mol (C-F), with carbon-carbon bonds in the middle of the range (75-85 kcal/g-mol)[3]. The carbon-hydrogen bond dissociation energy is about 90-100 kcal/g-mole (3.9-4.4 eV/molecule).

Hydrogen is the major gaseous product from radiolysis of most organic liquids and polymers that contain hydrogen. In the simplest case, a hydrogen molecule conceptually could be formed by breaking two C-H bonds and recombining the two hydrogen atoms. If all the radiation energy went into breaking bonds, then the energy needed to form one hydrogen molecule is given by twice the bond dissociation energy, or 2 x (3.9-4.4 eV)/molecule. This required energy results in an extreme upper bound G value estimated to be about 12 molecules generated per 100 eV of energy absorbed. This is an extreme upper bound because it ignores the H atoms that recombine with the parent molecule and the energy that is dissipated as heat.

---

[22] Gillen 1982. K. T. Gillen, R. L. Clough, and L. H. Jones, "Investigation of Cable Deterioration in the Containment Building of the Savannah River Nuclear Reactor," NUREG CR-2877, SAND81-2613, August 1982.

Most measured G values lie between 0.1 and 10.[4] Higher G values usually indicate a chain reaction has occurred. For example, the radiolysis products may chemically degrade the parent material, as occurs from HCl generated in pure PVC.

2.1.2.3.2 Factors Affecting the Fraction of Energy Absorbed by a Material

Factors affecting the fraction of energy absorbed by a material include the range of effectiveness of the radiation in the material, distribution of radioactive contaminants, and (in the case of alpha radiolysis) particle size of the radioactive contaminant (such as PuO_2 particles).

2.1.2.3.2.1 <u>Range of Effectiveness of the Radiation</u>

The range of alpha particles in gases, liquids, and solids must be considered both when comparing alpha with gamma radiolysis experiments on specific materials, and when evaluating the gas generation rates expected from actual waste drums. For example, the range of alpha particles in air at 0°C and 760 mm Hg pressure is approximated by Cember (1978)[8]:

$$Range(cm) = [1.24 \times E(MeV)] - 2.62, \text{ for } 4 < E < 8 \text{ MeV.}$$

For 5.5 MeV alpha particles, the range in air would be 4.2 cm. The presence of water vapor or other vapors would decrease that distance. The range of alpha particles in biological tissue, or other materials of low density, is given by Cember (1978)[8]:

$$Range = Range(air) \times (density \text{ of air})/(density \text{ of material})$$

$$= 4 \text{ cm} \times (1.2E\text{-}3 \text{ g/cm}^3)/(density \text{ of material}).$$

Plastics and cellulosics (or liquid water) have densities of about 1 g/cm^3. Therefore the range of alpha particles in typical combustible wastes or absorbed aqueous solutions is estimated to be about 5E-3 cm [(5E-3 cm x 1E4 microns/cm = 50 microns; 5E-3 cm/(2.54 cm/in) x 1E3 mils/in = 2 mils)].

Several conclusions that can be reached from the above calculations are:

(1)   For low-density materials less than about 2 mils thick, both alpha particles and gamma rays can penetrate completely through the material.

(2)   Materials more than about 4 cm away from all alpha-emitting radionuclides should not experience any alpha radiolysis.

(3)   Radiolysis of gases or vapors within 4 cm of alpha-emitting radionuclides will occur unless the alpha particles are first absorbed by other materials.

2.1.2.3.2.2 <u>Distribution of Radioactive Contaminants</u>

The distribution of radioactive contaminants can affect the rate of gas generation. This is especially important when the materials being irradiated are heterogeneous. For example, consider a drum containing mixed combustible and dry metal waste, where the thick metal pieces

are individually wrapped with plastic, and the activity all results from alpha decay. Several possible distributions of the alpha activity include the following:

(1)   All the activity is located in the interior of the metal pieces.

(2)   All of the activity is located on the exterior of the metal pieces, in contact with both the plastic wrapping and the metal pieces.

(3)   All of the activity is uniformly distributed in the mixed combustible waste.

The rate of gas production will be different for each of the three cases. In Case 1, no radiolytic gas will be generated. In Case 2, gas could be generated at a rate up to one-half the rate characteristic of plastic (no radiolytic gas is generated by metal). In Case 3, gas will be generated at a rate equal to the weighted average G value for the mixed combustibles. An upper-bound estimate of the quantity of radiolytic gas generated from a mixture of materials can be calculated by assuming that all of the emitted alpha energy is absorbed by the material having the highest G value.

If a plutonium dioxide particle is located on a surface, up to half the alpha particles may interact with gases or vapors above the contaminated surface, unless another surface is in contact with the first. The quantity of gas generated may be greater than calculated based only on the surface-contaminated material if a significant fraction of the atmosphere above the surface consists of organic vapors.

2.1.2.3.2.3 Particle Size of the Contaminant

The plutonium contaminants in CH-TRU wastes are usually in particle form as PuO_2 or hydroxides but may also be in the form of plutonium nitrate from solution in nitric acid. If the plutonium is in particle form, some of the alpha particles will interact with plutonium or oxygen atoms (in the process known as self-absorption), rather than with the waste material. Attachment B of this document presents a calculation of the fraction of alpha decay energy escaping from a particle of PuO_2 as a function of the PuO_2 particle radius.

The gas generation rate reported from particulate contamination could then be less than the rate predicted using maximum G values and all of the activity measured in the waste. For example, the $G(H_2)$ value for Pu-238 dissolved in nitric acid was observed to be about 2.5 times the $G(H_2)$ value for 2-micron particles of the oxide.[23] (These particles had probably agglomerated to larger particles.)

2.1.2.3.3 Use of G Values Measured by Non-Alpha Irradiation

Alpha radiolysis predominates in the CH-TRU wastes. However, many radiolysis experiments have been performed using gamma (or other) radiation. Some differences are found in the gases

---

[23] Bibler 1979. N. E. Bibler, "Gas Production from Alpha Radiolysis of Concrete Containing TRU Incinerator Ash, Progress Report 2, August 1, 1978 - November 30, 1978," E. I. DuPont de Nemours and Company, Savannah River Laboratory, DPST-78-150-2, April 1979.

produced in alpha radiolysis versus gamma radiolysis, but the results in most cases are very similar, as shown in Sections 2.1.3, 2.1.4, and 2.1.5. The quantities and compositions of the evolved gases should be comparable when:

(1)   The total absorbed dose for the gamma radiolysis experiment is similar to the total absorbed dose for the alpha radiolysis experiment.

(2)   The dose rate for the gamma radiolysis experiment is similar to the dose rate for the alpha radiolysis experiment.

(3)   For materials that are surface contaminated in an alpha radiolysis experiment, the gamma radiolysis experiment is performed on powders or thin films, to minimize diffusion effects in bulk materials.

2.1.3 Radiolysis of Liquids, Vapors, and Gases

G values for liquids are applicable to the following three waste forms: liquids absorbed onto various waste materials, liquids incorporated into a matrix such as concrete, and liquids used as plasticizers in plastics and rubbers. Radiolysis of vapors near contaminated surfaces may occur. The organic liquids are grouped into families based on their functional groups.[7] The functional group is the atom or group of atoms that defines the structure of a particular family of organic compounds, and, at the same time, determines their properties. For example, the functional group in alcohols is the -OH group, while in alkenes the functional group is the carbon-carbon double bond. A large part of organic chemistry is the chemistry of the various functional groups. A particular set of properties can be associated with a particular group wherever it is found. When a molecule contains a number of different functional groups, the properties of the molecule are expected to be roughly a composite of the properties of the various functional groups. (The properties of a particular group may be modified by the presence of another group, however.) Functional groups in macromolecules also determine their chemical reactions.

The major products of radiolysis are also influenced by molecular structure.[6] Chemical bonds are not broken randomly even though the excitation energy may exceed the bond dissociation energy. For solid materials for which the G values are unknown, structurally related organic liquids can provide estimates of maximum G values.

The radiolysis data are organized by families of liquids, which are based on functional groups (see Attachment A of this document for more details). Where data are available, G values at different LETs are shown.

Liquids that have G values for flammable gas greater than 4.1 are: saturated hydrocarbons, alcohols, ethers, ketones, and organic acids. Liquids that have G values for flammable gases less than 4.1 include unsaturated hydrocarbons, aromatic hydrocarbons, water, esters, halogenated hydrocarbons, aromatic halides, and commercial lubricant oils. G values for flammable gases for organic nitrogen compounds are low for those having aromatic characteristics or C-N triple bonds.

2.1.3.1   Radiolysis of Saturated Hydrocarbons

Saturated hydrocarbons contain only hydrogen and carbon atoms and single carbon-carbon bonds. They include most of the common petroleum fuels. An example of a saturated hydrocarbon is hexane, with the following structure:
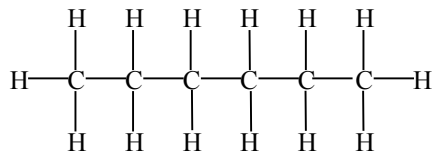
Table 2.1-2 presents G values for saturated hydrocarbons for irradiation at room temperature in vacuum. G(gas) is the G value for all gas produced.

From Table 2.1-2, the bounding $G(H_2)$ value is 5.6 for saturated hydrocarbons in the liquid phase at room temperature. In addition to hydrogen, other flammable gases may be generated. Newton[24] has observed some general characteristics of gas generation from saturated hydrocarbons. Normal saturated hydrocarbons yield principally hydrogen, with methane being produced only from the end groups. Therefore, the ratio of hydrogen to methane increases with increasing molecular weight. With branched-chain hydrocarbons (such as isobutane or neopentane), relatively more methane is produced, and the yield of methane increases with the number of methyl groups on the hydrocarbon chain.

Hall[6] reports an activation energy of about 3 kcal/mole for the $G(H_2)$ value for the liquid phase of neopentane and n-hexane. (See Section 2.1.2.3.1.2 for the use of activation energies in calculating the temperature dependence of G values.)

Table 2.1-2 — G Values for Saturated Hydrocarbons

Material	$G(H_2)$	$G(CH_4)$	G(gas)[a]	Comments	Reference
Vapor phase					
propane	8.2	0.4		alpha; vacuum	(1)
butane	9.0	1.2		alpha; vacuum	(1)
pentane	7.3	0.8		alpha; vacuum	(1)
hexane	5.6	0.8		alpha; vacuum	(1)
isobutane	7.4	2.7		alpha; vacuum	(1)
neopentane	2.0	2.0		alpha; vacuum	(1)

---

[24] Newton 1963. A. S. Newton, "Chemical Effects of Ionizing Radiation," in Radiation Effects on Organic Materials, Academic Press, New York, 1963, eds. R. O. Bolt and J. G. Carroll.

Table 2.1-2 — G Values for Saturated Hydrocarbons (Concluded)

Material	$G(H_2)$	$G(CH_4)$	$G(gas)^a$	Comments	Reference
Liquid phase					
pentane	4.2	0.4		electron; vacuum	(1)
	4.2	0.2	5.4	electron; vacuum	(2)
hexane	5.0	0.2	5.2	electron; vacuum	(1)
	5.0	0.1	7.2	electron; vacuum	(2)
cyclohexane	5.6	0.1	5.7	electron; vacuum	(1)
	5.3	0	5.3	alpha; vacuum	(1)
	7.7	--		fission fragments; vacuum	(3)
heptane	4.7	0.1		electron; vacuum	(1)
octane	4.8	0.1		electron; vacuum	(1)
	4.6	0.1		gamma; air	(4)
	4.2	--		alpha; air	(4)
nonane	5.0	0.1		electron; vacuum	(1)
decane	5.2	0.1		electron; vacuum	(1)
dodecane	4.9	0.1		electron; vacuum	(1)
hexadecane	4.8	0		electron; vacuum	(1)
2-methylpentane	4.0	0.5		electron; vacuum	(1)
2,2-dimethyl-butane	2.0	1.2		electron; vacuum	(1)
neopentane	1.6	3.7	5.6	gamma; vacuum	(2)

Refs.: (1) Spinks 1976[3], p. 365; (2) Hall 1963[6], p. 71; (3) Gaumann 1968[25]; (4) Bibler 1977[26].

Note: ^{a}G(gas) includes miscellaneous gaseous hydrocarbons C_2-C_4.

2.1.3.2 Radiolysis of Unsaturated Hydrocarbons

Unsaturated hydrocarbons are hydrocarbons that have at least one double or triple carbon-carbon bond. Examples include acetylene, ethylene, 1-hexene, and cyclohexene. The compound 1-hexene has the following structure.
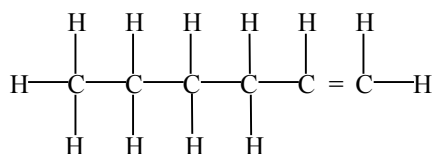
$G(H_2)$ values for unsaturated hydrocarbons are generally much smaller than for saturated hydrocarbons, even when the only structural difference occurs in a small area of a long molecule (e.g., hexane compared to 1-hexene). Table 2.1-3 gives G values for three unsaturated hydrocarbons.

---

[25] Gauman, 1968.

[26] Bibler 1977. N. E. Bibler and E. G. Orebaugh, "Radiolytic Gas Production from Tritiated Waste Forms, Gamma and Alpha Radiolysis Studies," E. I. DuPont de Nemours and Company, Savannah River Laboratory, DP-1459, July 1977.

Table 2.1-3 — G Values for Three Unsaturated Hydrocarbons

Material	$G(H_2)$	$G(CH_4)$	$G(gas)^a$	Comments	Reference
ethylene[b]	1.2	0.1	2.8	electron; vacuum	(1)
cyclohexene	1.3	0	1.3	gamma; vacuum	(2)
	3.0	0	3.0	alpha; vacuum	(2)
1-hexene	0.8	0	0.8	electron; vacuum	(1)

Refs.:   (1) Hall 1963[6], p.78; (2) Spinks 1976[3], p. 384.
Notes: [a]$G(gas)$ includes C_2H_2.
          [b]Gas phase.

Radiolysis products of liquid cyclohexene and their G values are listed in Table 2.1-4 for both gamma and alpha (1.5 MeV) radiation.[3]

Table 2.1-4 — Radiolysis Products and G Values for Liquid Cyclohexene

Product	G (Product)	
	^{60}Co γ-Ray	1.5 MeV α
H_2	1.3	3.0
cyclohexane	1.0	0.3
2,2'-bicyclohexenyl (II)	1.8-1.9	0.4
3-cyclohexylcyclohexene (III)	0.5-0.6	0.5
bicyclohexyl (IV)	0.2	0.1
polymer, unidentified dimer (as C_6 units)	8.9-9.8	6.1

Ref.:   Spinks 1976[3], Table 8.6.

2.1.3.3 Radiolysis of Aromatic Hydrocarbons

An aromatic hydrocarbon has a closed ring structure and resonance-stabilized unsaturation. The stability of aromatic compounds is attributed to the presence in the aromatic ring system of electrons in pi orbitals, which can dissipate energy throughout the ring system. This reduces the probability that excited or ionized aromatic molecules will dissociate. Alternative modes of energy dissipation are favored that do not result in dissociation of the molecule.[3] Examples include benzene, xylene, and discrete-ring polyphenyls. All of the aromatic hydrocarbons have very low G values for hydrogen and total gas, as shown in Table 2.1-5.

Aromatic hydrocarbons are good protective agents for a large number of chemicals because they have many low-lying excited states, have low ionization potentials, and are themselves radiation resistant.[24] The transfer of energy from higher excited states or charge exchange with the ion of the primary compound results in dissipation of energy in the aromatic hydrocarbon. For example, cyclohexane is protected from radiolytic decomposition by small amounts of added benzene. Internal protective agents can be built into molecules by adding aromatic groups.

Table 2.1-5 — G Values for Several Aromatic Hydrocarbons

Material	$G(H_2)$	$G(CH_4)$	G(gas)	Comments	Reference
benzene	0.6	0	0.8	alpha; vacuum	(1)
	~0	~0	~0	gamma; vacuum	(1)
	~0	~0	~0	electron; vacuum	(3)
toluene	0.6	0	0.6	alpha; vacuum	(1)
	0.1	~0	0.1	gamma; vacuum	(1)
	0.1	~0	0.1	electron; vacuum	(2)
p-xylene	0.2	0	0.2	gamma; vacuum	(1)
ethyl benzene	0.2	~0	0.2	electron; vacuum	(2), (3)
	0.2	~0	0.2	gamma; vacuum	(1)
	0.2	~0	0.2	reactor; vacuum	(2)
isopropyl benzene	0.2	0.1	0.3	gamma; vacuum	(1)
	0.2	0.1	0.3	electron; vacuum	(2), (3)
	0.3	0.1	0.4	alpha; vacuum	(3)
	0.2	0.1	0.3	reactor; vacuum	(2)
tert-butyl benzene	0.1	0.1	0.2	electron; vacuum	(2), (3)
	0.2	~0	0.2	reactor; vacuum	(2)
mesitylene	0.2	~0	0.2	electron; vacuum	(3)
biphenyl	[a]	[a]	~0	electron; vacuum	(2)
	[a]	[a]	0.1	reactor; vacuum	(2)
p-terphenyl	~0	~0	~0	electron; vacuum	(2)
	~0	~0	~0	reactor; vacuum	(2)

Refs.:   (1) Spinks 1976[3], p. 388; (2) Hall 1963[6], p. 91; (3) Rad. Effects 1963[27], p. 63.
Notes: [a]not listed;
           ~0 denotes a value <0.1.

2.1.3.4   Radiolysis of Water

Table 2.1-6 presents G values for radiolysis of water. $G(H_2)$ strongly depends on LET, increasing by a factor of 3-4 from gamma radiolysis to alpha radiolysis. (Note that LET for alpha particles decreases for increasing alpha particle energy that is greater than 1.5 MeV.)

---

[27] Rad. Effects 1963. "Radiation Effects Handbook," S-146, Institute of Electrical and Electronics Engineers, Inc., June 1963.

Table 2.1-6 — G Values for Water[a,b]

Radiation Type	pH	$G(H_2)$	Reference
Vapor phase			
gamma, e	not given	0.5	(1)
Liquid phase			
gamma, e	0.5	0.4	(1),(2)
	3 to 13	0.45	(1),(2)
6.4 MeV He^{++}	not stated	1.1^d	(2)
^{244}Cm alpha (5.8 MeV)	not stated	1.3	(3)
5.3 MeV alpha $(Po)^c$	0.5	1.6	(1)
^{252}Cf alpha, beta, and fission fragments	0.4M-H_2SO_4	1.7	(4)

Refs.:   (1) Spinks 1976[3], p. 258; (2) Burns 1981[28]; (3) Bibler 1975[29]. Bibler 1974[30];

Notes: [a]"e" means accelerated electrons.
       [b]$G(O_2)$ values not reported; maximum $G(O_2)$ would be 1/2 $G(H_2)$.
       [c]Po = polonium.
       [d]G(H2) value from curve fit to data from seven authors at a wide range of LET values.

The maximum $G(H_2)$ value for water is 1.6 for either gamma or alpha radiation. The maximum $G(O_2)$ value for water would be 0.8. Addition of nitrates to water lowers the production of hydrogen, but can increase the production of oxygen.

Bibler[30] measured gas evolution from aerated nitric acid or sodium nitrate-0.4-M H_2SO_4 irradiated by Cm-244 and Pu(IV)-239 alpha particles. The nitrate ions scavenged the precursors of hydrogen and reduced $G(H_2)$ as observed in gamma radiolysis experiments. Above 1-M NO_3^- concentration, oxygen and nitrite ions were produced as a result of direct energy absorption by nitrate ions.

The $G(H_2)$ value in alpha radiolysis experiments was found to decrease sharply from about 1.3 for zero concentration of NO_3^-, to 0.7 at 1-M NO_3^-, to about 0.25 at 2.5-M NO_3^-. The decrease in $G(H_2)$ was more pronounced for Co-60 gamma irradiation than for alpha irradiation. This

[28] Burns 1981. W. G. Burns and H. E. Sims, "Effect of Radiation Type in Water Radiolysis," J. Chem. Soc., Faraday Trans. I 77, pp. 2803-2813, 1981.

[29] Bibler 1975. N. E. Bibler, "Radiolysis of 0.4 M Sulfuric Acid Solutions with Fission Fragments from Dissolved Californium-252. Estimated Yields of Radical and Molecular Products that Escape Reactions in Fission Fragment Tracks," J. Phys. Chem. 79, pp. 1991-1995, 1975.

[30] Bibler 1974. N. E. Bibler, "Curium-244 Radiolysis of Nitric Acid. Oxygen Production from Direct Radiolysis of Nitrate Ions," J. Phys. Chem. 78, pp. 211-215, 1974.

effect has been attributed by Bibler and others to nitrate ions being more efficient hydrogen scavengers for gamma irradiation than for alpha irradiation. The $G(O_2)$ variation with NO_3^- concentration was approximately linear, from about $G(O_2)=0.25$ at zero concentration NO_3^- to $G(O_2)=0.75$ at 5.6-M NO_3^-. Agitation of the samples was necessary to release all of the generated O_2, much of which otherwise stayed in solution.

Bibler[30] reports measurements of gas produced from irradiation of 0.4-M sulfuric acid by Cf-252, which is a transuranic isotope that decays by alpha emission as well as spontaneous fission. The total absorbed dose from Cf-252 is due to alpha particles, fission fragments, and beta particles from decay of the fission fragments. The net $G(H_2)$ value reported from all contributions was 1.7. The fission fragment contribution (LET of 400 eV/A) was calculated to have $G(H_2)=2.1$.

$G(H_2)$ values and equilibrium concentrations of H_2 for irradiated water are controlled by a back reaction of H_2 with the OH^- radical to form water.[31,26] This back reaction is much more efficient for gamma radiation than for alpha radiation, resulting in a $G(H_2)$ value for gamma radiolysis 3-4 times lower than that for alpha radiolysis. The gas pressure above the water also was found to reach an equilibrium value at a much lower pressure for gamma radiolysis than for alpha radiolysis.

Another scavenger species that could compete with H_2 for OH^- is Cl^-, present in salt brines. The results of an experimental program to measure gas generation from radiolysis of salt brines are reported by Gray[31]. The brine was prepared by dissolving Permian Basin salt, consisting primarily of NaCl with a small amount of calcium sulfate, in deionized water. The irradiations were conducted in pressure vessels. The alpha radiolysis tests were terminated as the pressure approached the capacity of the pressure transducers. Gas compositions for both gamma and alpha radiolysis were roughly two parts H_2 to one part O_2 in most cases. The gamma radiolysis experiments reached an equilibrium pressure of about 100 atm, while the alpha radiolysis experiments were extrapolated to reach an equilibrium pressure of about 275 atm.

Alpha radiolysis experiments conducted by Bibler[32] on the free water in concrete demonstrated that below 100°C, the H_2 production rate is independent of temperature and radiation dose rate.

---

[31] Gray 1984. W. J. Gray and S. A. Simonson, "Gamma and Alpha Radiolysis of Salt Brines," PNL-SA-12746, 1984 Fall Meeting of the Materials Research Society in Boston, Mass., November 1984.

[32] Bibler 1981. N. E. Bibler, "Gas Production from Alpha Radiolysis of Concrete Containing TRU Incinerator Ash, Progress Report 4, September 1, 1979 - August 31, 1980," E. I. DuPont de Nemours and Company, Savannah River Laboratory, DPST-80-150-2, March 1981.

2.1.3.5 Radiolysis of Alcohols

Alcohols are compounds of the general formula ROH, where R is any alkyl or substituted alkyl group.[7] The group may be open-chain or cyclic; it may contain a double bond, a halogen atom, or an aromatic ring. All alcohols contain the hydroxyl (-OH) group, which determines the properties characteristic of this family. Compounds in which the hydroxyl group is attached directly to an aromatic ring are called phenols, and differ markedly from the alcohols. A glycol is a dihydroxy alcohol, containing two hydroxyl groups. For example, ethylene glycol has the structure

$$CH_2 \quad\text{—}\quad CH_2$$
$$|\qquad\quad|$$
$$OH \qquad OH$$
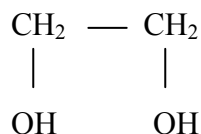
Table 2.1-7 presents G values for many alcohols.

2.1.3.6 Radiolysis of Ethers

Ethers are compounds of the general formula R-O-R, Ar-O-R, or Ar-O-Ar.[7]

Table 2.1-8 presents G values for many ethers. The maximum reported value of $G(H_2)$ is 3.6. Almost all of the other radiolysis gases or vapors are also flammable. Branching in the alkyl group decreases hydrogen evolution but increases hydrocarbon yields.[6]

2.1.3.7 Radiolysis of Aldehydes and Ketones

Aldehydes are compounds of the general formula RCHO; ketones are compounds of the general formula RR'CO.[7] The groups R and R' may be aliphatic or aromatic. Both aldehydes and ketones contain the carbonyl group, C=O, and are often referred to collectively as carbonyl compounds. It is the carbonyl group that largely determines the chemistry of aldehydes and ketones. For example, the structure of acetone is

$$CH_3 \quad\text{—}\, C=0$$
$$|$$
$$CH_3$$
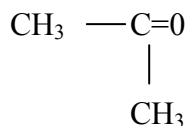
Table 2.1-9 presents G values for propionaldehyde. Table 2.1-10 illustrates the effect of LET on the gaseous products of acetone. Table 2.1-11 presents G values for several ketones, including acetone. The maximum total G value for flammable gas production from gamma or alpha radiolysis of these aldehydes or ketones is 3.5.

The series consisting of formaldehyde, acetaldehyde, and acetone was irradiated in the gas phase with electrons.[6] Hydrogen, CO, and CO_2 were the principal products from formaldehyde. Replacing one or both hydrogen atoms of the formaldehyde molecule with CH_3 groups (giving acetaldehyde or acetone) resulted in lower radiolytic production of CO_2 and H_2, but gave substantial yields of alkanes and alkenes. This result was considered by those authors to be as expected on the basis of a group-to-product correlation.

Table 2.1-7 — G Values for Alcohols

Material	$G(H_2)$	$G(CO)$	$G(CH_4)$	$G(gas)$[a,b]	Comments	Reference
Vapor phase						
ethanol	10.8	1.2	0.9	12.9	electron; vacuum	(1)
methanol	10.8	1.0	0.3	12.1	gamma; vacuum	(1)
Liquid phase						
ethanol	5.0	0.1	0.6	5.7	gamma; vacuum	(1)
	3.5	0.1	0.4	4.5	alpha; vacuum	(2)
	4.1	0.1	0.4	4.6	alpha; vacuum	(3)
methanol	5.4	0.1	0.7	6.2	gamma; vacuum	(1)
	3.5	0.2	0.4	4.5	alpha; vacuum	(2)
	4.0	0.2	0.2	4.4	gamma; vacuum	(3)
methanol	major product is formaldehyde				gamma; oxygen	(1)
1-propanol	4.4	--	--	4.4[c]	gamma; vacuum	(1)
	2.8	0.1	0.1	3.0	alpha; vacuum	(3)
2-propanol	3.7	--	1.5	5.2[c]	gamma; vacuum	(1)
n-propanol	2.8	--	0.1	3.9	alpha; vacuum	(2)
1-butanol	4.6	--	--	4.6[c]	gamma; vacuum	(1)
	3.6	0.1	0.1	4.3	alpha; vacuum	(3)
t-butanol	1.0	--	3.6	4.6[c]	gamma; vacuum	(1)
n-butanol	3.6	--	0.1	4.3	alpha; vacuum	(2)
1-octanol	3.5	0.1	~0	3.7	alpha; vacuum	(3)
1-decanol	3.5	~0	~0	3.6	alpha; vacuum	(3)

Refs.: (1) Spinks 1976[3], pp. 410, 417, 420; (2) Rad Effects, 1963[27], pp. 59-61; (3) Hall 1963[6], p. 92.

Notes: [a]Water vapor is generated but is not included.

[b]Other highly volatile products, such as formaldehyde, acetylene, ethylene, ethane, acetaldehyde, ethyl ether, and others, are also generated. G(gas) values greater than the sum of $G(H_2)$, $G(CO)$, and $G(CH_4)$ have included these vapors.

[c]Only major products were listed.

Table 2.1-8 — G Values for Ethers in the Liquid Phase

Material	$G(H_2)$	$G(CO)$	$G(CH_4)$	$G(gas)$[a]	Comments	Reference
ethyl ether	3.4	--	0.4	3.8	gamma; vacuum	(1)
	3.6	0.1	0.2	3.9	alpha; vacuum	(2)
ethyl n-butyl ether	3.3	0.1	0.1	3.5	alpha; vacuum	(2)
dibutyl ether	2.9	--	0.1	3.0	gamma; vacuum	(1)
n-butyl ether	2.7	0.1	0.1	2.9	alpha; vacuum	(2)
ethyl tertbutyl ether	2.0	0.1	0.8	2.9	alpha; vacuum	(2)
isopropyl ether	2.2	~0	1.5	8.4	gamma; vacuum	(3)
	2.4	0.1	0.9	5.8	alpha; vacuum	(3)
di-isopropyl ether	2.4	--	1.7	4.1	gamma; vacuum	(1)
dioxan	2.1	0.3	--	2.4	gamma; vacuum	(1)
tetrahydrofuran	2.6	--	--	2.6	gamma; vacuum	(1)

Refs.:   (1) Spinks 1976[3], pp. 421-423; (2) Hall 1963[6], p. 98; (3) Newton 1963[24], p. 55.

Note: [a]Other gases or highly volatile products, such as formaldehyde, acetylene, ethylene, ethane, acetaldehyde, alcohols, and others, are also generated. G(gas) values greater than the sum of $G(H_2)$, $G(C_O)$, and $G(CH_4)$ have included these other gases or vapors.

Table 2.1-9 — G Values for Propionaldehyde

Material	$G(H_2)$	$G(CO)$	$G(CH_4)$	$G(gas)$[a]	Comments
propionaldehyde	1.2	1.6	0.1	4.4	electron; vacuum

Refs.:   Hall 1963[6], p. 102.

Note: [a]G(gas) includes C_2-C_4 hydrocarbons.

Table 2.1-10 — Effect of LET on the Gaseous Products of Acetone

Radiation -dE/dx(eV/nm)	^{60}Co- γ 0.2	6.9-MeV He-ions 131	67-MeV C-ions 390	65.7-MeV N-ions 553
$G(H_2)$	0.96	1.47	2.36	2.71
$G(CO)$	0.56	0.80	1.05	1.22
$G(CH_4)$	1.76	0.97	0.99	0.96
$G(C_2H_4)$	0.04	0.12	0.21	0.24
$G(C_2H_6)$	0.30	0.50	0.56	0.64
$G(gas)$	3.62	3.86	5.17	5.77

Ref.:   Spinks 1976[3], Table 8.19.

Table 2.1-11 — G Values for Three Ketones

Material	G(H$_2$)	G(CO)	G(CH$_4$)	G(gas)[a]	Comments	Reference
acetone	1.0	0.6	1.8	3.6	gamma; vacuum	(1)
	1.5	0.8	1.0	3.9	alpha; vacuum	(1)
	0.9	0.8	2.6	4.8	gamma; vacuum	(2)
methyl ethyl ketone	1.2	0.8	0.9	6.8	gamma; vacuum	(2)
diethyl ketone	1.2	1.5	0.1	7.7	gamma; vacuum	(2)

Refs.:   (1) Spinks 1976[3], p. 427; (2) Hall 1963[6], p. 102.
Note: [a]G(gas) includes C$_2$-C$_4$ hydrocarbons.

2.1.3.8 Radiolysis of Carboxylic Acids

Carboxylic acids contain the carboxyl group

$$
\begin{array}{c}
\quad\quad O \\
\quad\quad \parallel \\
— C \\
\quad\quad \backslash \\
\quad\quad OH
\end{array}
$$
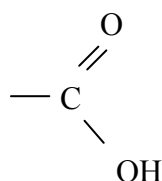
attached to either an alkyl group (RCOOH) or an aryl group (ArCOOH).[7] For example, acetic acid, CH$_3$COOH, has the structure

$$
\begin{array}{c}
CH_3 — C{=}O \\
\quad\quad\quad | \\
\quad\quad\quad OH
\end{array}
$$
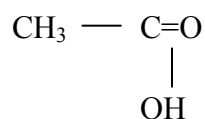
Whether the group is aliphatic or aromatic, saturated or unsaturated, substituted or unsubstituted, the properties of the carboxyl group are essentially the same.

Table 2.1-12 gives G values for two carboxylic acids that are liquids at room temperature. G values for some carboxylic acids that are solids at room temperature are given in Section 2.1.5.

Table 2.1-12 — G Values for Carboxylic Acids (Liquids at Room Temperature)

Material	$G(H_2)$	$G(CO)$	$G(CO_2)$	$G(CH_4)$	G(gas)	Comments	Reference
acetic acid	0.5	0.2	5.4	3.9	10.5	gamma; vacuum	(1)
	0.5	0.4	4.0	1.4	7.2	alpha; vacuum	(1)
propionic acid	0.8	0.3	3.9	0.5	5.5	alpha; vacuum	(2)

Refs.:   (1) Spinks 1976[3], pp. 428-429; (2) Hall 1963[6], p. 108.
Note: [a]G(gas) may include C_2; water vapor is also generated but is not included.

2.1.3.9 Radiolysis of Esters

Esters are functional derivatives of carboxylic acids in which the -OH of the carboxyl group has been replaced by -OR'.[7] Phosphate esters are discussed separately. For example, the structure of methyl acetate is

$$CH_3 — C=O$$
$$|$$
$$O—CH_3$$
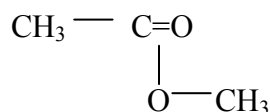
The emulsifier for Envirostone[R], a gypsum-based material used to solidify organic and low pH aqueous sludges and liquid waste, has been identified as a polyethyl glycol ester. Many plasticizers added to polymers to form commercial plastics are esters, such as dioctyl phthalate. Table 2.1-13 gives G values for many esters. Note that benzyl acetate, which includes a benzene ring in its structure, has a much lower $G(H_2)$ value than the other esters.

Table 2.1-13 — G Values for Esters

Material	$G(H_2)$	$G(CO)$	$G(CO_2)$	$G(CH_4)$	G(gas)[a]	Comments	Reference
methyl acetate	0.8	1.6	1.0	2.0	5.7	gamma; vacuum	(1)
	0.9	1.6	0.8	2.1	5.6	gamma; vacuum	(2)
	0.6	1.2	0.4	0.8	3.4	electron; vacuum	(2)
ethyl acetate	0.9	1.1	--	1.6	3.6	gamma; vacuum	(2)
isopropyl acetate	0.9	1.2	0.8	0.9	5.6	alpha; vacuum	(2)
	0.5	0.8	0.6	1.0	3.6	electron; vacuum	(2)
n-propyl acetate	0.8	1.1	0.6	0.4	4.0	electron; vacuum	(2)
benzyl acetate	0.1	0.2	1.6	0.8	2.7	electron; vacuum; aromatic character	(2)

Table 2.1-13 — G Values for Esters (Concluded)

Material	$G(H_2)$	$G(CO)$	$G(CO_2)$	$G(CH_4)$	$G(gas)^a$	Comments	Reference
di (2-ethyl) hexyl sebacate	1.0	0.3	0.2	~0	1.8	electron; vacuum	(3)
	1.0	0.3	0.2	~0	1.5	gamma; vacuum	(4)
di (2-ethyl) hexyl adipate	0.9	0.5	0.2	~0	1.7	gamma; vacuum	(4)
pentaerythritol ester	0.8	0.8	0.3	~0[b]	1.9	gamma; vacuum	(4)

Refs.: (1) Spinks 1976[3], p. 430; (2) Hall 1963[6], p. 104; (3) Rad. Effects 1963[27], p. 62; (4) Arakawa 1983a.[33]

Note: [a]$G(gas)$ may include C_2 hydrocarbons or vapors from volatile liquids, such as aldehydes, alcohols, or ethers.

[b]The value of 0.3 in the reference appears to be in error (0.03 vs. 0.3).

2.1.3.10 Radiolysis of Phosphate Esters

Phosphate esters have one of the following structures[7]:
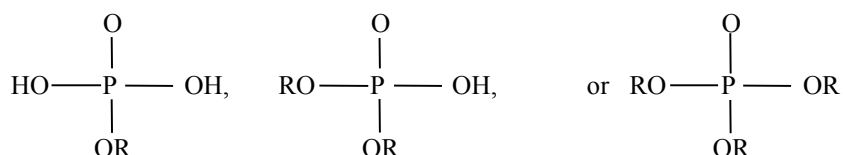
Table 2.1-14 gives G values for phosphate esters. Tricresyl phosphate contains three benzene rings and has a much lower $G(H_2)$ value than either trioctyl or tributyl phosphate.

Table 2.1-14 — G Values for Phosphate Esters

Material	$G(H_2)$	$G(CO)$	$G(CO_2)$	$G(CH_4)$	$G(gas)^a$	Comments	Reference
tricresyl phosphate	0.05	~0	~0	~0	0.06	gamma; vacuum; aromatic character	(1)
tributyl phosphate	2.0	--	--	0.3	2.3	gamma	(2)
trioctyl phosphate	2.3	~0	~0	0.1	2.6	gamma; vacuum	(1)

Refs.: (1) Arakawa 1983a[33]; (2) Holland 1978[34].

Note: [a]$G(gas)$ may include C2 hydrocarbons

---

[33] Arakawa 1983a. K. Arakawa, et al., "Radiation-Induced Gas Evolution from Commercial Lubricant Base Oil," Nuclear Technology 61, pp. 533-539, 1983.

[34] Holland 1978. J. P. Holland, et al., "The Radiolysis of Dodecane-Tributylphosphate Solutions," Nuclear Instruments and Methods 153, pp. 589-593, 1978.

Tri-n-butyl phosphate (TBP), an organic ester of phosphoric acid, is used as an extractant in the reprocessing of nuclear fuel. Radiolysis experiments have been conducted to determine the decomposition of TBP in different phases of the extraction system. The Purex process uses solution of TBP in dodecane.[35]

Ladrielle[35] conducted both gamma and alpha radiolysis experiments in solutions of TBP in dodecane at room temperature. The average alpha particle energy from the cyclotron beam interacting with the solution was estimated to be 10.5 MeV. Pure TBP and dodecane were also irradiated. Radiolysis of pure TBP resulted in the formation of mono and dibutylphosphate, butanol, and saturated hydrocarbons (C_5 to C_8). Radiolysis of pure dodecane yielded hydrocarbons (C_5 to C_{11}). Lower molecular weight hydrocarbons (C_4 and below) were neglected in this study.

Holland[34] performed gamma radiolysis experiments on TBP, dodecane, and mixtures of TBP and dodecane. All samples were treated with dry clean helium for a period of four to eight hours. The number of moles of gas volatile at 161 K was determined by PVT analysis. A sample of the gas extracted was analyzed at 40 C by gas chromatography. Values of $G(H_2)=6.7$ and $G(CH_4)=0.05$ were determined for dodecane. Corresponding G values for pure TBP were $G(H_2)=2.0$ and $G(CH_4)=0.3$. Mixtures of TBP and dodecane were also irradiated, with dodecane electron fractions of 40%, 70%, 80%, 90%, and 95%. Plots of $G(H_2)$ versus TBP electron fraction were nonlinear. The yield of hydrogen was less than would be predicted by the mixture law (the yield of acid was greater).

Aromatic hydrocarbons, such as benzene, toluene, and cyclohexene protect TBP, while saturated hydrocarbons such as hexane, cyclohexane, and dodecane sensitize TBP to radiolytic degradation.[36] Carbon tetrachloride also sensitizes TBP radiolysis. Barney found that chlorinated aromatic hydrocarbons also provided more protection to TBP for alpha radiolysis than did the chlorinated unsaturated hydrocarbons. The rate of chloride ion formation in 20% TBP mixtures with various chlorinated hydrocarbon diluents was also measured. The relative rates were in the ratio 1/0.7/0.5 for carbon tetrachloride/trichloroethylene/ tetrachloroethylene. No detectable chloride ion formation was found for 1,2,4-trichlorobenzene or o-dichlorobenzene.

2.1.3.11 Radiolysis of Halogenated Hydrocarbons

Halogenated hydrocarbons are hydrocarbons in which at least one and possibly all of the hydrogen atoms have been replaced by halogen atoms (the major functional group for these materials). Radiolysis of halogenated hydrocarbons can be strongly affected by the presence of oxygen or moisture, and chain reactions can occur involving HCl for chlorinated hydrocarbons.

---

[35] Ladrielle 1983. Ladrielle, et al., "Alpha and Gamma Induced Radiolysis of Tributyl-Phosphate," Radiochem. Radioanal. Letters 59, pp. 355-364, 1983.

[36] Barney 1977. G. S. Barney and D. G. Bouse, "Alpha Radiolysis of Tributyl Phosphate - Effect of Diluents," Atlantic Richfield Hanford Company, ARH-ST-153, April 1977.

2.1.3.11.1   Radiolysis of Carbon Tetrachloride

Radiolysis of carbon tetrachloride, CCl_4, represents a simple example of radiolysis of an organic halogen compound because the radicals produced have limited possible reactions. Only two products are found: chlorine and hexachloroethane (not a gas). The observed G values for both products are 0.65 to 0.75 for gamma radiation.[3] When carbon tetrachloride is irradiated in the presence of oxygen, phosgene gas and chlorine are formed, each with a G value for gamma radiation of 4.3.[3]

Kazanjian[37] measured gas generation from carbon tetrachloride contaminated with plutonium dioxide and mixed with calcium silicate to form a paste. The initial atmosphere was air. The only gaseous product found was carbon dioxide, with a G value of 0.6. After the oxygen was completely depleted in about 40 days, the gas production rate became essentially nil. Kazanjian remarked that finding only carbon dioxide was puzzling because previous studies had shown that chlorine and phosgene were the only gaseous products. He hypothesized that chlorine was not detected because of its high reactivity. Phosgene can react with water to form HCl and CO_2[38]. Another possibility is that the calcium silicate, while radiolytically inert, could sorb radiolysis products, such as chlorine. Table 2.1-15 gives G values for carbon tetrachloride.

Table 2.1-15 — G Values for Carbon Tetrachloride

Radiation Type	G(Products)	Comments	Reference
gamma	G(gas)=0.7-0.8 G(Cl$_2$)=0.7-0.8	vacuum	(1),(2)
gamma	G(gas)=8.6	oxygen	(1)
alpha	G(gas)=0.6 G(CO$_2$)=0.6	air; CCl$_4$ mixed with calcium silicate to form a paste	(3)

Refs.:   (1) Spinks 1976[3], pp. 401-403; (2) Rad. Effects 1963[27] p. 62; (3) Kazanjian 1976[37]

2.1.3.11.2 Radiolysis of Aromatic Halides

The aromatic halides chlorobenzene, bromobenzene, and iodobenzene consist of a benzene ring with one hydrogen atom replaced by a chlorine, bromine, or iodine atom, respectively.

Table 2.1-16 lists G values for several aromatic halides. Very low $G(H_2)$ values are found, as for the aromatic hydrocarbons.

---

[37] Kazanjian 1976. A. R. Kazanjian, "Radiolytic Gas Generation in Plutonium Contaminated Waste Materials," Rockwell International, Rocky Flats Plant, RFP-2469, October 1976.

[38] Kazanjian 1969. A. R. Kazanjian and A. K. Brown, "Radiation Chemistry of Materials Used in Plutonium Processing," The Dow Chemical Company, Rocky Flats Division, RFP-1376, December 1969.

Table 2.1-16 — G Values for Aromatic Halides

Material	G(Products)	G(gas)[a]
chlorobenzene	$G(H_2)\sim 0$; $G(HCl)=1.4$; $G(Cl_2)\sim 0$	1.4
bromobenzene	$G(H_2)\sim 0$; $G(HBr)=2.3$; $G(Br_2)=0.2$	2.5
iodobenzene	$G(H_2)\sim 0$; $G(HI)\sim 0$; $G(I_2)=2.0$	2.0

Ref.:   Spinks 1976[3], p. 407.

Note: [a]Gamma irradiation in a vacuum.

2.1.3.11.3 Radiolysis of Miscellaneous Halogenated Hydrocarbons

Some of the halogenated hydrocarbons that may be present in CH-TRU wastes are chloroform, methylene chloride, 1,1,1-trichloroethane, and 1,1,2-trichloro-1,2,2-trifluoroethane (freon-113).

The amounts and species of gases generated from gamma radiolysis of liquid chloroform are dependent on temperature and dose rate and, in particular, on traces of oxygen and moisture that induce chain reactions. Aqueous solutions of chloroform do not decompose by a chain reaction.[3] Measured values of G(HCl) from about 5 up to 11 have been reported at 22-25°C (Ottolenghi 1961[39], Chen 1960[40]) for pure chloroform.

In the presence of oxygen, chloroform takes part in a radiation-initiated chain reaction. Nearly 100 chloroform molecules are decomposed per 100 eV of energy absorbed[41]. Most of the radiolysis products are hydrolyzed by water to produce hydrochloric acid.

Kazanjian[37] measured gas generation from the alpha radiolysis of Chlorothene-VG solvent, which is a trade name for 1,1,1-trichloroethane. The samples were mixed with calcium silicate to form a paste. The total pressure decreased for the first 30 days because of oxygen depletion; then it increased because of evolved gases. The main products measured were hydrogen, carbon dioxide, and dichloroethylene. Kazanjian remarked that formation of dichloroethylene inferred the production of hydrogen chloride, and that the hydrogen chloride probably was not detected because of its high reactivity. Calculations using Kazanjian's data show average G values for

---

[39] Ottolenghi 1961. M. Ottolenghi and G. Stein, "The Radiation Chemistry of Chloroform," Radiation Research 14, pp. 281-290, 1961.

[40] Chen 1960. T. H. Chen, et al., "Radiolysis of Chloroform and Carbon Tetrachloride," J. Phys. Chem. 64, pp. 1023-1025, 1960.

[41] Schulte 1953. J. W. Schulte, et al., "Chemical Effects Produced in Chloroform by Gamma-Rays," J. Am. Chem. Soc. 75, pp. 2222-2227, 1953.

CO_2 and H_2 of 0.3 and 0.2, respectively; and G(gas)=0.7. The G values did not decrease with increasing dose.

Getoff [42] performed gamma irradiation of oxygenated waste water containing 1,1,1-trichloroethane and found $G(Cl^-)$=0.4.

Kazanjian[38,43] performed gamma radiolysis experiments on Baker reagent-grade trichloroethylene. Trichloroethylene is a highly sensitive compound, and very little energy input is necessary to initiate decomposition. In the absence of air, there were only two major products: hydrochloric acid and chloroacetylene, each with a G value of 0.25. A chain reaction was observed to occur when trichloroethylene was irradiated in the presence of oxygen. Extremely high yields were obtained, but the products were difficult to analyze because of their high reactivity. The major products were determined to be dichloroacetyl chloride, phosgene, and trichloroethylene oxide. There was no HCl or Cl_2 measured. Rapid reaction of the products with water to form HCl made it possible to analyze for total acidity. The total acid yield was measured by shaking the irradiated solvent with water and titrating the mixture with standardized NaOH solution. The $G(H^+)$ obtained was 4600 at room temperature[43] and increased with increasing temperature with an activation energy value of 2.2 kcal/mole.

Kazanjian[38] also measured the products from gamma irradiation of Alk-Tri^R, a commercial brand of trichloroethylene, which contains diisopropylamine for light stabilization. $G(H^+)$ was found to be 1600. Acid yields for this material would be expected to increase to the yields obtained for the reagent grade chemical as the additives were depleted through continued irradiation.

Perchloroethylene is expected to have a radiation chemistry similar to that of trichloroethylene and to produce an extremely high yield of acidic products in the presence of oxygen[38].

Alfassi and co-workers have performed gamma radiolysis experiments on two Freons, $CFCl_3$ and CF_2Cl_2, in the liquid phase.[44,45] A variety of C-F-Cl compounds were found with maximum measured G value for products of 2.6 in the presence of oxygen. All of the products were gases or highly volatile liquids.

Table 2.1-17 gives G values for miscellaneous organic halogen compounds.

---

[42] Getoff 1985. N. Getoff and W. Lutz, "Radiation Induced Decomposition of Hydrocarbons in Water Resources," Radiat. Phys. Chem. 25, pp. 21-26, 1985.

[43] Kazanjian 1970. A. R. Kazanjian and D. R. Horrell, "The Radiation-Induced Oxidation of Trichloroethylene," J. Phys. Chem. 75, pp. 613-616, 1971.

[44] Alfassi 1982. Z. B. Alfassi, "The Radiation Chemistry of CFCl3 in the Liquid Phase," Radiochem. Radioanal. Letters 56, pp. 333-342, 1982.

[45] Alfassi 1983. Z. B. Alfassi and H. Heusinger, "The Radiation Chemistry of CF2Cl2 in the Liquid Phase," Radiat. Phys. Chem. 22, pp. 995-1000, 1983.

Table 2.1-17 — G Values for Miscellaneous Organic Halogen Compounds

Material	G(Products)	Comments	Reference
chloroform[a]	G(HCl)=5.3	gamma; vacuum	(1)
methylene chloride	G(HC1)=4.9	gamma; vacuum	(2)
1,1,1-trichloroethane	G(gas)=0.7; G(H_2)=0.2; G(CO_2)=0.3; G(dichloroethylene)=0.2	alpha; with or without O_2 present	(3)[b]
	G(Cl^-)=0.4	gamma; O_2 present in aqueous solution	(4)
trichloroethylene	G(H^+)=4600[a] G(HCl)=0.25	gamma; oxygen present gamma; vacuum	(5) (5),(6)
Freons	G(gas)=2.6(max); G(C-F-Cl compounds)=1.6; G(CO_2)=0-1.1	gamma; with or without O_2 present	(7),(8)

Refs.:   (1) Spinks 1976[3], p. 403; (2) Rad. Effects 1963[27], p. 62; (3) Kazanjian 1976[37]; (4) Getoff 1985[42]; (5) Kazanjian 1970[43]; (6) Kazanjian 1969[38]; (7) Alfassi 1982[44]; (8) Alfassi 1983[45].

Notes: [a]G(H^+) is large for irradiation in oxygen. A chain reaction occurs in the liquid.
[b]Average G values calculated using author's data.

2.1.3.12 Radiolysis of Organic Nitrogen Compounds

Organic nitrogen compounds are basically hydrocarbons where a functional group has been replaced by an NO_2, NH_2, or other group containing one or more nitrogen atoms. Amides (such as propionamide) are functional derivatives of carboxylic acids in which the -OH of the carboxyl group has been replaced by -NH_2[7]. Amines have the general formula RNH_2, R_2NH, or R_3N, where R is any alkyl or aryl group. In many of their reactions, the final products depend on the number of hydrogen atoms attached to the nitrogen atom. Two examples of amines are methylamine (CH_3NH_2) and analine, which has the NH_2 group attached to a benzene ring. Some of the heterocyclic compounds containing nitrogen (such as pyrrole, pyrazole, pyridine, and pyrimidine) have aromatic properties, while others, including 3-pyrroline and pyrrolidiene, do not.

G values for radiolysis of organic nitrogen compounds that have aromatic characteristics are low, as were the G values for radiolysis of aromatic hydrocarbons. Table 2.1-18 lists the G values for the products generated by the gamma radiolysis of many liquid organic nitrogen compounds. Ammonia is one of the products formed for a few of the compounds.

Table 2.1-18 — G Values for Liquid Organic Nitrogen Compounds[a]

Material	G(Products)	Comments
nitromethane	G(HCHO)=2.0	
nitrobenzene	G(N$_2$)=0.16	
acetonitrile	G(H$_2$)=0.67; G(CH$_4$)=0.65; G(HCN)=0.2	C≡N bond
methylamine	G(H$_2$)=5.4; G(CH$_4$)=0.18	
aniline	G(H$_2$)=0.12; G(NH$_3$)=0.25; G(C$_6$H$_6$)=0.04	contains benzene ring
propionamide	G(H$_2$)=0.14; G(CO)=2.6; G(CH$_4$)=0.93	
pyrrole	G(H$_2$)=0.20	aromatic N-C bonds
3-pyrroline	G(H$_2$)=2.34	
pyrollidine	G(H$_2$)=6.35	
pyrazole	G(H$_2$)=0.04; G(N$_2$)=0.12	aromatic N-C bonds
tetrazole	G(H$_2$)=trace; G(N$_2$)=0.96	aromatic N-C bonds
pyridine	G(H$_2$)=0.025	aromatic N-C bonds
pyrimidine	G(H$_2$)=0.030	aromatic N-C bonds

Ref.:   Spinks 1976[3], Table 8.22.

Note: [a]Gamma irradiation in vacuum. Other liquid products are also formed.

A value of G(gas)=10.1 was reported for gamma irradiation at room temperature of mono-n-butylamine (Mirchi 1981[46]). Major gas constituents were hydrogen [G(H$_2$)=5.6] and ammonia [G(NH$_3$)=4.0]. For dibutylamine and tri-n-butylamine, measurements of G(H$_2$) values at room temperature were 3.6 and 2.7, respectively. In all three cases, the total G value for hydrocarbon gases was 0.5.

Diethylenetriaminepentaacetic acid (DTPA) is a polyamino-carboxylic acid used as an eluting agent for the purification of Cm-244 by cation exchange chromatography. DTPA has been irradiated in aqueous solution by alpha and gamma radiation sources (Bibler 1972[47]). In some experiments, the solutions were degassed before irradiation, and the amounts of radiolytically produced gases that were noncondensible at -196°C and at -78°C were determined. The products were identified by mass spectrometry. Gamma radiolysis of solutions of DTPA in 4-M HNO$_3$ or 0.4-M H$_2$SO$_4$ produced CO$_2$ and H$_2$, with measured G values of 6.5 and 4.2, respectively. Gases produced in the alpha radiolysis experiments were not reported. However, measured G values for the destruction of DTPA were much lower for the alpha radiolysis experiments than for the gamma radiolysis experiments, indicating that gas production for alpha radiolysis should also be much lower than for gamma radiolysis.

---

[46] Mirichi 1981. R. Mirichi, et al., "Selected Problems of Radiation Stability of Some Solvents and Amines Used in the Reprocessing of Nuclear Fuel," Nukleonika 26, pp. 827–848, 1981.

[47] Bibler 1972. N. E. Bibler, "Gamma and Alpha Radiolysis of Aqueous Solutions of Diethylenetriaminepentaacetic Acid," J. Inorg. Nucl. Chem. 34, pp. 1417-1425, 1972.

2.1.3.13 Radiolysis of Commercial Lubricants

Commercial lubricants consist of paraffinic, naphthenic, and aromatic hydrocarbons. The aromatics have much lower G values than the paraffins but are largely removed from the oils by refining because of their poor viscosity-temperature properties (Carroll 1963[48]).

G values have been measured for many different commercial lubricants using gamma irradiation at room temperature at a dose rate of 1 Mrad/h and absorbed doses ranging from 100 to 3,000 Mrad (Arakawa 1983a[33]). Graphs of the amount of evolved gas versus dose were nearly linear even at high absorbed dose, indicating nearly constant G values.

G values for Texaco Regal A motor oil, used in machining operations at the RFETS, were measured by Kazanjian using Co-60 gamma irradiation (Kazanjian 1969[38]) and alpha irradiation from Pu-239 (Kazanjian 1976[37]). In the gamma irradiation experiment, samples of the oil were irradiated under vacuum or sealed under 500 torr air. Values of $G(H_2)$ at 8.4 Mrad absorbed dose were 2.3 for the vacuum experiment and 1.8 for the experiment in air. The author did not consider this difference significant. At 8.4 Mrad absorbed dose, $G(-O_2)=1.6$, decreased from a value of 3.0 at 1.4 Mrad.

In the alpha radiolysis experiment, the Texaco oil was contaminated with plutonium dioxide and mixed with calcium silicate to form a paste. About 15% of the alpha energy could have been absorbed by the calcium silicate, which was considered to be radiation stable. In the first experiment the materials were contained in an initial air atmosphere in a valved stainless steel vessel. The oxygen concentration decreased from 21% to 5% over the course of the 100-day experiment. For the second experiment the vessel was evacuated and backfilled with helium. Calculations using Kazanjian's data show that as the absorbed dose increased, the G values for H_2 and total gas increased from about 1.6 to 2.8-2.9 for the first experiment. During the second experiment in vacuum, the G values decreased from about 2.3 to 1.9-2.1. The cause for these changes in G values is unknown. Maximum values for these experiments are listed in Table 2.1-18.

Zerwekh (Zerwekh 1979[13]) measured gas generated from the alpha radiolysis of vacuum pump oil (DuoSeal) absorbed on vermiculite. Two experimental cylinders were prepared. One cylinder contained 62 mg of Pu-238 in the oxide form dispersed in 35 g of oil, which was then absorbed on 17.5 g of vermiculite. The other cylinder contained the same amounts of oil and vermiculite but only half as much PuO_2. The gases in the cylinders were sampled each time the pressure reached 15-17 psig, and then the pressure was reduced to 1 psig. The O_2 concentration was less than 0.1% at the first sampling. The gas generated was predominantly hydrogen, with a small amount of methane. Concentrations of CO and CO_2 did not exceed 0.7% (each) at any time during the experiment. The maximum G(gas) value observed was about 1.7. The initial G(gas) value observed for the sample contaminated with 32 mg of PuO_2 was about 10% higher than for the sample contaminated with 62 mg of PuO_2.

---

[48] Carroll 1963. J. G. Carroll and R. O. Bolt, "Lubricants," in <u>Radiation Effects on Organic Materials,</u> Academic Press, New York, 1963, eds. R. O. Bolt and J. G. Carroll.

G values for Cm-244 alpha and Co-60 gamma radiolysis of DuoSeal vacuum pump oil absorbed on vermiculite were measured by Bibler (Bibler 1977[26]) at various dose rates, absorbed doses, and mass fraction of oil. (Vermiculite is a hydrated magnesium-aluminum-iron silicate, and produced no H_2 when irradiated.) Usually, 2.5 ml of the oil was absorbed onto each gram of vermiculite. At low gamma dose rates (1.5-4.8E5 rad/hr), a $G(H_2)$ of 2.0 was calculated based on energy absorbed only by the organic material. The composition of the evolved gas was about 96% H_2, 3% CO_2, and 1% CH_4. Experiments conducted at a dose rate of 1.4E7 rad/hr (gamma) showed that $G(H_2)$ was directly proportional to the amount of organic material present, indicating that the energy absorbed by the vermiculite was not transferred to the organic material.

The corresponding alpha radiolysis experiment using vacuum pump oil absorbed on vermiculite contaminated with 7.2 mg Cm-244 (dose rate 1.4E6 rads/hr) resulted in a $G(H_2)$ value of 2.7. No decrease in G values with increasing absorbed dose was observed for the alpha radiolysis experiment.

Rykon lubricating grease was irradiated under vacuum and in air using a Co-60 gamma source (Kazanjian 1969[38]). The gas yield was low and consisted mostly of hydrogen, with an approximate value of $G(H_2)$=1.

Table 2.1-19 gives G values for many commercial lubricants. The maximum G values for commercial lubricants are G(gas)=2.9 and $G(H_2)$ = 2.8.

2.1.3.14 Radiolysis of Gases

Radiolysis of the nitrogen/oxygen mixture found in air produces a small amount of ozone, as well as oxides of nitrogen (Spinks 1976[3]). Back reactions lead to an equilibrium concentration of these gases of a few ppm for ozone to a few percent for NO_2 and N_2O. The NO yields are much smaller (Kazanjian 1969[38]). When moisture is present, the main product is nitric acid, which is formed until the water vapor is exhausted (Spinks 1976[3], Kazanjian 1969[38]). G values are around 1 for nitric acid formation but vary with water concentration (Kazanjian 1969[38]).

Gaseous carbon dioxide is almost unaffected by ionizing radiation (Spinks 1976[3]), possibly due to a back reaction between CO and ozone to form CO_2 plus O_2.

2.1.4 Radiolysis of Polymers

Radiation effects in organic solids are generally similar to those for the same compound in the liquid state when allowance is made for the restricted mobility of the active species in the solid. Polymers, including materials such as polyethylene, PVC, and cellulose, are common organic solids found in CH-TRU wastes. Attachment A of this document describes the families of polymers and their use in commercial plastics. Other solids, such as solidified organic liquids, aqueous sludges, and bitumen, are discussed in Section 2.1.5. Some of the polymers discussed in this chapter occur in the liquid state at room temperature.

Table 2.1-19 — G Values for Many Commercial Lubricants

Material/ Radiation Type	G(Products)	Comments	Reference
Mineral oils			
gamma	G(gas)=2.8; G(H$_2$)=2.7; G(CH$_4$)=0.05	vacuum; highest G values for four paraffin oils	(1)
Naphthenic neutral oil			
gamma	G(gas)=0.9; G(H$_2$)=0.9	vacuum	(1)
Poly-alpha-olefin oil			
gamma	G(gas)=2.4; G(H$_2$)=2.3	vacuum	(1)
Ester lubricants			
gamma	G(gas)=2.6; G(H$_2$)=2.3; G(CH$_4$)=0.1; G(CO)~0	vacuum; highest G values for 5 oils[a]	(1)
Aromatic lubricants			
gamma	G(gas)=0.6; G(H$_2$)=0.5	vacuum; highest G values for 7 aromatic oils	(1)
Silicones			
gamma	G(gas)=2.3; G(H$_2$)=0.6 G(CH$_4$)=1.4; G(C$_2$H$_6$)=0.3	vacuum; highest G values for 2 silicones	(1)
Texaco Regal-A machining oil			
alpha (^{239}Pu)[b]	G(gas)=2.9; G(H$_2$)=2.8; G(HC)[c]=0.1	in air, before or after oxygen depletion; maximum values; mixed with calcium silicate to form a paste	(2)[b]
gamma	G(H$_2$)=2.3	vacuum; 8.4 Mrad	(3)
gamma	G(H$_2$)=1.8	500 torr O$_2$; 8.4 Mrad	(3)
gamma	G(H$_2$)=2.1	500 torr O$_2$; 1.4 Mrad	(3)
DuoSeal vacuum oil			
alpha (^{238}Pu)	G(gas)=1.7; G(H$_2$)~1.6	in air after oxygen depleted; sorbed on vermiculite	(4)
alpha (^{244}Cm)	G(gas)=2.8; G(H$_2$)=2.7; G(CO$_2$)=0.1	in air	(5)
gamma	G(gas)=2.1; G(H$_2$)=2.0; G(CO$_2$)=0.1	in air; extrapolated to zero dose	(5)
Rycon grease			
gamma	G(H$_2$)=1	vacuum or air	(3)

Refs.:   (1) Arakawa 1983a[33]; (2) Kazanjian 1976[37]; (3)Kazanjian 1969[38]; (4) Zerwekh 1979[13]; (5) Bibler 1977[26].
Note: [a]Includes oils based on di-2-ethylhexyl sebacate (DOS), di-2-ethylhexyl adipate (DOA), pentaerythritol ester, tricresyl phosphate (TCP), and trioctyl phosphate (TOP).
[b]Calculated using author's data. Assumes all decay energy was absorbed by the oil (85% by weight).
[c]HC = hydrocarbons.

The controlling factor in the behavior of polymers under irradiation, as under most other environmental influences, is the chemical structure (Sisman 1963[49]). Additives to improve physical or aging properties affect changes produced by radiation.

For example, polystyrene demonstrates the stabilizing effect of a regularly recurring phenyl group on the main chain (Sisman 1963[49]). The protective effect appears to depend on closeness to the phenyl group (not more than six carbon atoms away). A part of the stability of polystyrene must be assigned to the low mobility of the molecular segments in the solid.

Radiolysis of polymers generally results in two types of reactions: (a) chain scission and (b) crosslinking. Chain scission (degradation) is the term used for breaking of main-chain bonds in polymer molecules, which results in the formation of species of lower molecular weight. When scission of the polymer is predominant, structural strength and plasticity are rapidly lost. The polymer may actually crumble to a powder. Crosslinking results in network structures that are insoluble and infusible because of increased molecular weight and size. Generally, competition occurs between the two reaction mechanisms.

In the absence of oxygen, polymers can be divided into classes according to their tendency to degrade or crosslink. Tables 2.1-20 through 2.1-22 list common polymers in order of their decreasing resistance when irradiated to net molecular-weight change for polymers that

Table 2.1-20 — Radiation Resistance of Common Polymers that Predominantly Crosslink[a]

Polymer	Characteristics
poly(vinyl carbazole)	aromatic, N in main chain
polystyrene	aromatic
analine-formaldehyde	aromatic, N in main chain
Nylon[R]	N in main chain (amide)
polymethyl acrylate	ester
polyacrylonitrile	C-N triple bond
styrene-butadiene rubber	aromatic, unsaturated
polybutadiene	unsaturated
polyisoprene	unsaturated
nitrile-butadiene rubber	C-N triple bond, unsaturated
polyethylene oxide	ether
polyvinyl acetate	ester
polyvinyl methyl ether	
polyethylene	saturated
silicone	

Ref.:   Sisman 1963[49].
Note: [a]Listed in order of decreasing resistance to net molecular-weight change.

---

[49] Sisman 1963. O. Sisman, et al., "Polymers," in Radiation Effects on Organic Materials, Academic Press, New York, 1963, eds. R. O. Bolt and J. G. Carroll.

Table 2.1-21 — Radiation Resistance of Common Polymers that are Borderline Between Predominant Crosslinking and Scission[a]

Polymer	Characteristics
polysulfide rubber	S in main chain
polyethylene terephthalate	aromatic, ester
polyvinyl chloride	halogen
polyvinylidene chloride	halogen
polypropylene	saturated

Ref.:   Sisman 1963[49].

Note: [a]Listed in order of decreasing resistance to net molecular-weight change.

Table 2.1-22 — Radiation Resistance of Common Polymers that Scission Predominantly[a]

Polymer	Characteristics
phenol-formaldehyde	aromatic
polymethyl methacrylate	ester
polyvinyl alcohol	alcohol
polytetrafluoroethylene	halogen
polyisobutylene	saturated
cellulose	alcohol/ether

Ref.:   Sisman 1963[49].

Note: [a]Listed in order of decreasing resistance to net molecular-weight change.

predominantly crosslink, are borderline between crosslinking and scission, or that predominantly undergo scission, respectively. Oxygen enhances the degradation of most polymers (polymethyl methacrylate is one exception).

Ether-type oxygen linkages occur in the main chain in polyethylene oxide. Cellulose is made up of glucose residues joined through acetal linkages (ether links formed between hydroxyl and carbonyl groups). Cellulose and cellulose esters and ethers undergo scission, probably resulting from a break in the acetal link rather than rupture of the glucose ring (Sisman 1963[49]).

Commercial plastics and papers contain additives that modify the properties of the base polymer in the material. In general, the additives improve the radiation stability of the commercial materials and reduce G values for flammable gases.

Additives and nonpolymer components can be divided into two categories: active and inert materials. The active additives can be subdivided into two classes: the energy-sink materials and the chemical reactants. The aromatic ring acts as an energy sink incorporated intramolecularly in the polymer. Antioxidants are usually complex aromatic amines or phenols, which should have low G values as a result of their aromatic characteristics (Sisman 1963[49]).

Scission of polymethyl methacrylate has been reduced by the addition of aromatic compounds dissolved in the polymer (Bopp 1963[50]). Protection was shown to be concentration dependent. For several of the additives, no dose dependence was found, indicating that the additives were not being radiolytically degraded, but in other cases, a dose dependence was observed. Antioxidants and aromatic stabilizers and plasticizers are frequently used to enhance durability of mechanical properties. Polyethylene and hydrocarbon rubbers normally require a small quantity of antioxidant for stability during hot processing.

From the observed G values for flammable gas [G(flam gas)], the expected relationships between the G(flam gas) values for structurally related polymers are shown in Table 2.1-23.

Table 2.1-23 — Expected Relative G(flam gas) Values for Polymers from G(flam gas) Values in Structurally Related Liquids

High
Hydrocarbon polymers containing only saturated C-C bonds
Polymers containing alcohol functional groups
Polymers containing ether functional groups
Medium
Hydrocarbon polymers containing unsaturated C-C bonds
Polymers containing ester functional groups
Low
Polymers with aromatic characteristics

Notes: High: liquid G(flam gas)=5-7; Medium: liquid G(flam gas)=2-3; Low: liquid G(flam gas)<1.

Radiolysis experiments on polymers that are discussed in this chapter are organized into the following groups, which follow the approximate order of high to low G values for flammable gas expected for synthetic polymers containing only carbon, hydrogen, nitrogen, and oxygen:

(1)   Hydrocarbon polymers containing only saturated C-C bonds (polyethylene, polypropylene, ethylene-propylene rubber, and polyisobutylene)

(2)   Polymers containing alcohol functional groups (polyvinyl alcohol and polyethylene glycol)

(3)   Polymers containing ether functional groups (cellulose, urea formaldehyde, polyoxymethylene, polypropylene oxide, and polyvinyl formal)

(4)   Hydrocarbon polymers containing unsaturated C-C bonds (polybutadiene and polyisoprene)

(5)   Polymers containing ester functional groups (polymethyl methacrylate and polyvinyl acetate)

---

[50] Bopp 1963. C. D. Bopp, et al., "Plastics," in Radiation Effects on Organic Materials, Academic Press, New York, 1963, eds. R. O. Bolt and J. G. Carroll.

(6)   Polymers with aromatic characteristics (polystyrene, polysulfone, polycarbonate, and polyethylene terephthalate and other polyesters)

Additional groupings include halogen-containing polymers and miscellaneous polymers:

(7)   Polymers containing halogens (polyvinyl chloride, polychloroprene, chlorosulfonated polyethylene, polytetrafluoroethylene, polychlorotrifluorethylene, chlorinated polyether, rubber hydrochloride, and polyvinylidene chloride.

(8)   Miscellaneous polymers (polyamides, ion-exchange resins, and others).

The maximum G values are summarized in Table 2.1-24.

2.1.4.1   Radiolysis of Hydrocarbon Polymers Containing Only Saturated C-C Bonds

Polymers included in this section are polyethylene, polypropylene, ethylene-propylene rubber, and polyisobutylene. The polymers in this group produce hydrogen as the principal radiolysis gas. Small amounts of other hydrocarbons are formed. The maximum $G(H_2)$ value is 4.0 for polyethylene; the maximum G(flam gas) value is 4.1 for polyethylene.

2.1.4.1.1 Polyethylene

Polyethylene has the repeat unit:

— (CH_2) —

Polyethylene materials are generally divided into two classes: low-density polyethylene (LDPE) and high-density polyethylene (HDPE). Polyethylene bags and a 90-mil HDPE rigid drum liner are commonly used polyethylene products that are found in CH-TRU wastes. Unirradiated polyethylene softens in the range of 70 to 90°C, and melts to a viscous liquid at about 115 to 125°C (Spinks 1976[3]). Some of the G values and gas species produced by radiolysis of polyethylene depend on whether or not oxygen is present.

2.1.4.1.1.1 Radiolysis of Polyethylene in the Absence of Oxygen

When irradiated, polyethylene crosslinks in the absence of oxygen and evolves a considerable amount of gas (80-95% hydrogen along with other simple aliphatic hydrocarbons). The amount of volatile hydrocarbons produced by radiolysis of polyethylene increases while the hydrogen yield decreases, as the degree of chain branching increases. The evolution of hydrogen and hydrocarbon gases is accompanied both by an increase in unsaturation in the polymer chain and by an increase in crosslinking density (Chapiro 1962[10]).

Table 2.1-24 — Summary of Maximum G Values for Polymers at Room Temperature[a]

Group[b]	Polymer	G(H$_2$)	G(flam gas)	G(net gas)[c]
S-HC	polyethylene	4.0	4.1	4.1
	polypropylene	3.3	3.4	3.4
	ethylene-propylene	d	d	d
	polyisobutylene	1.6	2.4	2.4
Al	polyvinyl alcohol	3.1	3.1	3.1
	polyethylene glycol	3.5	3.5	3.5
Eth	cellulose	3.2	3.2	10.2
	cellulose nitrate	e	e	6.0[f]
	urea formaldehyde	2.4	2.8	2.8
	polyoxymethylene	2.1	5.6	14.1
	polypropylene oxide	1.1	e	e
	polyvinyl formal	e	e	5.6[f]
U-HC	polybutadiene	0.5	0.5	0.5
	polyisoprene	0.7	0.9	0.9
Est	polymethyl methacrylate	0.4	2.0	4.1
	polyvinyl acetate	0.9	1.4	1.4
Ar	polystyrene	0.2	0.2	0.2
	polysulfone	0.1	0.1	0.1
	polycarbonate	<0.1	<0.1	0.8
	polyesters	0.3	0.3	<0.8
	polyphenyl methacrylate	<0.1	<0.1	1.3
Hal	polyvinyl chloride	0.7	0.7	2.6
	polychloroprene	0.1	0.1	0.7
	chlorosulfonated polyethylene	0.3	0.3	0.6
	polychlorotrifluoro-ethylene	0	0	1.1
	polytetrafluoroethylene	0	0	<0.3
	chlorinated polyether	0.7	0.8	0.8
	rubber hydrochloride	0	0	<2.1
	polyvinylidene chloride	0	0	<2.1
M	polyamides	1.1	1.2	1.5
	ion-exchange resins	1.7	1.7	2.1

Notes: [a]Values listed are those most appropriate for CH-TRU waste, i.e., above 10 Mrad absorbed dose or for commercial rather than for pure materials
[b]S-HC = saturated hydrocarbon, Al = alcohol functional group, Eth = ether functional group, U-HC = unsaturated hydrocarbon, Est = ester functional group, Ar = aromatic character, Hal = halogen functional group, and M = miscellaneous
[c]G(net gas)is the net G value, and includes depletion of oxygen when applicable
[d]Values are intermediate between those for polyethylene and those for polypropylene
[e]Not reported
[f]Calculated on the basis of G(gas) = factor x G(gas) for polyethylene; factor=1.5 for cellulose nitrate, factor=1.4 for polyvinyl formal, and G(gas)=4.1 for polyethylene

Experimental measurements of G values from radiolysis of polyethylene in a vacuum, using reactor, gamma, accelerated electron, and x-ray radiation, are shown in Table 2.1-25 from Chapiro 1962[10]. Chapiro also plotted the data in an Arrhenius plot and found a temperature dependence with an activation energy of about 0.8 kcal/mole. From these data, Chapiro concluded that the G value for hydrogen at room temperature is about 4.1 and about 3.2 near the glass-transition temperature of -120°C. G values for volatile hydrocarbon formation were found to be usually less than 0.1. More recent experiments, discussed later in this section, have measured lower $G(H_2)$ values, and a maximum $G(H_2)$ value is established at $G(H_2)=4.0$.

Table 2.1-25 — Summary of G Values for Hydrogen and Methane for Radiolysis of Polyethylene in a Vacuum

Material[a]	Type of Radiation and Irradiation Temperature[b]	$G(H_2)$	$G(CH_4)$
LDPE	reactor (70°C)	4.0	0.08
LDPE	800 keV electrons	5.0	0.9
LDPE	reactor	5.0[c]	--
LDPE	Co^{60} gamma	3.75	--
LDPE and HDPE	2 MeV electrons (-196°C to +80°C)	3.1	--
PE	Co^{60} gamma	4.0	--
PE	reactor (80°C)	7.0	--
HDPE	800 keV electrons		
Marlex-50[R]	(-170 to 34°C)	3.75	0.07
Marlex-50[R]	136°C	5.5	0.13
Marlex-50[R]	240°C	5.8	0.17
LDPE	50 kV x-rays, 13°C	2.5	0.15
LDPE	50 kV x-rays, 80°C	3.0	0.36
HDPE	50 kV x-rays, 10°C	2.8	0.03
HDPE	50 kV x-rays, 80°C	3.0	0.09

Ref.:   Chapiro 1962[10], Table IX.I.

Note: [a]LDPE = low density polyethylene; HDPE = high density polyethylene. "High pressure" = "low density"; "low pressure" = "high density"; (Wiley 1986[51]).
   [b]Liquid above about 130°C.
   [c]G(gas).

One set of gamma irradiation experiments examined the effect of molecular weight on the $G(H_2)$ value for crystalline samples of polyethylene in the absence of oxygen (Mandelkern 1972[18]). A maximum value of $G(H_2)=4$ was found for the higher molecular weights studied (2.5-4.5×10^4); a $G(H_2)$ value as low as 2.8 was found for the lowest molecular weight studied (2×10^3).

---

[51] Wiley 1986. The Wiley Encyclopedia of Packaging Technology, John Wiley & Sons, New York, 1986, ed. M. Bakker.

Zerwekh (Zerwekh 1979[13]) contaminated pieces of LDPE bags (0.05 mm thick) with Pu-238 dissolved in 2-M HNO_3. In other experiments, pieces of the HDPE drum liner material (2.3 mm thick, 100% cross-linked) were contaminated with Pu-238 as chloride solution. The materials were allowed to dry, then placed into stainless steel cylinders. Gases were sampled and the pressure reduced to 1 psig when the pressure in a cylinder reached 15-17 psig. Almost all of the oxygen had been depleted by the time of first sampling. Gas compositions were determined using a mass spectrometer. The majority of the gas produced from LDPE in these alpha radiolysis experiments was hydrogen. The maximum G(gas) value measured for LDPE was 1.7.

The HDPE experiment, containing 62 mg of Pu-238, never pressurized to 15 psig (even after 1,300 days). At day 674, a gas sample was taken, and consisted of 5% H_2, 17% CO_2, and 77% N_2, with very small amounts of CH_4, O_2, and CO.

Kosiewicz (Kosiewicz 1981[12]) performed alpha radiolysis experiments on samples of commercial LDPE. The composition of the generated gas was 98% H_2, 1% CH_4, and 1% CO plus CO_2. Kosiewicz has reviewed his experimental data, and has corrected the originally published G values. The measured value of G(gas) was 2.0-2.4. Typically, 50 g of the material was cut into small squares onto which the TRU contaminant (Pu-238 or Pu-239 oxide powder) was distributed. A second piece of the test material was placed over the first to contain the plutonium. The initial atmosphere inside the experimental cylinders was air at local atmospheric pressure at Los Alamos of 77 kPa (11.2 psia). The gases in the cylinders were sampled and the pressures relieved when the pressure had increased to 100 kPa over ambient pressure. The rate of gas generation was calculated from the rate of pressure change. (This method results in an underestimate of the G values for generated gases while oxygen is present inside the experimental cylinder.)

Mitsui (Mitsui 1979[52]) measured gas generation from films made from Hizex 1200P polyethylene powder containing no antioxidant that were gamma irradiated in a vacuum. Values of $G(H_2)$ obtained at different temperatures were 3.0 at 30°C, 3.2 at 50°C, 3.4 at 70°C, and 3.6 at 100°C. From these data the authors calculated an activation energy of 0.6 kcal/g-mole for formation of H_2.

Kang (Kang 1966[53]) measured $G(H_2)$ values for polyethylene (Marlex-6002[R] film) as a function of temperature and dose. The room temperature $G(H_2)$ value varied from 3.7 (extrapolated to zero dose) to 3.3 (at an absorbed dose of 13 Mrad or more). A large increase in G value from 3.7 to 5.6 was observed when polyethylene was heated from room temperature to the liquid state at 140°C. The $G(H_2)$ values extrapolated to zero dose for the temperatures studied were: 3.68 at room temperature, 3.73 at 60°C, 3.81 at 80°C, 4.05 at 100°C, and 4.11 at 120°C. (The values at 60 and 120°C yield an activation energy of 0.4 kcal/g-mole.)

---

[52] Mitsui 1979. H. Mitsui and Y. Shimizu, "Kinetic Study of the Gamma Radiolysis of Polyethylene," J. Polym. Sci., Polymer Chem. Ed. 17, pp. 2805-2813, 1979.

[53] Kang 1966. H. Y. Kang, et al., "The Radiation Chemistry of Polyethylene. IX. Temperature Coefficient of Cross-Linking and Other Effects," J. Am. Chem. Soc. 89, pp. 1980-1986, 1966.

Krasnansky (Krasnansky 1961[54]) performed gamma radiolysis experiments (6 Mrad absorbed dose) in vacuum on various commercial packaging materials. The measured value of G(gas) was reported to be between 1.6 and 3.2 for samples of both low- and high-density polyethylene. Both LDPE and HDPE generated 90-91% H_2 and 3% CO_2. The major difference in the observed gas composition was that the HDPE sample produced 6.5% CO and 0.5% propane, while the LDPE sample produced 2.5% propane, 2% ethane, and 1.5% ethene. The authors stated that the relatively high proportion of CO and CO_2 could have been a result of oxidation of the polyethylene prior to the irradiation.

Bowmer (Bowmer 1977[55]) measured G values from two types of LDPE and one type of HDPE at 30 and 150°C using gamma irradiation in a vacuum of small (5-35 mg) or large (0.5-2.5 g) samples. For the small samples, the following G values were obtained at 30°C: HDPE, G(H_2)=2.9, G(HC)=0.01; LDPE-1, G(H_2)=3.5, G(HC)=0.09; LDPE-2, G(H_2)=3.1, G(HC)=0.1. Values for G(H_2) increased by about 11% for LDPE and 53% for HDPE when the irradiation temperature was changed from 30°C to 150°C.

G(H_2) values about 25% lower were observed for the large samples, even when they were heated at 150-200°C for 60-90 minutes to allow volatiles to escape from the materials (Bowmer 1977[55]). This effect was attributed to reactions of double bonds and trapped polymer radicals with hydrogen atoms and molecules for the large samples, for which the hydrogen pressure was an order of magnitude higher than in the small samples.

G values for various gases generated from the irradiation of polyethylene when oxygen is absent or has been depleted are listed in Table 2.1-26 for experiments not reported by Chapiro (Chapiro 1962[10]). The highest value of G(H_2) in these experiments at room temperature was 4.0. The data listed in the table for Kosiewicz (Kosiewicz 1981[12]) are values that incorporate a correction for a calculational error in the original data, supplied by that author.

2.1.4.1.1.2 <u>Radiolysis of Polyethylene in the Presence of Oxygen</u>

In an early gamma radiolysis experiment, the change in the total gas pressure was measured for irradiation of high-density polyethylene in pure oxygen. The G value for oxygen consumption [G(-O_2)] was found to be at least twice the sum of the G values for oxygen-containing gas molecules. The rest of the oxygen was assumed to be converted to peroxides and hydroxyl groups in the polyethylene (Dole 1973a[56]).

---

[54] Krasnansky 1961. V. J. Krasnansky, et al., "Effect of Gamma Radiation on Chemical Structure of Plastics," <u>SPE (Society of Plastics Eng.) Trans. 1</u>, pp. 133-138, 1961.

[55] Bowmer 1977. T. N. Bowmer and J. H. O'Donnell, "Nature of the Side Chain Branches in Low Density Polyethylene: Volatile Products from Gamma Radiolysis," <u>Polymer 18</u>, pp. 1032-1040, 1977.

[56] Dole 1973a. M. Dole, "Oxidation of Irradiated Polymers," in <u>The Radiation Chemistry of Macromolecules,</u> Vol. II, Academic Press, New York, 1973, ed. M. Dole.

Table 2.1-26 — G Values for Polyethylene (Oxygen Depleted or Absent)

Radiation Type	G(Products)	Comments	Reference
gamma	$G(H_2)$=6.2 (max)	no oxygen, 130°C	(1)
gamma	$G(H_2)$=2.8-4.0[a]	no oxygen, room temp	(1)
alpha (^{238}Pu)	$G(gas)$=1.7 (90-98% H_2)	oxygen depleted from initial air atmosphere; room temp	(2)
alpha (^{238}Pu)	$G(gas)$=2.0-2.4 (98% H_2, 1% CH_4, 1% CO_2 + CO)	oxygen depleted from initial air atmosphere; 20°C; corrected data	(3)
gamma	$G(H_2)$=3.0	vacuum; 30°C	(4)
gamma	$G(H_2)$=3.2	vacuum; 50°C	(4)
gamma	$G(H_2)$=3.4	vacuum; 70°C	(4)
gamma	$G(H_2)$=3.6	vacuum; 100°C	(4)
gamma	$G(H_2)$=3.7	vacuum; 25°C to 60°C	(5)
gamma	$G(H_2)$=3.8	vacuum; 80°C	(5)
gamma	$G(H_2)$=4.05	vacuum; 100°C	(5)
gamma	$G(H_2)$=4.11	vacuum; 120°C	(5)
gamma	1.6 $G(gas)$ 3.2 (92% H_2, 2-8% CO+CO_2, 0-6% HC)[b]	vacuum; room temp	(6)
gamma	$G(H_2)$=2.9;$G(HC)$=0.01[b]	HDPE; vacuum; 30°C	(7)
gamma	$G(H_2)$=4.5;$G(HC)$=0.03[b]	HDPE; vacuum; 150°C	(7)
gamma	$G(H_2)$=3.5;$G(HC)$=0.09[b]	LDPE; vacuum; 30°C	(7)
gamma	$G(H_2)$=3.9;$G(HC)$=0.18[b]	LDPE; vacuum; 150°C	(7)
gamma	$G(H_2)$=3.1;$G(HC)$=0.11[b]	LDPE; vacuum; 30°C	(7)
gamma	$G(H_2)$=3.5;$G(HC)$=0.36[b]	LDPE; vacuum; 150°C	(7)

Refs.: (1) Mandelkern 1972[18]; (2) Zerwekh 1979[13]; (3) Kosiewicz 1981[12] (data corrected by that author); (4) Mitsui 1979[52]; (5) Kang 1966[53]; (6) Krasnansky 1961[54]; (7) Bowmer 1977[55].

Notes: [a]Values were 3.9, 3.4, 3.6, 4.0, 3.9, 3.2, 3.4, and 2.8, depending on the molecular weight and degree of crystallinity.
[b]HC = hydrocarbons.

Relative amounts of gaseous products were measured for gamma irradiation of commercial samples of LDPE and HDPE in air and in vacuum up to 5.6 Mrad absorbed dose.[57] For both low- and high-density polyethylene, greater amounts of products per gram of material were obtained for irradiation in air than in vacuum (a ratio of 2.0 for LDPE and 1.4 for HDPE). The corresponding ratios of hydrogen production in air versus in vacuum were 1.8 for LDPE and 1.2 for HDPE. The LDPE produced 1.6 times the gaseous products of the HDPE in air, and 1.2 times the products of HDPE in vacuum. The second most abundant product for irradiation in air was carbon dioxide. All of the oxygen in the sample tubes was consumed for both types of polyethylene films. The experiments were repeated for an absorbed dose of 0.93 Mrad. Radiolysis of the LDPE exposed to air generated only carbon dioxide, while the $G(H_2)$ value for HDPE was higher than at 5.6 Mrad. These results contradict trends observed in most other radiolysis experiments on polyethylene and lower the credibility of Bersch's data on polyethylene.

Arakawa[58] performed gamma radiolysis of low- and high-density polyethylene in the presence of oxygen to examine the effect of antirad additives. For the pure polymers, hydrogen and carbon dioxide were the primary gases evolved. For LDPE, values of $G(H_2)=3.3$ and $G(CO_2)=1.3$ were obtained; for HDPE, values of $G(H_2)=3.2$ and $G(CO_2)=4.1$ were measured. The addition of propyl-fluoranthene, an antirad additive, reduced the $G(H_2)$ values by 15-30%. Radiolysis of an ethylene-propylene copolymer showed that the $G(H_2)$ value was independent of the amount of oxygen present.

Fourteen samples of polyethylene sheet used for bags (presumably LDPE) were gamma irradiated in the presence of oxygen (Kazanjian 1969[38]). Hydrogen was the only significant product, and a value of $G(H_2)=2.2$ was obtained. Oxygen consumption occurred; a value of $G(-O_2)=8.1$ was measured.

Kazanjian (Kazanjian 1976[37]) obtained radiolysis data during the time period when oxygen was being depleted for alpha radiolysis of LDPE bags contaminated with Pu-238 oxide powder (9.0 mg of Pu-238 to 3.6 g of material). The experiment was conducted for a total of 267 days, starting with an air atmosphere. The $G(gas)$ and $G(H_2)$ values calculated from these data show sharp decreases with time from $G(gas)=1.7$ to $G(gas)=0.7$ and $G(H_2)=1.3$ to $G(H_2)=0.7$ after 36 days of exposure. This decrease in G values could have been caused by (1) a very strong dependence of the G values on absorbed dose, (2) much higher G values in the presence of oxygen, or (3) experimental error. The oxygen initially present had been completely depleted by day 21 (5.8E22 eV absorbed energy). The $G(-O_2)$ value was about 3. Only small quantities of CO or CO_2 were detected, with maximum G values of 0.1 and 0.3, respectively.

Polyethylene and polyethylene oxide were gamma irradiated in oxygen in the presence of carbon tetrachloride (Jellinek 1983[15]). In both cases, chloroform was evolved. The G(scission) values

---

[57] Bersch 1959. C. F. Bersch, et al., "Effect of Radiation on Plastic Films," Modern Packaging 32, pp. 117-168, l959.

[58] Arakawa 1983b. K. Arakawa, et al., "Radiation-Induced Oxidation of Polymers. Effect of Antioxidant and Antirad Agent on Oxygen Consumption and Gas Evolution," J. Polym. Sci.: Polym. Chem. Ed. 21, 1983 (preprint).

increased for polyethylene from about 10 in oxygen to about 32 in oxygen mixed with carbon tetrachloride.

G values for various gases evolved from the irradiation of polyethylene when oxygen is present are listed in Table 2.1-27. The maximum measured value of $G(H_2)$ at room temperature when oxygen was present was 3.5, with the exception of Bersch's (Bersch 1959[57]) anomalous measurement of $G(H_2)=5.4$.

2.1.4.1.1.3 Hydrogen G Value for Polyethylene

Even at elevated temperature, almost all of the reported $G(H_2)$ values for polyethylene are less than 4.0. All of the $G(H_2)>4$ values that were found in the technical literature are for experiments conducted prior to 1962. The credibility of the experiments is questionable, as noted in the discussion, or the data were obtained using reactor radiation, where calculation of the absorbed dose is questionable. The available $G(H_2)$ data from alpha radiolysis experiments are in the 1.6-2.4 range. It is concluded that $G(H_2)=4.0$ and $G(flam\ gas)=4.1$ for polyethylene provide upper bound $G(H_2)$ and $G(flam\ gas)$ values for commercial polyethylene materials.

2.1.4.1.2 Polypropylene

Polypropylene has the repeat unit:

$$\text{——} \quad (CH_2\ CH) \quad \text{——}$$
$$|$$
$$CH_3$$
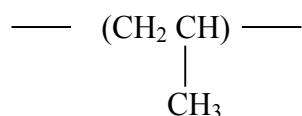
Polypropylene is termed isotactic if the methyl groups are on the same side of the chain, and atactic if the arrangement is random. The isotactic polymer is the more common commercially (Bopp 1963[50]).

Polypropylene may be manufactured into fibers (Herculon[R] is one example) or into molded shapes. Ful-Flo[R] filters used at the RFETS for filtering liquid wastes are made of polypropylene.

The maximum G values for hydrogen and total flammable gas are $G(H_2)=3.3$ and $G(flam\ gas)=3.4$.

2.1.4.1.2.1 Radiolysis of Polypropylene in the Absence of Oxygen

Hydrogen is the major gas produced from the gamma irradiation of polypropylene in a vacuum at room temperature, as shown in Table 2.1-28. Traces of methane and carbon monoxide are also found (Schnabel 1963[59]).

---

[59] Schnabel 1963. W. Schnabel and M. Dole, "Radiation Chemistry of Isotactic and Atactic Polypropylene. I. Gas Evolution and Gel Studies," J. Phys. Chem. 67, pp. 295-299, 1963.

Table 2.1-27 — G Values for Polyethylene (Oxygen Present)

Radiation Type	G(Products)	Comments	Reference
gamma	$G(-O_2)$=10.0, $G(H_2O)$=2.5, $G(CO)$=1.0, $G(CO_2)$=0.6	30°C; only measured gases containing oxygen	(1)
gamma	$G(H_2)$=2.2; $G(-O_2)$=8.1	LDPE bags; room temp	(2)
gamma	$G(gas)$=5.3;$G(H_2)$=3.5; $G(-O_2)$=14.0;$G(CO_2)$=1.3; $G(CO)$=0.6;$G(CH_4)$=0.1	LDPE; room temp; pure material; 20 Mrad	(3)
gamma	$G(gas)$=3.9;$G(H_2)$=2.8 $G(-O_2)$=7.4;$G(CO_2)$=0.9; $G(CO)$=0.2	LDPE; room temp; contained antirad additive; 20 Mrad	(3)
gamma	$G(gas)$=8.6;$G(H_2)$=3.2 $G(-O_2)$=29;$G(CO_2)$=4.1; $G(CO)$=1.3	HDPE; room temp; pure material; 20 Mrad	(3)
gamma	$G(gas)$=5.6;$G(H_2)$=2.2; $G(-O_2)$=12.1;$G(CO_2)$=2.8; $G(CO)$=0.6	HDPE; room temp; contained antirad additive; 20 Mrad	(3)
gamma	$G(gas)$=6.4;$G(H_2)$=5.4; $G(CO_2)$=0.6;$G(CO)$=0.1[a]	LDPE; room temp; commercial material; 5.6 Mrad	(4)
gamma	$G(gas)$=3.9;$G(H_2)$=3.1; $G(CO_2)$=0.6[b]	HDPE; room temp; commercial material; 5.6 Mrad	(4)
gamma	$G(gas)$=2.7;$G(H_2)$=0; $G(CO_2)$=2.7	LDPE; room temp; commercial material; 0.93 Mrad	(4)
gamma	$G(gas)$=8.5;$G(H_2)$=4.0; $G(CO_2)$=3.4;$G(CO)$=1.1	HDPE; room temp; commercial material; 0.93 Mrad	(4)
alpha (Pu-238)	$G(gas)$=1.7; $G(H_2)$=1.3; $G(-O_2)$=3; $G(CO_2)$=0.3; $G(HC)$=0.1[b]	LDPE bags; room temp; water vapor also detected.	(5)

Refs.:   (1) Dole 1973a[56], (2) Kazanjian 1969[38], (3) Arakawa 1983b[58]; (4) Bersch 1959[57]; (5) Kazanjian 1976[37].

Notes: [a]Water vapor, oxygenated hydrocarbons and unsaturated hydrocarbons also were detected.

[b]Calculated from author's data; HC = hydrocarbons; maximum G values are given.

Table 2.1-28 — G Values for Polypropylene (Oxygen Absent)

Radiation Type	G(Products)	Comments	Reference
gamma	G(gas)=2.4-2.9 $G(H_2)$=2.3-2.8, $G(CH_4)$=0.1	vacuum; room temp; actactic and isotactic PP	(1)
gamma	G(gas)=3.0; $G(H_2)$=2.9; $G(CH_4)$=0.1	vacuum; 10 Mrad; room temp; isotactic PP film	(2)
gamma	G(gas)=3.5; $G(H_2)$=3.3; $G(CH_4)$=0.1	vacuum; 10 Mrad; room temp; isotactic PP powder	(2)
gamma	G(gas) 3.2; (95% H_2, 1% CO_2, 1% CO, 3% CH_4)	vacuum; room temp; film	(3)
gamma	G(gas)=3.8; $G(H_2)$=3.2; $G(CH_4)$=0.1[a]	vacuum; 0.1 MGy (10 Mrad); room temp; stabi-lized isotactic PP film	(4)
gamma	G(gas)=3.0; $G(H_2)$=2.8; $G(CH_4)$=0.1[a]	vacuum; 0.2 MGy (20 Mrad); room temp; stabi-lized isotactic PP film	(4)

Refs.:   (1) Geymer 1973[60]; (2) Hegazy 1981a[63]; (3) Krasnansky 1961[54]; (4) Hegazy 1986[61].
Note: [a]Author's G values for gas constituents do not add up to his G(gas) value.

Polypropylene and other polymers have been gamma irradiated in the presence of carbon tetrachloride or chloroform in order to modify the polymer (Ramanan 1981[62]). When polypropylene fibers were immersed in carbon tetrachloride, generated HCl gas was collected by cooling the irradiated ampoules to 77 K and then breaking them under distilled water. The HCl released was estimated by following the change in pH. High yields of HCl were measured (Ramanan 1981[62]).

---

[60] Geymer 1973. D. O. Geymer, "Radiation Chemistry of Substituted Vinyl Polymers. Polypropylene," in The Radiation Chemistry of Macromolecules, Vol. II, Academic Press, New York, 1973, ed. M. Dole.

[61] Hegazy 1986. E. A. Hegazy, et al., "Radiation Effect on Stabilized Polypropylene," Radiat. Phys. Chem. 27, pp. 139-144, 1986.

[62] Ramanan 1981. G. Ramanan, et al., "Gamma Irradiation of Polypropylene Fibers in the Presence of Carbon Tetrachloride," J. Appl. Polym. Sci. 26, pp. 1439-1451, 1981.

2.1.4.1.2.2 Radiolysis of Polypropylene in the Presence of Oxygen

Hegazy (Hegazy 1981a[63]) measured a G value for oxygen consumption of about 4 for oxidative radiolysis of isotactic polypropylene (PP) film at ambient temperature and 150 torr initial oxygen pressure (which approximates the oxygen partial pressure in ambient air). The sum of the G values for production of oxygen containing gases (CO_2 and CO) was less than 0.3, suggesting that most of the consumed oxygen had combined with polymer chains.

Table 2.1-29 lists G values for radiolysis of polypropylene in the presence of oxygen.

Table 2.1-29 — G Values for Polypropylene (Oxygen Present)

Radiation Type	G(Products)	Comments	Reference
gamma	G(gas)=3.0; G(H_2)=2.5; G(CH_4=0.1; G(CO)=0.1; G(CO_2)=0.2, G($-O_2$)=4.2	150 torr O_2 initial pressure; 20 Mrad; room temp; isotactic PP film	(1)
gamma	G(gas)=2.9; G(H_2)=2.6; G(CH_4)=0.1; G(CO)=0.1 G(CO_2)=0.2; G($-O_2$)=5.0[a]	150 torr O_2 initial pressure; 0.2 MGy (20 Mrad); stabilized isotactic PP film	(2)

Refs.:   (1) Hegazy 1981a[63]; (2) Hegazy 1986[61].
Note: [a]Author's G values for gas constituents do not add up to his G(gas) value.

G(scission) values increased for polypropylene from about 5 in oxygen to about 33 in oxygen mixed with carbon tetrachloride vapor (Jellinek 1983[15]); chloroform was evolved.

2.1.4.1.3 Ethylene-Propylene Rubber

G values for ethylene-propylene rubbers (EPR, EPDM) are close to G values for polyethylene and polypropylene (Arakawa 1983b[58], Arakawa 1987[64], Decker 1973[65]).

---

[63] Hegazy 1981a. E. A. Hegazy, et al., "Radiation-Induced Oxidative Degradation of Isotactic Polypropylene," J. Appl. Polym. Sci. 26, pp. 1361-1372, 1981.

[64] Arakawa 1987. K. Arakawa, "Oxygen Consumption and Gas Evolution by Radiation-Induced Oxidation in Ethylene-Propylene-Diene Terpolymers," J. Polym. Sci.: Part A: Polym. Chem. 25, pp. 1713-1716, 1987.

[65] Decker 1973. C. Decker, et al., "Aging and Degradation of Polyolefins. III. Polyethylene and Ethylene-Propylene Copolymers," J. Polym. Sci.: Polym. Chem. Ed. 11, pp. 2879-2898, 1973.

2.1.4.1.4 Polyisobutylene

The repeat unit for polyisobutylene is:

$$\begin{array}{c} CH_3 \\ | \\ \overline{\quad\quad}(CH_2C)\overline{\quad\quad} \\ | \\ CH_3 \end{array}$$
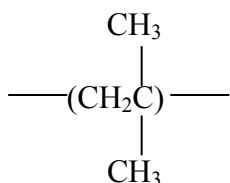
Bohm (Bohm 1982[66]) summarized several radiolysis experiments conducted on polyisobutylene. The composition of the gas evolved from polyisobutylene during gamma radiolysis experiments conducted in vacuum was approximately 95% hydrogen and methane, with the remainder composed of isobutylene and other fragments. Values of $G(H_2)$=1.3-1.6 and $G(CH_4)$=0.5-0.8 have been reported for gamma radiolysis experiments. A G(gas) value of only 0.9 was measured for mixed reactor radiation. Gas production in polyisobutylene is attributed to the fracture of side chains.

2.1.4.2 Radiolysis of Polymers Containing Alcohol Functional Groups

Polymers containing alcohol functional groups include polyvinyl alcohol and polyethylene glycol.

Gas generation from polyvinyl alcohol that was gamma irradiated in a vacuum at 12°C, -78°C, and -196°C was measured by Okada (Okada 1967[67]). Over 99% of the gas evolved was hydrogen. G(gas) values were measured to be 3.1 at 12°C, 2.0 at -78°C, and 1.5 at -196°C (maximum activation energy = 0.6 kcal/g-mole). [The corresponding G(gas) value at 25°C would be unchanged from the value at 12°C because of the low activation energy for gas generation.]

Polyethylene glycol (commercial name, Carbowax), having a molecular weight of 6,000, was irradiated using Co-60 gamma rays in a vacuum at room temperature (Nitta 1959[68]). The maximum G(gas) value measured was 3.5. The gas consisted primarily of hydrogen with some methane, acetylene, and carbon monoxide. Experiments conducted on a 4,000-molecular-weight Carbowax at various temperatures showed only a minor change in the G(gas) value from -196°C to 70°C (2.4 to 2.1) (Nitta 1961b[69]).

---

[66] Bohm 1982. G. Bohm, "Radiation Chemistry," Rubber Chem. Tech. 55, pp. 575-666, 1982.

[67] Okada, 1967. T. Okada, "Radiolysis of Poly (Vinyl Alcohol)," in Annual Report of the Japanese Assn. for Radiation Research on Polymers, Vol. 8, pp. 33-43, 1967.

[68] Nitta 1959. I. Nitta, et al., "Irradiation Effects of Co-60 Radiation on Polyethylene Glycol," in Annual Report of the Japanese Assn. for Radiation Research on Polymers, Vol 1., pp. 320-328, 1959.

[69] Nitta 1961b. I. Nitta, et al., "Effect of Radiation on Polyethylene Glycol," in Annual Report of the Japanese Assn. for Radiation Research on Polymers, Vol. 3, AEC-tr-6372, pp. 445-453, 1961.

2.1.4.3 Radiolysis of Polymers Containing Ether Functional Groups

Polymers containing ether functional groups include cellulose, urea formaldehyde, polyoxymethylene, polypropylene oxide, and polyvinyl formal. The polymers in this group generate gases that contain oxygen, even when irradiated in a vacuum. Another polymer in this group is polyethylene oxide. G values for cellulose and urea formaldehyde have been shown to be strongly dependent on the absorbed dose, at least for gamma radiolysis. For absorbed doses greater than 10 Mrad, the maximum value of $G(H_2)$ is 3.2 for cellulose. One of the polymers in this family (polyoxymethylene) generates other flammable gases that cause the G(flam gas) value to exceed 4.1, and another (polyvinyl formal) has a measured G(gas) that is 1.4 times the G(gas) value for polyethylene. For this reason, polyoxymethylene and polyvinyl formal are permitted in CH-TRU wastes only in trace amounts.

2.1.4.3.1 Cellulose

Cellulose is a linear macromolecule consisting of monomeric units with the empirical formula $C_6H_{10}O_5$. Cellulosic materials commonly present in the CH-TRU wastes include paper, cloth, wood, and Benelex[R], which is composed of wood fiber plus phenolic resin. Other commercial materials that contain cellulosics include cellophane, cellulose acetate (used to manufacture Rayon[R], molded items, paints, coatings), and ethyl cellulose (used to manufacture paints, molded items).

Natural cotton cellulose, having lattice type I, is about 70-80% crystalline and 20-30% amorphous. The other commercially important form of cellulose has lattice Type II, which is commonly referred to as mercerized cotton, and usually consists of regenerated cellulosic materials, paper, and wood products. Cellulose lattice type II is less ordered than cellulose lattice type I and is usually about 60% crystalline.[70] Differences between these types of cellulose may cause differences in the amount and composition of radiolysis gases.

Authors differ as to whether the presence of oxygen affects the radiation chemistry of cellulose. The results of experiments conducted both in the absence and presence of oxygen are summarized at the end of this section.

Sulfite cellulose, dried to a constant weight at 378 K, was irradiated using Co-60 in sealed, evacuated ampules of known volume, as well as in a medium of air and argon (Ershov 1986[71]). The experimental data for each of the media were not reported. The authors stated that the irradiation medium did not appreciably affect the rate at which the products were generated. The dose rate was 20 kGy/h (2 Mrad/h). The volume of gas generated was determined according to the pressure in the ampules. For total absorbed doses from 100-300 kGy (10-30 Mrad) and room temperature, a value of G(gas)=10.2 (31% H_2, 59% CO_2, 9% CO, and 1% CH_4) was observed. At liquid nitrogen temperature of 77 K, a value of G(gas)=6.0 (48% H_2 and 52% CO_2) was observed.

---

[70] Arthur 1970. J. C. Arthur, Jr., "Graft Polymerization onto Polysaccharides," in <u>Advances in Macromolecular Chemistry 2</u>, Academic Press, London, 1970, ed. by W. M. Pasika, pp. 1-87.

[71] Ershov 1986. B. G. Ershov, et al., "Mechanism of the Radiation Chemical Conversions of Cellulose," translated from <u>Khimiya Vysokikh Energii 20</u>, pp. 142-147, 1986.

Concentrations of radiolytically generated carboxyl, carbonyl, and aldehyde groups were measured using thin-layer chromatography for samples of powdered native cellulose that were gamma irradiated in air and in a vacuum (Dziedziela 1984[72]). No gases were measured. Some of the samples were outgassed for four days before irradiation. In all cases, yields of functional groups increased linearly with absorbed dose, indicating constant G values. For each functional group, the samples irradiated in a vacuum display two straight-line portions, with the low-dose part of the graph coincident with the straight line found for irradiation in oxygen. The authors attribute this effect to traces of oxygen from air still left in the samples, in spite of outgassing, and conclude that formation of functional groups occurs according to the same mechanism as in air up to the exhaustion of oxygen absorbed on the surface of the cellulose. For each functional group, the slope of the second line is much lower, indicating a lower G value in the absence of oxygen. The ratio of the G value in air to the G value in a vacuum for each of the functional groups was equal to 3:1.

Cotton cellulose was irradiated under oxygen or nitrogen atmosphere with Co-60 in the dose range 0-130 kGy (0-13 Mrad) (Bludovsky 1984[73]). The yields of the nongas radiolytic products were measured. The samples were analyzed immediately after irradiation to eliminate any effects of reactions occurring after the irradiation. No differences were observed in the qualitative composition of the products between those produced in nitrogen versus those produced in oxygen atmosphere. In all cases the presence of oxygen increased the yields of radiolytic products. The ratios of the yields varied from nearly 1 up to 1.7. The ratio of the chain scission G value in oxygen to the chain scission G value in nitrogen was 1.3.

Arthur (Arthur 1970[70]) reports the G values for gamma irradiation of cotton cellulose I at absorbed doses of 14E20-42E20 eV/g (22-67 Mrad) in vacuum, oxygen, air, and nitrogen atmospheres. The three measurements in a nitrogen atmosphere at different doses show a total absorbed dose effect, with the G(gas) value reduced from 4.5 at 22E20 eV/g (35 Mrad) to 4.0 at 38E20 eV/g (61 Mrad). All of the difference in G values comes from changes in the G(CO) value with absorbed dose. [The ratio of the G values for carbon-containing gases generated in air or oxygen to the values for gases generated in nitrogen at low dose is about 1.4, which agrees with the data of Bludovsky (Bludovsky 1984[73]). However, significant differences were seen in the gas composition.]

In one experiment (Dalton 1963[74]), samples of purified American cotton weighing 0.1-2 g were outgassed at 60°C, and electron irradiation was conducted in a vacuum at ambient temperature. The evolved gas consisted almost entirely of hydrogen. A G value near 2 was obtained at (relatively) high doses (75-400 Mrad), while the G value near 6 was obtained at 0.1 Mrad. A G value of about 3 was obtained at 5 Mrad. As discussed in Section 2.1.2.3.1.5, the dose experienced by plastics or paper irradiated by Pu-238 or Pu-239 alpha particles is at least

---

[72] Dziedziela 1984. W. M. Dziedziela and D. Kotynska, "Functional Groups in Gamma-Irradiated Cellulose," Radiat. Phys. Chem. 23, pp. 723-725, 1984.

[73] Bludovsky 1984. R. Bludovsky, et al., "The Influence of Oxygen on the Radiolytical Products of Cellulose," J. Radioanal. Nucl. Chem. Letters 87, pp. 69-80, 1984.

[74] Dalton 1963. F. L. Dalton, et al., "Gas Yields from Electron-Irradiated Cotton Cellulose," Nature 200, pp. 862-864, 1963.

22-23 Mrad. Therefore, the G value of 6 measured for 0.1 Mrad absorbed dose is not applicable to CH-TRU wastes.

Purified American cotton samples were also irradiated in a vacuum without outgassing, and a gas mixture of 82% H_2, 5% CO, and 13% CO_2 was obtained. A value for G(gas) was not reported for that experiment (Dalton 1963[74]). The difference in the gas composition was attributed to oxidation processes involving residual oxygen dissolved in the material.

Kazanjian (Kazanjian 1976[37]) measured gas consumption and generation from Pu-238 alpha irradiation of both wet and dry Kimwipes[R] (paper tissues). The Kimwipes[R] were cut up, and the plutonium oxide powder was added to the material in increments and the mixture shaken or stirred in a container. The wet Kimwipes[R] contained 11.9 g of water to 4.8 g of paper tissues. The initial atmosphere was air.

G values were calculated using Kazanjian's data for both dry and wet Kimwipes[R]. In both cases, the G values decreased as the dose increased. G(gas) decreased from about 1.1 initially to about 0.5 at 6.0E23 eV for dry Kimwipes[R], and from about 0.6 initially to about 0.3 at 4.5E23 eV absorbed dose for wet Kimwipes[R]. All of the G values were significantly lower for wet Kimwipes[R] compared to the values for dry Kimwipes[R]. This is attributed to some of the alpha decay energy being absorbed by water rather than by the cellulose.

The composition of the evolved gas from wet Kimwipes[R] was richer in hydrogen than for dry Kimwipes[R] (73% vs. 55%) with smaller concentrations of hydrocarbons. The graphs of moles of evolved gas versus time remained approximately linear until oxygen was depleted, then began to decrease in slope. This could be caused by an absorbed dose effect or lower G values in the absence of oxygen.

Zerwekh (Zerwekh 1979[13]) performed alpha radiolysis experiments on two different mixtures of cellulosic materials, one dry mixture and one wet mixture. The dry mixture consisted of paper wipes, paper tissues, embossed paper towel with polyethylene backing, cheesecloth, and cotton laboratory smock material. The final composition of the evolved gas from the dry mixture contained about 60% H_2, 25% CO_2, plus a small amount of CH_4 [estimated from Figure 10 of Zerwekh (Zerwekh 1979[13])]. The initial composition of the evolved gas contained higher concentrations of CO_2, up to a maximum of about 50%. The wet mixture consisted of damp cheesecloth contaminated with Pu-238 as chloride solution. The final composition of the evolved gas contained about 55% H_2 and 35% CO_2 [estimated from Figure 13 of Zerwekh (Zerwekh 1979[13])]. The initial composition of the evolved gas contained about 85% H_2 and 5% CO_2. The high initial concentration of H_2 may indicate that radiolysis of the water dominated early in the experiment, but radiolysis of the cheesecloth dominated near the end of the experiment (1,000 days). G(gas) values for dry cellulosic materials fell to about half of their initial values after about 750 days (1.2E25 eV absorbed energy).

In one of Zerwekh's experiments, gas generation from two identical cylinders was compared, where one cylinder was sampled and the pressure relieved at 15 psig, and the other one sampled and the pressure relieved only when the pressure reached 100 psig. From a plot in Zerwekh 1979[13], the rate of gas pressure buildup in the low-pressure cylinder was about twice the rate of

gas pressure buildup in the high-pressure cylinder. The evolved gases had the same composition, but water was also found in the high-pressure cylinder.

Bibler (Bibler 1976[19]) conducted alpha radiolysis experiments using Cm-244 solution (5-M nitric acid), which was absorbed by paper tissue that was dried and folded to surround the Cm-244 deposit. The evolved gas collected at constant pressure consisted of 49% H_2, 36% CO_2, and 15% CO. The value of G(gas) decreased to G(gas)=0.6 at 2.5E23 eV absorbed dose. A value of G(gas)=1.9 was measured during the first five hours of one experiment, with the first measurement taken at about 4E19 eV absorbed dose. Three different concentrations of Cm-244, up to a factor of 4 difference, were used in the experiments, and all observations appeared to fit the same curve of G(gas) versus absorbed dose.

Kosiewicz (Kosiewicz 1981[12], corrected) measured G(gas) values of about 1.9 at very low absorbed dose and about 1.5 from paper at a total absorbed dose of about 5E23 eV. The G(gas) value decreased to half its initial value after an absorbed dose of about 2.5E24 eV. The radiolytic gas composition was about 61% H_2, 26% CO_2, and 13% CO and nearly independent of total absorbed dose. Oxygen was initially present, but was rapidly depleted. Water vapor was not measured. Typically, 50 g of the material was cut into 1.5- to 3.0-cm squares onto which the finely divided plutonium dioxide (either Pu-239 or Pu-238) was distributed. A second piece of the test material was placed over the first to sandwich the plutonium particles. The sample vessel was a stainless steel cylinder instrumented with a pressure gauge or transducer. The gases in the cylinders were sampled and the pressures relieved when the pressure had increased to 100 kPa over the ambient pressure.

One set of experiments on paper was conducted in an argon atmosphere to measure the initial G(gas) value (at low dose) (Kosiewicz 1981[12], corrected). Data points started at absorbed dose as low as about 0.5E23 eV, for 0.016 Ci of Pu-238 per g of waste. A G(gas) value of 1.4 was estimated. A similar experiment with air as the initial atmosphere reached a maximum G(gas)=1.4 at about 4E23 eV. The first measured value of G(gas) was about 30% lower than the maximum value, probably because oxygen depletion was occurring.

Zerwekh (Zerwekh 1979[13]) measured the rate of gas evolution from mixed cellulosic materials at -13°C, 20°C, and 55°C to be 2.59 kPa/day, 3.45 kPa/day, and 4.93 kPa/day, respectively. The composition of the evolved gas was generally independent of temperature (although the experiment at 55°C also generated a gaseous component of molecular weight about 60). After corrections for thermal expansion of the gas, the activation energy calculated from these data by this author ranges from 0.8 kcal/mole (-13°C, 20°C) to 1.3 kcal/g-mole (20°C, 55°C).

Kosiewicz (Kosiewicz 1981[12]) also performed experiments to measure the temperature dependence of radiolysis of cellulosic materials, represented by paper. High dose rates (640E5 nCi/g) were used so that radiolysis would produce the majority of the gas and other potential modes of gas generation, such as thermal degradation, could be neglected. The rate of gas evolution was measured for experiments conducted at both 20 and 70°C. The higher temperature experiment initially had a rate of gas evolution that was 70% greater than for the lower temperature experiment. The difference in the rate of gas evolution was observed to decrease with increasing dose. At 180E23 eV absorbed dose, the difference had decreased to about 30%.

(The activation energy for a 70% or 30% increase would be 2.1 kcal/g-mole or 1.0 kcal/g-mole, respectively.) The composition of the evolved gases was not significantly different for the two experiments.

Table 2.1-30 presents a summary of G values for several cellulosic materials when oxygen is absent or has been depleted. Table 2.1-31 presents the results of irradiation experiments conducted when oxygen is present.

2.1.4.3.2 Urea-Formaldehyde

Urea-formaldehyde has been examined as a possible solidification medium for power reactor wastes (Colombo 1977[75]). Gamma radiolysis experiments in vacuum were conducted on a urea-formaldehyde formulation using Borden Casco-Resin 2^R that was catalyzed with a 25 wt% solution of sodium bisulfate in water. Measured values of G(gas) and G(H_2) were strongly dose-dependent: at 0.1 Mrad, G(gas)=21 and G(H_2)=4.8; at 1 Mrad, G(gas)=8.6 and G(H_2)=6.5; at 10 Mrad, G(gas)=2.8 and G(H_2)=2.4, and at 100 Mrad, G(gas)=2.0 and G(H_2)=1.3

2.1.4.3.3 Polyoxymethylene

Krasnansky (Krasnansky 1961[54]) measured gas evolution from plastic films exposed to gamma radiation to determine their order of radiation stability. Polyacetyl (polyoxymethane) had a value of G(gas) 8.1 for an absorbed dose of 6 Mrad. For that polymer, the gas consisted of 69% CO_2, 8% H_2, 2% methanol, 15% methane, and 6% dimethyl ether. (The minimum G value for all flammable gases would be about 5.6.)

Dole (Dole 1973d[76]) reported analysis (by gas chromatography) of the gas evolved from electron irradiation of polyoxymethylene at 30°C and 0.1 torr pressure. In addition to hydrogen [G(H_2)=1.7], formaldehyde [G(HCHO)=4], methane [G(CH_4)=0.1], carbon monoxide [G(CO)=0.1] and various oxygen-containing gases were detected. Gases excluded were oxygen, carbon dioxide, C_2 hydrocarbons, methanol, dimethyl ether, and butyl alcohol.

Sobashima (Sobashima 1959[77]) measured G values for gas generation from polyoxymethylene (Delrin 500X from DuPont) exposed to gamma irradiation in vacuum at room temperature. The G(gas) value measured was 14.1 at low doses. The gas composition was the following: 15% H_2, 67% CO_2, 1% CO, 10% CH_4, 1% methyl formate, 2% methyl ether, and 3% other.

---

[75] Colombo 1977. P. Colombo and R. M. Neilson, Jr., "Properties of Radioactive Wastes and Waste Containers, Quarterly Progress Report July-September 1976," Brookhaven National Laboratory Associated Universities, Inc., BNL-NUREG-50617, 1977.

[76] Dole 1973d. M. Dole, "Polyoxymethylene," in The Radiation Chemistry of Macromolecules, Vol. II, Academic Press, New York, 1973, ed. M. Dole.

[77] Sobashima 1959. S. Sobashima, et al., "Irradiation Effects on Polyoxymethylene," in Annual Report of the Japanese Assn. for Radiation Research on Polymers, Vol. 1, AEC-tr-6231, pp. 329-338, 1959.

Table 2.1-30 — G Values for Cellulosic Materials (Oxygen Absent or Depleted)

Material/Radiation Type	G(Products)	Comments	Reference
Sulfite cellulose			
gamma	G(gas)=10.2; G(H_2)=3.2 (31% H_2, 59% CO_2, 9% CO,1% CH_4)	vacuum, air, or oxygen; room temp; 10-30 Mrad	(1)
Cotton cellulose I			
gamma	G(gas)=3.7; G(H_2)=1.3 (35% H_2, 22% CO, 43% CO_2)	vacuum; room temp; 33E20 eV/g (53 Mrad)	(2)
gamma	G(gas)=4.5; G(H_2)=1.0 (22% H_2, 56% CO, 22% CO_2)	nitrogen; room temp; 22E20 eV/g (35 Mrad)	(2)
gamma	G(gas)=4.1; G(H_2)=1.0 (24% H_2, 51% CO, 24% CO_2)	nitrogen; room temp; 32E20 eV/g (51 Mrad)	(2)
gamma	G(gas)=4.0; G(H_2)=1.0 (25% H_2, 50% CO, 25% CO_2)	nitrogen; room temp; 38E20 eV/g (61 Mrad)	(2)
American cotton			
electrons	G(gas) 6; G(H_2)≤6	vacuum + outgassing; room temp; 0.1 Mrad	(3)
electrons	G(gas)~3; G(H_2)~3	vacuum + outgassing; room temp; 5 Mrad	(3)
electrons	G(gas)~2.5; G(H_2)~2.5 (98% H_2, 1% CO, 0.4% CO_2)	vacuum + outgassing; room temp; 25 Mrad	(3)
electrons	G(gas)=2.0	vacuum + outgassing; room temp; 75-100 Mrad	(3)
electrons	G(gas) not reported (82% H_2, 5% CO, 13% CO_2)	vacuum w/o outgassing; room temp; 48 Mrad	(3)
Mixed cellulosics (dry)			
alpha (Pu-238)	G(gas)~0.5; G(H_2)~0.3 (60% H_2, 25% CO_2, 15% misc)[a]	oxygen depleted from initial air atmosphere; room temp; after 1,000 days of exposure	(4)
Cheesecloth (wet)			
alpha (Pu-238)	G(gas)~1.3; G(H_2)~0.7 (55% H_2, 35% CO_2, 10% misc)[a]	oxygen depleted from initial air atmosphere; room temp; after 1,000 days of exposure	(4)
Paper			
alpha (Pu-238, -239)	G(gas)≤1.5; G(H_2)≤0.9 (61% H_2, 26% CO_2, 13% CO)	oxygen depleted from initial air atmosphere; room temp; ≥3E23eV for 50 g material; corrected data	(5)
Paper			
alpha (Pu-238, -239),	G(gas)=1.44	argon; room temp; corrected data	(5)

Refs.:   (1) Ershov 1986[71]; (2) Arthur 1970[70]; (3) Dalton 1963[74]; (4) Zerwekh 1979[13]; (5) Kosiewicz 1981[12], corrected.

Note: [a]Estimated from author's data.

Table 2.1-31 — G Values for Cellulosic Materials (Oxygen Present)

Radiation Type	G(Products)	Comments	Reference
Cotton cellulose I			
gamma	G(gas)=6.2; G(H$_2$)=1.2 (19% H$_2$, 27% CO, 55% CO$_2$)	oxygen; 42E20 eV/g (67 Mrad); room temp	(1)
gamma	G(gas)=5.5; G(H$_2$)=0.7 (13% H$_2$, 60% CO, 27% CO$_2$)	air; 14E20 eV/g (22 Mrad); room temp	(1)
Mixed cellulosics (dry)			
alpha (Pu-238)	G(gas)~1.6; G(H$_2$)~0.6 (40% H$_2$, 40% CO$_2$; (20% misc)[b]	air; room temp first measurement that was taken	(2)
Cheesecloth (wet)			
alpha (Pu-238)	G(gas)~1.6; G(H$_2$)~1.4 (85% H$_2$, 5% CO$_2$, 10% misc)[b]	air; room temp; first measurement that was taken	(2)
Kimwipes[R] (dry)			
alpha (Pu-238)	G(gas)=1.1; G(H$_2$)=0.6 (55% H$_2$, 9% CO, 32% CO$_2$, 3% HC)[a]	air; room temp	(3)
Kimwipes[R] (wet)			
alpha (Pu-238)	G(gas)=0.6; G(H$_2$)=0.4 (73% H$_2$, 5% CO, 22% CO$_2$)[a]		(3)
Paper tissue			
alpha (Cm-244)	G(gas)≤1.9; G(H$_2$)≤0.9 (49% H$_2$, 36% CO$_2$, 15% CO)	air; room temp	(4)

Refs.:   (1) Arthur 1970[70]; (2) Zerwekh 1979[13]; (3) Kazanjian 1976[37]; (4) Bibler 1976[19].

Note: [a]Calculated from author's data.
          [b]Estimated from author's data.

The maximum G value for flammable gases or vapors would be 4.4. The G(gas) values measured at different irradiation temperatures were G(gas)=6.1 at -196°C, G(gas)=9.4 at 20°C, and G(gas)=22.7 at 50°C (Nitta 1961a[78]).

2.1.4.3.4 Polypropylene Oxide

Polypropylene oxide is more susceptible to degradation under irradiation than polypropylene, and yields less hydrogen (Geymer 1973[60]). For irradiation in vacuum, measured G values for H_2, CH_4, and CO were 1.0, 0.1, and 0.3 for atactic polypropylene oxide, and 1.1, 0.1, and 0.4 for isotactic polypropylene oxide, respectively. G values for other oxygen-containing gases were not discussed. Measured G(OH) values were 1.8 for atactic polypropylene oxide and 1.7 for isotactic polypropylene oxide, compared to a value of 4.5 for polyoxymethylene.

2.1.4.3.5 Polyvinyl Formal

Polyvinyl formal was one of the many commercial plastics irradiated by Bopp and Sisman using the Oak Ridge National Laboratory (ORNL) Graphite Reactor (see Section 2.1.4.8 for more details). The value of G(gas) measured for polyvinyl formal was 1.4 times the value of G(gas) measured for polyethylene.

2.1.4.4 Radiolysis of Hydrocarbon Polymers Containing Unsaturated C-C Bonds

Polybutadiene and polyisoprene (Latex[R]) contain unsaturated C-C bonds. The G values for polybutadiene (and copolymers) and polyisoprene (Latex[R]) are given in Table 2.1-32.

Table 2.1-32 — G Values for Polybutadiene (and Copolymers) and Polyisoprene

Material/Radiation Type	G(Products)	Comments	Reference
Polybutadiene and copolymers			
gamma, electrons,	G(gas)≤0.5;	vacuum or air;	(1)
and reactor	G(H_2+CH_4)≤0.5	room temp	
Latex[R] gloves			
alpha (Pu-238)	G(gas)=0.4;G(H_2)=0.4	oxygen depleted; room temp	(2)
Isoprene[R] gloves			
alpha (Pu-238)	G(gas)<0.9;G(H_2)<0.7[a]	oxygen depleted; room temp	(3)

Refs.:   (1) Bohm 1973[79]; (2) Kazanjian 1976[37]; (3) Zerwekh 1979[13].

Note: [a]Estimated from author's data.

---

[78] Nitta 1961a. I. Nitta, et al., "Effect of Radiation on Polyoxymethylene," in Annual Report of the Japanese Assn. for Radiation Research on Polymers, Vol. 3, AEC-tr-6372, pp. 437-443, 1961.

[79] Bohm 1973. G. G. A. Bohm, "Radiation Chemistry of Elastomers," in The Radiation Chemistry of Macromolecules, Vol. II, Academic Press, New York, 1973, ed. M. Dole.

2.1.4.5   Radiolysis of Polymers Containing Ester Functional Groups

Polymers containing ester functional groups include polymethyl methacrylate (PMMA) and polyvinyl acetate. The maximum measured value of G(flam gas) for these two polymers is 2.0.

2.1.4.5.1 Polymethyl Methacrylate (PMMA)

Polymethyl methacrylate has the repeat unit:

$$
\begin{array}{c}
CH_3 \\
| \\
——\ (CH_2C)\ —— \\
| \\
O{=}COCH_3
\end{array}
$$
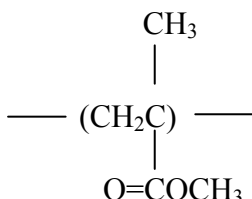
Two common materials made of PMMA are Plexiglas[R] and Lucite[R].

Because PMMA has a high glass-transition temperature (about 106°C), free radicals created within the material at lower temperatures are trapped and can persist days after irradiation. Gases generated from the free radicals are also trapped, and the larger molecular components can be released only by heating the sample (near the glass transition temperature) (Dole 1973c[80]). Even in the absence of oxygen, chain scission dominates. The melting temperature decreases as the absorbed dose increases, from about 140°C at zero dose to about 110°C at 100 Mrad absorbed dose (Jellinek 1978[11]).

G values for PMMA measured using nonalpha irradiation (probably in a vacuum) differ among authors. The main volatile products formed are H_2, CO_2, CO, CH_4, propane, and methyl methacrylate monomer. The individual G values vary depending on temperature and the type of ionizing radiation; and G(gas)<2 (Chapiro 1962[10], Bolt 1963[14]).

Busfield (Busfield 1982[81]) summarized measurements of volatile products from PMMA that was gamma irradiated in vacuum at 30°C. The highest G value for volatile products was 4.1, which included gases and highly volatile liquids including methyl alcohol, dimethyl ether, methyl formate, dimethoxymethane, and methyl acetate. The highest G value for all flammable gases or vapors was 2.2.

Kazanjian (Kazanjian 1976[37]) measured gas generated from alpha radiolysis of 12.8 g of shredded Plexiglas[R] contaminated with 1 g of Pu-239 oxide powder, initially in an air atmosphere. After 100 days of exposure, about half of the remaining gas was replaced with helium, and the experiment continued for an additional 347 days. Calculations were made of

---

[80] Dole 1973c. M. Dole, "Radiation Chemistry of Substituted Vinyl Polymers. Polymers that Primarily Degrade on Irradiation," in The Radiation Chemistry of Macromolecules, Vol. II, Academic Press, New York, 1973, ed. M. Dole.

[81] Busfield 1982. W. K. Busfield, et al., "Radiation Degradation of Poly (Styrene-co-Methylmethacrylate). 2. Protective Effects of Styrene on Volatile Products, Chain Scission and Flexural Strength," Polymer 23, pp. 431-434, 1982.

G values as functions of absorbed dose using Kazanjian's data. G(gas) values appeared to be gradually decreasing with time from about 2 initially to 1.0 at 450 days (5.0E23 eV absorbed dose) with no apparent differences between the two phases of the experiment. The value of $G(H_2)$ fell from 0.4 initially to less than 0.2 in the same time period. The initial G value for oxygen consumption was $G(-O_2) \sim 3.8$. The oxygen was considerably reduced after 19 days but was not completely exhausted.

G values for PMMA are summarized in Table 2.1-33.

Table 2.1-33 — G Values for PMMA

Radiation Type	G(Products)	Comments	Reference
alpha (Pu-238)	very low	oxygen depleted; room temp; Lucite[R]	(1)
alpha (Pu-239)	G(gas)=2.0 (23% H_2, 42% CO, 23% CO_2, 11% CH_4, 2% HC)[a]	oxygen depleted; room temp; Plexiglas[R]	(2)
gamma	G(gas)=4.1; $G(H_2)$=0.3; G(CO)=1.3 $G(CH_4)$=0.6; $G(CO_2)$=0.8; G(vapors)=1.1[c]	vacuum; 30°C; PMMA; worst case of three experiments	(3)
various	G(gas) < 2	vacuum; room temp; PMMA	(4), (5)

Refs.:   (1) Zerwekh 1979[13]; (2) Kazanjian 1976[37]; (3) Busfield 1982[81]; (4) Chapiro 1962[10], (5) Bolt 1963[14].

Note: [a]Calculated from author's data; HC = hydrocarbons.
        [c]Vapors include methyl alcohol, dimethyl ether, methyl formate, methyl acetate, and dimethoxymethane.

2.1.4.5.2 Polyvinyl Acetate

Measurements of G values for gas generation from polyvinyl acetate at 20 Mrad absorbed dose from gamma irradiation in a vacuum are reported by Graessley (Graessley 1973[82]). The value of G(gas) obtained was 1.4. The evolved gas consisted of 64% H_2, 34% CH_4, and 2% CO_2 + CO. Small amounts of acetic acid also were evolved but were not detected in the mass spectrometer analysis.

---

[82] Graessley 1973. W. W. Graessley, "Polyvinyl Acetate," in The Radiation Chemistry of Macromolecules, Vol. II, Academic Press, New York, 1973, ed. M. Dole.

2.1.4.6 Radiolysis of Polymers with Aromatic Characteristics

Polymers having aromatic characteristics include polystyrene, polysulfone, polycarbonate, polyethylene terephthalate and polyesters, and others. These polymers are characteristically low [G(gas) is usually less than 0.8]. Other polymers in this group, for which scant radiolysis data are available, include polyurethane, analine-formaldehyde, styrene-butadiene rubber, phenol-formaldehyde, phenolic resin, epoxy resin, and polyimides.

2.1.4.6.1 Polystyrene

The repeat unit for polystyrene is:

$$\text{———}(CH_2CH)\text{———}$$
$$|$$
$$\text{Aromatic Ring}$$
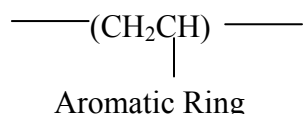
One common material composed of polystyrene is Styrofoam[R]. Polystyrene contains aromatic rings and exhibits the low G values and relatively strong LET effects characteristic of aromatic compounds [G(H$_2$) is 0.2 or less] (Parkinson 1973[83]). Production of very small amounts of methane and benzene by radiolysis has also been observed. Bersch (Bersch 1959[57]) measured G(H$_2$)=0.1 and G(gas)=0.3 for gamma radiolysis of polystyrene in air and G(gas)<0.1 in a vacuum. Busfield (Busfield 1982[81]) reported an even lower value of G(H$_2$)=0.03.

The values of G(scission) increased for polystyrene from about 10 in oxygen to about 45 in oxygen mixed with carbon tetrachloride (Jellinek 1983[15]).

2.1.4.6.2 Polysulfone

G values for polysulfone have been reported for gamma and electron irradiation of several different materials (Giori 1984[84]). The value of G(gas) ranged from 0.01 to 0.1. Hydrogen, methane, carbon monoxide, and carbon dioxide composed most of the gas generated.

2.1.4.6.3 Polycarbonate

Krasnansky (Krasnansky 1961[54]) measured gas evolution from commercial polycarbonate powder exposed to gamma radiation in vacuum. The value of G(gas) calculated from his data was less than 0.8. Most of the gas was carbon dioxide or carbon monoxide. The value of G(H$_2$) was less than 0.012.

Samples of polycarbonates were irradiated in vacuum at room temperature using a Co-60 source.[85] The measured value of G(gas) was 0.9, 97% of which was carbon monoxide or carbon dioxide.

---

[83] Parkinson 1973. W. W. Parkinson and R. M. Keyser, "Radiation Chemistry of Substituted Vinyl Polymers. Polystyrene and Related Polymers," in The Radiation Chemistry of Macromolecules, Vol. II, Academic Press, New York, 1973, ed. M. Dole.

[84] Giori 1984. C. Giori and T. Yamauchi, "Effects of Ultraviolet and Electron Radiations on Graphite-Reinforced Polysulfone and Epoxy Resins," J. Appl. Polym. Sci. 29, pp. 237-249, 1984.

2.1.4.6.4 Polyethylene Terephthalate and Other Polyesters

Commercial polyesters include Dacron^R and Mylar^R. Polyethylene terephthalate (PET) is the polymer on which these materials are based. Oxygen atoms appear in the backbone of the molecule as well as in side branches. One or more aromatic rings occur in the backbone or side branches; consequently, low G values are expected. Table 2.1-34 lists G values for several polyesters. The hydrogen chloride reported by Krasnansky (Krasnansky 1961[54]) that was evolved from polyester III was believed to have resulted from the breakdown of the coating on that material.

Table 2.1-34 — G Values for Polyesters

Material/Radiation Type	G(Products)	Comments	Reference
PET			
gamma, electrons	G(gas)=0.1-0.3; G(H_2)=0.01-0.02 (CO+CO_2=83-90%)		(1)
gamma	G(gas)=0.3; G(H_2)<0.1	air; room temp; 5.6 Mrad	(2)
gamma	G(gas)<0.1	vacuum; room temp; 5.6 Mrad	(2)
Polyester I			
gamma	G(gas)≤0.2; G(H_2)<0.1 (34% H_2, 56% CO_2, 6% HC, 4% other^a)^b	vacuum; room temp; 6 Mrad	(3)
Polyester II			
gamma	G(gas)≤0.8; G(H_2)<0.1 (18% H_2, 82% CO_2)^b	vacuum; room temp; 6 Mrad	(3)
Polyester III			
gamma	G(gas)≤0.2;G(H_2)=0.3 (60% H_2,24% CO_2, 16% CH_4+HCl)	vacuum; room temp; 6 Mrad	(3)

Refs.:   (1) Turner 1973[86]; (2) Bersch 1959[57]; (3) Krasnansky 1961[54].

Notes: ^{a}Other = methyl chloride.

^{b}Calculated from author's data.

---

[85] Amamiya 1959. A. Amamiya and S. Sekigawa, "Irradiation Effects on Polycarbonates," in <u>Annual Report of the Japanese Assn. for Radiation Research on Polymers</u>, Vol 1., pp. 469-476, 1959.

[86] Turner 1973. D. T. Turner, "Radiation Chemistry of Some Miscellaneous Polymers. Polyethylene Terephthalate," <u>The Radiation Chemistry of Macromolecules</u>, Vol. II, Academic Press, New York, 1973, ed. M. Dole.

2.1.4.6.5 Other Polymers Containing Aromatic Rings

Polyphenyl methacrylate produced G values for gamma irradiation in vacuum that were determined to vary from 1.3 for a high molecular weight polymer to 0.7 for a low molecular weight polymer (Raghunath 1983[87]). The majority of the gas in each case was CO. The value of $G(H_2)$ was less than 0.1. Scission of the ester group appeared to be the most important degradation process.

2.1.4.7 Radiolysis of Polymers Containing Halogens

Polymers containing halogen atoms include polymers that also contain hydrogen (e.g., polyvinyl chloride, polychloroprene, chlorosulfonated polyethylene, and polyvinylidene chloride) and polymers that contain no hydrogen (i.e., polytetrafluroethylene and polychlorotrifluoroethylene).

For the polymers containing both halogen and hydrogen atoms, the G values for production of possible gas species, such as HCl, H_2, etc., are strongly dependent on the plasticizers and stabilizers added to the base polymers. Where G values for commercial materials have been measured, these are used for the maximum G values applicable to CH-TRU wastes, rather than G values for the pure polymers. Maximum values are $G(H_2)$=0.7-0.8 and $G(gas)$=3.2.

2.1.4.7.1 Polyvinyl Chloride (PVC)

The repeat unit for polyvinyl chloride (PVC) is:

$$\text{------ } (CH_2CH) \text{ ------}$$
$$|$$
$$Cl$$
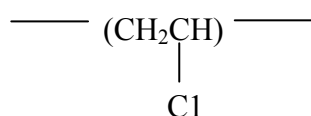
PVC is found in many of the CH-TRU wastes as a packaging material, such as the 10-mil PVC box liner or 10-mil PVC O-ring bag. Various forms of PVC also appear in combustible wastes. PVC and its copolymers are used in electrical components, in Tygon[R] tubing, and in Pylox[R] gloves.

The conventional technique for commercial PVC heat stabilization is the addition of a stabilizer or a combination of stabilizers to the polymer. Most PVC heat stabilizers are organometallic salts containing calcium, zinc, barium, cadmium, or lead. Most traditional stabilizers function as hydrogen chloride acceptors, which reduce the catalytic effect of evolved HCl gas (Kelen 1983[88]).

Brittle polymers such as PVC are usually plasticized to produce flexible films and containers. Tricresyl phosphate, the original plasticizer for commercial PVC, has been replaced by phthalic acid esters, such as dioctyl phthalate (DOP). Plasticizers may be external plasticizers, such as

---

[87] Raghunath 1983. S. Raghunath, et al., "Effect of Co-60 Gamma-Rays on Polyphenyl Methacrylate Obtained by Gamma-ray Irradiation," Radiat. Phys. Chem. 22, pp. 1023-1027, 1983.

[88] Kelen 1983. T. Kelen, Polymer Degradation, Van Nostrand Reinhold Company, New York, 1983.

the phthalates, or internal plasticizers that form copolymers with vinyl chloride, such as vinyl acetate, ethylene, or methyl acrylate. Citric acid esters, epoxidized oils, and dioctyl adipate are substituted for DOP for food packaging materials. Low molecular weight polyesters are also used as nonvolatile plasticizers (Wiley 1986[51]).

A typical Ca/Zn-stabilized PVC compound for food packaging films consists of 100 parts PVC, 30-70 parts plasticizer, 2-3 parts Ca/Zn stabilizer, 1-2 parts epoxidized soybean oil, and 0.1-0.2 part stearic acid. Electrical insulation and jacketing for wires and cables are generally made from PVC formulations that are stabilized by lead (Kelen 1983[88]).

The strong effect of the plasticizers and stabilizers on the radiolysis of PVC is demonstrated by the differences in the composition of the radiolysis gas, which varies from 85% H_2, to 83% HCl, to 70% CO_2 depending on the specific formulation and whether oxygen is present.

2.1.4.7.1.1 Radiolysis of PVC in the Absence of Oxygen

Values of G(HCl) up to 13 at room temperature, increasing to 23 at 70°C, have been reported for electron irradiation in a vacuum of unstabilized Geon 101^R PVC powder (Miller 1959[89]). The evolved gas was collected in a stainless-steel irradiation cell. The PVC powder was outgassed for several hours while the temperature was raised, then the sample was irradiated to doses of 5-20 Mrad. Following irradiation, the cell was allowed to stand for one hour at room temperature, allowing diffusion of the HCl out of the PVC particles to a constant pressure reading. Cooling of the evolved gas into a liquid nitrogen trap showed that at least 95% was condensable and that little or no hydrogen (noncondensable) was formed. The author assumed all of the condensable product was HCl, which is a reasonable assumption for pure PVC that had been thoroughly outgassed before irradiation. For irradiation at 70°C, the irradiation cell was immediately quenched in liquid nitrogen to cool the sample to room temperature in less than 5 minutes, to avoid collecting gas resulting from purely thermal degradation. G values were also measured at low temperatures, down to -145°C. Very little change in the G value occurred between 0 and -145°C. The minimum value of G(HCl) measured was 5.6.

Lawton (Lawton 1961[90]) performed similar experiments involving electron irradiation of Geon 101^R PVC powder and measured values of G(H_2)=0.4 and G(HCl)=0.5 for irradiation at -196°C. He reported a chain dehydrochlorination process that occurred at temperatures as low as -70°C and concluded that Miller's value (Miller 1959[89]) of G(HCl)=5.6 at -196°C was not the true radiation yield.

The gas yield from irradiation of samples of commercial PVC depends strongly on the materials added to the PVC resin, and even on the solvent used to dissolve the resin. Szymanski

---

[89] Miller 1959. A. A. Miller, "Radiation Chemistry of Polyvinyl Chloride," J. Phys. Chem. 63, pp. 1755-1759, 1959.

[90] Lawton 1961. E. J. Lawton and J. S. Balwit, "Electron Paramagnetic Resonance Study of Irradiated Polyvinyl Chloride," J. Phys. Chem. 65, pp. 815-822, 1961.

(Szymanski 1976[91]) reports a value of G(HCl)=8-9 for films prepared by dissolving PVC resin in tetrahydrofuran (THF) and a value of G(HCl)=4-5 for films prepared using cyclohexanone as the solvent. The HCl yield was measured by determining the chloride concentration. Films containing various concentrations of three different stabilizers were prepared using THF, and irradiated with Co-60 gamma radiation at room temperature to a dose of about 3 Mrad. (It is unclear whether oxygen was present during the irradiation.) Addition of 2-3% p-terphenyl or Tinuvin P[R] decreased the value of G(HCl) to 5. Addition of 1% Epidian 5[R] (an epoxy resin) decreased the value of G(HCl) to about 0.3.

Additional experiments were performed using PVC films formulated with 18% DOP (plasticizer) and 1-5% metallic soaps as stabilizers. Values of G(HCl) ranged from 1.7 to nearly 0, with most in the range of 0.3-0.7 (Szymanski 1976[91]). For three of the films, no HCl was detected. The average value of G(HCl) for 19 formulations of plasticized, stabilized PVC was $G(HCl)_{avg}$=0.54. A value of G(HCl) for 18% DOP plasticizer but no stabilizer was G(HCL)=3.1.

Gamma radiolysis of pure PVC powder and plasticized PVC film was studied with and without oxygen present to determine the effects of additives and oxygen on the gases generated (Hegazy 1981b[92]). (His experiments conducted with oxygen present are discussed in Section 2.1.4.7.1.2.) Oxygen consumption and gas evolution were measured by gas chromatography and mass spectrometry. The PVC film contained PVC, DOP, epoxy oil, and Ca-Zn stearate compounds in the ratio of 100/50/5/2. The dose rate was 1 Mrad/hr, and the experiments were conducted at room temperature. In the absence of oxygen, the amount of hydrogen produced as a function of absorbed dose remained linear (constant G value) up to about 80 Mrad absorbed dose. CO_2 and CH_4 production began to decrease at about 30 Mrad absorbed dose.

For pure PVC powder irradiated to 10 Mrad absorbed dose in a vacuum, G values obtained were G(gas)=8.4, $G(H_2)$=0.2, and G(HCl)=8.2. At 60 Mrad absorbed dose, the values were G(gas)=5.2, $G(H_2)$=0.2, and G(HCl)=4.9. The plasticized/stabilized PVC film displayed much lower G values than the pure PVC powder and produced different ratios of gases depending on the absorbed dose. For PVC film irradiated in a vacuum to 10 Mrad absorbed dose, the following G values were obtained: G(gas)=0.3, $G(H_2)$=0.1, and G(HCl)=0.03. At 21 Mrad absorbed dose, the values were G(gas)=0.3, $G(H_2)$=0.2, and G(HCl)=0.03; while at 60 Mrad absorbed dose, the values were G(gas)=1.7, $G(H_2)$=0.2, and G(HCl)=1.4. The increases in G(gas) and G(HCl) with absorbed dose were attributed to degradation of the stabilizers and DOP above 20 Mrad absorbed dose (Hegazy 1981b[92]), probably through reaction with radiolysis products.

---

[91] Szymanski 1976. W. Szymanski, et al., "Increase of Poly (Vinyl Chloride) Stability Towards Ionizing Radiation. II. Effects of Epidian Addition in PVC Films. III. Effects of the Addition of Ethylene Glycol Bis-beta-Aminocrotonate in PVC Foils," Nukleonika 21, pp. 277-283, 1976.

[92] Hegazy 1981b. E. A. Hegazy, et al., "Radiation-Induced Oxidative Degradation of Poly (vinyl Chloride)," J. Appl. Polymer Sci. 26, pp. 2947-2957, 1981.

Rigid PVC films containing stabilizers and anti-oxidants in the range of 0.2-0.5 wt% were gamma irradiated in a vacuum and at various oxygen pressures (Zahran 1985[93]). For a rigid PVC film in a vacuum irradiated to 10 Mrad absorbed dose, G values obtained were G(gas)=2.9, G(H_2)=0.2, and G(HCl)=2.7; while in a vacuum at 20 Mrad absorbed dose, the values were G(gas)=2.6, G(H_2)=0.2, and G(HCl)=2.4 (Zahran 1985[93]). Oxygen consumption and gas evolution were analyzed using gas chromatography.

Arakawa[94] measured gas evolution and oxygen consumption of PVC gamma irradiated at room temperature in a vacuum and in an oxygen environment and used gas chromatography to determine the gas composition. Three samples containing various plasticizers and stabilizers were tested. One sample (model formulated PVC) contained PVC, DOP, tribasic lead sulfate, stearic acid, and clay #33 in the proportions 100/50/5/1/10. The other two samples were of unknown composition but were considered to be representative of insulating materials used for electric cables. All three samples had G(gas) values of 1.4 or less at 20 Mrad absorbed dose. The gas generated from each of the two unknown samples contained 50% or more CO_2. CO_2 generation has also been noted in the thermal degradation of PVC stabilized using basic lead carbonates (Michell 1986[95]).

From these experiments it appears that the plasticizers added to flexible PVC films, in addition to the stabilizers, have a major effect in reducing the G(HCl) value.

Modified PVC, containing 6.5-15.7 mole % N,N-dimethyl dithiocarbamate or 8.3-17.5 mole% N,N-diethyl dithiocarbamate, was irradiated with gamma rays from Co-60 at room temperature under vacuum (Nakagawa 1976[96]). The evolved gases were measured and analyzed with a mass spectrometer. G values were much lower [G(gas)=0.1-0.3] than those measured for pure PVC, and little (if any) HCl was detected. Major peaks in the mass spectra of the gaseous products were measured at mass 28 (CO_2), mass 32, and mass 60. No peaks were reported at mass 2 (H_2) or mass 16 (CH_4).

Kazanjian (Kazanjian 1969[38]) measured radiolysis products from nine samples of PVC bag material used at the RFETS irradiated using a Co-60 gamma source. The measured hydrogen G value was G(H_2)=0.11. The tubes containing the irradiated PVC were opened under water, shaken, and titrated with 0.04-N NaOH to determine the yield of water soluble acid. The acid yield, most of which was HCl, gave G(HCl)=0.21.

---

[93] Zahran 1985. A. H. Zahran et al.,"Radiation Effects on Poly (vinyl chloride) -- I. Gas Evolution and Physical Properties of Rigid PVC Films," Radiat. Phys. Chem. 26, pp. 25-32, 1985.

[94] Arakawa 1986. K. Arakawa, et al., "Radiation-Induced Gas Evolution in Chlorine-Containing Polymer. Poly (vinyl chloride), Chloroprene Rubber, and Chlorosulfonated-Polyethylene," Radiat. Phys. Chem. 27, pp. 157-163, 1986.

[95] Michell 1986. E. W. J. Michell, "True Stabilization: A Mechanism for the Behavior of Lead Compounds and Other Primary Stabilizers Against PVC Thermal Dehydrochlorination," J. Vinyl Technology 8, pp. 55-65, 1986.

[96] Nakagawa 1976. T. Nakagawa and Y. Fujiwara, "Radiation Protection of Poly (vinyl chloride) by N,N-Dialkyl Dithiocarbamate Substitution," J. Appl. Polym. Sci. 20, pp. 753-763, 1976.

Kazanjian (Kazanjian 1976[37]) measured radiolytic gas generation from PVC O-ring bags attached to glove box ports at the RFETS. The bags were cut into pieces and contaminated with PuO_2 powder. Two samples were prepared, one contaminated with 1 g of Pu-239 oxide, the other contaminated with 13.5 mg of Pu-238 oxide. The initial atmosphere was air in each experiment. In both cases, the primary gas produced was hydrogen. Measurements were continued in the Pu-239 experiment after the vessel was partially evacuated to estimate the void volume. No HCl was detected using a mass spectrometer (possibly due to reactions with the stainless steel test vessel or the inlet of the instrument).

G values for hydrogen were calculated from Kazanjian's data for both the Pu-239 and Pu-238 experiments. Taken as a whole, the data are consistent with a value of $G(H_2)$ of about 0.6. At doses above 3E23 eV (about 100 days of exposure), the Pu-238 $G(H_2)$ value appeared to be decreasing slightly.

Kosiewicz (Kosiewicz 1979[97], Kosiewicz 1981[12]) measured gas generated by alpha radiolysis of PVC Pylox[R] gloves. The contaminant, in the form of finely divided powders of PuO_2 (either Pu-239 or Pu-238), was distributed onto squares of the material 2.5-3 cm on a side. A second piece of the test material was placed over the first to sandwich the plutonium. Gases in the cylinders were sampled and the pressures relieved when the pressure had increased to 100 kPa over the ambient pressure of about 77 kPa. The gas composition observed was 85% hydrogen with small amounts of methane, carbon dioxide, and carbon monoxide. No HCl was detected, but it may have been absorbed by the steel cylinder walls or inlet of the measuring instrument. The (Kosiewicz 1981[12], corrected) values of G(gas) were about 0.8 at 20°C for a dose rate of 5E22 eV/day and about 6.3 at 70°C for a dose rate of 3E20 eV/day. The G(gas) value appeared to be increasing with time (Kosiewicz 1979[97]), perhaps indicating depletion of stabilizers or plasticizers was occurring.

Zerwekh (Zerwekh 1979[13]) performed similar experiments using PVC and vinyl Bakelite[R] 0.3-mm thick bag materials used to package wastes removed from glove boxes. The materials were cut into pieces approximately 5 x 5 cm and contaminated with Pu-238 dissolved in 2-M HNO_3. The solution was placed on the materials with a medicine dropper in as uniform a pattern as possible. The solution was allowed to evaporate, and then the test materials were loaded into all-glass systems used to reduce absorption of any HCl generated. Orsat-type gas burets were used to collect the gases produced. The maximum radionuclide contamination level was 62 mg of heat-source grade Pu on 52.5 g of waste (specific activity of about 14 Ci/g). Vinyl Bakelite[R] produced 100 cm^3 of gas in 69 days. The gas contained 4% H_2, 2% CO, 0.9% CO_2, and 0.2% CH_4. No Cl or HCl was detected in the gas using a mass spectrometer, but wet chemical analysis found 0.06% Cl. The PVC bagout material produced only 10 cm^3 of gas in 335 days, containing 0.6% H_2, 0.1% CO, 1.0% CO_2, and 0.1% CH_4. The balance of each sample was oxygen-depleted air. [The final O_2 concentrations were not reported, so the $G(H_2)$ and G(gas) values cannot be calculated from Zerwekh's data.]

---

[97] Kosiewicz 1979. S. T. Kosiewicz, et al., "Studies of Transuranic Waste Storage Under Conditions Expected in the Waste Isolation Pilot Plant (WIPP), Interim Summary Report October 1, 1977--June 15, 1979," Los Alamos National Laboratory, LA-7931-PR.

G values for pure PVC irradiated in a vacuum are listed in Table 2.1-35. HCl is the primary gas produced. Table 2.1-36 lists G values for plasticized or stabilized PVC irradiated in a vacuum or after oxygen depletion.

In most instances, $G(H_2)$ 0.3 at room temperature. The highest value of $G(H_2)$ reported was 0.7 for alpha irradiation. A bounding value at room temperature, therefore, appears to be $G(H_2)_{max} = 0.7$.

Table 2.1-35 — G Values for Pure PVC (in Vacuum)

Radiation Type	G(Products)	Comments	Reference
electrons	G(gas)=G(HCl)=13	30°C	(1)
electrons	G(gas)=G(HCl)=23	70°C	(1)
gamma	G(HCl)=4-9	room temp; 3 Mrad; only HCl detectable by measurement technique	(2)
gamma	G(gas)=8.4; $G(H_2)$=0.2; G(HCl)=8.2	room temp; 10 Mrad	(3)
gamma	G(gas)=8.8; $G(H_2)$=0.3; G(HCl)=8.0	room temp; 20 Mrad	(4)

Refs.:   (1) Miller 1959[89]; (2) Szymanski 1976[91]; (3) Hegazy 1981b[92]; (4) Arakawa 1986[94].

Table 2.1-36 — G Values for Plasticized and/or Stabilized PVC (Oxygen Absent or Depleted)

Material/Radiation Type	G(Products)	Comments	Reference
Films w/stabilizers gamma	G(HCl)=0.3-5	vacuum; room temp; 3 Mrad; only HCl detectable by measurement technique	(1)
gamma	G(gas)=2.9; $G(H_2)$=0.2; G(HCl)=2.7	vacuum; room temp; 10 Mrad	(2)
Films w/stabilizers and plasticizers gamma	G(HCl)=0-1.7 (most 0.3-0.7);$G(HCl)_{avg}$=0.54	vacuum; room temp; 3 Mrad; only HCl detectable by measurement technique	(1)
gamma	G(gas)=0.3; $G(H_2)$=0.1; G(HCl)=0.03[a]; G(CO)=0.1; $G(CO_2)$=0.1	vacuum; room temp; 10-20 Mrad	(3)
gamma	G(gas)=1.4; $G(H_2)$=0.1; G(HCl)=1.2 (8% H_2, 83% HCl, 5% CO, 3% CO_2, 1.2% HC)[b] G(gas)=0.7; $G(H_2)$=0.2; G(HCl)=0.1 (26% H_2, 14% HCl, 8% CO, 50% CO_2, 1.4% HC)[b] G(gas)=1.1; $G(H_2)$=0.2; G(HCl)=0.1 (15% H_2, 8% HCl, 9% CO, 66% CO_2, 2% HC)[b]	vacuum; room temp; 10 Mrad; three different materials	(4)
alpha (Pu-238, -239)	G(gas)=0.7; $G(H_2)$=0.6 (83% H_2, 12% CO + CO_2, 5% HC)[b]	oxygen depleted; room temp; O-ring bags	(5)
alpha (Pu-238)	G(gas)~0.8; $G(H_2)$=0.7 (85% H_2, 2% CH_4, 6% CO_2, 7% CO)[c]	oxygen depleted; 20°C; Pylox[R] gloves; corrected data	(6)
alpha (Pu-239)	G(gas)~6.3; $G(H_2)$=5.3 (85% H_2, 2% CH_4, 6% CO_2, 7% CO)[c]	oxygen depleted; 70°C; Pylox[R] gloves; corrected data	(6)

Refs.: (1) Szymanski 1976[91]; (2) Zahran 1985[93]; (3) Hegazy 1981b[92]; (4) Arakawa 1986[94]; (5) Kazanjian 1976[37]; (6) Kosiewicz 1981[12] (corrected).

Notes: [a]At an absorbed dose of 60 Mrad, G(HCl)=1.4.

[b]HC = hydrocarbons; calculated using author's data.

[c]An increase from G(H2)=0.7 to G(H2)=5.3 between 20°C and 70°C corresponds to an activation energy of 8.1 kcal/mole; see Section 2.1.2.3.1.2.

2.1.4.7.1.2 Radiolysis of PVC in the Presence of Oxygen

Zeppenfeld (Zeppenfeld 1967[98]) irradiated PVC (apparently pure PVC) with Co-60 gamma rays in the presence of oxygen. The HCl formed was absorbed in water and then titrated. The HCl yield as a function of radiation dose was a straight line through the origin, with a G(HCl) value of 46 at about 95°C (estimated from the author's data). Experiments conducted at several different temperatures between about 84 and 119°C yielded an activation energy of 5 kcal/g-mole. The corresponding value of G(HCl) at 25°C would be 9.4.

Pure PVC powder and PVC film containing PVC, DOP, epoxy oil, and Ca-Zn stearate compounds in the ratio of 100/50/5/2 were irradiated at various oxygen pressures (Hegazy 1981b[92]). The dose rate was 1 Mrad/h, and the experiments were conducted at room temperature. At an absorbed dose of 20 Mrad with an initial oxygen pressure of 150 torr (the oxygen partial pressure in ambient air), plasticized PVC again produced much less gas than pure PVC. For pure PVC powder, G values measured were G(gas)=10, G(H_2)=0.1, G(HCl)=8.0, and G(-O_2)=11.3. For PVC film, G values measured were G(gas)=2.4, G(H_2)=0.2, G(HCl)=1.7, and G(-O_2)=6. Corresponding results at an oxygen pressure of 500 torr are: for pure PVC powder, G values measured were G(gas)=20.3, G(H_2)=0.1, G(HCl)=15, and G(-O_2)=29; for PVC film, G values measured were G(gas)=5.9, G(H_2)=0.2, G(HCl)=5.0, and G(-O_2)=11 (Hegazy 1981b[92]).

Rigid PVC films containing stabilizers and anti-oxidants in the range of 0.2-0.5 wt% were gamma irradiated in a vacuum and also at various oxygen pressures (Zahran 1985[93]). At an absorbed dose of 20 Mrad with an initial oxygen pressure of 150 torr, G values for rigid PVC film were G(gas)=6.1, G(H_2)=0.1, G(HCl)=5.9, and G(-O_2)=2.9.

Gas evolution and oxygen consumption were measured for three samples of PVC containing various plasticizers and stabilizers that were gamma irradiated at room temperature with oxygen present (the O_2 concentration was not stated) (Arakawa 1986[94]). The formulations of these samples are discussed in Section 2.1.4.7.1.1. Pure PVC powder was also studied. G(gas) for the pure PVC powder was much higher (21.6) than G(gas) for any of the plasticized/stabilized samples (1.4-5.0). Radiolysis of the model-formulation PVC produced primarily HCl, while the two commercial samples of unknown composition produced primarily CO_2 (as was the case for irradiation in vacuum). Values of G(H_2), however, were consistently between 0.2 and 0.3 for all four PVC samples studied.

Examination of the efficiency in forming a gel fraction in gamma radiolysis of plasticized PVC samples in air led Krylova (Krylova 1979[99]) to conclude that the plasticizers were functioning as anti-rad additives. The plasticizers, containing esters with long hydrocarbon chains, appeared to break down more readily than the PVC base polymer. Energy transfer from the PVC molecules to the plasticizer molecules seemed to be occurring.

---

[98] Zeppenfeld 1967. G. Zeppenfeld and L. Wuckel, "On the Mechanism of the Radiation Oxidation of Poly (Vinyl Chloride)," in Proceedings of the Second Tihany Symposium, Akademiai Kiado, Budapest, 1967.

[99] Krylova 1979. S. V. Krylova, et al., "Effect of Plasticizers on the Behavior of Polyvinyl Chloride in γ-Irradiation," Polym. Sci. 21, pp. 749-757, 1979.

Table 2.1-37 lists G values for PVC irradiated in the presence of oxygen. The highest value of $G(H_2)$ observed for PVC irradiated at room temperature, with or without oxygen present, is $G(H_2)=0.7$.

2.1.4.7.2 Polychloroprene

Neoprene rubber is composed of polychloroprene. G values for polychloroprene are listed in Table 2.1-38.

2.1.4.7.3 Chlorosulfonated Polyethylene

Hypalon[R] gloves are composed of chlorosulfonated polyethylene. Lead oxide is often incorporated into the glove material to provide gamma shielding. Table 2.1-39 provides G values for chlorosulfonated polyethylene (Hypalon[®]).

2.1.4.7.4 Polytetrafluoroethylene (PTFE) and Polychlorotrifluoroethylene

Both polytetrafluoroethylene and polychlorotrifluoroethylene contain no hydrogen in their base polymers. Polychlorotrifluoroethylene has the repeat unit:
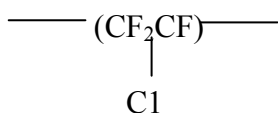
$$\overline{\qquad} (CF_2CF) \overline{\qquad}$$
$$\vert$$
$$Cl$$

Bersch (Bersch 1959[57]) measured gas evolution in air and in a vacuum from gamma radiolysis of two brands of Kel-F[R], which has polychlorotrifluoroethylene as the base polymer. The maximum value of G(gas) calculated from Bersch's data was 1.1 in air versus 0.1 in vacuum. Almost all of the radiolysis gas produced in air consisted of CO_2.

Polytetrafluoroethylene (PTFE) has the repeat unit:

$$\overline{\quad}(CF_2)\overline{\quad}$$

Teflon[R] is a trade name for PTFE. Teflon[R] is similar in structure to polyethylene; however, all of the hydrogen atoms are replaced by fluorine atoms. Differences in the energy relationships between possible chemical reactions lead to the generation of hydrogen gas from polyethylene but no fluorine gas from Teflon[R] (Dole 1973b[100]).

---

[100] Dole 1973b. M. Dole, "Radiation Chemistry of Some Miscellaneous Polymers. Fluoropolymers," in The Radiation Chemistry of Macromolecules, Vol. II, Academic Press, New York, 1973, ed. M. Dole.

Table 2.1-37 — G Values for PVC (Oxygen Present)[a]

Material/ Radiation Type	G(Products)	Comments	Reference
Pure PVC			
gamma	$G(gas)=10.3$; $G(H_2)=0.1$; $G(HCl)=8.0$; $G(CO)=1.0$; $G(CO_2)=1.2$; $G(-O_2)=11.3$	150 torr O_2; 20 Mrad; room temp	(1)
gamma	$G(gas)=21.6^{a}$; $G(H_2)=0.2$ (1% H_2, 85% HCl, 4% CO, 10% CO_2)[b] $G(-O_2)=37.7^{b}$	O_2 pressure not reported[c]; room temp	(2)
Films w/stabilizers			
gamma	$G(gas)=6.1$; $G(H_2)=0.1$; $G(HCl)=5.9$; $G(-O_2)=2.9$	150 torr O_2; room temp	(3)
Films w/stabilizers and plasticizers			
gamma	$G(gas)=2.4$; $G(H_2)=0.2$; $G(HCl)=1.7$; $G(CO)=0.2$; $G(CO_2)=0.2$; $G(-O_2)=6$	150 torr O_2; 20 Mrad; room temp	(1)
gamma	$G(gas)=5.0^{a}$; $G(H_2)=0.3$ $G(HCl)=2.6$ (5% H_2, 52% HCl, 6% CO, 37% CO_2)[b] $G(-O_2)=8.1^{b}$	O_2 pressure not reported; 10 Mrad; room temp	(2)
gamma	$G(gas)=1.4^{a}$; $G(H_2)=0.2$; $G(HCl)=0.2$; (15% H_2, 15% HCl, 17% CO, 51% CO_2, 1% HC)[b] $G(-O_2)=6.9^{b}$	O_2 pressure not reported; 10 Mrad; room temp	(2)
gamma	$G(gas)=1.9^{a}$; $G(H_2)=0.2$; $G(HCl)=0.2$; (10% H_2, 10% HCl, 9% CO, 70% CO_2, 1% HC)[b] $G(-O_2)=6.6^{b\backslash}$	O_2 pressure not reported; 10 Mrad; room temp	(2)
gamma	$G(H_2)=0.11$; $G(HCl)=0.21$	G(HCl) determined from G(acid)	(4)

Refs.:   (1) Hegazy 1981b[92]; (2) Arakawa 1986[94]; (3) Zahran 1985[93]; (4) Kazanjian 1969[38].
Note: [a]See also Kazanjian 1976[37].
         [b]Calculated using author's data.
         [c]Probably ambient pressure (~760 torr).

Table 2.1-38 — G Values for Polychloroprene

Material/ Radiation Type	G(Products)	Comments	Reference
Pure polychloroprene			
gamma	G(gas)=3.5; G(H_2)=0.2 (5% H_2, 93% HCl, 1% CO_2)[a]	vacuum; room temp	(1)
gamma	G(gas)=7.7; G(H_2)=0.3 (4% H_2, 39% HCl, 14% CO, 43% CO_2)[a]	oxygen; room temp	(1)
Commercial Neoprene[R]			
alpha (Pu-238)	G(gas)=0.03; G(H_2)=0.03 (95% H_2, 3% CO_2, 1% CO, 1% CH_4)	oxygen depleted; room temp; corrected data	(2)
alpha (Pu-238)	G(gas)<0.1; G(H_2)<0.1[b]	oxygen depleted; room temp	(3)
gamma	G(gas)=0.2; G(H_2)=0.1 (35% H_2, 16% HCl, 3% CO, 43% CO_2, 3% SO_2)[a]	vacuum; room temp; model compound	(1)
gamma	G(gas)=0.3; G(H_2)=0.1 (29% H_2, 17% HCl, 1% CO, 50% CO_2, 3% SO_2)[a]	vacuum; room temp; special compound	(1)
gamma	G(gas)=0.6; G(H_2)<0.1 (6% H_2, 7% HCl, 8% CO, 79% CO_2)[a]	oxygen; room temp; model compound	(1)
gamma	G(gas)=0.7; G(H_2)=0.1 (17% H_2, 9% HCl, 9% CO, 58% CO_2, 1% CH_4, 6% SO_2)[a]	oxygen; room temp; special compound	(1)

Refs.: (1) Arakawa 1986[94]; (2) Kosiewicz 1981,[12] corrected (3) Zerwekh 1979[13].

Notes: [a]Calculated from author's data.
[b]Estimated from author's data.

Table 2.1-39 — G Values for Hypalon[R]

Material/Radiation Type	G(Products)	Comments	Reference
Pure Hypalon[R]			
gamma	G(gas)=5.0; G(H_2)=0.6 (12% H_2, 42% HCl, 9% CO_2, 37% SO_2)	vacuum; room temp	(1)
gamma	G(gas)=7.8; G(H_2)=0.5 (6% H_2, 62% HCl, 2% CO, 20% CO_2, 10% SO_2)	oxygen; room temp	(1)
Commercial Hypalon[R]			
alpha (Pu-238)	G(gas)=0.15; G(H_2)=0.15 (96% H_2, 1% CH_4, 2% CO_2, 1% CO)	oxygen depleted from initial air atmosphere; room temp; corrected data	(2)
alpha (Pu-238)	G(gas)<0.1; G(H_2)<0.1[a]	oxygen depleted from initial air atmosphere; room temp; dry box gloves	(3)
alpha (Pu-239)	G(gas)=0.4; G(H_2)=0.2; (56% H_2, 42% CO_2, 2% HC)[b]	oxygen present; room temp; Neoprene-Hypalon glove box gloves	(4)
gamma	G(gas)=0.3; G(H_2)=0.3 (90% H_2, 8% CO_2, 2% CO)	vacuum; room temp; model compound	(1)
gamma	G(gas)=0.4; G(H_2)=0.3 (66% H_2, 33% CO_2, 1% CO)	vacuum; room temp; special compound	(1)
gamma	G(gas)=0.5; G(H_2)=0.3 (59% H_2, 31% CO_2, 10% CO)	oxygen; room temp; model compound	(1)
gamma	G(gas)=0.6; G(H_2)=0.3 (52% H_2, 44% CO_2, 4% CO)	oxygen; room temp; special compound	(1)

Refs.:   (1) Arakawa 1986[94]; (2) Kosiewicz 1981,[12] corrected; (3) Zerwekh 1979[13]; (4) Kazanjian 1976[37].
Note: [a]Estimated from author's data.
          [b]Calculated from author's data.

Teflon[R] is one of the most stable polymers with respect to heat, solvents, and most corrosive chemicals. In contrast, this polymer is extremely sensitive to radiation and incurs marked damage to its mechanical properties after relatively low radiation doses.

2.1.4.7.4.1 Radiolysis of PTFE in the Absence of Oxygen

While authors disagree about the details of PTFE radiolysis in the absence of oxygen, they agree that the total gas generation rate is relatively low. Pure PTFE contains no hydrogen, so

radiolysis of commercial Teflon[R] should yield little or no hydrogen-containing gases.
Table 2.1-40 gives G values for PTFE in the absence of oxygen.

Table 2.1-40 — G Values for PTFE (Oxygen Depleted or Absent)

Radiation Type	G(Products)	Comments	Reference
gamma	G(gas)=0.3 for condensable gases	vacuum; room temp	(1)
reactor	(primarily CF_4; no G value given)		(2)
reactor	G(gas)=0.02-0.05 ($CO_2 + CO$)		(2)
alpha (Pu-238)	G(gas)=0.06 (0% H_2, 0.2% CH_4, 16.8% CO_2, 83% CO)	oxygen depleted from initial air atmosphere; room temp; Teflon[R], corrected data	(3)

Refs.:   (1) Dole 1973b[100]; (2) Chapiro 1962[10], (3) Kosiewicz 1981,[12] corrected.

2.1.4.7.4.2 Radiolysis of PTFE in the Presence of Oxygen

Irradiation of PTFE in the presence of oxygen increases the rate of degradation. Gamma irradiation of powdered PTFE resulted in a G value for oxygen consumption of $G(-O_2)$=5. A G value of 3.5 for condensable gases was measured; a large percentage of the gas was carbonyl fluoride. The G value for condensable gases (0.33) for irradiation in a vacuum was much smaller (Dole 1973b[100]).

G(scission) values for PTFE increased from about 7 in oxygen to about 26 in oxygen mixed with carbon tetrachloride vapor (Jellinek 1983[15]). The evolved gas was CCl_3F.

Table 2.1-41 gives G values for PTFE in the presence of oxygen.

Table 2.1-41 — G Values for PTFE (Oxygen Present)

Radiation Type	G(Products)	Comments
gamma	$G(-O_2)$=5, G(gas)=3.5	oxygen present; for condensable gases mostly CF_2O produced

Ref.:   Dole 1973b[100].

2.1.4.7.5 Other Polymers Containing Halogens

Krasnansky (Krasnansky 1961[54]) measured gas evolution from commercial chlorinated polyether film exposed to gamma radiation in vacuum. The value of G(gas) calculated from his data was less than 0.8, with hydrogen composing 86% of the gas and butene 1.4%.

Bersch (Bersch 1959[57]) measured gas evolution in air and in a vacuum from gamma radiolysis of rubber hydrochloride (Pliofilm[R]) and two brands of polyvinylidene chloride. For these polymers, measured G values were much smaller than those for polyethylene [G(gas)$_{max}$=2.1 for polyvinylidene chloride in vacuum], and the evolved gas for the polymers when irradiated in air consisted mostly of CO_2.

2.1.4.8 Radiolysis of Miscellaneous Polymers

Radiolysis experiments have been conducted for a variety of additional polymers and commercial plastics.

2.1.4.8.1 Polyamides

Polyamides include materials, such as Nylon[R], which contain H-N bonds as well as H-C and C=O bonds. Nomex[R], used in filters, is an aromatic polyamide (EPRI 1981[101]). G values for polyamides are summarized in Table 2.1-42. Polyacrylonitrile contains C=N bonds and should also have low G values (see Section 2.1.3.12 for a discussion of structurally-related liquids).

2.1.4.8.2 Ion-Exchange Resins

The vast majority of ion-exchange resins used are synthetic organic resins (Pillay 1986[102]). G values vary, depending on the resin and the ionic form. Pillay (Pillay 1986[102]) reports G values for many different ion-exchange resins. The bounding values are G(gas) 2.1, and G(H$_2$) 1.7 for Zeocarb-215[R] resin (wet) (Mohorcic 1968[103]). Most G(gas) and G(H$_2$) values are much lower. Kazanjian (Kazanjian 1976[37]) obtained a value of G(gas)=0.1 for Dowex-1[R] resin.

2.1.4.8.3 Other Miscellaneous Polymers

Some specialty materials have been developed to be highly sensitive to radiation. These include the poly(olefin sulfone)s, which have very high G values for production of SO_2, hydrogen, and olefins. For example, a value of G(gas) of 71 is reported for polyhexene-1-sulfone (Jellinek 1978[11]). These materials are not used in common commercial plastics.

---

[101] EPRI 1981. Georgia Institute of Technology, "Radiation Effects on Organic Materials in Nuclear Plants," Electric Power Research Institute, EPRI NP-2129, November 1981.

[102] Pillay 1986. K. K. S. Pillay, "The Effects of Ionizing Radiations on Synthetic Organic Ion Exchangers," J. Radioanaly. Nuc. Chem., Articles 97/1, pp. 135-210, 1986.

[103] Mohorcic 1968. G. Mohorcic and V. Kramer, "Gasses Evolved by Co-60 Radiation Degradation of Strongly Acidic Ion Exchange Resins," J. Polym. Sci.: Part C, pp. 4185-4195, 1968.

Table 2.1-42 — G Values for Polyamides

Material/ Radiation Type	G(Products)	Comments	Reference
Polymid MXD-6[R] gamma	$G(gas)=0.1^a$; $G(H_2)<0.1^a$ (75% H_2, 25% CO_2)	vacuum; room temp; 36 Mrad	(1)
Nylon 66[R] gamma	$G(gas)=0.5^a$; $G(H_2)=0.4^a$ (82.5% H_2, 16% CO, 1.5% CO_2)	vacuum; room temp; 36 Mrad	(1)
Nylon 6-6[R] gamma	G(gas) not reported; $G(H_2)=0.4$	vacuum; room temp	(2)
Nylon II[R] gamma	$G(gas)=1.5^a$; $G(H_2)=1.1^a$ (75% H_2, 22.5% CO; 0.5% CO_2; 2% CH_4)	vacuum; room temp; 36 Mrad	(1)
Aromatic polyamide not reported	G(gas) not reported; $G(H_2)=0.01$		(3)

Refs.:   (1) Krasnansky 1961[54]; (2) Dole 1983[104]; (3) Zimmerman 1973[105].
Note: [a]Calculated from author's data.

The radiation stability of various commercial plastics was studied in the 1950s by members of the ORNL by irradiating the materials in the ORNL Graphite Reactor (Bopp 1953[106], Bopp 1955[107], Bopp 1963[50]). The radiation exposure was converted to absorbed dose using the chemical composition of the material. The data as reported in Bopp (Bopp 1963[50]) were arbitrarily scaled up to match a higher G value for polyethylene, indicating some uncertainty in the absolute values. Because of inherent dosimetry problems in these early studies, these data are used only in a qualitative sense to establish the gas generation potential of the materials with

[104] Dole 1983. M. Dole, "Effects of Radiation Environments on Plastics," in The Effects of Hostile Environments on Coatings and Plastics, American Chemical Society, Washington, D. C., 1983, ed. D. P. Garner, pp. 17-24.

[105] Zimmerman 1973. J. Zimmerman, "Radiation Chemistry of Some Miscellaneous Polymers. Polyamides," The Radiation Chemistry of Macromolecules, Vol. II, Academic Press, New York, 1973, ed

[106] Bopp 1953. C. D. Bopp and O. Sisman, "Radiation Stability of Plastics and Elastomers," Oak Ridge National Laboratory, ORNL-1373, July 1953.

[107] Bopp 1955. C. D. Bopp and O. Sisman, "Radiation Stability of Plastics and Elastomers," Nucleonics 13, pp. 28-33, 1955.

respect to polyethylene (one of the materials irradiated). G values obtained from these experiments relative to polyethylene are listed in Table 2.1-43.

Table 2.1-43 — G(gas) Values for Miscellaneous Commercial Plastics (Relative to Polyethylene)

Material	G(gas) Value Relative to Polyethylene[a]
cellulose nitrate	1.5
polyvinyl formal	1.4
polyethylene	1.0
allyl diglycol carbonate	0.6
ethyl cellulose	0.5
methyl methacrylate	0.5
cellulose propionate	0.5
cellulose acetate butyrate	0.4
Nylon[R]	0.4
phenolics (no filler, or cellulosic or mineral filler)	<0.3
urea formaldehyde (cellulosic filler)	0.3
Silastic[R]	0.3
cellulose acetate	0.3
butyl rubber	0.3
natural rubber-butyl rubber mixtures	<0.3
melamine formaldehyde (cellulosic filler)	0.2
Selectron 5038[R] polyester	0.2
natural rubber with fillers	<0.2
natural rubber	0.1
Thiokol ST[R]	0.09
Neoprene[R]	<0.06
casein plastic	0.05
Mylar[R] film	0.05
Plaskon[R] alkyd	0.03
triallyl cyanurate	0.02
aniline formaldehyde	0.01
furane resin (asbestos & carbon filler)	<0.01
polystyrene	<0.01
styrene-butadiene copolymer	<0.01

Ref.:   Bopp 1953[106].
Note: [a]Calculated from author's data.

Only two materials, polyvinyl formal and cellulose nitrate, had higher G(gas) values than polyethylene in the ORNL reactor irradiation experiments. The composition of the evolved gas was not reported. The major use of polyvinyl formal is in heat-resistant nonconductive electrical wire enamels and other coatings (Deanin 1972[108]). Because of its thermal instability, cellulose nitrate does not have wide application in commonly used materials in general commerce, except

---

[108] Deanin 1972. R. D. Deanin, <u>Polymer Structure, Properties and Applications</u>, Chaners Books, Boston, 1972.

in photographic film and lacquers (cellulose nitrate commonly is the film remaining after the volatile constituents have evaporated) (Deanin 1972[108]). As a result, polyvinyl formal and cellulose nitrate will be present in the CH-TRU wastes only in trace amounts.

2.1.5 Radiolysis of Non-Polymer Solids

Other common solid materials in the CH-TRU wastes are solidified liquid wastes, solid organic acids, asphalt, and miscellaneous inorganic materials.

2.1.5.1 Radiolysis of Solidified Liquid Wastes

Solidified liquid wastes include sludges, concretes, and gel-like or monolithic structures that bind liquid wastes so that free liquids are minimized.

2.1.5.1.1 Aqueous Sludges

One common sludge is produced at the RFETS by the neutralization of nitric acid solutions in the plutonium recovery process. The sludge consists of hydroxides of calcium, sodium, potassium, silicon, magnesium, aluminum, iron, and other metals at lower concentrations (Kazanjian 1981[109]). The water and nitrate content of the sludge can vary.

Kazanjian (Kazanjian 1981[109]) conducted experiments on this sludge to determine the radiolytic gas yields as a function of water and nitrate content. The nitrate concentration in the material was determined to be 10.2 wt%, and the water content was 52 wt%. The water content was varied either by drying or adding water to the as-received sludge. Mass spectrometric analysis of the gases evolved under drying conditions showed that the weight loss was essentially all due to water evaporation. In order to examine the effect of the nitrates on gas yields, nitrate salts were removed by washing the sludge with water. All of the experiments were conducted at lowered pressure to permit more accurate analysis of the evolved gases using mass spectrometry.

The experiments were conducted using gamma radiation. The dose rate was 4.45E5 rad/h, except for the 75% water sample, which was irradiated at 3.8E5 rad/h.

The results show that decreasing the water content of the sludge decreases the rate of gas generation. Small amounts of CO and NO_x were also observed. Removing nitrates from the sludge changed the amount and composition of the evolved gas. Oxygen generation was virtually eliminated. Hydrogen evolution in these samples, which contained about 65% water, was up to three times greater than hydrogen evolution obtained from sludge containing nitrate. The measured value of $G(H_2)$ varied from 0.23 to 0.43. [The largest $G(H_2)$ value observed (0.43) is very close to the value of 0.45 for $G(H_2)$ measured for gamma irradiation of liquid water at high pH (see Section 2.1.3.4).] A maximum value of $G(O_2)$ of 0.9 was found in the nitrate sludges from the radiolysis of nitrates. These findings are in agreement with other experiments on the radiolysis of nitric acid and solid inorganic nitrates.

---

[109] Kazanjian 1981. A. R. Kazanjian and M. E. Killion, Results of experiments on radiolytic gas generation from sludge, Rockwell International, Rocky Flats Plant, personal communication.

Sludge from waste water processing at Mound Laboratory, composed primarily of carbon, iron, and calcium compounds, is immobilized in Portland cement (Lewis 1983[110]). A sample of the sludge was contaminated with heat-source plutonium dioxide, consisting of particles averaging 20 microns in size, and mixed with cement. The sludge/cement contained 20 wt% water. The G(gas) value measured was 0.21 (for generated gases only), consisting almost entirely of hydrogen; the G(-O_2) value was 0.13. A small amount of nitrogen was also generated.

Gas generation from cemented caustic waste resulting from immobilization at Mound Laboratory of 1-N NaOH contaminated scrubber solution in Portland cement is reported in Lewis (Lewis 1983[110]). The caustic waste was contaminated with heat-source plutonium in the form of PuO_2 particles averaging 20 microns in size. The caustic/cement waste form contained 22 wt% water. The measured G(gas) value was 0.26, consisting of about equal amounts of oxygen and hydrogen [G(O_2)=0.11 and G(H_2)=0.13]. A small amount of nitrogen was also generated.

2.1.5.1.2 Concretes

The cement-based and other hydraulic binders used for immobilization of wastes require water in their curing reactions. Generally, some excess water remains in the materials in a closed-pore system (Dole 1986[111]). Radiolysis of this unbound water contributes most of the gas generation from within these solidified radioactive wastes.

High-level radioactive sludges at the SRS were simulated using Fe_2O_3, MnO_2, or equimolar mixtures of the two compounds, which were solidified in high-alumina cement (Bibler 1976[19], Bibler 1978[112]). For all tests, the simulated wastes were 40 wt% of the dry cement-waste mixtures. Irradiation of this material with Co-60 gamma rays generated a gas consisting predominantly of hydrogen. The hydrogen pressure reached a steady-state value; higher pressures corresponded to higher dose rates. The equilibrium pressure also depended on the specific material being irradiated, with equilibrium pressures in descending order for Fe_2O_3-cement, neat cement, and MnO_2-cement. In all three cases, oxygen was partially consumed to form hydrogen peroxide, as verified by chemical analysis of the irradiated concrete.

In alpha radiolysis experiments conducted on the same concretes, oxygen was a product as well as hydrogen, composing 20 to 50% of the evolved gas. Up to 200 psi, no steady-state pressure was reached. The average value of G(H_2) was 0.21 (Bibler 1978[112]).

---

[110] Lewis 1983. E. L. Lewis, "TRU Waste Certification: Experimental Data and Results," Monsanto Research Corporation, Mound Laboratory, MLM-3096, September 1983.

[111] Dole 1986. L. R. Dole and H. A. Friedman, "Radiolytic Gas Generation from Cement-Based Waste Hosts for DOE Low-Level Radioactive Wastes," preprint of a presentation at the Symposium on the Effects of Radiation on Materials, Seattle, Washington, June 1986.

[112] Bibler 1978. N. E. Bibler, "Radiolytic Gas Production from Concrete Containing Savannah River Plant Waste," E. I DuPont de Nemours and Company, Savannah River Laboratory, DP-1464, January 1978.

The effect of adding NO_3^- or NO_2^- ions was also examined (Bibler 1978[112]). In low-dose-rate (0.09 Mrad/hr) gamma radiolysis tests, added NO_3^- or NO_2^- did not lead to additional pressurization. O_2 was still consumed, and H_2 was still produced. At the high dose rate (28 Mrad/hr), O_2 was a product, indicating that a different radiolytic process dominates at this dose rate. Also, a steady-state pressure was not reached.

Gas generation from a concrete consisting of a mixture of Portland cement and gypsum-perlite plaster mixed with water in the ratio of approximately 1.7:1 was measured by Bibler (Bibler 1977[26]). The value of G(gas) measured in the gamma radiolysis experiment was 0.03. Hydrogen was the only gas produced. As the hydrogen pressure increased, back reactions occurred to reduce the rate of hydrogen formation, resulting in a steady-state pressure that depended on the dose rate. Oxygen in the air was partially consumed, and nitrogen was unaffected. For the alpha radiolysis tests, Cm-244 was dissolved in the water used to make the concrete, ensuring that the Cm-244 was in direct contact with the elements in the concrete. In four tests with varying amounts of Cm-244, $G(H_2)$ was constant and equal to 0.6, a value 20 times greater than measured in the gamma radiolysis experiment. As with gamma radiolysis, oxygen was partially consumed and nitrogen was unaffected. However, a steady-state pressure was not attained even at about 200 psi of hydrogen.

Bibler (Bibler 1980[113]) conducted a series of alpha radiolysis experiments to study radiolysis of CH-TRU wastes immobilized in concrete, especially incinerator ash. Drying the concrete at 200°C reduced the water content from 35 to 7.4% (80% reduction) but greatly reduced the $G(H_2)$ value from 0.38 to 0.0002. The water remaining was thought to be involved in hydration reactions and not as easily degraded as the free water remaining in the concrete after curing.

The similarity in the radiolysis results for concrete and water led Bibler (Bibler 1977[26]) to conclude that the metal oxides of the concrete do not significantly alter the radiation chemistry of the water, even when the water is incorporated in the concrete. In gamma radiolysis tests, O_2 in the air sealed in the container was partially consumed, while N_2 was unaffected. A steady-state H_2 pressure up to 45 psig was attained. Higher equilibrium pressures were seen for the higher dose rates in the experiment. The values of $G(H_2)$ were measured to be 0.03 for all dose rates.

In the alpha radiolysis experiments on concrete, a value of $G(H_2)$=0.6 was measured, independent of the amount of Cm-244. This $G(H_2)$ value was a factor of 20 times higher than the $G(H_2)$ value measured for gamma radiolysis. As with gamma radiolysis, oxygen was partially consumed while N_2 was unaffected. In contrast to gamma radiolysis, a steady-state pressure was not attained even to about 200 psig H_2.

Tests were also performed (Bibler 1979[23]) to determine if self-absorption of alpha energy would occur when plutonium dioxide particles were added to concrete. The amount of energy absorbed by a particle depends on the size of the particle and its density. The value of $G(H_2)$ was decreased by about a factor of 2 for concrete containing PuO_2 particles having an average size of

---

[113] Bibler 1980. N. E. Bibler, "Radiolytic Gas Generation in Concrete Made with Incinerator Ash Containing Transuranium Nuclides," in Scientific Basis for Nuclear Waste Management, Vol. 2, pp. 585-592, 1980.

2 microns and a density about 80% of the maximum density, compared to concrete containing plutonium dissolved in nitric acid. (The particles may have agglomerated to form larger particles.) The calculated range of the Pu-238 alpha particles (in PuO_2 of the maximum theoretical density of 11.4 g/cm^3) is 11 microns (Bibler 1979[23]).

Bibler (Bibler 1979[23], Bibler 1980[113]) reported gas generation experiments on three types of concrete containing simulated TRU incinerator ash: high-alumina cement, Portland Type I cement, and Portland-pozzolanic cement. Simulated incinerator ash containing primarily CaO and TiO_2 was mixed with dry cement (30 wt% ash, 70 wt% cement). Pu-238 solution was added, and the resulting paste was transferred to a mold and cured to allow 30-40% of the free water to evaporate. $G(H_2)$ values ranged from 0.3 to 0.6. $G(H_2)$ values were unaffected by either dose rate or the pH of the water used to make the concrete. $G(H_2)$ could be decreased by reducing the water content of the concrete and by adding an organic acid (EDTA) to the concrete.

Bibler (Bibler 1979[23], Bibler 1980[113]) conducted further experiments on high-alumina and Portland Type I cements. He determined that addition of NO_3^- or NO_2^- ions to the water used to make the concrete lowered the alpha radiolysis $G(H_2)$ values by a factor of 20 for 6-M NO_3^- or a factor of 2.4 for 3-M NO_2^-. Oxygen was also produced from the concrete containing 6-M NO_3^-, while oxygen was consumed in the concrete containing 3-M NO_2^-.

Radiolysis experiments conducted at 70 and 100°C indicated that $G(H_2)$ for concretes does not increase with temperature below 100°C (Bibler 1979[23], Bibler 1980[113]). In fact, decreases in the hydrogen generation rate were noted, caused by evolution of free water from the concretes.

Bibler (Bibler 1979[23]) also compared $G(H_2)$ values measured for dissolved TRU contaminants versus contaminants present as small particles. When Pu-238 was added as PuO_2, $G(H_2)$ for high-alumina concrete was 0.21 compared to 0.55 determined using dissolved Pu-238. $G(H_2)$ for Portland Type I cement was 0.28 compared to 0.65. The PuO_2 particles used had an initial average size of 2 microns initially but could have agglomerated to larger particles.

Radiolysis of simulated radioactive waste immobilized in cement-based grouts was examined by Dole (Dole 1986[111]). All specimens were cured for 28 days before the radiolysis gases were collected. Some dewatered specimens were dried at elevated temperature for seven days in order to establish the role of the porewater in the production of radiolysis gases. Cm-244 was used as the contaminant in the alpha radiolysis experiments. Two waste streams were simulated: current acid waste and double-shell slurry (DSS) waste. Both waste streams were acidic and contained metal sulfates and nitrates. The cement used was low alumina cement. The authors stated that the gas tightness of their containers was unreliable, and seals were broken as the pressure increased. G(gas) values for the current acid waste samples were estimated that ranged from 0.32 to 0.43 for alpha radiolysis. When samples were dried at elevated temperature following cure, no evolved gas was detected. The DSS samples had much lower G(gas) values of 0.04-0.15 for alpha radiolysis and 0.02 for gamma radiolysis. Gas compositions remaining in the vessels at the end of the tests indicated generation of hydrogen in all of the tests; production of oxygen was reported in all six of the alpha radiolysis experiments using current acid waste. Only

the DSS waste was examined by both alpha and gamma radiolysis, and conflicting data were obtained for the two alpha radiolysis experiments.

Very low G values have been reported from irradiation of water present as the hydrate in crystals (Zagorski 1983[114]). Water in the hydrates appears to exhibit the property of an energy sink. This has been attributed to the presence of a hydrated electron that can absorb energy by changing its state. For example, KOH   0.5 H_2O was irradiated up to 1 MGy absorbed dose without generation of any observable H_2, O_2, or H_2O_2. The authors stated that this concept is also applicable to hydrates of organic materials.

2.1.5.1.3 Adsorbed or Absorbed Liquids

Radiolysis of adsorbed or absorbed liquids indicates that the sorbing medium can either be inert to radiation or can transfer energy to the sorbed liquid. Unless experimental data demonstrate that the binding medium is radiolytically inert (e.g., vermiculite), all of the radiation energy should be assumed to interact with the sorbed liquid.

Bibler (Bibler 1977[26]) reported gamma and alpha radiolysis experiments on octane or a commercial vacuum pump oil sorbed onto vermiculite. Hydrogen was evolved, and oxygen was consumed. $G(H_2)$ was found to vary linearly with the mass fraction of organic material. This suggested that the vermiculite absorbed some of the emitted energy, and it acted as an inert diluent (no energy transfer occurred between the vermiculite and the organic liquid). The extrapolated $G(H_2)$ values for 100% liquid were 3 for octane and 1.6 for oil at high dose rate. At lower dose rates, the $G(H_2)$ values reported were 4.5 for octane and 2.0 for oil. Radiolysis gases were produced in the nominal ratio of $H_2/CO_2/CH_4 = 1.0/0.03/0.01$.

Kinetic studies of water radiolysis in the presence of oxide systems have shown that the exposure of an oxide plus adsorbed water system to gamma radiation can result in energy transfer from the oxide to the water molecules (Garibov 1983[115]). Oxides studied included SiO_2, SiO_2-Al, SiO_2-Ca, Er_2O_3, La_2O_3, and Al_2O_3. Values of $G(H_2)$ measured indicate that the energy transferred from the oxide to the adsorbed water molecules can easily be 3-5 times the energy that is originally absorbed by the water. Very little gas generation was observed from irradiation of silica gel that had been evacuated to remove adsorbed water (Krylova 1967). Lower values of $G(H_2)$ were observed when the silica gel was purified. This effect was attributed to recombination of hydrogen precursors by the organic impurities on the surface of the silica gel.

Garibov (Garibov 1983[115]) also examined the effect of temperature on charge transfer in silica gel. Increasing the temperature at which the sample was irradiated decreased the value of $G(H_2)$ measured. This was attributed to a greater desorption rate of water molecules from the oxide surface, which inhibited effective energy transfer to adsorbed molecules, and to thermal annealing of radiation defects in the oxide phase.

---

[114] Zagorski 1983. Z. P. Zagorski, "Applied Aspects of Radiation Chemistry of Hydrates," in Proceedings of the Fifth Tihany Symposium on Radiation Chemistry, Akademiai Kiado, Budapest, 1983, pp. 331-336.

[115] Garibov 1983. A. A. Garibov, "Water Radiolysis in the Presence of Oxides," in Proceedings of the Fifth Tihany Symposium on Radiation Chemistry, Akademiai Kiado, Budapest, 1983, pp. 377-384.

Vereshchinskii (Vereschinskii 1964[116]) summarized radiolysis experiments conducted on pentane adsorbed on zeolites or silica gel. The observed values of $G(H_2)$ were examined as a function of the electron fraction of pentane when the system pentane-solid was irradiated. The total dose absorbed by the system was used in calculating the $G(H_2)$ value. The results depended to a great extent on the identity of the solids studied. In most cases, more hydrogen was generated than would be expected without energy transfer from the adsorbent to the pentane. The charge transfer appeared to affect only one mono-layer of the absorbed liquid. In contrast, radiolysis of water adsorbed on zeolites indicated that there is no energy transfer in that system (Krylova 1967).

2.1.5.2 Radiolysis of Solid Organic Acids

$G(H_2)$ values for some organic acids that are solid at room temperature have been reported in the range from 1.2 to 2.3 (Bolt 1963[14]). G(gas) values for the same materials range from 1.8 to 4.1. The maximum G value for flammable gas was 2.6. A value of $G(CO_2)$ up to 14 has been reported for one of the organic acids (isobutyric acid) (Spinks 1976[3]).

2.1.5.3 Radiolysis of Asphalt

A value of G(gas) for bitumen (asphalt) for low absorbed dose was estimated to be 1.3, with hydrogen being the primary gas evolved (Kosiewicz 1980[117], corrected). No dependence was seen on temperature from 20 to 70°C. Gamma radiolysis experiments reported by Burnay (Burnay 1987[118]) measured lower G values.

2.1.5.4 Radiolysis of Soil

Gas evolution from plutonium-contaminated soil was reported by Pajunen (Pajunen 1977[119]). The soil was removed from the Z-9 Trench, which had been used as a liquid waste disposal site for the Plutonium Finishing Plant at the Hanford site. The waste solutions were acidic and consisted of aluminum, magnesium, calcium, and other metal nitrate salt wastes; degraded solvents (15% tributyl phosphate or dibutylbutyl phosphate in CCl_4); and other organics, such as solvent washings, fabrication oil, and other waste materials from hood and equipment flushes (Ludowise 1978[120]). The top 30 cm of soil in the trench was mined. The soil moisture content ranged between 0.2 and 25.5 wt%, averaging approximately 5 wt%. Organic content averaged 7.1 wt % with a range of 0.2 to 46.4 wt %. The highest value of G(gas) calculated from Pajunen's data was 1.6, for a soil having a combined organic and moisture content of about

---

[116] Vereshchinskii 1964. I. V. Vereshchinskii and A. K. Pikaev, Introduction to Radiation Chemistry, Israel Program for Scientific Translations, Ltd., Jerusalem, 1964.

[117] Kosiewicz 1980. S. T. Kosiewicz, "Gas Generation from the Alpha Radiolysis of Bitumen," Nuclear and Chemical Waste Management 1, pp. 139-141, 1980.

[118] Burnay 1987. S. G. Burnay, "Comparative Evaluation of and Radiation Effects in a Bitumenisate," Nuclear and Chemical Waste Management 7, pp. 107-127, 1987.

[119] Pajunen 1977. A. O. Pajunen, "Radiolytic Evolution of Gases from Z-9 Soils," Rockwell Hanford Operations, RHO-CD-13, July 1977.

[120] Ludowise 1978. J. D. Ludowise, "Report on Plutonium Mining Activities at 216-Z-9 Enclosed Trench," Rockwell International, Rockwell Hanford Operations, RHO-ST-21, September 1978.

15 wt%. The typical composition of the gas generated by the soils was 50% N_2, 14% O_2, 23% H_2, and 13% CO_2.

Soil samples from Mound Laboratory property were contaminated with heat-source plutonium in the form of PuO_2 particles averaging 20 microns in size (Lewis 1983[110]). Gas generation was measured from a soil sample that contained about 5 wt% water. The G(gas) value was 0.22, with G(H_2)=0.15 and G(CO_2)=0.07. Oxygen was consumed, with G($-O_2$)=0.10.

2.1.5.5 Radiolysis of Dry, Solid Inorganic Materials

Dry, solid inorganic materials do not generate hydrogen gas but may produce other gases (frequently oxygen).

Some common inorganic chemicals used in processing aqueous wastes include ferric sulfate, calcium chloride, and magnesium sulfate. One treatment process produces a precipitate of the hydrated oxides of iron, magnesium, aluminum, silicon, etc. (Kazanjian 1981[109]). Various nitrates and carbonates can also be present (Clements 1985a[121], Clements 1985b[122]).

The yield of nitrite ions is more frequently measured in gamma radiolysis of solid nitrates than is the oxygen yield. For stoichiometric decomposition, a value of G(O_2) should be one-half of the G(NO_2^- value. A value of G(O_2)<1.3 has been determined (Johnson 1970[123]). G values measured for gamma radiolysis of barium, potassium, and sodium chlorates had G(Cl^-)<1.8 and G(O_2)<4.0.

For alkali and alkaline earth perchlorates, values of G(Cl^-)<1.1 and G(O_2)<5.3 were measured. Careful tests were conducted to detect the presence of ozone and free chlorine, but neither of those gases was observed (Johnson 1970[123]).

2.1.6 Comparison of Laboratory G Values With Effective G Values Measured for Drums of CH-TRU Wastes

Actual CH-TRU wastes consist of general laboratory waste (glass, crucibles), combustible materials (paper, plastic), organic shielding materials (Benelex[R], Plexiglas[R]), metals, sludges or concreted wastes, and various other materials. The materials are contaminated with TRU radionuclides in solution (such as dilute nitric acid) or in particle form (such as PuO_2). Typically, several different contaminated materials are present in a given waste container. The G value calculated for actual CH-TRU wastes is an effective G value. All of the radioactivity present in the waste container is assumed to be absorbed by the waste materials, when actually some self-absorption of the alpha decay energy occurs inside particulate contamination.

---

[121] Clements 1985a. T. L. Clements, Jr. and D. E. Kudera, "TRU Waste Sampling Program: Volume I--Waste Characterization," EG&G Idaho, Inc., EGG-WM-6503, September 1985.

[122] Clements 1985b. T. L. Clements, Jr. and D. E. Kudera, "TRU Waste Sampling Program: Volume II--Gas Generation Studies," EG&G Idaho, Inc., EGG-WM-6503, September 1985.

[123] Johnson 1970. E. R. Johnson, <u>The Radiation-Induced Decomposition of Inorganic Molecular Ions</u>, Gordon and Breach Science Publishers, New York, 1970.

The following discussion is applicable to RH-TRU waste forms as well, given the similar physical and chemical forms of the waste. While RH-TRU wastes have higher gamma and beta radiation emissions, G values are expected to be lower than the maximum values discussed in this appendix. Since data exist primarily for CH-TRU waste containers, a discussion of these data is included below.

Effective G values have been measured for drums of actual CH-TRU wastes. On the whole, the effective hydrogen G values are much lower than maximum hydrogen G values for the waste forms based on the material in the waste form with the highest G value. For drums of combustible wastes, the maximum $G(H_2)$ value determined in controlled experiments was 2.1 versus a possible value of 4.0 based on laboratory experiments. For drums of sludge, the maximum $G(H_2)$ value measured was 0.3 versus a possible value of 1.6 based on laboratory experiments.

Sources of information for gas generated from actual CH-TRU wastes include examinations of drums retrieved from storage at the Idaho National Engineering and Environmental Laboratory (INEEL) (Clements 1985a[121]) and at LANL (Warren 1985[124], Clements 1985a[121]), and experiments measuring gas composition and pressure for newly generated drums of wastes at the RFETS (Clements 1985b[122], Kazanjian 1985[125]), at LANL (Clements 1985b[122], Zerwekh 1986[126]) and at the SRS (Ryan 1982[127]).

2.1.6.1 Retrieved Drums of CH-TRU Wastes

G values for radiolytic gas production from unvented retrieved drums can only provide lower limits, because of uncertainties in the rates at which gases can permeate through the drum gaskets or diffuse through gaps between the gaskets and sealing surfaces. [Tests conducted at INEEL indicate that drums will vent when pressurized above 20 psig (Clements 1985a[121]).] Only gas in the drum headspace was sampled, and the concentrations of generated gases could have been higher inside the waste bags.

A total of 209 waste containers (199 drums) of wastes that originated at the RFETS were retrieved from storage at INEEL (Clements 1985a[121]). A sample of the headspace gas in each drum was taken and analyzed. Internal pressure and void volume for gas accumulation were measured, and the containers were opened and the wastes examined. All but seven of the waste drums had been sealed with nonporous styrene-butadiene gaskets.

---

[124] Warren 1985. J. L. Warren and A. Zerwekh, "TRU Waste-Sampling Program," Los Alamos National Laboratory, LA-10479-MS, August 1985.

[125] Kazanjian 1985. A. R. Kazanjian, et al., "Gas Generation Results and Venting Study for Transuranic Waste Drums," Rockwell International, Rocky Flats Plant, RFP-3739, 1985.

[126] Zerwekh 1986. A. Zerwekh and J. L. Warren, "Gas Generation and Migration Studies Involving Recently Generated Pu-238-Contaminated Waste for the TRU Waste Sampling Program," Los Alamos National Laboratory, LA-10732-MS, July 1986.

[127] Ryan 1982. J. P. Ryan, "Radiogenic Gas Accumulation in TRU Waste Storage Drums," E. I. du Pont de Nemours & Co., Savannah River Laboratory, DP-1604, January 1982.

A lower limit for the hydrogen G value was calculated (by this author) for each of the drums using reported alpha activity, void space, pressure, time since drum closure, and hydrogen concentration in the headspace. Almost all of the drums had minimum $G(H_2)$ values less than 1.0. Those that had minimum $G(H_2)$ values greater than 1.0 and activity greater than 0.1 Ci (the specific activity of Pu-239 is 0.07 Ci/g) are listed in Table 2.1-44.

One possible source of a high apparent G value is that the time period for gas generation may have been underestimated. The storage times are based on the dates the drums were sealed, while wastes may have been placed into the drum weeks or months prior to the closure date. Four of the drums had calculated effective G values of 6.0 or higher. These include one drum of combustibles and three drums of cemented sludges and solutions containing organic complexing chemical wastes.

Solidified liquid organic wastes, including cemented sludges and solutions and organic sludges, will not be transported until more information is available on their potential for hydrogen (or other flammable) gas generation.

Combustible waste Drum No. 76-02898 had a calculated $G(H_2)$ value of 6.0, which is above the bounding laboratory value of 4 (at room temperature). The most probable explanation for the high calculated $G(H_2)$ value is that the drum contained a significant amount of Am-241. Drum No 76-02898 was lead-lined, a procedure necessary when Am-241 is present in higher concentration than in usual weapons-grade plutonium. This was the only one of the combustible waste containers that was lead lined. The original assay listed 32 g Pu and no Am. A second assay, conducted on a NaI system using a 100-second count (not long enough to measure americium) listed 29 g Pu and no Am. Reassay records showed a measurement of 29 ± 16.3 g Pu.

Drums of CH-TRU wastes were also retrieved at LANL, but those drums had been closed with a gas-permeable sponge-rubber gasket. All of the LANL drums were at ambient pressure, demonstrating that flow or diffusion of gases through the porous gasket had occurred.

2.1.6.2 Newly Generated Waste Experiments

Experiments on newly generated wastes have been conducted at RFETS, LANL, and SRS.

2.1.6.2.1 Rocky Flats Environmental Technology Site Experiments

The gas generated inside each of 16 drums of newly generated wastes contaminated with weapons-grade plutonium was measured over a 13-week period as the second phase of a two-phase experiment (Clements 1985b[122], Kazanjian 1985[125]). Wastes were assayed as individual packages or by radiochemical analysis to determine total alpha activity. In Phase I, the drums were vented for three months using one of three potential venting devices (a filter, a semi-permeable gasket, or a Hanford vent clip). Drum pressure and gas concentrations in the drum headspaces were measured. At the conclusion of Phase I, the drums were purged with air, and a gas sample was taken to obtain the initial gas composition for the second phase of the study. In all cases the plug in the lid of the rigid liner was left out, so that the rigid liner was not a primary barrier for gas escape.

Table 2.1-44 — Data for RFETS Retrieved Waste Drums with G(H$_2$)$_{min}$ > 1.0^{a,b}

ID No.	Waste Form	Activity (Ci)	Time (days)	Gauge Pressure (mmHg)	Void Vol. (l)	Gas Composition						Minimum G Values			
						H$_2$	O$_2$	N$_2$	Ar	CO$_2$	HC	G(H$_2$)	G(CO$_2$)	G(HC)	G(gas)
22-01194	Combustibles	0.30	276	2.0	181	0.4	18.8	79.2	0.9	0.2	0.3	1.0	0.6	0.7	2.3
02-39371	combustibles^c	1.78	245	28.5	182	2.1	0.1	96.5	1.1	0.0	0	1.1	0	0	1.1
02-39465	combustibles	0.74	227	-19.0	179	0.9	17.2	79.4	0.9	1.1	0.3	1.1	1.3	0.3	2.7
02-39195	combustibles	0.15	307	-36.0	168	0.3	12.5	83.3	0.9	2.1	0.3	1.4	8.4	1.2	10.9
744-3829	cmt s&s	0.16	263	13.5	77	0.8	1.7	95.0	1.1	0.8	0.1	1.7	0.2	0.3	2.1
76-01642	spc slud	0.74	880	-43.0	151	7.5	5.6	85.2	1.0	0.0	0.6	1.9	0	0.2	2.1
76-02898	combustibles	2.15	326	87.5	171	18.2	0.0	64.6	0.8	15.2	0.8	6.0	5.0	0.2	11.3
744-3841	cmt s&s	0.15	256	5.4	76	2.7	2.8	91.8	1.1	0.0	0.3	6.3	0	0.6	6.9
744-3837	cmt s&s	0.17	256	5.5	38	6.2	0.2	90.7	1.1	0.0	0	6.4	0	0	6.4
744-2389	cmt s&s	0.20	4439	154.0	162	32.4	0.1	64.2	0.8	0.0	2.3	8.6	0	0.6	9.2

Notes: [a]cmt s&s = cemented sludges and solutions consisting of organic complexing chemical wastes; spc slud = an uncemented sludge packaged in polyethylene bottles inside a drum; HC = hydrocarbons.

[b]Ambient pressure at RFETS is about 613 mmHg; ambient pressure at INEEL is about 640 mmHg.

[c]Contained Ful-Flo^R (polypropylene) filters coated with grease.

The drum lids were sealed to the drums using Permatex Form-a-Gasket[R]. The drums were pressure tested and considered to be sealed if they held a pressure of 155 torr above atmospheric pressure for 3 hours with a pressure loss of no more than 5 torr. Two of the drums developed leaks of 41 torr and 28 torr. These values were not considered in determining the gas generation rates. The drum pressure and gas composition of samples taken from the drum headspace were recorded weekly. Gas compositions were determined by mass spectrometry.

While no gas samples were taken from inside the waste bags, the gas generation rates calculated from the drum headspace samples should give the gas generation rates inside the waste bags. In these experiments, hydrogen generated inside the inner waste bags had permeated through the layers of plastic in the drum into the drum headspace, and the hydrogen concentration increased linearly with time. When this occurs, the hydrogen concentrations in the inner waste bags, drum liner bags, and drum headspaces are all increasing at the same rate.

The G values for hydrogen, carbon dioxide, hydrocarbons, and total gas were calculated for each of the drums in the cited reports. Plots of hydrogen gas production versus time that are shown in the reports appear linear, indicating that absorbed dose effects were minimal. The G values so obtained are listed in Table 2.1-45. Figure 2.1-1 shows Ar, CO_2, H_2, hydrocarbons, and isopropanol partial pressures as functions of time for a drum containing leaded rubber gloves (Figure #16 in Table 2.1-45). (The isopropanol is attributed to the Permatex Form-a-Gasket[R] material.)

The high values of $G(H_2)$ for the organic setup waste form (solidified organics) are much greater than the $G(H_2)$ values of less than 3 that have been measured for oils. The radionuclide content of the drums was confirmed by reassaying samples of the sludge. The authors (Clements 1985b[122], Kazanjian 1985[125]) suggested that corrosion of the mild steel drum could be responsible for the high rate of hydrogen production. Corrosion can produce hydrogen gas in an anaerobic, wet atmosphere, which were the conditions inside each of the two drums after the first week of the experiment.

The relatively large amounts of CO_2 generated in several of the drums could have been caused by microbial action or chemical reactions. Measured $G(H_2)$ values for combustibles (maximum of 2.1) are all well within the maximum G value of 4 at room temperature established in Section 2.1.4. Measured $G(H_2)$ values for inorganic sludges (maximum of 0.3) are much lower than the maximum $G(H_2)$ value of 1.6 for water.

Table 2.1-45 — Effective G Values for RFETS Newly-Generated Waste Drums

Fig #	Waste Form Description	Effective G values			
		H$_2$	CO$_2$	HC	Total
1	inorganic sludge	0.30	0.01	--	0.31
2	inorganic sludge	0.28	0.01	--	0.29
3	inorganic sludge	0.19	0.01	--	0.92[a]
4	inorganic sludge	0.16	0.01	0.02	0.19
5	organic setup	15.1	0	--	15.1
6	organic setup	22.5	0	--	22.5
7	dry combustibles	2.1	1.6	--	3.7
8	dry combustibles	1.4	1.3	0.9	3.6
9	dry combustibles	0.79	0.47	--	1.26
10	dry combustibles	0.39	5.1	--	5.49
11	wet combustibles	0.74	0.17	--	0.91
12	wet combustibles	0.52	0.28	0.25	1.05
13	plastic & rubber	1.1	2.2	--	3.3
14	plastic & rubber	0.65	0.77	--	1.42
15	leaded rubber	0.32	6.4	--	6.72
16	leaded rubber	0.95	0.49	0.07	1.51

Notes: [a]Includes G(O$_2$)=0.72. All other G(O$_2$)s were negative.
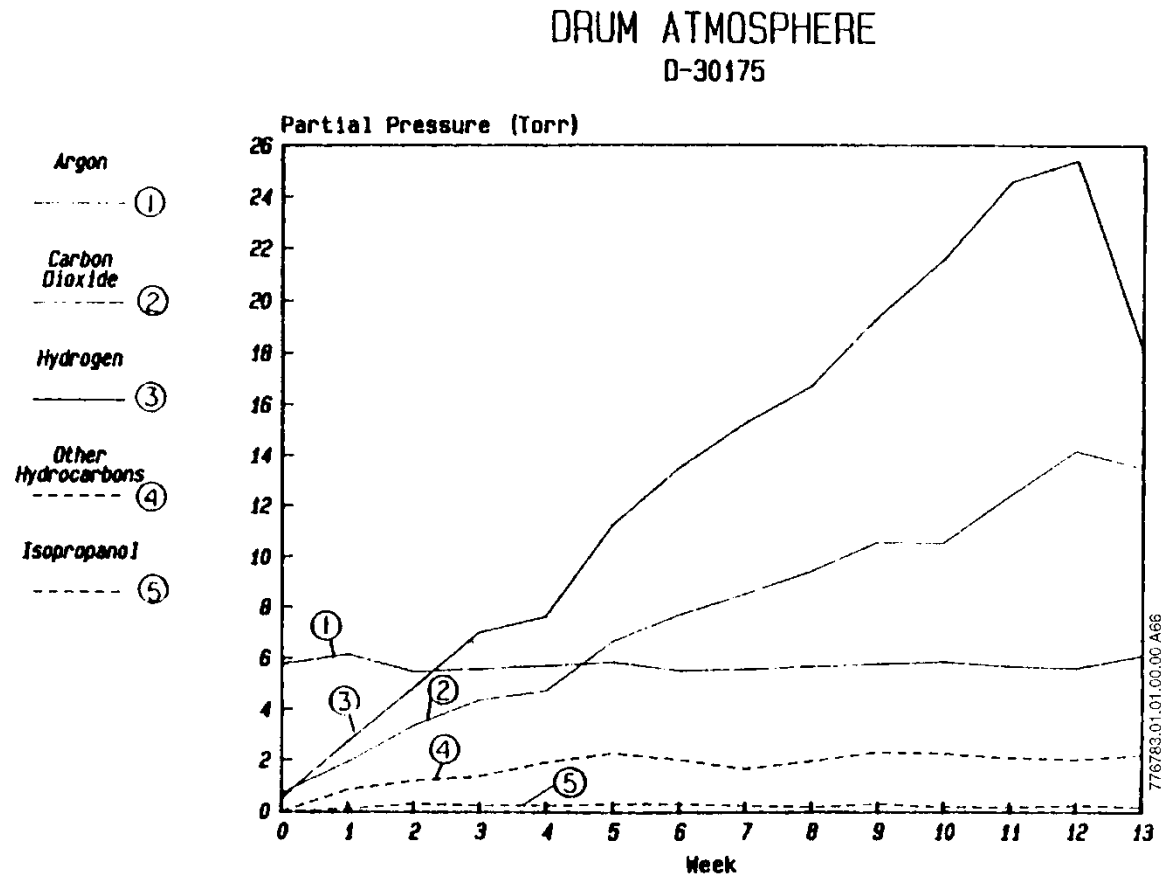
Figure 2.1-1 — Partial Pressures of Various Gases in a Drum of Newly-Generated Waste from RFP (Leaded Rubber Gloves)

2.1.6.2.2 Los Alamos National Laboratory Experiments

In the LANL experiments, six high-activity newly generated Pu-238 waste drums were examined to determine gas generation rates and the ability of filters to limit the hydrogen concentration in the drum. Two additional drums of wastes provided information on the permeation of hydrogen through the 90-mil high-density polyethylene rigid liner. The experiments were separated into the same two phases as the RFETS experiments.

All of the drums selected contained combustible materials. Each waste package within the drum was individually assayed using segmented gamma scan techniques, and the assay results for the individual packages were added to obtain the total activity. The wastes had been generated from three to eight months before the gas generation phase of the experiments began.

Gas generation data for five of the six drums of waste for which void volumes could be measured are listed in Table 2.1-46. An ambient atmospheric pressure at Los Alamos of 579 mm Hg was assumed for all cases. (Actual ambient pressures were obtained for sampling dates, but using those pressures did not reduce the scatter of the measurements.)

No observable decrease in G values appeared to occur in these experiments until after about 100 days into the experiment (for wastes that had been generated three to eight months before the experiments began). In another 200 days, the G values had dropped to about one-half of their initial values. A plot of gas yields versus time for drum BFB-116 is shown in Figure 2.1-2. The composition of the generated gas was 46% CO_2, 41% H_2, 12% CO, and 1% CH_4, comparable to the gas composition measured in laboratory radiolysis experiments on Hypalon[R] or Neoprene[R].

2.1.6.2.3 Savannah River Site Experiments

SRS initiated a series of experiments in 1976 to acquire data on drum pressures and gas compositions under actual storage conditions at SRS (Ryan 1982[127]). Four drums were filled with highly contaminated material consisting of typical SRS waste. Data were collected on a monthly basis for over four years. The waste materials were contained in plastic bags that were placed within a 90-mil-thick high-density polyethylene liner. The liner was sealed with an adhesive. The drum lids were locked on over a neoprene-butadiene O-ring gasket (specified to be nonporous), with a galvanized ring bolt. While sealing compound was used to hold the gasket in place on the drum lid, no adhesive was applied to the lower surface of the gasket. Valves and airtight bulkhead fittings were connected to each drum wall before the drums were filled with waste. A detailed inventory and radioactive material assay were conducted of each bag of waste materials. The test drums were placed in concrete culverts. The culverts, 7-ft high by 7-ft dia. cylindrical containers with 6-in. thick walls, were designed to contain 14 drums of waste in two tiers of seven. The culvert lids were grouted in place and sealed with epoxy.

About 100 days after the experimental drums had been filled with waste and sealed, the drums were placed into the culvert. Two thermocouple wires were included in the instrumentation, one attached to the drum that contained the greatest amount of radioactivity (Drum No. 122), the other suspended in the culvert to read the air temperature. Ryan (Ryan 1982[127]) reported most of the temperature data only for outside air. Where data were available, the drum surface

Table 2.1-46 — Effective G Values for LANL Newly-Generated Waste Drums[a]

Drum No.	Waste Form Description	Pkg.	Dates Start	End	^{238}Pu g	Ci	Void Vol.[c] l	Effective G Values Initial H2	Total	Final H2	Total
BFB-112	plastic, leaded gloves	7/28/83	4/10/84	2/22/85	1.2	16.8	198.1	0.3	0.6[b]	0.1	0.3
BFB-114	plastic, rags	9/23/83	12/29/83	3/30/84	15.6	218.4	201.1	0.4	0.7	0.1	0.6
BFB-116	leaded gloves	10/27/83	4/10/84	2/22/85	2.28	31.9	210.3	0.2	0.5[b]	0.1	0.2
BFB-118	rags, plastics, metals, metal oxides	10/27/83	4/10/84	1/29/85	4.92	68.9	201.3	0.4	0.8[b]	0.2	0.4
BFB-120	leaded gloves	1/03/84	8/10/84	3/06/85	1.6	22.4	215.6	0.2	0.4	0.1	0.3

Notes: [a]Calculated using authors' data; Drum BFB-113 has been omitted because of the scarcity of data in the sealed condition.

[b]Initial G values apply to the first 100 days of the 300-day experiment.

[c]Void volume for drum BFB-114 is the volume inside the rigid liner; other void volumes include the void between the rigid liner and the drum.
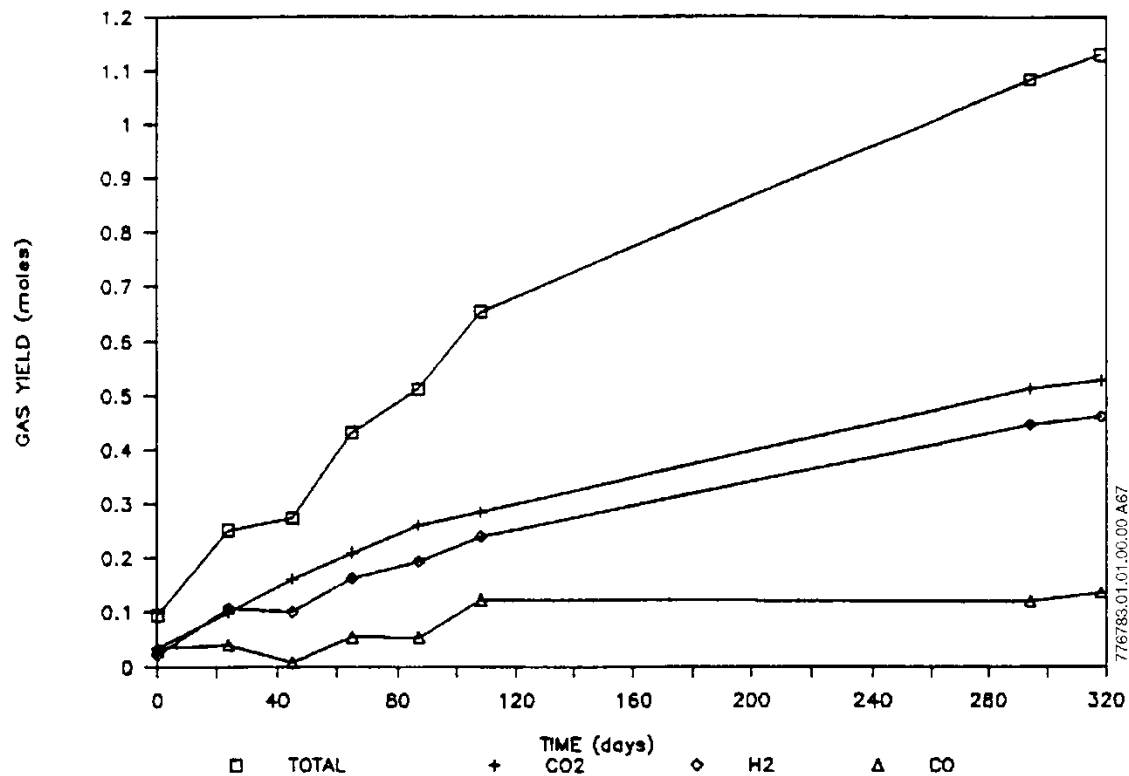
Figure 2.1-2 — Gas Yields vs. Time LANL Drum BFB-116 (Leaded Rubber Gloves)

temperature typically was no more than 5°C different from the outside air temperature, although one measurement showed a difference of 12°C.

The first gas samples were drawn 101 days after the drums were sealed. Subsequent samples were taken about every 30 days. The composition of ambient air was determined as part of the standardization of each gas analysis and was, on the average, 79% N_2, 21% O_2, and 0.1% CO_2. [The 1% Ar that is present in ambient air was not reported.]

Ryan (Ryan 1982[127]) plotted drum gas concentrations versus time and drum gauge pressures versus time. The gas composition of the culvert atmosphere was also measured. The largest hydrogen concentration measured in a culvert air sample was about 0.7 mole %. No appreciable hydrogen concentration was measured inside the culvert until day 993. Ryan stated that a significant quantity of gas was escaping from the drums at all times. This conclusion appears to be based on the maximum G values calculated from the largest (or close to largest) increases in the amounts of gas present, and then extrapolating the pressures from those G values. Ryan concluded that G(gas) appeared to be at least equal to 1.0 and more likely about 2.0.

Ryan's data (concentrations for each gas species, air temperature, gauge pressure, drum void volume, activity, and sampling date) were entered onto a spreadsheet that calculates moles of gas and G values as functions of time. Drums 119 and 121 appear to have leaked, while drums 120 and 122 could have been well sealed, at least for most of the four-year period. Plots of gauge pressure and total moles of gas present are shown in Figures 2.1-3 and 2.1-4 for drum 122. The cyclical behavior of the gauge pressure versus time plot corresponds to annual temperature variations.

Figure 2.1-5 shows a plot of $G(H_2)$ versus time, with the points chosen by Ryan checked. The plot illustrates the variability in the experimental data. The greatest slope of the curve (ignoring wide swings in the data) occurs at the beginning of the experiment, with $G(H_2)_{max}$=0.2. Similar evaluations performed for the other three drums show that the G values appear to be much less than 1, in agreement with laboratory data for the radiolysis of rubber.
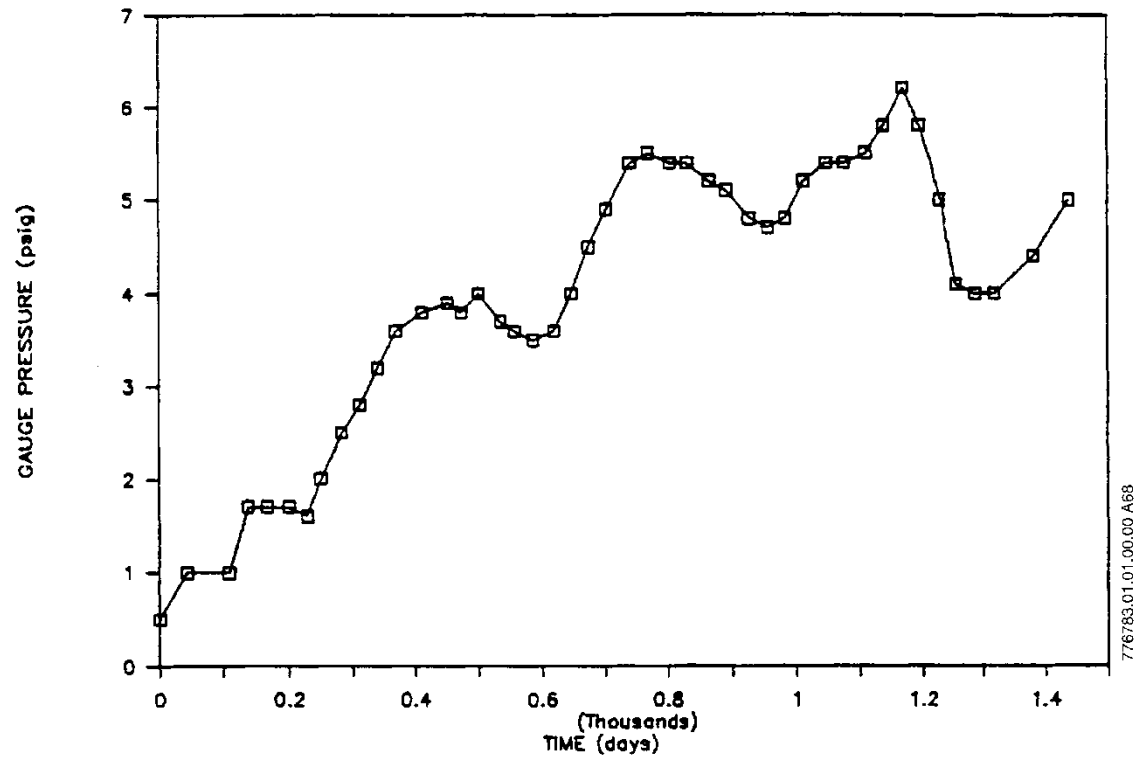
Figure 2.1-3 — Gauge Pressure in Drum 122 vs. Time
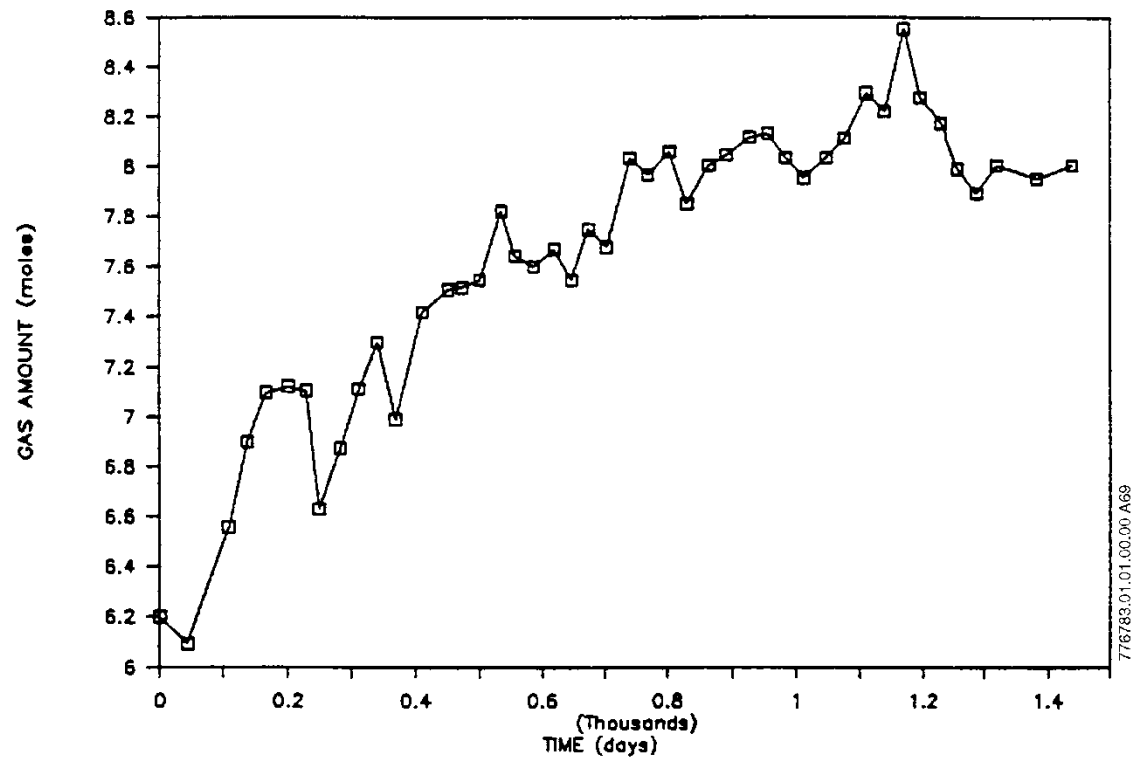
Figure 2.1-4 — Moles of Gas Present in Drum 122 vs. Time
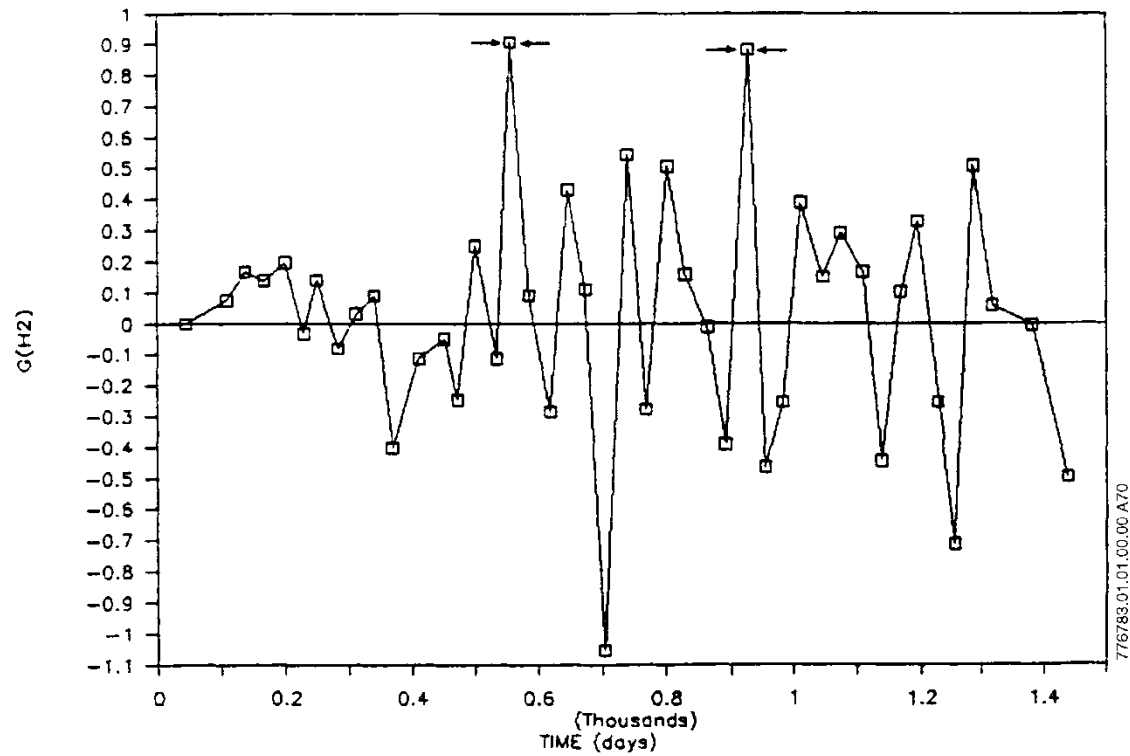
Figure 2.1-5 — G(H$_2$) vs. Time for Drum 122

This page intentionally left blank.

Attachment A
Chemical Properties and Commercial Uses of Organic Materials

Executive Summary

Almost all of the materials that are potential generators of gas from radiolysis are organic materials (water and inorganic materials containing water being the primary exceptions). These organic materials are hydrocarbons or their derivatives containing oxygen, nitrogen, halogens, or other atoms. Naturally occurring organic materials that are present in the CH-TRU wastes, such as cellulose, also may generate radiolytic gas.

Basic families of organic liquids are described in Section A1.1. Polymers and their use in commercial materials are discussed in Section A1.2. Section A1.3 illustrates structural features of many commercial polymers.

A1.1 Families of Organic Liquids

Common names for families of organic liquids are: the hydrocarbons [alkanes (paraffins), alkenes (olefins), alkynes, cyclic hydrocarbons, and aromatic hydrocarbons]; the oxygenated organic compounds [ethers, esters, alcohols, aldehydes, ketones, and organic acids]; and the organic derivatives of ammonia (called amines). Compounds having the same formula but different structures and properties are called isomers (Pierce 1970[1]). (Higher-molecular-weight members of these families may be solids at room temperature rather than liquids.)

Hydrocarbons, as the name implies, contain only hydrogen and carbon atoms. Except for methane (CH_4), the carbon atoms form chains that consist of two or more atoms. The main chain may also contain side branches of atoms.

The alkanes are saturated hydrocarbons in which only carbon-carbon single bonds occur. All of the alkane names end in "-ane," such as methane, ethane, propane, and butane. In the petroleum industry, a high-temperature process called cracking of the saturated hydrocarbons causes the molecules to separate into fragments that then recombine at random to form other hydrocarbons and hydrogen gas. The alkanes are used as fuels to generate energy by oxidation (combustion). The addition of halogens forms such compounds as carbon tetrachloride, chloroform, trichloroethylene, hydrogen chloride, and other halogenated compounds.

The alkenes (olefins) are unsaturated hydrocarbons that contain double carbon-carbon bonds. All of the names of the alkenes end in "-ene," such as ethene, propene, and butene. Many of the olefins polymerize, forming macromolecules having gram molecular masses on the order of 10^4 to 10^6.

In the alkynes, the double bond of the alkenes is replaced by a triple carbon-carbon bond. Acetylene is one of the common alkynes.

---

[1] Pierce 1970. J. B. Pierce, <u>The Chemistry of Matter</u>, Houghton Mifflin Company, Boston, 1970.

Cyclic hydrocarbons may be alkanes (such as cyclohexane), alkenes, or alkynes. All of the cyclic alkanes have saturated carbon-carbon bonds.

Aromatic hydrocarbons contain a benzene ring and include benzene, toluene, naphthalene, and xylene. Aromatic compounds may be formed by joining benzene rings together through the elimination of hydrogen, for example, biphenyl (two benzene rings). Naphthalene is an example of a condensed-ring structure and is used in the manufacture of alkyd resins. A hydrogen atom on a benzene ring can be replaced by other chemical species through halogenation, sulfonation, or nitration. Toluene is formed by replacing one of the hydrogen atoms in benzene by a methyl (CH_3) group. Xylene is formed by replacing two of the hydrogens by methyl groups. The location of the substituted groups determines the isomer (ortho, meta, para). Phenol is formed by adding a hydroxyl group (OH) to the benzene molecule and is used in the formation of Bakelite® plastics and glues.

Organic compounds may also contain oxygen. The oxygen atoms may be bonded between carbon atoms to form ethers or esters. Oxygen atoms may bond to single carbon atoms to form alcohols (ROH), ketones (RCOR'), aldehydes (RCOH), or carboxylic acids (RCOOH).

Individual alcohols are named by adding the suffix "-ol" to the name of the corresponding alkane, such as "methanol." Several different isomers of alcohols are possible as the number of carbons in the chain increases, such as in propanol and butanol. More than one hydroxyl (OH) group may be present in the molecule, such as for ethylene glycol and glycerol.

Aldehydes are formed by oxidation of alcohols which have an hydroxyl group on a terminal carbon atom. The simplest aldehyde is formaldehyde. It reacts with phenol and urea to form phenol-formaldehyde and urea-formaldehyde resins.

Ketones are formed by oxidation of a secondary alcohol. The simplest ketone is acetone.

The organic (carboxylic) acids contain the group -COOH attached to either an alkyl or an aryl group. Examples of these acids are formic acid, acetic acid, oleic acid, and oxalic acid. Long-chain organic acids are called fatty acids.

The reaction of a carboxylic acid with an alcohol produces an ester (RCOOR') plus water. Common names for esters end in "-ate." When there are no double or triple bonds between the carbon atoms, the materials are solids; otherwise, they are liquids at room temperature. Esters of low molecular mass are used as solvents, artificial flavors, and components in perfumes. Waxes contain esters formed by the reaction of long-chain acids and alcohols. Fatty-acid esters of glycerol are found in vegetable oils and animal fats. The less volatile esters (such as dioctyl phthalate) are commonly used as plasticizers. The reaction of fats with boiling sodium hydroxide solution forms soaps.

Amines are organic derivatives of ammonia. Amines are used in the production of polyamides, such as Nylon®. Proteins are also polyamides.

A1.2 Polymers

Polymers are natural or synthetic materials that are composed of very large molecules containing repeating structural units called monomers. The structural features of many commercial polymers are shown in Section A1.3.

Knowledge of the repeat unit can aid in interpreting or predicting the gases generated by radiolysis (or thermal degradation). Additives also can affect the gas generation potential of commercial materials made from polymers. Polymers composed of more than one kind of repeat unit are termed copolymers.

Various additives are combined with the base polymer or polymers in compounding to produce the final commercial composition and properties of a plastic. Liquid plasticizers are added to polymers such as polyvinyl chloride (PVC) or cellulose esters to increase their flexibility. These compounds are chosen for their relatively low volatility but may be lost from a material that is heated or aged for long periods of time. Plasticizers in PVC commonly compose about 30-40% of the total material. Most of the plasticizers are less solvent- and chemical-resistant than the polymer to which they are added. Many plasticizers may be extracted by oils or dry-cleaning solvents. Most of the plasticizers are combustible, and lower the flame resistance and softening points of the total composition (Deanin 1972[2]).

Stabilizers are added to the polymer to increase resistance to heat, ultraviolet light, or other forms of degradation. Most plastics contain antioxidants, which may be consumed eventually by chemical reactions with oxygen. Polymers that crosslink are often rendered quite sensitive to oxidative degradation by radiation. The use of effective antioxidants can significantly improve their radiation resistance. Materials added to obtain other desirable properties could result in a final product which is less radiation resistant than the base polymer. However, this does not appear to happen often. Inorganic fillers are usually effective in increasing radiation resistance by dilution of the base polymer (EPRI 1981[3]).

Organic phosphates and halogenated compounds are frequently added to polymers to increase their flame resistance. At the same time, these additives may decrease thermal and other types of stability, particularly if they contain organic halogen compounds (Deanin 1972[2]).

The CH-TRU wastes consist of commercial materials, containing plasticizers and stabilizers that can affect radiolytic gas production (both the composition and amount of gas). For this reason, maximum G values measured for commercial materials provide more realistic upper bounds for radiolytic gas generation than do the G values measured for pure polymers.

Chain lengths on the order of a hundred thousand monomer units are not uncommon in polymers (Sisman 1963[4]). Branched or network structures may be present. Most linear commercial

---

[2] Deanin 1972. R. D. Deanin, <u>Polymer Structure, Properties and Applications</u>, Chaners Books, Boston, 1972.

[3] EPRI 1981. Georgia Institute of Technology, "Radiation Effects on Organic Materials in Nuclear Plants," Electric Power Research Institute, EPRI NP-2129, November 1981.

[4] Sisman 1963. O. Sisman, et al., "Polymers," in <u>Radiation Effects on Organic Materials</u>, Academic Press, New York, 1963, eds. R. O. Bolt and J. G. Carroll.

polymers have a small amount of branching caused by impurities in the starting material or side reactions during the polymerization process. Polymers may be amorphous, crystalline, or contain regions of each. The linear polymers are used in a wide variety of molded and extruded objects. The solubility of linear polymers in solvents permits their use as paints, coatings, and films. Other applications include fibers, fabrics, tires, hoses, and gaskets.

Polymers are useful as electrical and thermal insulators. The rigidity and hardness of cross-linked polymers have been utilized in molded objects, which can be produced economically by thermally initiating cross-linking reactions within the mold. Polymers having network structures are generally insoluble. They have a strong tendency to retain their shape through rubber-like elasticity in materials with a low density of cross links or through high rigidity and hardness in heavily cross-linked materials (Sisman 1963[4]).

Table A1.2-1 lists the families of plastics (Dean 1987[5]). Cross-references of commercial names with the base polymers are available in Desk-Top Data Bank (1977[6], 1979[7], 1980[8]).

A1.2.1 Acetals

Acetal homopolymers are prepared from formaldehyde and consist of high-molecular-weight linear polymers of formaldehyde. They are among a group of high-performance engineering thermoplastics that resemble Nylon® in appearance (but not in properties). Trade names include Delrin® and Celcon®. Prolonged exposure to elevated temperatures results in the liberation of increasing amounts of formaldehyde. Acetals have relatively low radiation stability (Harper 1975[9]). Major applications for polyoxymethylene (an acetal) are in business machines, automotive gears and bearings, plumbing fittings, such as tub assemblies, and in consumer articles, such as aerosol containers (Deanin 1972[2]).

---

[5] Dean 1987. J. A. Dean, Handbook of Organic Chemistry, McGraw-Hill Book Company, New York, 1987.

[6] Desk-Top Data Bank 1977. Desk-Top Data Bank, Elastomeric Materials, The International Plastics Selector, Inc., San Diego, 1977.

[7] Desk-Top Data Bank 1979. Desk-Top Data Bank, Films, Sheets, and Laminates, The International Plastics Selector, Inc., San Diego, 1979.

[8] Desk-Top Data Bank 1980. Desk-Top Data Bank, Commercial Names and Sources for Plastics and Additives, The International Plastics Selector, Inc., San Diego, 1980.

[9] Harper 1975. C. A. Harper, Handbook of Plastics and Elastomers, McGraw-Hill Book Company, New York, 1975.

Table A1.2-1 — Families of Plastics

Acetals
Acrylics
      Polymethyl methacrylate (PMMA)
      Polyacrylonitrile (PAN)
Alkyds
Alloys
      Acrylic-polyvinyl chloride alloy
      Acrylonitrile-butadiene-styrene-polyvinyl chloride alloy (ABS-PVC)
      Acrylonitrile-butadiene-styrene-polycarbonate (ABS-PC)
Allyls
      Allyl-diglycol-carbonate polymer
      Diallyl phthalate (DAP) polymer
Cellulosics
      Cellulose acetate resin
      Cellulose-acetate-propionate resin
      Cellulose-acetate-butyrate resin
      Cellulose nitrate resin
      Ethyl cellulose resin
      Rayon$^{®}$
Chlorinated polyether
Epoxy
Fluorocarbons
      Polytetrafluoroethylene (PTFE)
      Polychlorotrifluoroethylene
      Perfluoroalkoxy (PFA) resin
      Fluorinated ethylene-propylene (FEP) resin
      Polyvinylidene fluoride
      Ethylene-chlorotrifluoroethylene copolymer
      Ethylene-tetrafluoroethylene copolymer
Polyvinyl fluoride
Melamine-formaldehyde
Melamine phenolic
Nitrile resins
Phenolics
Polyamides
      Nylon$^{®}$s
      Aromatic Nylon$^{®}$s
Polyamide-imide
Polyaryl ether
Polycarbonate
Polyesters
      Polyethylene terephthalate (PET)
      Unsaturated polyesters

Table A1.2-1 — Families of Plastics (Concluded)

Polyimide

Polymethyl pentene
Polyolefins
      Low-density polyethylene (LDPE)
      High-density polyethylene (HDPE)
      Ultrahigh-molecular-weight polyethylene
      Polypropylene
      Polybutylene
      Polyallomers
Polyphenylene oxide
Polyphenylene sulfide
Polyurethanes
Silicones
Styrenics
      Polystyrene
      Acrylonitrile-butadiene-styrene (ABS) copolymer
      Styrene-acrylonitrile (SAN) copolymer
      Styrene-butadiene copolymer
Sulfones
      Polysulfone
      Polyether sulfone
      Polyphenyl sulfone
Thermoplastic elastomers
Urea-formaldehyde
Vinyls
      Polyvinyl chloride (PVC)
      Polyvinyl acetate (PVAC)
      Polyvinylidene chloride
      Polyvinyl butyrate
      Polyvinyl formal
      Polyvinyl alcohol

Ref: Dean 1987[5].

A1.2.2 Acrylics

Polyacrylates are derivatives of acrylic acid. They are frequently used as coatings or paints. Polyethyl acrylate is used as a component of synthetic rubbers in which resistance to oils and high temperatures is important (Bopp 1963[10]). Polymethyl methacrylate (PMMA), a related compound, has common trade names of Plexiglas® and Lucite®. Acrylics are also made into fibers and fabrics, such as Orlon®, Acrilan®, and Creslan® (Rutherford 1963[11]).

---

[10] Bopp 1963. C —D. Bopp, et al., "Plastics," in <u>Radiation Effects on Organic Materials</u>, Academic Press, New York, 1963, eds. R. O. Bolt and J. G. Carroll.

[11] Rutherford 1963. H. A. Rutherford, "Textiles," in <u>Radiation Effects on Organic Materials</u>, Academic Press, New York, 1963, eds. R. O. Bolt and J. G. Carroll.

Polyacrylonitrile (PAN) is a member of the acrylic family that includes nitrogen atoms in its structure. Its major use is in the production of wool-like fibers used in sweaters, blankets, and carpeting (Deanin 1972[2]).

A1.2.3 Alkyds

Alkyds are thermosetting plastics that are widely used for molded electrical parts. They have high degrees of cross-linking (Deanin 1972[2]) and are chemically similar to polyester resins (Harper 1975[9]).

A1.2.4 Alloys

Polymer alloys are physical mixtures of structurally different homopolymers or copolymers. The mixture is held together by secondary intermolecular forces such as dipole interaction, hydrogen bonding, or van der Waals' forces. The physical properties of these alloys are averages based on composition (Dean 1987[5]). Polymer alloys include acrylic-polyvinyl chloride, acrylonitrile-butadiene-styrene-polyvinyl chloride (ABS-PVC), and acrylonitrile-butadiene-styrene-polycarbonate (ABS-PC). ABS alloyed or blended with polycarbonate results in a thermoplastic that is easier to process, has high heat and impact resistance, and is cheaper than polycarbonate alone.

A1.2.5 Allyls

Allyl polymers are linear thermoplastic structures. Molding compounds with mineral, glass, or synthetic fiber filling are used for electrical components. Allyl polymers include allyl-diglycol-carbonate and diallyl phthalate (DAP). Their benzene rings, a high degree of cross-linking, and the usual glass fiber reinforcement provide high rigidity and strength. Primary applications are in molded structural electrical insulation. Diallyl phthalate resin is also used for surfacing laminates in furniture and paneling (Deanin 1972[2]).

A1.2.6 Cellulosics

Cellulosics are a class of polymers that are prepared by various treatments of purified cotton or special grades of wood cellulose. Trade names include Tenite®, Ethocel®, and Forticel®. Cellulosics are among the toughest of thermoplastics, are generally economical, and are good insulating materials (Harper 1975[9]). The most prominent industrial cellulosics are cellulose acetate, cellulose acetate butyrate, cellulose propionate, and ethyl cellulose.

Cellulose butyrate, propionate, and acetate are tough and rigid, and useful for applications where clarity, outdoor weatherability, and aging characteristics are needed. The materials are fast-molding plastics and can be manufactured to have hard, glossy surfaces (Bopp 1963[10]). Major applications of these cellulose esters include blister packaging, pencils, lighting fixtures, tool handles, and tubing (Deanin 1972[2]). Ethyl cellulose is compatible with many other resins and with most plasticizers. These properties, along with its compatibility with cellulose nitrate, are responsible for its use in paints and as a coating for fabrics (Bopp 1963[10]).

Incompletely nitrated cellulose nitrate is used in molded objects, and as a constituent of lacquers and photographic film. Because of its flammability and tendency to decompose at high temperatures, cellulose nitrate is not used as a compression or injection molding material (Bopp

1963[10]). The nitrogen content for cellulose nitrate plastics is usually about 11%, for lacquers and cement base it is 12%, and for explosives it is 13% (Dean 1987[5]).

Cotton and cellulose acetate (Rayon®) are two cellulosics that are made into fibers. Cellulosics (cotton and wood) are blended in making paper. Cellophane is also based on cellulose (Deanin 1972[2]). Cellulose triacetate is used primarily in motion picture film and magnetic recording tape (Deanin 1972[2]). Cellulose ethers have applications where low temperature impact strength is needed, such as in instrument cases, electrical appliance parts, and tool handles. Different processing produces a polymer that is completely soluble in water and is used primarily as a thickening agent in foods, shampoo, latex paints, paper, and adhesives (Deanin 1972[2]).

A1.2.7 Epoxy

Epoxies and unsaturated polyesters are cross-linking resins that can be cured by chemical agents with little or no application of heat or pressure. They are frequently used in paints and finishes (Bopp 1963[10]).

A1.2.8 Fluorocarbons

Fluorocarbons include polytetrafluoroethylene (PTFE), polychloro-trifluoroethylene, perfluoroalkoxy (PFA) resin, fluorinated ethylene-propylene (FEP) resin, polyvinylidene fluoride, ethylene-chlorotrifluoroethylene copolymer, ethylene-tetrafluoroethylene copolymer, and polyvinyl fluoride.

These polymers have good abrasion and solvent resistance and electrical properties. Polyvinyl fluoride is used only as a film (Dean 1987[5]).

Polytetrafluoroethylene is the base polymer for Teflon®. Polychloro-trifluoroethylene resins may be processed by melting and can be molded as extruded. Kel-F® is one of the trade names (Harper 1975[9]). PFA resins are used as electrical insulations in flat cables and circuitry and in laminates used in electrical and mechanical applications. Fluorinated ethylene/propylene copolymer has applications in capacitors, cables, flexible belting, textile finishing, and printing (Deanin 1972[2]).

A1.2.9 Nitrile Resins

The principal monomer of nitrile resins is acrylonitrile.

A1.2.10 Polyamides

Polyamides are called nylons, which include hard materials used in mechanical parts as well as soft materials used for fibers and textiles. Aromatic nylons (also called aramids) are high temperature nylons such as Nomex®. Nomex® is used in sheet, fiber, and paper form for insulation (Harper 1975[9]) and in filters.

A1.2.11 Polyaryl Ether

Polyaryl ether is one of the relatively new thermoplastics that can be used for engineering applications in the automotive, appliance, and electrical industries. One trade name is Arylon® (Harper 1975[9]).

A1.2.12 Polycarbonate

Polycarbonates have high performance characteristics in engineering designs, which require very high impact strength. As with most plastics containing aromatic groups, polycarbonates have high radiation stability (Harper 1975[9]).

A1.2.13 Polyesters

Polyesters are used in the production of film and fibers. Glass reinforced polyesters are used in automotive, electrical/electronic, and other industrial applications replacing other plastics or metals. The basic polymer is polyethylene terephthlate (PET). Brand names include Mylar® (sheet) and Dacron® (fiber). Unsaturated polyesters are discussed under "Epoxies".

A1.2.14 Polyimides

Polyimides can be used at the highest temperatures among the commercially available plastics, and they are the strongest and most rigid (Harper 1975[9]). These materials can be used in various forms, including moldings, laminates, films, coatings, and adhesives.

A1.2.15 Polymethyl Pentene

Polymethyl pentene is another thermoplastic based on the ethylene structure. Applications for this material have been developed in the fields of lighting and in the automotive, appliance, and electrical industries (Harper 1975[9]).

A1.2.16 Polyolefins

The family of polyolefins includes various polyethylenes (low-density polyethylene, high-density polyethylene, ultrahigh-molecular-weight polyethylene), polypropylenes, polyethylene oxide, polypropylene oxide, and polybutylene.

Polypropylenes are chemically similar to polyethylenes (Harper 1975[9]). The material is termed isotactic if the methyl groups are on the same side of the chain and atactic if the arrangement is random. The isotactic polymer is more frequently used commercially (Sisman 1963[4]). The polymer is used to make molded items or fibers (Herculon is one example).

Commercial polyethylene oxide is waxy and fibrous. Because of its water solubility, it is used as a plasticizer and as an additive in non-polymeric materials rather than as a base polymer (Bopp 1963[10]).

Treatment of polyethylene with chlorine and sulfur dioxide decreases the crystallinity of the polyethylene and results in a rubbery material. Applications include wire and cable insulation,

liquid roof coatings, gaskets, floor tile, and shoe soles (Deanin 1972[2]). One trade name is Hypalon[®], which is used in fabricating glovebox gloves.

Polybutylene low-molecular-weight polymers are viscous liquids used in compounding adhesives, caulks, and sealants. High-molecular weight polymers are used in elastomers and sealants, such as butyl rubber (Deanin 1972[2]).

Polyallomers are polyolefin-type thermoplastic polymers produced from two or more different monomers, such as propylene and ethylene. In general, the properties of polyallomers are similar to those of polyethylenes and polypropylenes (Harper 1975[9]).

A1.2.17 Polyphenyl Polymers

Polyphenylene oxide is formulated by the oxidative coupling of phenolic monomers. This material is used for engineering applications. One trade name is Noryl[®]. Polyphenylene sulfide is a crystalline polymer, and is used for coatings and molded materials. One trade name is Ryton[®].

A1.2.18 Polyurethanes

The most common usage of polyurethane is in foams, which may be flexible or rigid (Deanin 1972[2]). These foams have applications as insulation, structural reinforcement, packaging, and gaskets (Harper 1975[9]).

A1.2.19 Silicones

Silicones are also called polysiloxanes. They are characterized by their three-dimensional branched-chain structure. Various organic groups (such as methyl, phenyl, vinyl) introduced within the polysiloxane chain impart certain characteristics and properties. Applications include waterproofing, paper coatings, elastomers, sealants, medical equipment, and transformers (Deanin 1972[2]).

A1.2.20 Styrenics

Polystyrene can be regarded as a substituted polyethylene with phenyl groups on alternate carbon atoms (Sisman 1963[4]). Polystyrene is highly rigid at room temperature, but the rigidity may be decreased and the impact strength increased by the addition of plasticizers. It can be used in moldings or in small electrical components, as well as in containers and other packaging items (Sisman 1963[4]). Common trade names are Lustrex[®] and Styron[®].

Styrene-acrylonitrile (SAN) copolymers are random, amorphous copolymers whose properties vary with molecular weight and copolymer composition. SAN resins are rigid, hard, transparent thermoplastics (Dean 1987[5]). Acrylonitrile-butadiene-styrene (ABS) copolymer is a thermoplastic resin. Trade names include Marbon Cycolac[®], Bason[®], and Lustran[®]. ABS plastics have hardness and rigidity without brittleness, at moderate costs (Harper 1975[9]). Styrene-butadiene copolymers are used in gaskets.

A1.2.21 Sulfones

Polysulfones are rigid, strong thermoplastics, and can be molded, extruded, or thermoformed into a wide variety of shapes. The chemical structure is highly resonating (contains benzene rings), resulting in high stability (Harper 1975[9]). Copolymers with olefins, however, have low radiation stability (Jellinek 1978[12]).

A1.2.22 Thermosetting Plastics

Thermosetting plastics are insoluble and infusible because of their three-dimensional structure. They are used chiefly as molding powders and as binders for laminates. Examples are phenol-formaldehyde, urea-formaldehyde, and melamine-formaldehyde. Common uses are in molded household items. Laminated sheets and tubes are widely used in electrical components or molded components of industrial equipment (Bopp 1963[10]).

A1.2.23 Vinyls

Vinyl polymers are structurally based on the ethylene chain (Harper 1975[9]).

Polyvinyl chloride (PVC) is a material with a wide range of rigidity or flexibility. PVC can be plasticized with a wide variety of materials to produce soft, yielding plastics. Without plasticizers, PVC is a strong, rigid material that can be machined, heat-formed, or welded by solvents or heat. Typical uses include wire and cable insulation and foam applications. PVC can also be made into film and sheet (Harper 1975[9]). Other uses are as a fabric coating, for upholstery and similar household articles, and for hoses and tubular items (Bopp 1963[10]).

Polyvinyl acetate (PVAC) is used in latex paints because of its quick-drying and self-priming properties, and resistance to weathering. It is also used in hot-melt and solution adhesives (Dean 1987[5]). Copolymers of polyvinylidene chloride and PVC are used to make Saran (Bopp 1963[10]).

Polyvinyl alcohol is made by the hydrolysis of polyvinyl acetate. It is soluble in water and resistant to most organic solvents. It is used in solvent-resistant hoses, diaphragms, and gaskets, and in coatings, textile sizing, and as an adhesive (Bopp 1963[10]).

Polyvinyl acetals, consisting of polyvinyl butyral, polyvinyl formal, and polyvinyl acetal, are the most abundantly used plastics related to polyvinyl alcohol. Polyvinyl formal is used in coating electrical wire. Polyvinyl acetal is tough and easy to mold, and is used for bottle caps, combs, and as a binder in heavily filled molded items. Polyvinyl butyral is a very important item of commerce as the interlayer in safety glass (Bopp 1963[10]).

A1.3 Structural Features of Commercial Polymers

The structural features of many commercial polymers are shown in Table A1.3-1.

---

[12] Jellinek 1978. H. H. G. Jellinek, Aspects of Degradation and Stabilization of Polymers, Elsevier Scientific Publishing Company, New York, 1978.

Table A1.3-1 — Structural Features of Commercial Polymers

Acrylonitrile/butaiene/styrene terpolymer (ABS)
$$—(CH_2CH \!=\! (CHCH)—$$
$$(CH_2CH)—(CH_2CH)—$$
$$(C \!\equiv\! N)$$

Alkyd
$$\overset{O\ O}{\underset{}{—(C\ \ COCH_2CHCH_2O)—}}$$
$$OC(CH_2)_7CH \!=\! CHCH_2CH \!=\! CH(CH_2)_4CH_2$$
$$O$$

Butadiene/acrylonitrile rubber (nitrile rubber or NBR)
$$—(CH_2CH \!=\! CHCH_2) —(CH_2CH)—$$
$$(C \!\equiv\! N)$$

Butadiene/styrene rubber (SBR or GR-S)
$$—(CH_2CH \!=\! CHCH_2) —(CH_2CH)—$$

Cellulose
$$—CH_2OH$$
$$CH—O$$
$$—(OCH \qquad CH)—$$
$$CH—CH$$
$$OH \quad OH$$

Table A1.3-1 — Structural Features of Commercial Polymers (Continued)

Cellulose Nitrate

$$\begin{array}{c} CH_2ONO_2 \\ | \\ CH \!-\! O \\ / \qquad \qquad \backslash \\ -(OCH \qquad \qquad CH)- \\ \backslash \qquad \qquad / \\ CH \!-\! CH \\ | \qquad | \\ OH \qquad ONO_2 \end{array}$$

Cellulose Triacetate

$$\begin{array}{c} O \\ \| \\ CH_2OCCH_3 \\ | \\ CH \!-\! O \\ / \qquad \qquad \backslash \\ -(OCH \qquad \qquad CH)- \\ \qquad O \quad CH \!-\! CH \quad O \\ \qquad \| \quad | \qquad | \quad \| \\ CH_3C \!-\! O \qquad O \!-\! CCH_3 \end{array}$$

Chlorosulfonated Polyethylene

$$-(CH_2CH_2)-(CH_2CH)-(CH_2CH)- $$
$$\qquad\qquad\qquad\qquad | \qquad\qquad | $$
$$\qquad\qquad\qquad\qquad Cl \qquad O\!=\!S\!=\!O $$
$$\qquad\qquad\qquad\qquad\qquad\qquad\qquad | $$
$$\qquad\qquad\qquad\qquad\qquad\qquad\qquad Cl $$

Diallyl Phthalate

$$\begin{array}{c} O \; O \\ \| \; \| \\ -(CH_2CHCH_2O\!-\!C \quad COCH_2CHCH_2)- \\ | \qquad\qquad\qquad\qquad | \end{array}$$

Epoxy Resin

$$\begin{array}{c} O \qquad\qquad\quad CH_3 \qquad\quad O \\ / \; \backslash \qquad\qquad | \qquad\qquad / \; \backslash \\ -CH_2 \!-\! CHCH_2O\!\!\ll\!\!\gg\!\! C \ll\!\!\gg OCH_2CH \!-\! CH_2 \\ | \\ CH_3 \end{array}$$

Table A1.3-1 — Structural Features of Commercial Polymers (Continued)

Ethyl Cellulose

$$CH_2OC_2H_5$$
$$CH-O$$
$$-(OCH \quad CH)-$$
$$CH-CH$$
$$OH \quad OC_2H_5$$

Ethylene/Ethyl Acrylate Copolymer

$$-(CH_2CH_2)-(CH_2CH)-$$
$$O=C-OC_2H_5$$

Ethylene/Propylene Copolymer

$$-(CH_2CH_2)-(CH_2CH)-$$
$$CH_3$$

Ethylene/Vinyl Acetate Copolymer

$$-(CH_2CH_2)-(CH_2CH)-$$
$$OCCH_3$$
$$\|$$
$$O$$

Fluorinated Ethylene/Propylen Copolymer

$$-(CF_2CF_2)-(CF_2CF)-$$
$$CF_3$$

Melamine-Formaldehyde

$$\begin{array}{c} N \quad CH_2)- \\ -(N-C \quad C-N-CH_2)- \\ N \quad N \\ C \\ -(CH_2-N-CH_2)- \end{array}$$

Table A1.3-1 — Structural Features of Commercial Polymers (Continued)

Nylon 6

$$-[(CH_2)_5\overset{\overset{\displaystyle O}{\|}}{C}-\overset{\overset{\displaystyle H}{|}}{N}]-$$

Nylon 11

$$-[(CH_2)_{10}\overset{\overset{\displaystyle O}{\|}}{C}-\overset{\overset{\displaystyle H}{|}}{N}]-$$

Nylon 12

$$-[(CH_2)_{11}\overset{\overset{\displaystyle O}{\|}}{C}-\overset{\overset{\displaystyle H}{|}}{N}]-$$

Nylon 610

$$-[(CH_2)_6\overset{\overset{\displaystyle H}{|}}{N}-\overset{\overset{\displaystyle O}{\|}}{C}(CH_2)_8\overset{\overset{\displaystyle O}{\|}}{C}-\overset{\overset{\displaystyle H}{|}}{N}]-$$

Nylon 66

$$-[(CH_2)_6\overset{\overset{\displaystyle H}{|}}{N}-\overset{\overset{\displaystyle O}{\|}}{C}(CH_2)_4\overset{\overset{\displaystyle O}{\|}}{C}-\overset{\overset{\displaystyle H}{|}}{N}]-$$
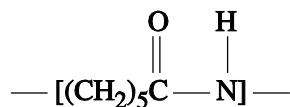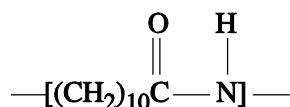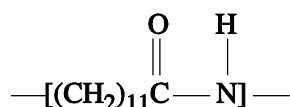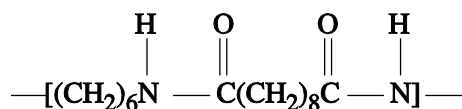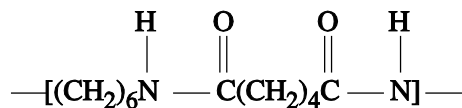
Phenol-formaldehyde
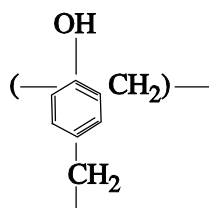
Phenoxy Resin
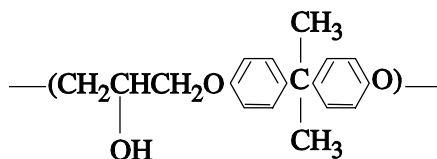
Table A1.3-1 — Structural Features of Commercial Polymers (Continued)

Polyacrylonitrile

$$— (CH_2CH) —$$
$$ | $$
$$C \equiv N$$
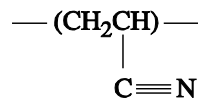
Polybenzimidazole
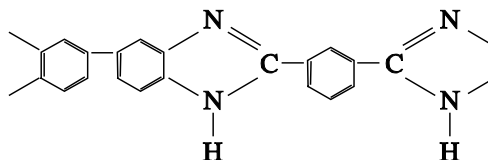
Poly-3,3-bis (chloromethyl) oxetane (Penton)

$$CH_2Cl$$
$$ | $$
$$— (OCH_2CCH_2) —$$
$$ | $$
$$CH_2Cl$$

Polybutadiene

$$— (CH_2CH = CHCH_2)$$

Poly-1-Butene

$$— (CH_2CH)$$
$$ | $$
$$C_2H_5$$
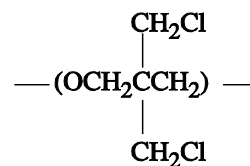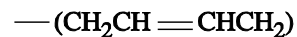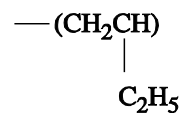
Polycarbonate

Polychloroprene (neoprene)

$$— (CH_2C = CHCH_2) —$$
$$ | $$
$$Cl$$

Table A1.3-1 — Structural Features of Commercial Polymers (Continued)

Polychlorotrifluoroethylene

$$— (CF_2CF) —$$
$$|$$
$$Cl$$

Poly (2,6-dimethylphenylene oxide) (PPO)

$$CH_3$$
$$(\langle\!\!\!\bigcirc\!\!\!\rangle - O)—$$
$$CH_3$$

Polyepichlorohydrin

$$— (CH_2CHO) —$$
$$|$$
$$CH_2Cl$$

Polyester Polyurethane

$$\begin{array}{cccccc} & O & O & & O & H & CH_3 \\ & \| & \| & & \| & | & \\ — [(CH_2CH_2OC(CH_2)_4CO]CH_2CH_2OC & —N & & \end{array}$$

$$N — CO)—$$
$$| \quad \|$$
$$H \quad O$$

Unsaturated Polyester (cured)

$$\begin{array}{cccc} & & O & O \\ & & \| & \| \\ —(CHCH_2OC \quad COCHCH_2OCCHCHCO)— \\ | & \| \| & | & | \\ CH_3 & O O & CH_3 & (CH_2CH\langle\!\!\!\bigcirc\!\!\!\rangle) \\ & & & | \end{array}$$

Polyether Polyurethane

$$\begin{array}{cccc} CH_3 & & O & H & CH_3 \\ | & & \| & | & \\ —(CH_2CHO)CH_2CH_2OC & —N & \end{array}$$

$$N — CO)—$$
$$| \quad \|$$
$$H \quad O$$

Table A1.3-1 — Structural Features of Commercial Polymers (Continued)

Polyethyl Acrylate

$$-(CH_2CH)-$$
$$|$$
$$O=COC_2H_5$$

High-Density Polyethylene

$$-(CH_2CH_2)-$$

Low-Density Polyethelene

$$-(CH_2CH_2)-(CH_2CH)-(CH_2CH)-(CH_2CH)-$$
$$\qquad\qquad\qquad | \qquad\quad | \qquad\quad |$$
$$\qquad\qquad\qquad C_2H_5 \quad C_4H_9 \quad C_nH_{2n+1}$$
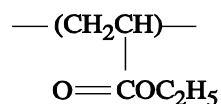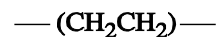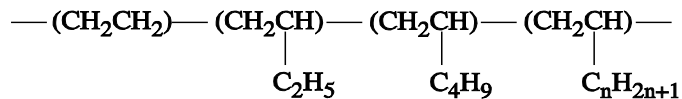
Polyethelene Oxide

$$-(CH_2CH_2O)-$$
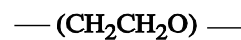
Poly(ethelene terephalate)

$$-(CH_2CH_2OC\langle\bigcirc\rangle CO)-$$
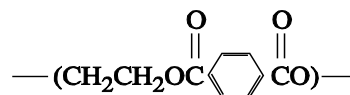
Polyimide

Polyisobutylene

$$CH_3$$
$$|$$
$$-(CH_2C)-$$
$$|$$
$$CH_3$$
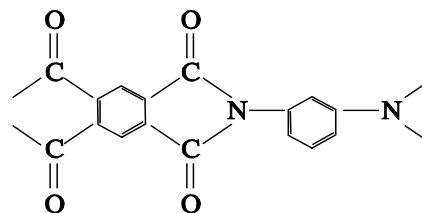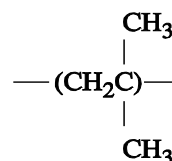
Table A1.3-1 — Structural Features of Commercial Polymers (Continued)

Polyisoprene (Natural Rubber)

$$— (CH_2C = CHCH_2) —$$
$$\quad\quad\quad\; |$$
$$\quad\quad\quad CH_3$$
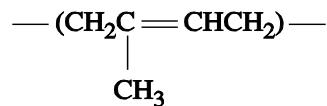
Polymethyl Metacrylate

$$\quad\quad\quad CH_3$$
$$\quad\quad\quad\; |$$
$$— (CH_2C) —$$
$$\quad\quad\quad\; |$$
$$\quad\; O = COCH_3$$
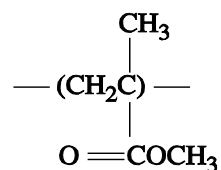
Poly (4-methylpentene-1)
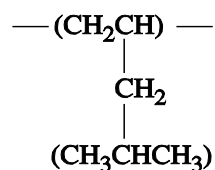
$$— (CH_2CH) —$$
$$\quad\quad\quad |$$
$$\quad\quad\; CH_2$$
$$\quad\quad\quad |$$
$$\; (CH_3CHCH_3)$$

Polyoxymethylene (Acetal)
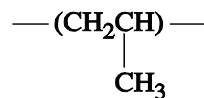
$$— (CH_2O) —$$

Polypropylene

$$— (CH_2CH) —$$
$$\quad\quad\quad |$$
$$\quad\quad\; CH_3$$

Polypropylene-Oxide

$$— (CH_2CHO) —$$
$$\quad\quad\quad\; |$$
$$\quad\quad\; CH_3$$

Poly-p-xylylene

$$— (CH_2 \hexagon CH_2) —$$
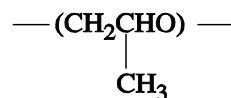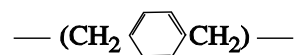
Table A1.3-1 — Structural Features of Commercial Polymers (Continued)

Polysulfide Elastomer

$$— (CH_2CH_2OCH_2OCH_2CH_2SSCH_2CH_2SS) —$$

Polysulfone
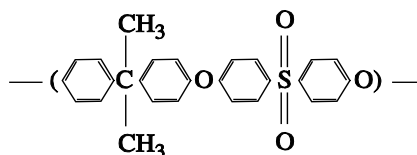
Polystyrene

Polytetrafluoroethylene

$$— (CF_2CF_2) —$$
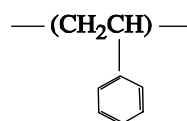
Polyvinyl Acetate
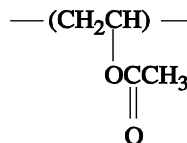
Polyvinyl Alchohol
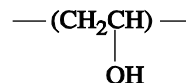
Polyvinyl Butyral
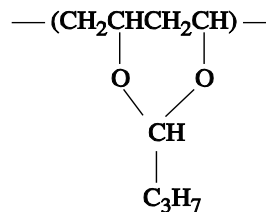
Table A1.3-1 — Structural Features of Commercial Polymers (Continued)

Polyvinyl Chloride
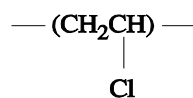
$$— (CH_2CH) —$$
$$|$$
$$Cl$$

Polyvinyl Ethyl Ether
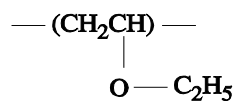
$$— (CH_2CH) —$$
$$|$$
$$O — C_2H_5$$

Polyvinyl Fluoride

$$— (CH_2CH) —$$
$$|$$
$$F$$

Polyvinyl Formal

$$— (CH_2CHCH_2CH) —$$
$$|\qquad|$$
$$O\qquad O$$
$$\diagdown\ \diagup$$
$$CH_2$$

Polyvinylidene Chloride

$$Cl$$
$$|$$
$$— (CH_2C) —$$
$$|$$
$$Cl$$

Polyvinylidene Fluoride

$$— (CH_2CF_2) —$$
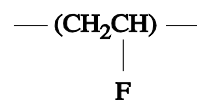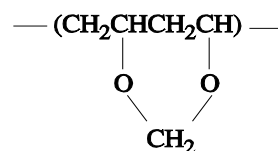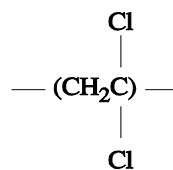
Polyvinyl Pyrrolidone

$$— (CH_2CH) —$$
$$|$$
$$N$$
$$\diagup\quad\diagdown$$
$$CH_2\qquad C = O$$
$$|\qquad\qquad|$$
$$CH_2 — CH_2$$
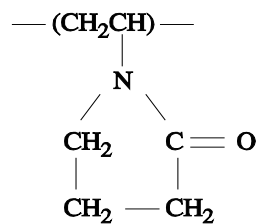
Table A1.3-1 — Structural Features of Commercial Polymers (Concluded)

Silicone

$$— (Si — O) —$$

with CH_3 groups above and below the Si.

Sodium Carboxymethyl Cellulose (CMC)

$$CH_2OCH_2CO^-Na^+$$

$$— (OCH \quad CH) —$$

with ring: $CH — O$, $CH — CH$, $OH \quad OH$

Styrene/Acrylonitrile Coplolymer

$$— (CH_2CH) — (CH_2CH) —$$

$$C \equiv N$$

Impact Styrene

$$— (CH_2CH = CHCH) —$$

$$— (CH_2CH) —$$

Urea-Formaldehyde

$$— (N — C — N — CH_2) —$$

with O above C, and $CH_2) —$ below N

Vinyl Chloride Vinyl Acetate Copolymer

$$— (CH_2CH) — (CH_2CH) —$$

$$Cl \quad\quad OCCH_3$$

$$O$$

Vinylidene Fluoride/Hexafluoroporylene Copolymer

$$— (CH_2CF_2) — (CF_2CF) —$$

$$CF_3$$

2.1-124

Attachment B
Absorption of Alpha Decay Energy Inside Particles of PuO$_2$

Executive Summary

This attachment derives the fraction of alpha decay energy escaping from a spherical particle of PuO$_2$ of radius r. The rate of energy deposition is calculated from an estimated Bragg curve for PuO$_2$.

B1.1 Introduction

Let

s = stopping distance of alpha particles in PuO$_2$,
a = radius of spherical particles of PuO$_2$.
E$_0$ = energy generated per unit volume.

The solution is separated into three cases: for Case I, the diameter of the particle is less than the stopping distance (2a < s), for Case II, the stopping distance is between the radius and the diameter of the particle (a ≤ s ≤ 2a), and for Case III, the radius of the particle is greater than the stopping distance (s < a).

The rate of alpha particle energy deposition inside the PuO$_2$ particle is calculated based on the estimated Bragg curve shown in Figure B1-1. This curve was generated by the program TRIM-88 "The Transport of Ions in Matter," copyrighted by J. P. Biersack and J. F. Ziegler (discussed in Ziegler 1985[1]).

The highest atomic number nucleus included in the program is U(92), so UO$_2$ with the density of PuO$_2$ (11.4 g/cm^3) was used to simulate PuO$_2$. Figure B1-2 shows the alpha particle energy in MeV versus distance traveled from its origin for alpha particles having initial energies of 5.15 MeV (Pu-239) and 5.49 MeV (Pu-238). [The total distance along the particle's path is somewhat greater, due to straggling that occurs at low energies when collisions of the alpha particle with nuclei become more important than interactions of the alpha particle with electrons.]

B2.1 Case I, 2a < s

The geometry of Case I is shown in Figure B2-1. The fraction of energy reaching point Q from point P along r' is

$$E_F = f(E_o, r')$$ (B2-1)

---

[1] Ziegler 1985. J. F. Ziegler, J. P. Biersack, and U. Littmark, <u>The Stopping and Range of Ions in Solids</u>, Vol. I, Pergamon Press, New York, N.Y., 1985.

ESTIMATED BRAGG CURVE FOR PUO2
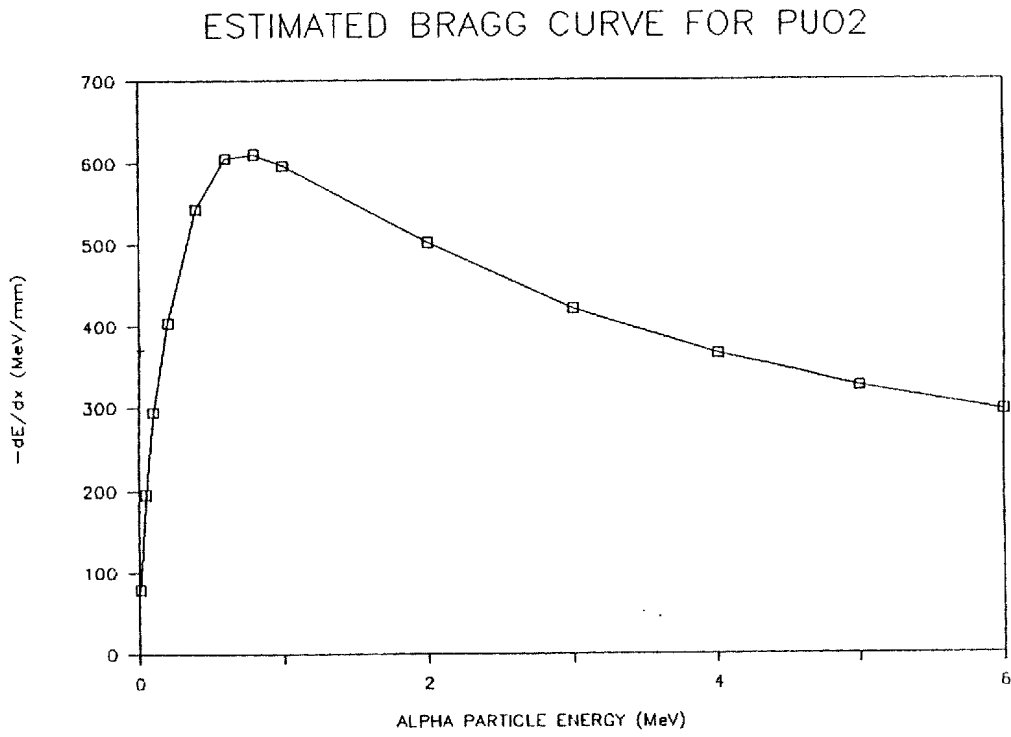
Figure B1-1
Estimated Bragg Curve for PuO$_2$
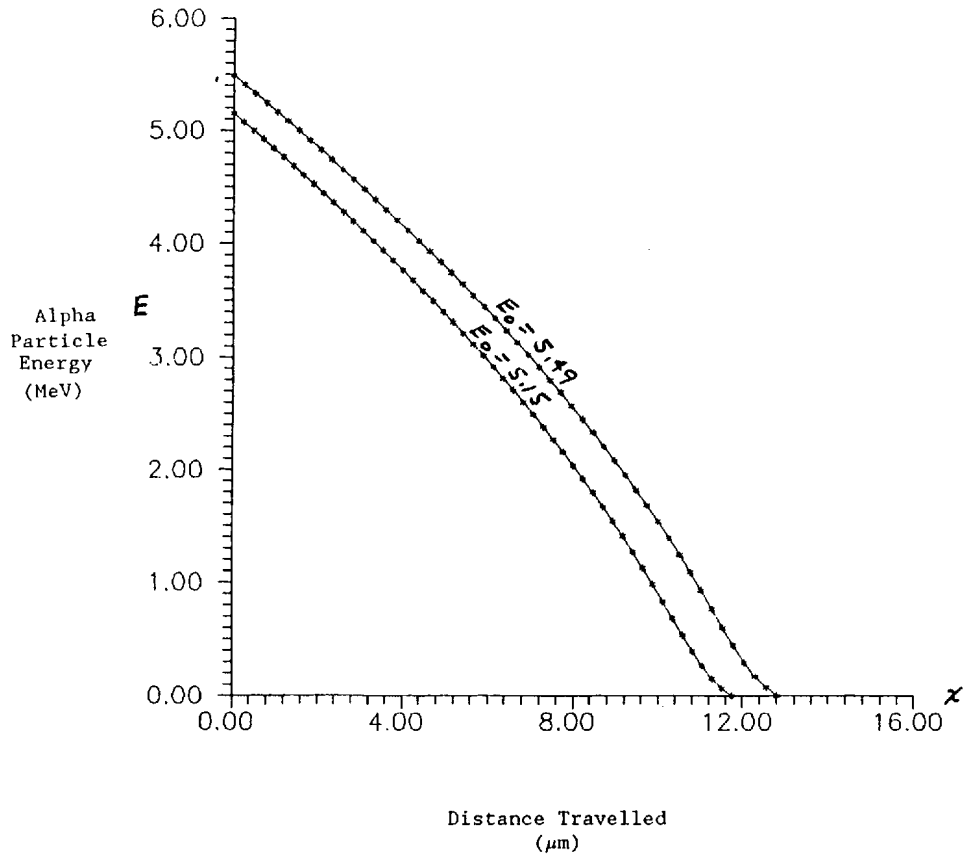
Figure B1-2
Alpha Particle Energy vs. Distance Traveled from Point of Origin

Where:

$$r'^2 = a^2 + r^2 - 2\ ar\ \cos\ \omega \qquad\qquad\text{(B2-2)}$$

since r' < s for this case, and f(E_0,r') is shown graphically in Figure B1-2 for two values of E_0.

The fraction of the area of a sphere centered at P, subtended by dϕ and revolved about the x axis is

$$A = \frac{r'd\phi 2\ \pi\ r'\ \sin\ \phi}{4\pi\ r'^2} \qquad . \qquad\qquad\text{(B2-3)}$$

The total energy reaching the boundary, a, from point P is

$$\rho(r) = 1/2 \int_0^\pi\ f(E_O, r') \sin \phi\ d\phi \qquad . \qquad\qquad\text{(B2-4)}$$

The total energy from all points, P, in the sphere is

$$E = \int_0^a\ 4\pi\ r^2 \rho(r)\ dr = 2\pi\ \int_0^a\ r^2 \int_0^\pi\ f(E_O, r') \sin \phi\ d\phi\ dr \qquad . \qquad\text{(B2-5)}$$

The fraction of energy generated in the sphere and escaping from the surface is

$$\frac{E}{E_r} = \frac{2\pi}{4/3\ \pi\ a^3 E_O} \int_0^a r^2\ \int_0^\pi\ f(E_O, r')\ \sin \phi\ d\phi\ dr \qquad\qquad\text{(B2-6)}$$

where r' is defined in Eq. (B2-2).

The law of signs allows cos ω to be expressed in terms of ϕ where

$$\frac{r'}{\sin \omega} = \frac{a}{\sin (\pi - \phi)} = \frac{a}{\sin \phi}, \qquad\qquad\text{(B2-7)}$$

$$r' = \frac{a \sin \omega}{\sin \phi} = \sqrt{a^2 + r^2 - 2\ ra\ \cos \omega}, \qquad\qquad\text{(B2-8)}$$

$$\frac{a^2 \sin^2 \omega}{\sin^2 \phi} = a^2 + r^2 - 2\ ra\ \cos \omega, \qquad\qquad\text{(B2-9)}$$

$$\frac{a^2}{\sin^2 \phi} (1 - \cos^2 \omega) = a^2 + r^2 - 2\ ra\ \cos \omega, \qquad\qquad\text{(B2-10)}$$

$$\frac{a^2}{\sin^2 \phi} \cos^2 \omega - 2\,ra\cos\omega + a^2 + r^2 - \frac{a^2}{\sin^2 \phi} = 0, \tag{B2-11}$$

$$\frac{a^2}{\sin^2 \phi} \cos^2 \omega - 2\,ra\cos\omega + r^2 - \frac{a^2\cos^2\phi}{\sin^2 \phi} = 0, \tag{B2-12}$$

$$\cos\omega = \frac{2\,ra \ \pm \ \sqrt{4r^2 a^2 - \dfrac{4a^2}{\sin^2 \phi}\left[r^2 - a^2\dfrac{\cos^2\phi}{\sin^2\phi}\right]}}{\dfrac{2a^2}{\sin^2\phi}} \tag{B2-13}$$

$$= \left[r \pm \sqrt{-\frac{r^2\cos^2\phi}{\sin^2\phi} + \frac{a^2\cos^2\phi}{\sin^4\phi}}\ \right]\frac{\sin^2\phi}{a} \tag{B2-14}$$

$$= \frac{r}{a}\sin^2\phi \pm \frac{|\cos\phi\,|\sin\phi\,|}{a}\sqrt{\frac{a^2}{\sin^2\phi} - r^2}, \tag{B2-15}$$

$$= \frac{r}{a}\sin^2\phi + \frac{\cos\phi}{a}\sqrt{a^2 - r^2\sin^2\phi}. \tag{B2-16}$$

The positive solution is chosen since when $\phi = 0$, $\omega = 0$ and when $\phi = \pi$, $\omega = \pi$, and when $r = 0$, $\omega = \phi$.

Therefore,

$$\cos\omega = \frac{r}{a}\sin^2\phi + \cos\phi\sqrt{1 - \left(\frac{r}{a}\right)^2\sin^2\phi}. \tag{B2-17}$$

B2.2 Case II, a ≤ s ≤ 2a

Case II is divided into two subcases. Figure B2-2 shows the geometry for Case IIa where $r \le$ s-a. The geometry for Case IIb is shown in Figure B2-3 where $r >$ s-a.

For Case IIa, tangency occurs when r = s-a. The total energy reaching the boundary, a, is

$$\rho(r) = \int_0^\pi f(E_O, r')\, \frac{r'\,d\phi\ \ 2\pi\,r'\sin\phi}{4\pi\,r'^2} \tag{B2-18}$$

since r' < s.

For Case IIb intersection occurs for r' = s. From Figure B2-3,

$$a^2 = r^2 + s^2 - 2\,rs\,\cos\,(\pi - \phi\,(r,s))\,, \tag{B2-19}$$

$$= r^2 + s^2 + 2\,rs\,\cos\,\phi\,(r,s)\,, \tag{B2-20}$$

$$\phi\,(r,s) = \cos^{-1}\frac{a^2 - r^2 - s^2}{2\,rs} \tag{B2-21}$$

The total energy reaching the boundary, a, is

$$\rho\,(r) = \int_0^{\phi(r,s)} f(E_o,r')\,\sin\,\phi\,d\phi\,dr \tag{B2-22}$$

Where r' is given in Eq. (B2-2) and cos ω is defined in Eq. (B2-17).

The fraction of energy generated in the sphere and escaping from the surface is

$$\frac{E}{E_T} = \frac{1.5}{a^3 E_0}\left[\int_0^{s-a} r^2 \int_0^{II} f(E_o,r')\sin\phi\,d\phi\,dr\right.$$

$$\left.+ \int_{s-a}^{a} r^2 \int_0^{\phi(r,s)} f(E_o - r')\,\sin\phi\,d\phi\,dr\,\right] \tag{B2-23}$$

or

$$\frac{E}{E_T} = \frac{3}{2a^3\,E_o}\int_0^{a} r^2 \int_0^{\phi\,(r,s)} f(E_o,r')\sin\phi\,d\phi\,dr \tag{B2-24}$$

where

$$\phi(r,s) = \pi \qquad\qquad\qquad if\ r \le s - a \tag{B2-25}$$

$$= \cos^{-1}\left[\frac{a^2 - r^2 - s^2}{2\,rs}\right] \quad if\ r > s - a\ \ . \tag{B2-26}$$

B2.3 Case III, s < a

In this case, the energy reaching the boundary a from point P is confined to a shell of thickness s as shown in Figure B2-4. The total energy is given by

$$\rho(r) = \int_0^{\phi(r,\ s)} f(E_O,r')\frac{r'\,d\phi\,2\pi\,r'\sin\phi}{4\pi\,r'^2} \tag{B2-27}$$

where Equation (B2-26) defines ϕ(r, s).

The fraction of energy generated in the sphere and escaping from the surface is

$$\frac{E}{E_T} = \frac{2\pi\, E_O}{4/3\,\pi\, a^3\, E_O} \int_{a-s}^{a} r^2 \int_{0}^{\phi\,(r,\,s)} f(E_O, r')\sin\phi\, d\phi\, dr\,. \qquad \text{(B2-28)}$$

B2.4 Numerical Solution

The fractional energy equations, E/E_T, were evaluated for particles with radii, a, between 0 and 100 microns and initial energies of 5.15 and 5.49 MeV. Adaptive 8-point Legendre-Gauss integration was performed with GAUS8 (see VanDevender 1984[2] and Cowell 1984[3]). An integration error tolerance of 10^{-4} was used. Figures B2-5 and B2-6 display fractional energy for $0 \geq a \geq 100$ and $0 \leq a \leq 20$, respectively, for $E_o = 5.15$ MeV. Table B2-1 lists the fraction of energy escaping from particles of various radii.

---

[2] VanDevender 1984. W. H. VanDevender, "Slatec Mathematical Subprogram Library Version 2.0," Sandia National Laboratories, SAND84-0281, April 1984.

[3] Cowell 1984. W. R. Cowell, <u>Sources and Development of Mathematical Software</u>. Prentice Hall, New York, N.Y., 1984.
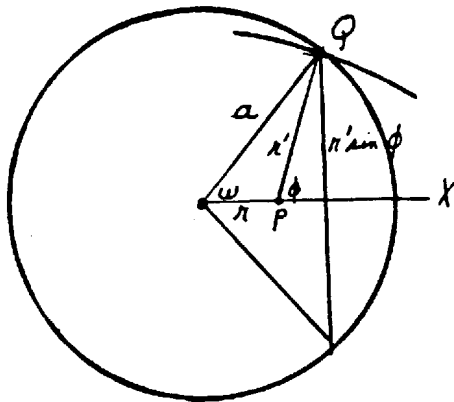
Fig. B2-1 Case I 2a < s
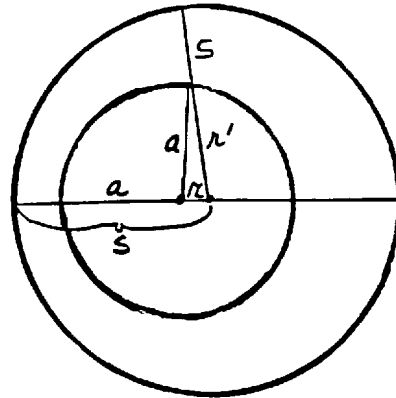
Fig. B2-2 Case IIa r ≤ s-a
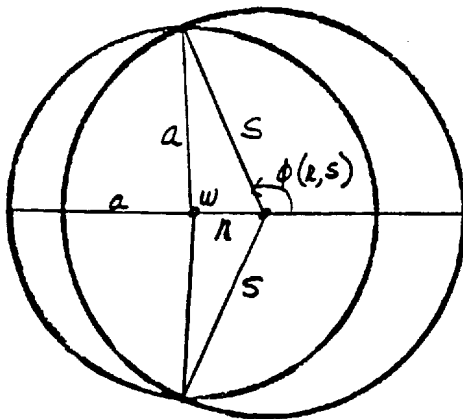
Fig. B2-3 Case IIb r > s-a
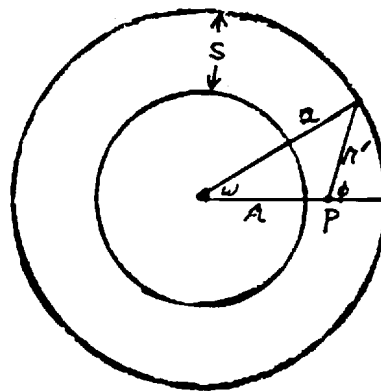
Fig. B2-4 Case III s < a
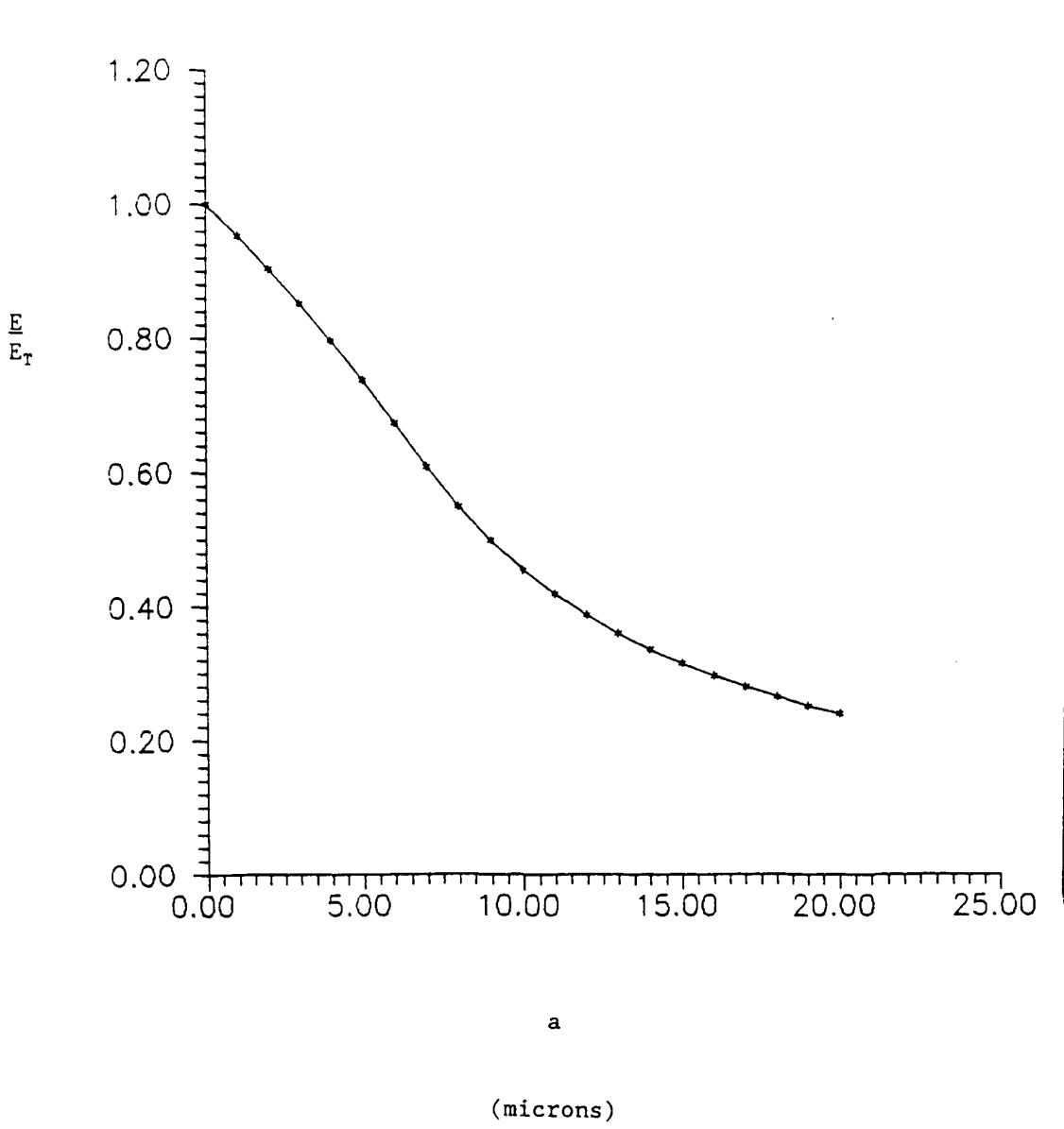
Figure B2-5
PuO$_2$ Fractional Energy vs. Radius for E$_o$ = 5.15 MeV
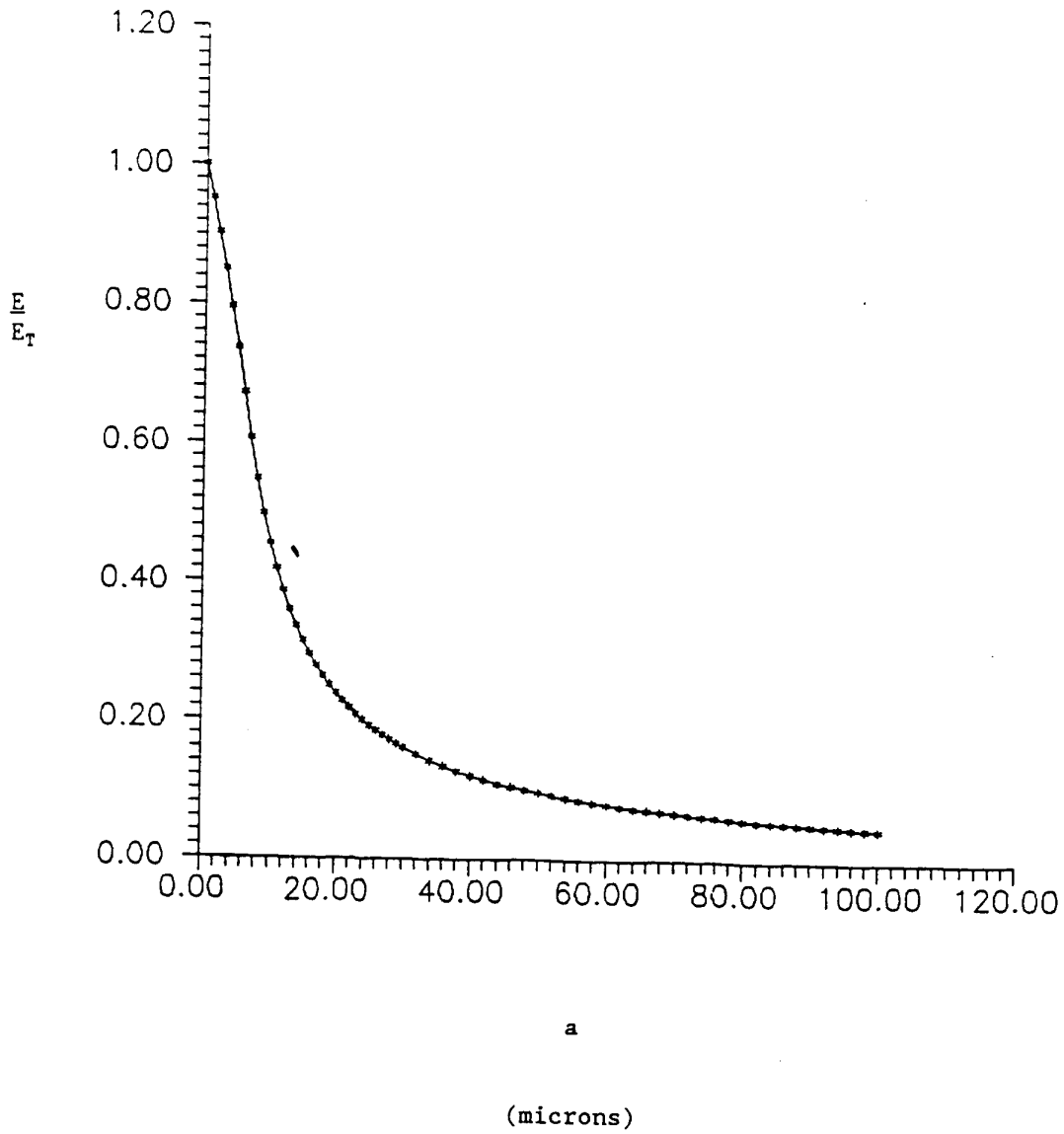
Figure B2-6
PuO$_2$ Fractional Energy vs. Radius E$_o$ = 5.15 MeV

Table B2-1 — Fraction of Alpha Particle Energy Escaping from PuO$_2$ Particles as a Function of Particle Radius and Initial Energy

Particle Radius (µm)	Fraction of Energy Escaping	
	Eo = 5.15 MeV	Eo = 5.49 MeV
9.5	0.476	0.515
7.0	0.607	0.647
4.5	0.766	0.790
3.5	0.823	0.840
2.5	0.877	0.888
1.5	0.927	0.934
0.75	0.964	0.967
0.28	0.987	0.988

This page intentionally left blank.

APPENDIX 2.2

G VALUES FOR RH-TRU WASTE

This page intentionally left blank.

2.2   G Values for RH-TRU Waste

2.2.1   Summary

This appendix defines the methodology for calculating G values for remote-handled transuranic (RH-TRU) payload content codes based on the radiolytic G values for waste materials that are discussed in detail in Appendix 2.1 of the RH-TRU Payload Appendices. Bounding G values for RH-TRU waste are discussed in Section 2.2.2. The radionuclides in RH-TRU materials can emit alpha, beta, or gamma radiations. The effective G values take into account the fraction of the alpha, beta, and gamma energy absorbed by the gas-generating materials in a given content code. The determination of applicable effective G values for RH-TRU waste content codes is discussed in Section 2.2.3. The use of the bounding and effective G values in arriving at content code-specific decay heat limits is described in Appendix 2.5 of the RH-TRU Payload Appendices.

In general, RH-TRU waste to be transported in the RH-TRU 72-B packaging can be classified into three waste types as follows:

- Solidified Inorganics

- Solid Inorganics

- Solid Organics.

Waste materials belonging to the three waste types are subdivided into waste content codes. Content codes that are currently part of the payload for the RH-TRU 72-B packaging are described in the RH-TRU Waste Content Codes (RH-TRUCON) document.[1] The chemicals present in a waste-specific content code under one of these waste types determine the gas generation potential of a given waste.

Bounding and effective G values are not established for solidified organic materials. As such, decay heat limits cannot be established for content codes describing solidified organic wastes. While not expected in general, any containers assigned to content codes for solidified organic wastes must be evaluated for compliance with the flammable gas generation rate limits as described in Appendix 2.5 of the RH-TRU Payload Appendices.

2.2.2   Bounding G Values for Waste Materials

As described in Appendix 2.1 of the RH-TRU Payload Appendices, the G value for a given material is determined primarily by the chemical properties of the material and its temperature. The effective G value is determined based on the fraction of the alpha, beta, and gamma energy absorbed by the gas generating materials in a given content code. Quantitative estimates of effective G values are discussed in Section 2.2.3.

G values are used in calculating decay heat limits to restrict hydrogen gas concentrations and total gas generated (equal to the total amount of gas generated minus the amount of oxygen consumed, if applicable), which supports the pressure calculations for the RH-TRU 72-B packaging. The calculational basis allows G values at room temperature (i.e., 70°F) to be

---

[1] U.S. Department of Energy (DOE), *Remote-Handled Transuranic Content Codes (RH-TRUCON)*, current revision, DOE/WIPP 90-045, U.S. Department of Energy, Carlsbad Field Office, Carlsbad, New Mexico.

corrected for higher or lower anticipated temperatures in the RH-TRU 72-B packaging inner vessel. The temperature dependence of G values is defined by the Arrhenius equation (see Appendix 2.1 of the RH-TRU Payload Appendices):

$$G_{eff}(T) = G_{eff}(T_{RT}) \exp \left\{ (E_a/R)[(T - T_{RT})/(T \times T_{RT})] \right\}$$

where,

$G_{eff}(T)$ = Effective G value at temperature, T (molecules/100 eV)

$G_{eff}(T_{RT})$ = Effective G value at room temperature, RT (molecules/100 eV)

E_a = G value activation energy for a gas species (kcal/mole)

R = Gas law constant (1.99E-3 kcal/mole-K)

T_{RT} = Absolute room temperature (294 K)

T = Absolute temperature of the target material (i.e., average contents temperature) (K).

Table 2.2-1 summarizes the maximum G values for hydrogen and net (total) gas, as well as the activation energies for the G values for the bounding waste materials that radiolytically generate gas and may be present in RH-TRU waste. RH-TRU wastes that can be classified as solidified inorganics, solid inorganics, or solid organics based on the chemicals and materials present in the waste in quantities greater than 1% (weight) and the list of allowable materials specified in the Remote-Handled Transuranic Waste Authorized Methods for Payload Control (RH-TRAMPAC)[2] (Table 4.3-1 of the RH-TRAMPAC) are bound by the G values summarized in Table 2.2-1. For solid organic materials other than those listed in Table 2.2-1, a bounding G value from Table 2.2-1 (e.g., polyethylene at 70ºF) shall be used provided that the material is allowed by Table 4.3-1 of the RH-TRAMPAC and is not a solidified organic material. Inorganic and nonhydrogenous materials do not generate hydrogen and have a G value of zero.

Table 2.2-1 – Summary of Maximum Hydrogen and Net Gas G Values and Activation Energies for Bounding Materials in RH-TRU Waste

Waste Material	Hydrogen Gas G Value at 70ºF (molecules/100 eV)	Net (Total) Gas G Value at 70ºF (molecules/100 eV)	Activation Energy (kcal/mole)
Water	$1.6x^{①}$	$2.4x^{①}$	0
Polyethylene	4.1	4.1	0.8
Polyvinyl Chloride	0.7	2.6	3.0
Cellulose	3.2	8.4	2.1
Organic Resins	1.7	2.1	2.1
Other Polymers	4.1	4.1	0.8

① x is the mass fraction of water in the waste.

---

[2] U.S. Department of Energy (DOE), *Remote-Handled Transuranic Waste Authorized Methods for Payload Control (RH-TRAMPAC)*, current revision, U.S. Department of Energy, Carlsbad Field Office, Carlsbad, New Mexico.

The G values for net (total) gas are used in pressure calculations, and include the effect of oxygen consumption, if oxygen was present in the experiment as discussed in Appendix 2.1 of the RH-TRU Payload Appendices.

With time and constant exposure to radiation, hydrogen is removed from hydrogenous waste materials, thus decreasing the number of hydrogen bonds available for further radiolytic breakdown. For these waste materials, as the amount of available hydrogen is reduced with time, the G value decreases with increasing dose toward a value that is defined as the "dose-dependent G value." Dose-dependent G values for the bounding waste materials are provided in Table 2.2-2. The methodology associated with the determination of dose-dependent G values is further discussed in Attachment A of this appendix. As noted in Attachment A, dose-dependent G values are not applicable to solidified aqueous waste materials and the dose-dependent G values for alpha and beta radiation are not temperature dependent.

Table 2.2-2 – Summary of Dose-Dependent Hydrogen G Values for Bounding Materials in RH-TRU Waste

Waste Material	α and β Radiation Hydrogen Gas G Value at 70°F (molecules/100 eV)	γ Radiation Hydrogen Gas G Value at 70°F (molecules/100 eV)
Water	$1.6x$①	$1.6x$①
Polyethylene	0.64	4.1
Polyvinyl Chloride	0.50	0.7
Cellulose	1.09	3.2
Organic Resins	1.09	1.7
Other Polymers	1.09	4.1

① x is the mass fraction of water in the waste.

The use of the maximum and dose-dependent G values for bounding waste materials in determining content code-specific decay heat limits is described in Appendix 2.5 of the RH-TRU Payload Appendices.

2.2.3   Effective G Values for Content Codes

This section describes the methodology used to determine an effective G value for a content code, based on the fraction of the alpha, beta, and gamma energy absorbed by the gas generating materials in the content code. The use of effective G values in determining content code-specific decay heat limits is described in Appendix 2.5 of the RH-TRU Payload Appendices, along with the mathematical formulations and a detailed example determination. The general approach is described below.

The equation for an effective G value can be written as:

$$G_{eff} = \sum_M (F_P \ x \ F_M) \ x \ G_M$$
$$= \sum_M (F_M \ x \ G_M) \ x \ F_P$$

where,

F_P =   Fraction of energy emerging from the particles

F_M =   Weight fraction of material M in waste

G_M =   Bounding G value for material M.

Fraction of Energy Emerging from the Particles

Fraction of Alpha Energy Available for Gas Generation

Attachment B of this appendix describes a mathematical calculation of the fraction of alpha decay energy that escapes from a spherical particle containing uniformly distributed TRU nuclides. Attachment B of this appendix shows that a maximum of 82% of the alpha decay energy escapes from particles of PuO_2 when the particle size distribution is taken into account.

RH-TRU wastes consist of solid inorganic materials (e.g., glass and metal) and solid organic materials (e.g., paper and plastic) that may have been contaminated with particles of radioactive material, usually in the oxide form and solidified inorganic aqueous sludges consisting of precipitated salts. Radioactive elements will co-precipitate with the salts or sorb on the hydroxide/oxide precipitates.

For waste containing contamination in solution (i.e., solidified wastes), a maximum of 100% of the alpha decay energy may emerge from the particles.

For waste forms using dose-dependent G values, a value of 1.0 is used for the fraction of alpha energy emerging from the particles because the experimentally determined dose-dependent G values already account for particle size distribution and the experiments were conducted with materials representative of TRU waste.

Fraction of Beta Energy Available for Gas Generation

For the determination of effective G values for RH-TRU content codes, it is assumed that all beta energy is available for gas generation.

Fraction of Gamma Energy Available for Gas Generation

As described in Appendix 2.5 of the RH-TRU Payload Appendices, absorbed dose estimates for gamma energy are used to determine the fraction of the gamma energy that is available for gas generation. Input parameters needed for these estimations include the waste geometry, waste density, and the isotopic composition of the waste. The mathematical analysis for these estimations is provided in Appendix 2.5 of the RH-TRU Payload Appendices. If these input parameters cannot be quantified for a content code, it is conservatively assumed in the decay heat calculations that all gamma energy is available for gas generation.

Weight Fractions of Materials in Waste

The chemical list for the content code is used to determine the weight fraction of the materials listed in Table 2.2-1 or Table 2.2-2. As noted in Section 2.2.2, for organic materials not listed in the tables or if specific information on the weight fraction is not available, default assumptions (e.g., all organic material is assumed to be polyethylene) are used in determining the effective G value for the content code.

Bounding G Value for Material

The bounding G values are listed in Table 2.2-1 or Table 2.2-2.

Attachment A
Use of Dose-Dependent G Values for RH-TRU Wastes
A1.0 Background

This attachment describes controlled studies and experiments that quantify the reduction in the rate of hydrogen gas generation (G value) over time based on the total dose received by the target matrix. With time and constant exposure to radiation, hydrogen is removed from the hydrogenous waste or packaging material (the matrix), thus decreasing the number of hydrogen bonds available for further radiolytic breakdown (the matrix is depleted). Therefore, when the alpha,beta-generating source is dispersed in the target matrix, it will affect only that portion of the target material that is present in a small spherical volume surrounding the source particle. As the amount of available hydrogen is reduced over time, the G value decreases with increasing dose toward a value that is defined as the "dose-dependent G value." This phenomenon of matrix depletion has been studied and observed in previous studies (see Appendix 2.1 of the RH-TRU Payload Appendices). A formal study was undertaken to quantify dose-dependent G values under strictly controlled conditions and evaluate their applicability to transuranic (TRU) wastes.[3] This attachment summarizes the results of this study and derives dose-dependent G values for TRU waste materials, as applicable. Section A5.0 of this attachment specifically discusses the application of these dose-dependent G values to remote-handled (RH)-TRU wastes.

A2.0 Overview of the Matrix Depletion Program

The Matrix Depletion Program (MDP), established as a joint venture by the U.S. Department of Energy (DOE) National TRU Waste Program and the DOE Mixed Waste Focus Area, was comprised of the following elements:

1. Laboratory experiments for the assessment of effective G values as a function of dose for matrices expected in contact-handled (CH)-TRU wastes (polyethylene, polyvinyl chloride, cellulose, etc.), as well as an assessment of the impact of other variables (isotope, temperature, etc.) on the dose-dependent G values.

2. Measurements of effective G values and hydrogen concentrations in real waste and comparisons with dose-dependent G values.

3. Analysis to calculate effective G values from fundamental nuclear and molecular mechanisms.

A total of 60 one-liter test cylinders containing the simulated TRU waste materials were used, with two replicates for each test. Solid waste matrices (plastics and cellulose) were prepared by sprinkling the radioactive isotope powders over the matrix, folding the matrix over the contaminated surfaces, securing them, and placing them in test cylinders. Solidified waste matrices (cement) were mixed with a solution of dissolved plutonium oxide, water, and sodium hydroxide to adjust the pH. The test cylinders were connected to measurement devices that

---

[3] Idaho National Engineering and Environmental Laboratory, "TRUPACT-II Matrix Depletion Program Final Report," INEL/EXT-98-00987, Rev. 1, prepared for the U.S. Department of Energy, Idaho Operations Office, Idaho Falls, Idaho (1999).

facilitated sampling of generated gases and quantifying the gas generation over time. The entire test apparatus was controlled by a personal computer through LABVIEW software.

All activities of the MDP were performed under a documented quality assurance (QA) program that specified the performance-based QA/quality control requirements for all aspects of the program.[4] The experiments under the MDP were designed using an U.S. Environmental Protection Agency established procedure to formulate data quality objectives. QA objectives for the MDP were defined in terms of precision, accuracy, representativeness, completeness, and comparability. All data were validated and verified pursuant to the performance objectives of the program. The MDP was run for a duration of approximately three years.

A3.0 Results and Conclusions from the MDP

Results from the MDP are described in detail in the MDP final report[3] and are summarized in Table A-1 in terms of the dose-dependent G values for each matrix tested.

For all matrices, these dose-dependent G values were achieved within a maximum dose of 0.006 watt*year (product of watts times years). For example, for a waste container with a watt loading of 0.1 watt, the dose-dependent G value shown in Table A-1 would be reached after 0.06 years or 22 days. The lower the watt loading, the longer it would take for the watt*year criteria to be satisfied and the dose-dependent G value to be applicable.

Table A-1 – Experimental Dose-Dependent G Values

Matrix	Number of Observations	Mean	Standard Deviation	95% Upper Tolerance Limit[①]
Cement	202	0.25	0.18	0.58
Dry Cellulose	302	0.27	0.18	0.59
Polyethylene	186	0.23	0.22	0.64
Polyvinyl Chloride	99	0.14	0.19	0.50
Wet Cellulose	276	0.44	0.36	1.09

①   Dose-dependent G values.

The following conclusions can be drawn from the results of the MDP:

- Increasing dose (product of the decay heat loading and elapsed time) decreases the effective G value for hydrogen due to depletion of the matrix in the vicinity of the alpha-emitting radioactive source particle. The lower G value, called the "dose-dependent G value," is applicable after a dose of 0.006 watt*years.

- As with initial G values, the dose-dependent G values are a function of the waste matrix.

- Dose-dependent G values for wet cellulosics were higher than those for dry cellulosics because of the presence of water.

- The dose-dependent G values were independent of temperature based on testing performed at room temperature and at 140°F.

---

[4] Connolly, M.J., G.R. Hayes, T.J. Krause, and J.S. Burt, "TRUPACT-II Matrix Depletion Quality Assurance Program Plan," INEL95/0361, Rev. 1, Idaho National Engineering and Environmental Laboratory, Idaho Falls, Idaho (1997).

- Experiments performed with different particle sizes show that while initial G values could be higher for smaller particle sizes, the dose-dependent G values for all particle sizes tested are bounded by the values shown in Table A-1.

- Previous experiments that included agitation of cylinders similar to those used in the MDP indicated that agitation did not affect dose-dependent G values.[3]

- Isotopic composition did not have a significant impact on the dose-dependent G values based on experiments performed with two different isotopes of Pu (Pu-238 and Pu-239).

Data from TRU waste containers at the Rocky Flats Environmental Technology Site and the Idaho National Engineering and Environmental Laboratory show that even when compared to the mean dose-dependent G values from the matrix depletion experiments, G values from real waste containers are lower. Theoretical analysis, using nuclear and molecular level mechanisms, also shows that hydrogen generation from radiolysis and matrix depletion is consistent with the experimental results from the MDP.

A4.0 Effects of Agitation on Dose-Dependent G Values

The effects of agitation on dose-dependent G values have been evaluated by previous studies at both the laboratory-scale and drum-scale levels, and agitation has been found to have no impact on dose-dependent gas generation rates. Agitation could occur under transportation conditions but, as shown below, does not cause redistribution of the radionuclides to a non-depleted portion of the waste matrix and therefore does not cause an increase in the dose-dependent G values as shown in this section.

The earliest study of the effects of agitation on gas generation rates was performed by Zerwekh at the Los Alamos National Laboratory (LANL) in the late 1970s.[5] Zerwekh prepared an experimental array of 300-cm^3 stainless steel pressure cylinders, each loaded with 52.5 grams of a single or a combination of TRU waste matrix materials. Materials tested included cellulosics, polyethylene (PE) (low-density) bags, PE (high-density) drum liner material, and other typical TRU waste material. Net gas G values as a function of elapsed time were derived for each of the test cylinders and showed the characteristic decrease in G value with dose. Thorough mechanical shaking of two of the cylinders on two different occasions did not affect the rate of gas generation.[5]

In a second study, researchers at LANL retrieved six drums of Pu-238 contaminated waste from storage to study gas generation.[6] The wastes were contained in 30-gallon drums and consisted of either mixed cellulosic wastes or mixed combustible wastes. The drums ranged in age from four to ten years. Two of the drums containing mixed combustible wastes were tumbled end over end in a drum tumbler for four hours.[6] The researchers also reported G values for three drums of newly generated waste that were previously characterized. All six retrieved drums had measured G values that were lower than those measured for newly generated drums. The researchers concluded that the retrieved drums' effective hydrogen G values corroborate the matrix depletion observed for the previous laboratory-scale experiments.[5] Also, because of the vigorous nature of

---

[5] Zerwekh, A. "Gas Generation from Radiolytic Attack of TRU-Contaminated Hydrogenous Waste." LA-7674-MS, Los Alamos National Laboratory, Los Alamos, New Mexico, 1979.

[6] Zerwekh, A., J. Warren, and S. Kosiewicz. "The Effect of Vibration on Alpha Radiolysis of Transuranic (TRU) Waste." Proceedings of Symposium on Waste Management, Tucson, Arizona, 1993.

the agitation experienced by two of the four-year-old drums, the researchers concluded that radionuclide redistribution does not occur under transportation conditions.[6]

More recently, experiments on alpha radiolysis were conducted at LANL by Smith, et al.[7], to determine radionuclide loading limits for safe on-site storage of containers at LANL. Simulated TRU waste matrices in the form of cellulose (cheesecloth and computer paper) and PE (bottle and bag material forms) were contaminated with pre-weighed amounts of Pu-238 oxide powder. The first PE experiment (referred to as PE test cylinder 1) used a PE bottle to allow any potential later redistribution of the radionuclide particles to fresh matrix surfaces. The radionuclide powder was poured into the bottle, which was sealed and gently rolled to allow contamination of the sides of the bottle. The bottle was returned to an upright position and the lid was punctured with an approximately 0.5-inch diameter hole to allow free movement of generated gas from the bottle to the test canister. It was noted that the Pu-238 oxide powder adhered to the walls of the bottle and very little, if any, collected at the bottom. The remaining five test sample matrices were prepared by uniformly sprinkling the powder across a letter-sized sheet of the waste matrix, folding the sheet in toward the center from each end, and finally rolling each sheet into a cylindrical shape of about 2 by 4 inches. The six test matrices were placed inside six cylindrical, 2.06-liter stainless steel sealed canisters. Gas samples were extracted periodically and analyzed by mass spectrometry.

The first test canister for each waste material was subjected to vigorous dropping, rolling several times, and shaking on day 188 to simulate drum handling and transportation that could result in redistribution of the Pu-238 oxide to fresh non-depleted portions of the waste matrix. Any agitation effects were expected to be most pronounced for the test canister containing the PE bottle in PE test cylinder 1, because some aggregation of the powder at the bottom of the bottle was expected. However, no change in the effective hydrogen G value was observed for either the cellulose or PE test canisters.

In summary, three separate studies have investigated the ability of agitation to redistribute radionuclide particles to non-depleted surfaces of TRU waste matrices. All three studies conclusively showed that the dose-dependent G values are not impacted by agitation during transportation. Application of dose-dependent effective G values to RH-TRU waste is discussed in Section A5.0.

A5.0 Application of Dose-Dependent G Values to RH-TRU Wastes

Dose-dependent G values, based on the results of the MDP, are in principle applicable to all TRU wastes. The phenomenon of matrix depletion primarily stems from the nature of the waste matrix and the type of penetrating radiation; thus, if the waste matrix and radiation type are properly accounted for, G value results obtained for CH-TRU waste are also applicable to RH-TRU waste.

With respect to waste matrix, dose-dependent G values are not applicable to solidified aqueous materials. For these waste forms, the solidified aqueous nature precludes observation of matrix depletion (as the matrix near the Pu is depleted, water can move to replace the depleted matrix).

---

[7] Smith, M.C., E.L. Callis, J.H. Cappis, E.M. Foltyn, R.S. Marshall, and J. Espinoza. "Alpha Radiolytic Gas Generation: Determination of Effective G-values." Benchmark Environmental Corporation, Albuquerque, New Mexico, 1997.

With respect to radiation type, both CH- and RH-TRU waste are characterized by large amounts of alpha and beta emitters; the primary difference between the two waste forms is the noticeable presence of gamma emitters in RH-TRU waste. Thus, while the G value for CH-TRU waste is dependent primarily on the emitted decay heat (since most or all of the alpha and beta radiation is absorbed by the waste matrix and contributes to hydrogen gas generation), the G value for RH-TRU waste is dependent on the actual fraction of the decay heat that is absorbed by the waste matrix.

Since the results of the MDP are applicable only to alpha and beta radiation (gamma radiation effects were not quantified), G values for RH-TRU waste can be separated into those for alpha and beta radiation and gamma radiation and treated accordingly. Thus, RH-TRU waste G values for alpha and beta radiation can be treated as dose-dependent and the lower "dose-dependent G value" may be used after a dose of 0.012 watt*years (twice the highest value recorded in the experiments). G values for gamma radiation can conservatively be treated as not dose-dependent and the maximum G value must be used (see Table 2.2-2 of this appendix).

This page intentionally left blank.

Attachment B

Mass-Weighted Fraction of Energy Escaping From PuO₂ Particles

B1.0 Introduction

This attachment demonstrates that a maximum of 82 percent of the alpha decay energy escapes from particles of PuO_2 when the particle size distribution is taken into account.

B2.0 Mass-Weighted Fraction of Energy Escaping from PuO₂ Particles

Attachment B of Appendix 2.1 of the RH-TRU Payload Appendices describes the mathematical calculation of the fraction of alpha decay energy that escapes from a spherical particle containing uniformly distributed transuranic (TRU) nuclides. As the PuO_2 particle radius exceeds the stopping distance of the alpha particles, some of the alpha particles are completely absorbed within the PuO_2 particle. Only the outer shell of the PuO_2 particle (11-12 µm thick) contains radionuclides whose alpha particles can escape from the PuO_2 particle.

Many different particle-size distributions for PuO_2 have been reported in the literature. Mishima in his examination of transport methods for PuO_2 powder for fuel considered 13 different distributions.[8] The PuO_2 used for fuel fabrication is required to be finely divided powder or co-precipitate so that it can be intimately blended with UO_2 to form a mixed oxide fuel. It is unlikely that the PuO_2 found in surface-contaminated waste would be as fine a powder as is used in fuel fabrication. High efficiency particulate air (HEPA) filters in glovebox exhaust systems will trap the smaller particles, which more easily become airborne. Size distributions for aerosols are applicable only to HEPA filters (which typically have inorganic filtration media). Small particles can also agglomerate, creating larger particles.

The particle size distribution used in this document was chosen by Schwendiman[9] as most appropriate for evaluating leakage from a transportation container for PuO_2 powder. The distribution corresponds to 1,000°C calcined plutonium oxalate with a 15-minute dispersion prior to measurement. This particle size distribution is listed in Table B-1. The particle size distributions in most wastes are expected to have larger mean particle sizes.

These data were converted to mass fraction of particles having diameters between two values, and the mass fraction was assigned to a diameter corresponding to the range midpoint. The fraction of the alpha decay energy escaping from each size particle was calculated with the results and the mass-weighted total energy escaping from the PuO_2 particles tabulated in Table B-2 for Pu-239 and Table B-3 for Pu-238.

The conclusion drawn is that at most 82% of the alpha decay energy from particulate contamination is available to interact with waste materials.

---

[8] Mishima, J., and C. G. Lindsey, "Investigation into the Feasibility of Alternative Plutonium Shipping Forms," Pacific Northwest Laboratory, Battelle Memorial Institute, NUREG/CR-3007, PNL-4507, 1983.

[9] Schwendiman, L. C., "Supporting Information for the Estimation of Plutonium Oxide Leak Rates through Very Small Apertures, "Battelle, Pacific Northwest Laboratories, BNWL-2198, NRC-12, 1977.

Table B-1 – PuO$_2$ Particle Size Distribution

Particle Diameter and Smaller (µm)	Cumulative Percent by Weight
20	100
18	99
10	81
8	56
6	39
4	20
2	4
1	1
0.5	0.15
0.1	0.1

Source: Schwendiman, L. C., "Supporting Information for the Estimation of Plutonium Oxide Leak Rates through Very Small Apertures," Battelle, Pacific Northwest Laboratories, BNWL-2198, NRC-12, 1977.

Table B-2 – Mass-Weighted Total Energy Escaping from PuO$_2$ Particles for Pu-239[1]

Midpoint Particle Radius (µm)	Fraction of Alpha Energy Escaping	Mass Fraction in Distribution	Mass-Weighted Fraction of Energy Escaping
9.5	0.48	0.01	0.005
7.0	0.61	0.18	0.110
4.5	0.77	0.25	0.193
3.5	0.82	0.17	0.139
2.5	0.88	0.19	0.167
1.5	0.93	0.16	0.149
0.75	0.96	0.03	0.029
0.28	0.99	0.01	0.010
TOTAL			0.802

[1] Particles have the size distribution given in Table B-1.

Table B-3 - Mass-Weighted Total Energy Escaping from PuO$_2$ Particles for Pu-238[①]

Midpoint Particle Radius (µm)	Fraction of Alpha Energy Escaping	Mass Fraction in Distribution	Mass-Weighted Fraction of Energy Escaping
9.5	0.52	0.01	0.005
7.0	0.65	0.18	0.117
4.5	0.79	0.25	0.198
3.5	0.84	0.17	0.143
2.5	0.89	0.19	0.169
1.5	0.93	0.16	0.149
0.75	0.97	0.03	0.029
0.28	0.99	0.01	0.010
TOTAL			0.820

[①] Particles have the size distribution given in Table B-1.

This page intentionally left blank.

APPENDIX 2.3

SHIPPING PERIOD – GENERAL CASE

This page intentionally left blank.

2.3   Shipping Period – General Case

2.3.1   Introduction

The purpose of this appendix is to develop, on a conservative basis, the time for the shipping period from closure until venting that should be considered for the analysis of gas generation in the RH-TRU 72-B package.

2.3.2   Background

A large number of shipments of remote-handled transuranic (RH-TRU) waste have been planned between U.S. Department of Energy (DOE) facilities and the Waste Isolation Pilot Plant (WIPP). These shipments will be made by a fleet of trucks, each capable of transporting a single RH-TRU 72-B package, or by rail. The analysis in this appendix is presented for the case of shipments by truck. Shipments by rail shall meet the 60-day total maximum shipping period requirement for truck shipments. Using administrative controls, a 10-day shipping period is applicable for shipments to WIPP or other receiving sites as presented in Appendix 2.4 of the RH-TRU Payload Appendices.

The RH-TRU 72-B packages are loaded on specially designed trailers that travel over public highways on specified routes. The waste transportation activity will span a 25-year period. Because of the large number of trips and because of the agreements for notification to the states through which these shipments will pass on their way to WIPP or other receiving site, a state-of-the-art satellite tracking system will be employed to monitor the progress and position of each shipment. This monitoring capability will be available to authorities in the affected states as well as the transportation management people at the WIPP site and other receiving sites.

2.3.3   Approach

The approach to be taken in establishing the shipping period will be to develop a normal or expected shipment time based on the planned loading, transport, and unloading times. Then a maximum shipment time will be based on adding to the normal shipment time delays caused by a number of factors. This maximum shipment time will assume that each of these delays occurs. The probability of each of these delays occurring is small. The joint probability of all of these delays occurring would be extremely small. Thus, the development of a maximum shipment time based on the sum of extended delays for each of the factors is considered to have a large margin of error. In the event that a particular shipment is experiencing delays (for one reason or another) resulting in an abnormal shipment time, close monitoring of the delay by WIPP will ensure minimum delays in the schedule.

2.3.3.1   Normal or Expected Shipment Time

The normal transport time is the sum of the times associated with loading the RH-TRU 72-B package, the normal transit time, and the unloading of the package. The loading time to be considered as important is the time interval from closing (sealing) the inner vessel (IV) until the truck leaves the waste shipper's facility. The transit time is that time interval beginning with

departure from the shipper's facility and ending with the arrival at the WIPP site or other receiving site. The unloading time is that time interval beginning with the arrival at the receiving site and ending with the venting of the IV. This total time defines the expected shipment time.

2.3.3.2 Off-Normal or Maximum Shipment Time

The maximum shipment time includes those delays that could extend the shipment time. These delays are:

- Delays in loading or releasing the truck at the shipper's facility.

- Delays in transit caused by adverse weather conditions leading to road closures, or road closures due to accidents involving other vehicles.

- Accidents involving the shipment vehicle. These delays would include the time required for notification of appropriate authorities (including the DOE Emergency Response Team), and the time to take corrective action. This corrective action may involve transfer of the RH-TRU 72-B package to a back-up truck, which would require the services of heavy equipment.

- Delays in transit caused by mechanical problems with the truck. This factor would include such things as tire problems, broken belts and hoses, and any other such minor problems.

- Delays caused by one or both of the drivers becoming ill.

- Delays in unloading the RH-TRU 72-B package at the WIPP site or other receiving site. These could potentially be caused by factors such as truck arrival at the start of a long holiday weekend or equipment problems at the receiving site.

2.3.4 Discussion

2.3.4.1 Normal or Expected Shipment Time

As stated previously, the normal or expected shipment time is that time interval beginning with the sealing of the IV at the shipper's facility and ending with the venting of the IV in the WIPP site or other receiving site.

2.3.4.1.1 RH-TRU 72-B Package Loading

The package is designed so that it can be loaded within one eight-hour shift. However, to be conservative, one day (24 hours) is allotted for this activity.

2.3.4.1.2 Transit Time

Specific routes have been selected for transport of waste between the DOE facilities and from each of the DOE facilities to the WIPP site. The distances for the primary DOE facilities to the WIPP site are given in Table 2.3-1.

Table 2.3-1 — Normal Transit Times

To WIPP From	Distance (Miles)	Transit Time in Hours (Miles per Hour)				Transit Time in Days (Miles per Hour)			
		40	45	50	55	40	45	50	55
ANL	1727	43.2	38.4	34.5	31.4	1.7	1.6	1.4	1.3
BCL	1910	47.8	42.4	38.2	34.7	1.9	1.8	1.6	1.4
Bettis	2178	54.5	48.4	43.6	39.6	2.2	2.0	1.8	1.7
GE-VNC	1474	36.9	32.8	29.5	26.8	1.5	1.4	1.2	1.1
Hanford	1808	45.2	40.2	36.2	32.9	1.8	1.7	1.5	1.4
INL	1392	34.8	30.9	27.8	25.3	1.4	1.3	1.2	1.1
KAPL-NY	2225	55.6	49.4	44.5	40.5	2.2	2.1	1.9	1.7
LANL	342	8.6	7.6	6.8	6.2	0.3	0.3	0.3	0.3
MFC	1393	34.8	31.0	27.9	25.3	1.4	1.3	1.2	1.1
ORNL	1440	36.0	32.0	28.8	26.2	1.4	1.3	1.2	1.1
SNL	326	8.2	7.2	6.5	5.9	0.3	0.3	0.3	0.2
SRS	1540	38.5	34.2	30.8	28.0	1.5	1.4	1.3	1.2
WVDP	2391	59.8	53.1	47.8	43.5	2.4	2.2	2.0	1.8

These shipments will all be made by trucks having two drivers. Regulations governing maximum driving and on-duty times are given in 49 CFR 395, "Hours of Service of Drivers."[1]

Experience at the Idaho National Laboratory (INL) has shown that shipments of this type can achieve an average speed of 45 mph. This average speed includes stops for vehicle inspections every two hours, fueling, meals, driver relief and state vehicle inspections.

The normal transit times range from 0.3 day for shipments from LANL to 2.2 days for shipments from the West Valley Demonstration Project as shown in Table 2.3-1. For the purpose of conservatism, three days is assumed for a maximum normal transit time.

2.3.4.1.3 Unloading

Normal unloading will be accomplished in less than a day. Once the truck has undergone the health physics survey and security checks, the tractor is disconnected, and a trailer jockey is connected to the trailer. The trailer and package are cleaned, and the trailer is moved to the unloading area. The RH-TRU 72-B package is removed from the trailer and placed into the unloading area. The lid is removed after the containment vessel has been vented through a facility gas-handling system, and other procedural steps are then taken. The normal unloading of a trailer will be accomplished in less than one day. The unloading time is, thus, conservatively assigned a value of one day.

---

[1] Title 49, Code of Federal Regulations, Section 395 (49 CFR 395), "Hours of Service of Drivers."

2.3.4.1.4 Total Normal or Expected Shipment Time

The total normal or expected shipment time is three to five days depending on the origin of the waste. Normal loading time is one day, transit time is one to three days and unloading time is one day.

2.3.4.2 Off-Normal or Maximum Shipping Time

2.3.4.2.1 Loading Delays

There are a number of factors that could extend the time interval between the sealing of the IV and the truck getting under way:

- Loading could begin on a day preceding a holiday weekend.

- Difficulty testing the IV or outer cask (OC) seals.

- Handling equipment failure.

In the most severe sequence, loading could begin on a day preceding a long (holiday) weekend. If, for example, loading began on a Friday afternoon preceding a three-day weekend, loading would not be completed until the following Tuesday. This would result in a four-day loading period.

The IV or OC seal may fail the leak test, which would generally call for some maintenance. The worst case would probably be a failure in the leak test equipment that could take up to two days to correct.

The crane or the lifting fixture with center of gravity load compensation could also fail, forcing a delay in any further loading until corrected. This could also take two days.

It would be very unlikely for more than two of these scenarios to happen simultaneously, so a total of six days is deemed to be a reasonable maximum time to account for delays associated with loading. If there were conditions that could cause long, totally unanticipated delays, the RH-TRU 72-B package can be vented at the shipper's facility.

2.3.4.2.2 Transit Time Delays

There are several factors that could extend the normal transit time of three days. Adverse weather conditions could lead to delays and road closures. A telephone survey of states in the waste shipment corridor states was conducted to ascertain a reasonable time to assume for weather delays. Table 2.3-2 provides the results of this survey. One can conclude from this survey that weather conditions may close a major highway for two to five days. Long-term interruptions in normal traffic caused by bridge outages etc., would result in rerouting traffic to alternate routes. Accidents involving other vehicles could also cause delays and road closures of up to a day. It is concluded that a total transit delay of five (5) days is reasonable to assume for weather delays or road closures.

Accidents involving the shipment vehicle itself could cause lengthy delays. These delays would include the accident response time for notifying appropriate authorities (including Radiological Assistance Teams, if required) and the time to take corrective action or to mitigate the accident. One day is conservatively assumed for the response to the accident. (In addition to normal accident responses, monitoring of the satellite tracking system would also facilitate an early response to accidents). Corrective action may involve retrieving the RH-TRU 72-B package from a damaged trailer (including the possibility that the truck could be over an embankment), and transferring it to a back-up truck. Special equipment such as cranes may be required to carry out these operations. An accident mitigation time of five days will be assumed. This time includes the time for delivery of a back-up truck, and the time to move in special heavy equipment and rig special lifting fixtures to retrieve and transfer the packages to the back-up vehicle.

Delays in transit could be caused by routine mechanical problems with the truck. These problems could include tire failures, broken belts and hoses, electrical failures and similar minor problems; or more significant problems necessitating bringing a back-up truck into service. It is conservatively assumed that appropriate responses to mechanical failures of the truck can be made in four days.

Lastly, one or both of the drivers could become ill during the trip, necessitating the possibility that one driver must do all the driving or relief drivers would have to be sent to wherever the truck is parked. If one driver has to do all the driving, the transit time would be doubled (i.e., add three days). If relief drivers are required, a two-day delay will occur to allow for travel time of the replacement driver(s).

Table 2.3-2 — Survey of Weather Related Delays on Interstate Highways of the TRU Waste Shipment Corridor Sites

State/City	Office Contacted	Date Contacted	Type of Weather Related Delays	Highway
1. Alabama/Montgomery	State DOT	2/4/88	24 hrs. max.	All
2. Arizona/Phoenix	Dept. of Public Safety	2/4/88	8 hrs. maximum for any type of emergency.	All
3. Arkansas/Little Rock	State DOT Construction of Maintenance	2/17/88	1/2 day maximum.	All
4. California/Sacramento	State DOT Highway Dept.	2/18/88	2 days due to snow every 2 to 3 years. Few minutes to 2 to 3 weeks due to flood. 2 weeks due to earthquake. Detours provided.	I-5 I-15 Route 14
5. Colorado/Denver	State DOT	2/5/88	12 hrs. maximum.	
6. Georgia/Atlanta	State DOT Maintenance	2/2/88	No information available.	
7. Idaho/Boise	State DOT	2/4/88	3 to 4 hrs. due to blizzard.	
8. Illinois/Springfield	State DOT	2/7/88	10 days because a bridge pier slipped. (Trucks were off the road for 14 days). Detours provided.	Northbound I-90, I-94
9. Indiana/Indianapolis	Dept. of Highway Operations	2/5/88	2 days due to snowstorm or blizzard/wind.	I-65
10. Kentucky/Frankfort	State DOT Highway Maintenance	2/5/88	8 hrs. maximum.	
11. Louisiana/Boston Range	State DOT Office of Highway Traffic and Planning	2/3/88	No information available.	
12. Mississippi/Jackson	State DOT Highway Dept.	2/17/88	None.	
13. Missouri/Jefferson City	Highway Patrol	2/4/88	1/2 to 1 day due to flooding. 1 to 1-1/2 days with detours provided.	I-70
14. Nevada/Carson City	State DOT Maintenance Div.	2/4/88	4 to 8 hrs. due to snow.	I-80
15. New Mexico/Santa Fe	State DOT	2/9/88	Closed periodically due to snow and/or wind but for a very short period of time.	Interstate
16. Ohio/Columbus	State DOT	2/5/88	8 hrs. maximum.	All
17. Oklahoma/Oklahoma City	State DOT	2/5/88	1 month due to a bridge was washed out on Cimmaron River.	I-35
18. Oregon/Salem	State DOT	2/4/88	8 hrs. maximum. Generally, usage of highway stopped for trucks/oversized vehicles for up to 8 hours for icy conditions	Interstate
19. South Carolina/ Columbia	State DOT State Dept. of Health and Control	2/3/88	No information but generally 8 hrs. maximum.	

State/City	Office Contacted	Date Contacted	Type of Weather Related Delays	Highway
20. Pennsylvania/ Harrisburg	State DOT	2/22/91	No information but generally 1 day maximum	Interstate
21. Tennessee/Nashville	State DOT	2/3/88	96 hours due to rain. 72 Hours due to rain/high water level.	State Route 54 N in Haywood County State Route 188
22. Texas/Austin	State DOT	2/16/88	2 to 3 hours due to flooding. 8 hours maximum due to snow.	I-20
23. Utah/Salt Lake City	State DOT Traffic Engr.	2/4/88	4 to 5 hours due to blizzard.	I-15
24. Washington/Olympia	State DOT	2/4/88	2 days due to avalanche.	I-90
25. West Virginia/ Charleston	State DOT	2/19/91	1 day maximum	I-70
26. Wyoming/Cheyenne	State DOT Motor Vehicle Safety	2/4/88	4 to 5 days predominantly due to weather.	I-80

2.3.4.2.3 Unloading Delays

Delays in unloading the RH-TRU 72-B package at the WIPP site or other receiving site could be caused by a number of factors: A truck could arrive at the receiving site late on a Friday preceding a three day weekend, and the normal processing and unloading would not be completed until the following Tuesday, causing a delay in unloading of approximately 5 days. There could be equipment problems that could cause delays in unloading the package. Venting and handling equipment could break down. A total unloading time of four days will be assumed if unloading begins just before a regular weekend or five days for a holiday weekend. This is a reasonable maximum time to account for delays associated with unloading because the package can be vented at the receiving site (using workers overtime) if a totally unanticipated chain of delays were to occur.

2.3.4.2.4 Total Off-Normal or Maximum Shipment Time

The total off-normal or maximum shipment time is summarized in Table 2.3-3. A maximum shipment time of 31 days is projected assuming the worst-case scenario of all off-normal occurrences happening in the same shipment.

Table 2.3-3 — Shipment Time Summary

Activity	Time (Days)
Normal Shipment Time	
Loading	1
Transit Time	1-3
Unloading	1
Maximum Normal Shipment Time	3-5
Off-Normal Shipment Time[a]	
Loading	6
Transit Time	
• Normal (maximum)	3
• Weather delays and road closures	5
• Accident response	1
• Accident Mitigation	5
• Truck maintenance problems	4
• Driver illness	2
Unloading	5
Maximum Off-Normal Shipment Time	31

[a]Adding all the times for relatively low-probability, independent delays provides a conservative value for the maximum off-normal transit time.

2.3.5 Summary and Conclusions

The total normal or expected shipment time from the DOE facilities to the WIPP site or other receiving site will be three to five days with the longest time associated with the trip from the West Valley Demonstration Project to WIPP. The maximum or off-normal shipment time that has been postulated to occur as a consequence of a series of accidents or other off-normal events and delays is 31 days. This maximum shipment time is six times the maximum normal expected shipment time. This justifies using a 31-day period for the basis of determining potential buildup of flammable concentrations in the RH-TRU 72-B package under the specified normal conditions with the absence of venting or operational controls during transport. However, to add an additional margin of safety, the shipping period is nearly double the maximum off-normal shipment time, or 60 days, which is more than an order of magnitude longer than the maximum normal shipment time.

APPENDIX 2.4

SHIPPING PERIOD – CONTROLLED SHIPMENTS

This page intentionally left blank.

2.4   Shipping Period – Controlled Shipments

2.4.1 Introduction

This appendix presents the shipping period determination for shipments designated as controlled shipments. For these shipments, the RH-TRU 72-B packaging is loaded at the site, transported from the site to the Waste Isolation Pilot Plant (WIPP) or other receiving site, and vented within a maximum of 10 days from the closure (or sealing) of the inner vessel (IV). The basis for the 10-day shipping period is defined in this appendix. The use of a 10-day controlled shipment is an option available to sites that elect to impose administrative controls to ensure compliance with the conditions described herein.

2.4.2 Approach

The shipping period is defined to begin with closure (or sealing) of the IV during loading at the shipping facility and end with venting of the IV during unloading. Conservative time estimates for the following activities were used in determining the shipping period for controlled shipments:

- Loading time

- Transport time

- Unloading time.

2.4.2.1   Loading Time

The loading time begins with the sealing of the IV and ends with the departure of the shipment of the package from the site. Activities to be completed during the loading time include leak testing and handling of the loaded package(s). As directed by site procedures for controlled shipments, these activities must be completed within 24 hours. If these activities are delayed beyond 24 hours, the package(s) must be vented and the closure process repeated in accordance with the administrative controls described in Section 6.2.3 of the Remote-Handled Transuranic Waste Authorized Methods for Payload Control (RH-TRAMPAC)[1].

2.4.2.2   Transport Time

The transport time begins with the departure of the shipment from the site and ends with the arrival of the shipment at the receiving site. The transport time is dependent upon the distance between the two sites and capabilities for efficient response to potential transport time delays. As shown in Table 2.4-1, at an average speed of 40 miles per hour (mph) the longest travel time from a site to WIPP is 59.8 hours [corresponding to the 2,391-mile distance from the West

---

[1] U.S. Department of Energy (DOE), *Remote-Handled Transuranic Waste Authorized Methods for Payload Control (RH-TRAMPAC)*, current revision, U.S. Department of Energy, Carlsbad Field Office, Carlsbad, New Mexico.

Valley Demonstration Project (WVDP) to WIPP]. Controlled shipments shall be made only when the shipping distance between the two sites is bound by that shown for the WVDP to WIPP in Table 2.4-1. This average speed takes into account stops for vehicle inspections every two hours, fueling, meals, driver relief, and state vehicle inspections. Controlled shipments between sites are not allowed if the proposed distance exceeds 2,391 miles.

Table 2.4-1 — Normal Transit Times

To WIPP From	Distance (Miles)	Transit Time in Hours (Miles per Hour)				Transit Time in Days (Miles per Hour)			
		40	45	50	55	40	45	50	55
ANL	1727	43.2	38.4	34.5	31.4	1.7	1.6	1.4	1.3
BCL	1910	47.8	42.4	38.2	34.7	1.9	1.8	1.6	1.4
Bettis	2178	54.5	48.4	43.6	39.6	2.2	2.0	1.8	1.7
GE-VNC	1474	36.9	32.8	29.5	26.8	1.5	1.4	1.2	1.1
Hanford	1808	45.2	40.2	36.2	32.9	1.8	1.7	1.5	1.4
INL	1392	34.8	30.9	27.8	25.3	1.4	1.3	1.2	1.1
KAPL-NY	2225	55.6	49.4	44.5	40.5	2.2	2.1	1.9	1.7
LANL	342	8.6	7.6	6.8	6.2	0.3	0.3	0.3	0.3
MFC	1393	34.8	31.0	27.9	25.3	1.4	1.3	1.2	1.1
ORNL	1440	36.0	32.0	28.8	26.2	1.4	1.3	1.2	1.1
SNL	326	8.2	7.2	6.5	5.9	0.3	0.3	0.3	0.2
SRS	1540	38.5	34.2	30.8	28.0	1.5	1.4	1.3	1.2
WVDP	2391	59.8	53.1	47.8	43.5	2.4	2.2	2.0	1.8

The potential factors that could delay the normal transport time are as follows:

- Adverse weather

- Vehicle accidents

- Mechanical problems with the truck

- Driver illness.

Administrative controls in place at the shipping site prohibit the initiation of a controlled shipment at times when adverse weather exists or is forecasted. Any transport time delays associated with adverse weather are expected to be minimal and are, therefore, adequately covered by the margin of safety included in this analysis (see Section 2.4.4).

Prompt emergency response, truck maintenance, and driver or equipment replacement during the transport of controlled shipments is ensured by the application of additional resources. Administrative controls applied to all RH-TRU waste shipments regardless of destination require the designation of a shipment as a "controlled shipment" prior to initiation of the shipment from the site. This designation provides a trigger that requires additional resources to be available in order to provide accelerated response to avoid any significant delay during the transport time. This controlled shipment protocol is in addition to the routine use of the TRANSCOM system at WIPP, which provides continuous tracking of the shipment during transport regardless of its destination (i.e., to WIPP or other receiving site).

Vehicle accidents have the potential for the longest transport time delays due to the time required to respond and perform required corrective actions. Based on the training programs provided to local emergency response personnel along the transport routes, accident response time would be minimal (less than one hour). However, additional time may be required for notification and response of other appropriate authorities such as Radiological Assistance Teams (if required). Deployment of other appropriate authorities from WIPP, the shipping facility, or other intermediate site, whichever is closer, would take no more than 1 day to reach an accident scene. Prompt mitigation of any accident is ensured by the application of WIPP protocol for controlled shipments. Due to the additional resources available during controlled shipments, up to 2 days is considered appropriate for completing accident corrective actions. This time includes deployment of a backup truck and trailer, retrieving and transferring the package(s) to the backup vehicle, and performing any necessary surveys and/or inspections to confirm the shipment is prepared for continued transport.

Truck maintenance associated with common mechanical problems could result in transport time delays. The majority of routine mechanical problems (flat tires, belt or hose failures, etc.) can be rectified in a matter of hours. A worst-case mechanical problem would result in the need for a replacement truck, which is included in the time estimated for vehicle accident mitigation as described above.

The last remaining potential scenario for delaying the transport time is driver illness. The additional resources available for controlled shipments ensure prompt replacement of an ill driver. The time required to replace a driver is conservatively estimated as 1 day.

As a result of WIPP protocols applied to shipments designated as controlled shipments, a 5-day transport time accounts for any unexpected impact to the expected transport time.

2.4.3 Unloading Time

The unloading time begins with the arrival of the shipment at the receiving site and ends with the venting of the IV. Normal unloading will be accomplished in less than one day (24 hours). Section 6.2.3 of the RH-TRAMPAC outlines administrative controls imposed to ensure venting of the IV within 9 days of shipment departure from the shipping site[1].

2.4.4 Summary and Conclusions

Based on a loading time of 24 hours, an estimated transport time of less than 60 hours, and an unloading time of 24 hours, the normal expected shipping period for controlled shipments is 4 to 5 days. Using a conservatively estimated transport time of 5 days, the maximum expected shipping period for controlled shipments is 7 days. The additional contingency of a 3-day margin of safety results in a maximum shipping period of 10 days. Table 2.4-2 provides a summary of the activities comprising the shipping period.

Table 2.4-2 – Shipping Period Analysis Summary

Activity	Normal Expected Time (days)	Maximum Time Used in Analysis (days)
Loading Time	<1	1
Transport Time	1-3	5
Unloading Time	<1	1
Margin of Safety	–	3
Shipment Time	3-5	10

This analysis justifies using a 10-day period as the basis for determining compliance with gas generation requirements under rigorous operational controls during loading, transport, and unloading as specified in this appendix.

Sample shipping time data based on over 2,530 shipments of contact-handled transuranic waste to WIPP to date are shown in Table 2.4-3. As shown, all shipments have been made in well under 10 days even without the use of administrative controls specified in this appendix. Therefore, the controlled shipments completed under the conditions specified in this appendix will readily comply with the 10-day shipping period.

Only shipments designated as controlled shipments and, therefore, subject to the protocol described in this appendix and the administrative controls specified in Section 6.2.3 of the RH-TRAMPAC[1] for loading and unloading are eligible for evaluation using the 10-day shipping period.

Table 2.4-3 – Sample Shipping Time Data

To WIPP From	Total Number of Shipments as of 04-20-04	Average Shipping Time (hours)*	% of Time Shipments are Completed within Average Time	Shipping Time Delays	
				Duration of Maximum Delay	Explanation
ANL	11	43	100%	N/A	N/A
Hanford	76	43	98%	2 days	Weather delay; delay occurred at Hanford Site prior to shipment departure
INL	603	32	98%	5 days	Weather delay; delay occurred en route; shipment was returned to INEEL and delayed prior to second departure
LANL	71	9	98%	1 day	Delay occurred at LANL as the result of generator site issues prior to shipment departure
NTS	7	30	100%	N/A	N/A
RFETS	1,389	18	99%	2 days	Weather delay; delay occurred at RFETS prior to shipment departure and en route following departure
SRS	346	36	99%	3.7 days	Weather delay; delay occurred at SRS prior to shipment departure

*Average shipping times are estimated based on average speeds of 50 miles per hour and include time associated with safety inspections, fuel and food stops, and driver breaks.

N/A = Not applicable.

This page intentionally left blank.

APPENDIX 2.5

COMPLIANCE METHODOLOGY FOR GAS GENERATION REQUIREMENTS

This page intentionally left blank.

2.5 Compliance Methodology for Gas Generation Requirements

2.5.1 Summary

The hydrogen concentration must be maintained at or below 5% by volume within any confinement layer and the inner vessel (IV) during transport of the remote-handled transuranic (RH-TRU) waste materials. This appendix describes the logic and methodology used to evaluate compliance with this requirement for waste to be shipped in the RH-TRU 72-B. This methodology shall be implemented in the determination of flammable (gas/volatile organic compound [VOC]) concentration limits for each content code under the direction of the WIPP RH-TRU Payload Engineer.

Compliance with the 5% (by volume) limit on the hydrogen concentration can be demonstrated by one of two methods:

- **Compliance with Flammable Gas Generation Rate Limit:** The 5% (by volume) restriction on hydrogen concentration may be converted into a limit on the allowable flammable gas generation rate (FGGR) per container. If it can be shown for a given container that this limit can be met, the hydrogen concentration will remain at or below 5% under transportation conditions. A generalized procedure for determining the FGGR of a container is provided in Appendix 3.1 of the RH-TRU Payload Appendices. FGGR limits for each RH-TRU content code are specified in the RH-TRUCON document.[1]

- **Compliance with Decay Heat Limit:** Because radiolysis of the waste materials is the primary mechanism by which hydrogen is generated in TRU waste, the 5% (by volume) restriction on hydrogen concentration may be converted into a limit on the allowable decay heat per container. If it can be shown for a given container that this limit can be met, the hydrogen concentration will remain at or below 5% under transportation conditions. Procedures for determining the decay heat value for a container are described in Section 3.1 of the Remote-Handled Transuranic Waste Authorized Method for Payload Control (RH-TRAMPAC).[2] Decay heat limits for each RH-TRU content code are specified in the RH-TRUCON document.[1]

For each content code, the limit on the hydrogen concentration can be met either by complying with the FGGR limit or the decay heat limit. Specific examples of the determination of the FGGR and decay heat limits are provided in Section 2.5.5 and Section 2.5.6, respectively. Parameters that govern the FGGR and decay heat limits are summarized below:

FGGR Limit Parameters

- Waste packaging configuration (i.e., the number and type of confinement layers).

- Release rates of hydrogen from each of these confinement layers.

---

[1] U.S. Department of Energy, "RH-TRU Content Codes (RH-TRUCON)," DOE/WIPP 90-045, current revision, U.S. Department of Energy, Carlsbad Field Office, Carlsbad, New Mexico.

[2] U.S. Department of Energy, "Remote Handled Transuranic Waste Authorized Methods for Payload Control (RH-TRAMPAC)," current revision, U.S. Department of Energy, Carlsbad Field Office, Carlsbad, New Mexico.

- Operating pressure and temperature for the payload in the RH-TRU 72-B packaging IV during the shipping period.

- Void volume inside the container and in the IV outside the RH-TRU canister available for gas accumulation.

- Duration of the shipping period.

Decay Heat Limit Parameters (in addition to the FGGR limit parameters)

- Waste density and geometries of the RH-TRU canister and any inner containers.

- Hydrogen generation potential quantified by the G value for the waste material (the number of molecules of hydrogen produced per 100 eV of energy absorbed).

- Isotopic composition.

- Fraction of the gamma energy absorbed by waste material that could potentially generate hydrogen. [Packaging may include plastic bags or sheeting, or high-density polyethylene (HDPE) neutron shielding within the neutron shielded canister.]

2.5.2   Methodology for Determining Compliance with Gas Generation Requirements

Figure 2.5-1 is a flowchart showing the methodology used to demonstrate compliance with the 5% (by volume) limit on hydrogen concentration in the RH-TRU 72-B package. Appendices 4.1, 4.5, and 4.6 of the RH-TRU Payload Appendices demonstrate that chemical, biological, and thermal gas generation mechanisms are insignificant in the RH-TRU 72-B package. Because radiolysis of the waste materials is the primary mechanism by which hydrogen is generated in TRU waste, the 5% hydrogen concentration limit can be converted into limits on FGGR and decay heat. As shown in Figure 2.5-1, if potentially flammable VOCs exceed 500 parts per million, the 5% hydrogen concentration restriction is replaced by a reduced allowable flammable gas concentration (AFGC) that is then converted into similarly reduced limits on FGGR and decay heat in accordance with the methodology documented in Section 5.0 of the RH-TRAMPAC[2].

As shown in Figure 2.5-1, compliance with the limit on hydrogen concentration can be demonstrated by meeting either the FGGR or decay heat limit:

- If the actual FGGR for a container (as determined through the methodology of Appendix 3.1 of the RH-TRU Payload Appendices) is less than the FGGR limit specified by the content code for the container, the hydrogen concentration limit will be met. The determination of the FGGR limits for a content code is discussed in Section 2.5.3.
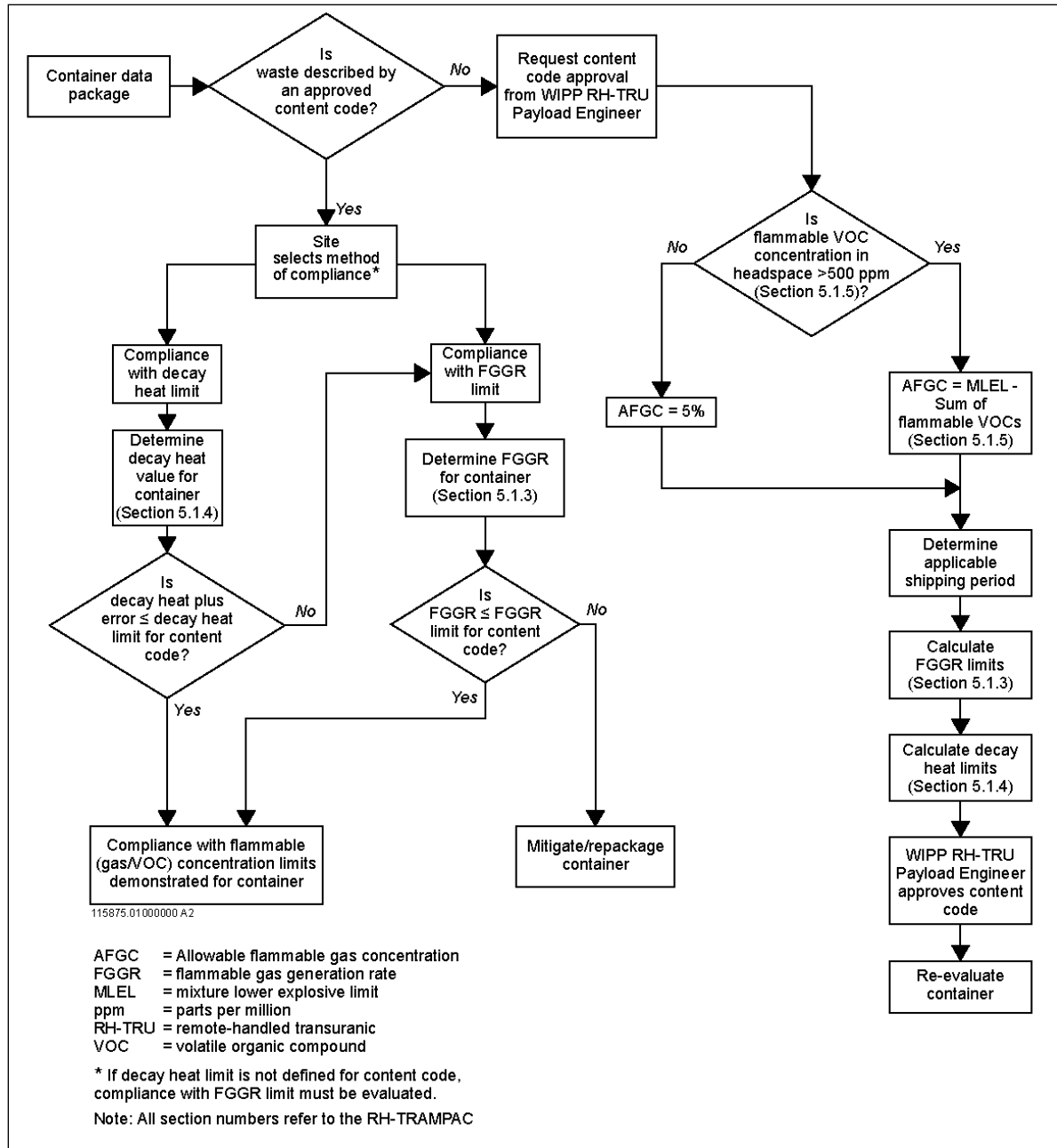
Figure 2.5-1 – Methodology for Compliance with Flammable (Gas/VOC) Concentration Limits

- If the decay heat value plus error for a container (determined as described in Section 3.1 of the RH-TRAMPAC) is less than the decay heat limit specified by the content code for the container, the hydrogen concentration limit will be met. The determination of the decay heat limits for a content code is discussed in Section 2.5.4.

Numerical examples for each compliance option are presented in Section 2.5.5 and Section 2.5.6.

2.5.3 Determination of FGGR Limits for Content Codes

2.5.3.1 Input Parameters

The parameters needing quantification include the following:

Waste Packaging Configuration and Release Rates

Each content code has a unique packaging configuration that is completely defined. A confinement layer is any boundary that restricts, but does not prohibit, the release of hydrogen gas across the boundary. Release rates of hydrogen through typical confinement layers used for RH-TRU waste packaging have been quantified at the reference temperature of 25°C (298 K)[3] and are summarized in Table 2.5-1. Packaging configurations that allow free release of hydrogen (e.g., punctured plastic bags, bags open at the end, pieces of plastic sheeting wrapped around the waste for handling, or metal cans with closures that allow free hydrogen release) are not considered confinement layers. Any other type of confinement layer (other than those with release rates listed in Table 2.5-1) shall be shown, by testing or analysis, to be equivalent to one of the confinement layers in Table 2.5-1 for purposes of minimum hydrogen release. "Equivalency" may be established by demonstration of a hydrogen release rate greater than or equal to one of the values specified in Table 2.5-1. In determining FGGR limits for content codes, the WIPP RH-TRU Payload Engineer shall use the release rates specified in Table 2.5-1 as the default values for confinement layers. Content code-specific release rates determined to be equivalent to those listed in Table 2.5-1 shall be documented by the site and approved by the WIPP RH-TRU Payload Engineer as described in Section 1.5 of the RH-TRAMPAC.

Release rates increase with increasing temperature[3]. To ensure the conservative calculation of FGGR limits, the release rate values in Table 2.5-1 (quantified at 25ºC [298 K]) are adjusted to those that occur at the lowest operating temperature (see "Temperature" below). Release rates may be calculated at any temperature as diffusivity varies with temperature raised to the 1.75 power. Thus, the release rate of a confinement layer at temperature absolute, T_2 (in K), may be calculated from the release rate at 298 K (25°C) listed in Table 2.5-1 through the following relationship:

Release Rate (T_2) = Release Rate (at 298 K from Table 2.5-1) $(T_2/298 \text{ K})^{1.75}$

---

[3] U.S. Department of Energy, "CH-TRU Waste Payload Appendices," current revision, U.S. Department of Energy, Carlsbad, New Mexico.

Table 2.5-1 – Release Rates of Hydrogen Through Common Confinement Layers

Confinement Layer	Release Rate (mole/sec/mol fraction) at 298 K (25°C)
Breather vent on can	5.18E-6
Filtered bag	1.075E-5
Fold-and-tape or twist-and-tape liner bag	4.67E-6[2]
Heat-sealed bag	$$RR = \frac{\rho\,A_p\,P_g}{x_p}\,\frac{mole}{22,400\,cm^3\,(STP)}$$ where, RR = Release rate of hydrogen, mole/sec/mol fraction H_2 ρ = Hydrogen permeability, cm^3 (STP) cm^{-1} (cm Hg)$^{-1}$ s^{-1} [3.6E-10 for polyvinylchloride and 8.6E-10 for polyethylene] A_p = Permeable surface area, cm^2 P_g = Gas pressure, 76 cm Hg x_p = Bag thickness, cm
Inner drum liner filter	3.70E-6
Drum filter	3.70E-6
Fixed lid canister filter (high diffusivity) [1]	9.34E-5
Fixed lid canister filter [1]	1.48E-5
Removable lid canister filter [1]	1.48E-5
NS15 neutron shielded canister open-cell urethane foam gaskets (2 ea. – combined)	7.38E-4[3]
NS30 neutron shielded canister open-cell urethane foam gaskets (2 ea. – combined)	7.96E-4[3]
NS15 neutron shielded canister filter[1]	1.48E-5
NS30 neutron shielded canister filter[1]	1.48E-5

[1]   Release rate meets the minimum filter specifications of Section 2.4 of the RH-TRAMPAC.

[2]   Release rate is valid for all temperatures.

[3]   Shaw Environmental, Inc., "Diffusivity and Flow Rates of PORON® Gaskets in RH-TRU Neutron Shielded Canisters," Shaw Environmental, Inc., December 2009.

Void Volumes in Confinement Layers

The void volumes for the confinement layers are based on waste generation and packaging processes. Outer void volumes are based on volumes of the inner containers.   For example, the void volume in the RH-TRU 72-B packaging IV with a canister is 450 liters, based on the size of the canister and the IV. The void volume in a canister with three 55-gallon drums is 240 liters based on the external volume of the three 55-gallon drums and the internal volume of the canister. Void volumes within drums and other inner containers and confinement layers are based on waste characterization data and conservative estimates documented by the sites for specific content codes approved by the WIPP RH-TRU Payload Engineer. When characterization data are not available, the conservative (i.e., minimum) default void volume values listed in Table 2.5-2 shall be used by the WIPP RH-TRU Payload Engineer to calculate FGGR limits. As shown in Table 2.5-2, a conservative void volume of 1 liter shall be used for any confinement layer without characterization data in order to minimize the FGGR limit. The default void volume for a canister containing up to three 55-gallon drums is listed in Table 2.5-2. If fewer than three 55-gallon drums or other inner containers, or drums of a smaller size, are packaged in a canister, the void volume value may be adjusted to account for the additional void volume. For example, for a canister with two 55-gallon drums, the additional void volume is added to the default value, and the resulting void volume is 240 liters + 208 liters (volume of a 55-gallon drum) = 448 liters.

Table 2.5-2 – Default Void Volumes in Confinement Layers

Confinement Layer	Void Volume (Liters)
Can	1
Bag layer	1
Inner drum liner	1
Drum	1
Canister (fixed or removable lid with waste directly loaded)	1
Canister (fixed or removable lid containing up to three 55-gallon drums)	240
NS15 neutron shielded canister (containing up to three approximately 15-gallon drums)	296
NS30 neutron shielded canister (containing up to three approximately 30-gallon drums)	335
RH-TRU 72-B packaging IV	450

Pressure

The pressure is assumed to be isobaric and equal to one atmosphere. The mole fraction of hydrogen in each void volume would be smaller if pressurization was considered, resulting in a greater FGGR limit. Furthermore, the amount of hydrogen gas generated during the shipping period would be negligible compared to the quantity of air initially present at the time of sealing the RH-TRU 72-B packaging.

Temperature

The input parameter affected by temperature is the release rates through different confinement layers. These release rates increase with increasing temperature.[3] Therefore, the minimum release rate and minimum FGGR limit occur at the lowest operating temperature. The FGGR limit calculations use the lowest operating temperature of -20°F, so that the minimum (i.e., the most restrictive) FGGR limit is obtained. This provides an additional margin of safety in the determination of the FGGR limit for each content code.

2.5.3.2 Mathematical Analysis

The FGGR limit for each content code is calculated using numerical solutions to differential equations that describe the unsteady-state mass balances on hydrogen within each confinement volume of the RH-TRU 72-B packaging. The FGGR that will yield 5 volume percent hydrogen within the innermost layer of confinement is not known *a priori* and is calculated using the iterative scheme described below.

In addition to the input parameters described in Section 2.5.3.1, the following assumptions have been made in deriving the governing equations:

- Hydrogen is an ideal gas and the ideal gas law applies.

- Hydrogen is assumed to be non-reactive with any materials in the payload container.

- FGGR is not reduced by depletion of the waste matrix.

- The concentration of hydrogen within each of the layers of confinement prior to loading in the RH-TRU 72-B packaging is assumed to be at steady-state (generation rate equals release rate). This assumption provides an additional margin of safety as maximum hydrogen concentrations exist at steady-state conditions.

The following list defines the variables that are used in the description of the mathematical framework.

Variables

n_i	=	Moles of hydrogen within void (i.e., confinement) volume "*i*" (mol).
k_i	=	Effective release rate of hydrogen across the confinement layer "*i*" (mol day^{-1} atm H$_2^{-1}$).
X_i	=	Mole fraction hydrogen in void (i.e., confinement) volume "*i*" (dimensionless).
R_i	=	Release rate of hydrogen across the confinement layer "*i*" (L/day).
V_i	=	Void volume within confinement layer "*i*" (L).
t	=	Time (days).
R	=	Gas law constant (0.08206 atm L mol^{-1} K^{-1}).
T	=	Absolute temperature (K).
P	=	Absolute pressure (1 atm).
P_i	=	Partial pressure hydrogen inside void (confinement) volume "*i*" (atm H$_2$)

2.5-7

CG   =   FGGR of innermost confinement layer (mol/sec).

N_i =   Number of generators in void (i.e., confinement) volume "*i*".

Subscripts

i   =   Void (i.e., confinement) volume for confinement layer "*i*".

NVV =   Number of void (i.e., confinement) volumes.

1   =   Innermost confinement volume or layer.

c   =   Canister void volume (i.e., the same layer as NVV-1)

IV   =   RH-TRU 72-B packaging IV void volume.

For brevity in subsequent discussions, a parameter C_1 is defined as:

Equation 1

$C_1 = CG \; x \; R \; x \; T \, / \, P$

In the determination of FGGR limits, a computer program is used to perform the iterative calculations. The steps in the calculational procedure are as follows: For a given content code, the number of void (i.e., confinement) volumes, the void volumes, and the release rates of hydrogen across confinement layers are read from an input data file. An initial gas generation rate, CG, of 1×10^{-8} mole/second per innermost confinement layer (ICL) is assumed. Prior to transport in the RH-TRU 72-B packaging, the concentration of hydrogen within each layer of confinement is assumed to be at steady-state. At steady state, the release rates of hydrogen across each layer are equal to the FGGR. The steady-state concentrations of hydrogen within each volume of confinement are evaluated from the equations below. It is assumed that the RH-TRU canister void volume (denoted by the subscript "NVV-1," or simply "c") has also attained a steady-state concentration of hydrogen prior to transport as an added margin of safety. For the case of the NS15 or NS30 neutron shielded canister, any flammable gas generation due to interaction of gamma energy with the neutron shield insert (HDPE) is conservatively assumed to be generated within the innermost layer of confinement.

The generation of hydrogen within the innermost layer, release across confinement layers, and accumulation within the confinement volumes during transport are simulated by numerically solving the system of hydrogen mass balance differential equations for each void volume. The derivation of the general system of differential equations representing hydrogen mass balances is presented below:

Innermost void (confinement) volume (i = 1)

The hydrogen mass balance within the innermost void (confinement) volume is:

Equation 2

Accumulation   =   Generation − removal by transport in response to concentration gradient

In terms of parameters, the hydrogen mass balance may be expressed as:

Equation 3

$$\frac{dn_1}{dt} = CG - k_1 \, (P_1 - P_2)$$

Applying the ideal gas law and assuming isobaric conditions such that P is constant total system pressure yields:

Equation 4

$$\frac{PV_1}{RT} \frac{dX_1}{dt} = CG - k_1 \, P \, (X_1 - X_2)$$

Rearranging terms and defining R_1 as k_1RT yields the following equation:

Equation 5

$$\frac{dX_1}{dt} = \frac{C_1}{V_1} - \frac{R_1 \, (X_1 - X_2)}{V_1}$$

Void (confinement) volumes (i = 2 to NVV-2)

The hydrogen mass balances in void volumes i = 2 to NVV-2, where the number of generators in void volume "i" is N_i, are given as:

Equation 6

$$\frac{dn_i}{dt} = N_i \, k_{i-1} \, (P_{i-1} - P_i) - k_i(P_i - P_{i+1}) \; \textit{for i = 2 to NVV} - 2$$

Applying the ideal gas law and assuming isobaric conditions such that P is constant total system pressure yields:

Equation 7

$$\frac{PV_i}{RT} \frac{dX_i}{dt} = N_i \, k_{i-1} \, P \, (X_{i-1} - X_i) - k_i P \, (X_i - X_{i+1}) \; \textit{for i = 2 to NVV} - 2$$

Rearranging terms and defining R_i as k_iRT yields the following equation:

Equation 8

$$\frac{dX_i}{dt} = \frac{N_i \, R_{i-1} \, (X_{i-1} - X_i)}{V_i} - \frac{R_i \, (X_i - X_{i+1})}{V_i} \; \textit{for i = 2 to NVV} - 2$$

Canister void (confinement) volume (i = NVV-1 = c)

The hydrogen mass balance in the canister void volume with the number of generators in the canister, N_c, is:

Equation 9

$$\frac{dn_c}{dt} = N_c k_{c-1}(P_{c-1} - P_c) - k_c(P_c - P_{IV})$$

Applying the ideal gas law and assuming isobaric conditions such that P is constant total system pressure yields:

Equation 10

$$\frac{PV_c}{RT}\frac{dX_c}{dt} = N_c k_{c-1} P(X_{c-1} - X_c) - k_c P(X_c - X_{IV})$$

Rearranging terms and defining R_c as $k_c RT$ yields the following equation:

Equation 11

$$\frac{dX_c}{dt} = \frac{N_c R_{c-1}(X_{c-1} - X_c)}{V_c} - \frac{R_c(X_c - X_{IV})}{V_c}$$

RH-TRU 72-B Packaging IV void (confinement) volume (i = NVV = IV)

The hydrogen mass balance in the RH-TRU 72-B packaging IV void volume is:

Equation 12

$$\frac{dn_{IV}}{dt} = k_c(P_c - P_{IV})$$

Applying the ideal gas law and assuming isobaric conditions such that P is constant total system pressure yields:

Equation 13

$$\frac{PV_{IV}}{RT}\frac{dX_{IV}}{dt} = k_c P(X_c - X_{IV})$$

Rearranging terms and using the definition of R_c defined previously (as $k_c RT$) yields the following equation:

Equation 14

$$\frac{dX_{IV}}{dt} = \frac{R_c(X_c - X_{IV})}{V_{IV}}$$

This system of differential equations (i.e., Equations 5, 8, 11, and 14) is solved numerically. Numerical solution implies obtaining the mole fractions of hydrogen in each void volume as a function of time. The solution proceeds until the simulation time equals the shipping period duration.

Derivation of the Steady-State Concentrations in Confinement Layers

At steady-state prior to loading in the RH-TRU 72-B packaging, the concentration of hydrogen outside the RH-TRU canister is zero (i.e., in Equation 14, $X_{IV} = 0$) and there is no accumulation of hydrogen within any confinement void. The steady-state concentrations in the different confinement layers are determined through the following algebraic equations.

For the ICL (i.e., $i = 1$), the steady-state hydrogen mass balance becomes:

Equation 15

$$\frac{dX_1}{dt} = 0 = \frac{C_1}{V_1} - \frac{R_1\,(X_1 - X_2)}{V_1}$$

For void volumes $i = 2$ to NVV-2 where the number of generators in void volume "i" is N_i, the steady-state hydrogen mass balances are given as:

Equation 16

$$\frac{dX_i}{dt} = 0 = \frac{N_i\,R_{i-1}\,(X_{i-1} - X_i)}{V_i} - \frac{R_i\,(X_i - X_{i+1})}{V_i} \; for\; i = 2\; to\; NVV - 2$$

For the canister, the hydrogen concentration outside the canister is assumed to be zero (i.e., $X_{IV} = 0$) such that at steady state Equation 11 becomes:

Equation 17

$$\frac{dX_c}{dt} = 0 = \frac{N_c\,R_{c-1}(X_{c-1} - X_c)}{V_c} - \frac{R_c\,X_c}{V_c}$$

The steady-state concentrations are then used to define the initial state of the system (i.e., hydrogen mole fractions within each confinement volume) at the time the RH-TRU 72-B packaging is sealed for transport as explained below.

For each container, an initial FGGR is assumed. Using the assumed FGGR, the steady-state concentrations in all void volumes for each container are calculated using the appropriate steady-state equations listed above. The steady-state concentrations serve as initial conditions for the solution of the system of differential mass balance equations representing the generation, accumulation, and transport of hydrogen within the various confinement volumes during transport. The appropriate system of differential equations (i.e., Equations 5, 8, 11, and 14) is solved numerically using the initially assumed FGGR for the container. Based on the predicted concentration within the ICL, the FGGR is adjusted accordingly. With the updated FGGR, the steady-state hydrogen mole fractions and the system of differential mass balances are solved again. The FGGR within the ICL is iteratively adjusted and the process is repeated until the predicted ICL hydrogen concentration is 0.05 mole fraction at the end of the shipping period. The FGGR that yields this concentration is the FGGR limit for that container and is specified in the content code approved by the WIPP RH-TRU Payload Engineer. A numerical example of this mathematical analysis is presented in Section 2.5.5.

2.5.4   Determination of Decay Heat Limits for Content Codes

2.5.4.1   Input Parameters

The calculation of decay heat limits requires knowledge of the FGGR limits. Therefore, the input parameters required to calculate FGGR limits are also required to calculate decay heat limits. In addition, the following parameters are needed:

Temperature

The input parameters affected by temperature are the release rates through different confinement layers and the G values for the waste materials. The minimum decay heat limits are determined by the ratio of these two parameters. In other words, the higher the release rate, the higher the decay heat limit; the higher the G value, the lower the decay heat limit. The dependence of G values on temperature is documented in Appendix 2.2 of the RH-TRU Payload Appendices. The temperature that yields the minimum decay heat limit for each content code is used as the calculation input parameter.

Based on the values presented in Table 3.4-3 and Table 3.4-4 of the RH-TRU 72-B SAR, the average payload temperatures (T_{ap} in ^{o}F) are approximately linear functions of the decay heat (Q in watts). Thus, the average payload temperature will vary for each content code. The relationships are represented by the following linear regression equations:

Paper Waste

$T_{ap} = 1.08288 \, Q + 123.593$

Metallic Waste

$T_{ap} = 0.18123 \, Q + 124.436$

The calculation of the decay heat limits for content codes is based on an iterative process until the applicable relationship is satisfied. The decay heat limits are calculated at 244 K and at the temperature that satisfies the applicable relationship for average payload temperature as a function of payload decay heat. The minimum value is selected as the decay heat limit for the content code. This provides an additional margin of safety in the determination of the decay heat limit for each content code.

Bounding G Values

The G value is a measure of the amount of gas generated from a waste material per unit (100 eV) of radioactive material present. Bounding G values of hydrogen for the different waste materials found in RH-TRU waste are presented in Appendix 2.2 of the RH-TRU Payload Appendices. If the bounding G values are used in the calculation of decay heat limits instead of the effective G values (see below), information for determining the effective G value and absorbed dose estimate described below is not required. The WIPP RH-TRU Payload Engineer shall determine the bounding G value for a content code using the chemical composition information provided by the site and the methodology specified in Appendix 2.2 of the RH-TRU Payload Appendices. The use of bounding G values is a conservative approach, and assumes that all energy in the waste is absorbed by the waste. This approach shall be used by the WIPP RH-TRU Payload Engineer if the parameters required for the calculation of effective G values and absorbed dose estimates cannot be quantified for a given content code.

Effective G Values

The logic of determining the effective G values, which accounts for the fraction of energy absorbed by the waste and the dose absorbed by the matrix material, is presented in Appendix 2.2 of the RH-TRU Payload Appendices. For alpha energy, 82.0% of the total energy is available for absorption by the waste material (except for waste containing contamination in solution, in which case 100% of the total energy is available). For beta energy, all of the energy is available for absorption by the waste material. For gamma energy, estimation of the amount of absorbed energy requires knowledge of the waste properties. For waste packaged in the neutron shielded canisters (NS15 or NS30), the shield insert (HDPE) must be included in the determination of the total waste density and gas generation from gamma energy.

The WIPP RH-TRU Payload Engineer shall determine the effective G value for a content code using the radionuclide and chemical composition information provided by the site and the methodology specified in Appendix 2.2 of the RH-TRU Payload Appendices. The WIPP RH-TRU Payload Engineer may conservatively use the bounding G values provided in Appendix 2.2 if the absorbed dose estimations cannot be quantified for a given content code.

Knowledge of the isotopic composition is necessary in order to establish what percentage of the emitted energy is due to alpha, beta, or gamma emitters. Absorbed dose estimates for the gamma energy in the waste also require a knowledge of the following waste properties:

- Waste density
- Container geometry.

The gamma energy absorbed by the waste is a function of the gamma emission strength, the quantity of gamma ray energy that is absorbed by collision with a waste particle, and the number of particles that interact with the gamma ray. Therefore, gamma energy absorption increases with increasing waste density. For a given waste density, a larger container will contain more particles, and, therefore, a higher percentage of the gamma ray energy would be absorbed than in a smaller container.

The methodology for using the dose-dependent G values specified in Appendix 2.2 of the RH-TRU Payload Appendices is presented in Section 2.5.4.2.

2.5.4.2 Compliance with Watt*Year Criteria

Containers may be evaluated for compliance with decay heat limits determined using dose-dependent G values if compliance with the criteria of >0.012 watt*year can be demonstrated. A discussion and derivation of watt*year criteria is provided in Attachment A of Appendix 2.2 of the RH-TRU Payload Appendices. Demonstration of compliance with the >0.012 watt*year criteria for a given container is carried out as follows:

1. Determine the effective G value and decay heat limit (Q) for the content code using the dose-dependent G values for alpha and beta radiation and non-dose-dependent G values for gamma radiation provided in Table 2.2-2 of Appendix 2.2 of the RH-TRU Payload Appendices.

2. Determine decay heat limit that excludes the gamma radiation contribution (Q_{allow}) as a function of the FGGR limit (Cg) and effective G value for the content code as follows:

Equation 18

$$Q_{allow} = \frac{Cg \ * \ N_A \ * \ 1.602(10)^{-19} \ watt\text{-}sec/eV}{G}$$

where,

Cg   =   FGGR limit for the content code obtained using the methodology described in Section 2.5.3.

G   =   Effective G value for the content code (molecules of hydrogen formed/100 electron volts [eV] emitted energy)

N_A =   Avogadro's number (6.023×10^{23} molecules/mole).

3. Determine the Q/Q_{allow} ratio, which represents the minimum fraction of the total container decay heat that excludes the gamma radiation contribution.

4. Calculate the decay heat value for a container ($Q_{watt*yr}$) needed to evaluate compliance with the watt*year criteria as:

Equation 19

$$Q_{watt*yr} = \frac{Q}{Q_{allow}} * Q_{actual}$$

where, Q_{actual}, is the actual decay heat value for the container.

5. The watt*year for the container is calculated as $Q_{watt*yr}$ times the elapsed time, and this value is compared to the >0.012 watt*year criteria. The elapsed time is the time between the generation of the container and the time of the compliance evaluation. If the resulting watt*year value is greater than 0.012 watt*year, the container may be evaluated for compliance with the decay heat limit calculated using the dose-dependent G value (Q) determined in Step 1 and provided in the content code approved by the WIPP RH-TRU Payload Engineer.

2.5.4.3   Mathematical Analysis

The mathematical analysis for calculating the decay heat limits for a content code includes the following inputs:

- Isotopic composition (e.g., activity fractions) of the waste within the container based on characterization data at a known point in time

- Elapsed time between the time associated with the isotopic composition and the time of compliance evaluation

- Waste composition (i.e., weight fractions of materials)

- G values for waste material, densities of waste material, and container geometry

- Shipping period duration.

This evaluation consists of iterating on the total activity (decay heat) until the FGGR is equal to the FGGR limit calculated in accordance with Section 2.5.3.

The methodology for calculating FGGR as a function of waste parameters is described in the RadCalc program.[4,5,6] This program calculates the radiolytic production of hydrogen in the waste matrix of radioactive waste and contains a robust decay algorithm that calculates the activity of a radionuclide and its associated daughter products using the Oak Ridge Isotope Generation and Depletion Code (ORIGEN) database.[4,5,6]

The quantity of hydrogen that may be potentially generated during transport in the RH-TRU 72-B packaging is a function of the amount of energy absorbed by the waste. The relationship between gas generation production potential and energy absorption is expressed by the effective G value. The amount of energy absorbed by the waste due to radioactive decay is a function of the isotopic composition and the specific activity of each nuclide (Ci/g of waste) and the density of the waste. The decay modes considered in these calculations are alpha, beta, and gamma emissions. For alpha emissions, 82% of the emitted energy is assumed to be absorbed by the waste (see Appendix 2.2 of the RH-TRU Payload Appendices). All beta-emitted energy is assumed to be absorbed by the waste. Only a percent of gamma energy will be absorbed by the waste and is a function of radionuclide composition, waste density, and container geometry. The RadCalc program calculates the absorbed gamma dose in the waste material.[4,5,6] The production of hydrogen is calculated by multiplying the total decay heat, or energy, produced of radiation type *j* for radionuclide *i* by the fraction of decay heat, or energy, absorbed in the waste material for that radiation type by the effective G value for the *jth* radiation type. Summing this product for all radiation types and radionuclides and multiplying by a conversion factor will result in an FGGR. Specifically, the FGGR (i.e., CG), is calculated as:

---

[4] Duratek Technical Services and Josephson Engineering Services 2005, RadCalc Volume I: User's Manual, current version, Duratek Technical Services and Josephson Engineering Services, Richland, Washington (http://www.radcalc.energy.gov).

[5] Duratek 2002a, RadCalc Volume II: Technical Manual, current version, Duratek Federal Services, Inc., Northwest Operations, Richland, Washington (http://www.radcalc.energy.gov).

[6] Duratek 2002b, RadCalc Volume IV: Database Manual, current version, Duratek Federal Services, Inc., Northwest Operations, Richland, Washington (http://www.radcalc.energy.gov).

Equation 20

$$CG = K \sum_{ij} G_j \, D_i \, E_{ij}$$

where,

i	=	Index for radionuclide
j	=	Index for radiation type (alpha, beta, or gamma)
G_j	=	Effective G value for radiation type j (molecules/100 eV)
D_i	=	Total number of disintegrations per unit time for radionuclide "i" (disintegrations/sec)
E_{ij}	=	Total energy absorbed per disintegration (eV/disintegration)
K	=	Conversion factor (1 / Avogadro's number) (1.66044×10^{-24} mole/molecule).

For known discrete gamma radiation, the total energy absorbed is calculated as follows:

Equation 21

$$E_{i\gamma} = \sum E_{i\gamma k} \, A_{i\gamma k} \, F(\rho, E_{i\gamma k}) + \overline{E'_{i\gamma}}$$

where,

k	=	Index for each discrete gamma "k"
$E_{i\gamma k}$	=	k^{th} discrete gamma energy
$A_{i\gamma k}$	=	Fraction of decays exhibiting the kth gamma
$F(\rho, E_{i\gamma k})$	=	Fraction of energy absorbed in the waste matrix (calculated through a polynomial regression equation as a function of waste density and energy emitted)
$\overline{E'_{i\gamma}}$	=	Electromagnetic radiation not accounted for amongst the known discrete gammas, usually very low energy x-rays.

For alpha and beta radiation, the total energy absorbed is simply the average recoverable decay heat, or energy, for the given disintegration type per disintegration. $E_{i\gamma k}$, and $A_{i\gamma k}$ data are taken from the Fusion Energy Nuclear Data Library (FENDL)/D-2.0 database.[4,5,6]

The decay heat limit for a container is conservatively calculated by the RadCalc program at the end of a user-specified decay time to be equal to the total recoverable energy. The decay heat limit is calculated as:

Equation 22

$$Q = K \sum_i A_i \, E_i$$

where,

Q   =   Decay heat (watt)

K   =   Conversion factor of 5.9×10^{-9} W/(Ci-eV)

A_i =   Activity in curies of nuclide "i"

E_i =   Total recoverable energy per disintegration of nuclide "i" (eV).

The total recoverable energy for a disintegration of each nuclide "i" is calculated in the RadCalc program as:

Equation 23

$$E_i = E_{\alpha,i} + E_{\beta,i} + E_{\gamma,i}$$

where,

$E_{\alpha,i}$ =   Average recoverable alpha energy per decay for radionuclide "i"

$E_{\beta,i}$ =   Average recoverable energy per decay for beta radiation for radionuclide "i"

$E_{\gamma,i}$ =   Average energy per decay for all gamma radiations for nuclide "i."

$E_{\alpha,i}$, $E_{\beta,i}$, and $E_{\gamma,i}$ originate from the FENDL/D-2.0 database.[4,5,6]

The activities or masses of the various radionuclides based on characterization data are specified as input to the RadCalc program. The time to decay the source is also specified as input to the program (i.e., the elapsed time between isotopic determination and compliance evaluation). RadCalc will perform decay and in-growth calculations and calculate the isotopic composition and decay heat of a container at the end of a user-specified decay time. The total activity is adjusted until the RadCalc calculated FGGR is equal to the FGGR limit calculated through the methodology in Section 2.5.3. The corresponding decay heat calculated by the RadCalc program then defines the decay heat limit for the container and is specified in the content code approved by the WIPP RH-TRU Payload Engineer.

2.5.5 Example Flammable Gas Generation Rate Limit Calculation

2.5.5.1 Introduction

This section provides an example calculation of the FGGR limits for Content Code ID 325B. A copy of Content Code ID 325B is provided in Section 2.5.7.

2.5.5.2 ID 325B Content Description and Waste Packaging Configuration

The waste consists of solid organic materials. The waste is packaged either in two 7.5-gallon metal cans or in one 5-gallon and one 10-gallon metal can. The metal cans are not considered layers of confinement because the lid of each can does not have a gasket, and there are holes drilled in the can sides to accommodate the placement of a lifting cable attachment. The metal cans are placed in a fiber drum pouch spreader, an inner polyvinyl chloride (PVC) pouch with a high-efficiency particulate air filter vent, a polyethylene drum liner, an outer PVC pouch with a filter vent, and a 17H 30-gallon drum with a filter vent or an opening in the drum lid. The inner PVC pouch is placed inside a rigid polyethylene liner without a lid. The liner and its contents

are then heat-sealed inside the outer PVC pouch. A maximum of three 30-gallon drums are placed into the RH-TRU canister with a fixed lid.

2.5.5.3 Operating Temperature Range

The minimum release rates are those at the lowest operating temperature of 244 K (-20ºF) and will yield the minimum FGGR limit. For purposes of calculating decay heat limits, the FGGR limit at the average payload contents temperature (T_{ap}) is needed. As stated in Section 2.5.4.1, an iterative process is used to determine the decay heat limit such that the relationship for T_{ap} as a function of payload decay heat for paper waste is satisfied. The calculation of the FGGR limit at T_{ap} is included in this section for use in calculating the decay heat limits, as shown in Section 2.5.6. As discussed in Appendix 2.2 of the RH-TRU Payload Appendices, there are two sets of G values for each content code depending on whether a container has satisfied the >0.012 watt*year dose criterion. Thus, there are two payload decay heat limits for each content code corresponding to the two G values. Because of the dependence of T_{ap} on the payload decay heat, there are also two values of T_{ap} for the example Content Code ID 325B. As a result of the iterative process (see Section 2.5.4.1), a T_{ap} of 324.3 K (124.0ºF) corresponding to a payload decay heat limit of 0.3963 watt is valid when dose ≤0.012 watt*year, and a T_{ap} of 324.7 K (124.8ºF) corresponding to a payload decay heat limit of 1.0820 watt is valid when dose >0.012 watt*year. The FGGR is always calculated at the lower of the two T_{ap} (i.e., when dose ≤0.012 watt*year) values as the flammable gas release rates and the FGGR are lower at the lower T_{ap} value.

2.5.5.4 Confinement Layer Flammable Gas Release Rates

From Table 2.5-1, the hydrogen release rate across a heat-sealed polymer bag (RR) is:

Equation 24

$$RR = \frac{\rho\, A_p\, P_g}{x_p} \frac{mole}{22,400\, cm^3\,(STP)}$$

where,

RR   =   Release rate of hydrogen (mole/sec/mol fraction H_2)

ρ   =   Hydrogen permeability [cm^3 (STP) cm^{-1} (cm Hg)$^{-1}$ s^{-1}]

Ap   =   Permeable surface area (cm^2)

Pg   =   Gas pressure (76 cm Hg)

xp   =   Bag thickness (cm).

The temperature dependence of gas permeability across a polymer can be defined by an Arrhenius equation:

Equation 25

$$\rho = \rho_0\, \exp\!\left(\frac{-E_a}{RT}\right)$$

where,

E_a =   Activation energy associated with gas permeability (kcal)

R   =   Gas constant defined as 1.99E-3 kcal/(mol K)

T   =   Absolute gas temperature (K).

For a hydrogen permeability for PVC of 3.6E-10 cm^3(STP) cm^{-1} (cm Hg)$^{-1}$ s^{-1} at 77°F (298.2 K)[7] with an activation energy of 1.9 kcal/mole, the constant, ρ_0, is defined as 8.89E-9 cm^3 (STP) cm^{-1} (cm Hg)$^{-1}$ s^{-1}. The hydrogen permeability for PVC at 244 K is calculated from Equation 25 as:

$$\rho = 8.89E\text{–}9\ cm^3(STP)\,cm^{-1}(cmHg)^{-1}s^{-1}\ \exp\left(\frac{-1.9\,kcal/mole}{1.99E\text{–}3\,kcal/(mole\,K)\times 244\,K}\right)$$

$$\rho = 1.78E\text{-}10\ cm^3\,(STP)\ cm^{-1}\ (cm\ Hg)^{-1}\ s^{-1}$$

Similarly (for use in calculating the decay heat limit), the hydrogen permeability for PVC at 324.3 K is calculated as 4.68E-10 cm^3 (STP) cm^{-1} (cm Hg)$^{-1}$ s^{-1}.

The minimum permeable surface area inside the 30-gallon waste drum was calculated based on the waste drum configuration described by IT Corporation for this waste[8]. The permeable surface area of a PVC pouch is defined by its minimum height and diameter. The maximum outside diameters of the 7.5-gallon steel cans and polyethylene drum liner are 15 in (38.1 cm) and 18 in (45.7 cm), respectively. The 30-gallon drum has a useable height of 28 in (71.1 cm). The diameters of the inner and outer PVC pouches are conservatively assumed to be 16 in (40.6 cm) and 17 in (43.2 cm), respectively. Because of the presence of a fiberboard pouch spreader and polyethylene drum liner, the heights of the inner and outer PVC pouches are assumed to be 26 in (66.0 cm) and 27 in (68.6 cm), respectively. The dimensions of the inner PVC pouch, assumed to be that of a cylinder, are used to define the surface of both PVC pouches. The surface area along the side and top of the cylinder define the total surface area. The permeable area of each PVC layer was calculated to be 9,700 cm^2, and its thickness is 20 mils (0.0508 cm). The release rate by hydrogen permeation through a PVC pouch at 25°C (298 K) is calculated from Equation 24 to be:

$$RR = \frac{3.6E-10\,cm^3(STP)\,cm^{-1}(cmHg)^{-1}s^{-1}\times 9700\,cm^2\times 76\,cmHg}{0.0508\,cm}\ \frac{mole}{22{,}400\,cm^3(STP)}$$

$$RR = 2.34E\text{-}7\ mole/s\ at\ 25°C\ (298\ K)$$

The release rates by hydrogen permeation through a PVC pouch at 244 K and 324.3 K were calculated from Equation 24 to be 1.15E-7 mole/s and 3.03E-7 mole/s, respectively.

Temperature-corrected hydrogen diffusivity values across filter vents used on the filtered PVC pouches, on the 30-gallon drum, and on the fixed lid canister at an absolute temperature, $D(T_2)$, can be defined in terms of the minimum hydrogen diffusivity across the same filter vent at the measured temperature, T_1, of 25°C (298 K) such that:

---

[7] Perry, R. H., D. W. Green, and J. O. Maloney, 1984, Perry's Chemical Engineers' Handbook, Sixth Edition, McGraw-Hill Book Company, New York, New York.

[8] IT Corporation, July 2003, "AK Documentation Report for INEEL-Stored Remote-Handled Transuranic Waste from Argonne National Laboratory-East," Revision 0, IT Corporation, Albuquerque, New Mexico.

Equation 26

$$D(T_2) = D(T_1)\left(\frac{T_2}{T_1}\right)^{1.75}$$

The release rates (hydrogen diffusivities) of the filters on the PVC pouch, 30-gallon drum, and fixed lid canister at 25°C (298 K) are 1.075E-5 mole/s/mole fraction, 3.70E-6 mole/s/mole fraction, and 9.34E-5 mole/s/mole fraction, respectively, from Table 2.5-1.

The effective release rate across the filtered PVC pouch is by a combination of diffusion and permeation. Thus, the effective release rate is the sum of the two release rates:

　　　　1.075E-5 + 2.34E-7 = 1.10E-5 mole/s/mole fraction

The applicable flammable gas release rates for ID 325B are listed in Table 2.5-3.

Table 2.5-3 – Release Rates of Hydrogen Through Confinement Layers for Content Code ID 325B

Confinement Layer	Release Rate (mole/s/mol fraction) at 298 K (25°C)	Release Rate (mole/s/mol fraction) at 244 K	Release Rate (mole/s/mol fraction) at 324.3 K
Filtered PVC Pouch	1.10E-5	7.70E-6	1.28E-5
Drum Filter	3.70E-6	2.61E-6	4.29E-6
Canister Filter (Fixed Lid)	9.34E-5	6.58E-5	1.08E-4

Based on the packaging configuration, the release of flammable gas from the waste occurs in series through the filtered PVC pouches, the 30-gallon drum filter, and the fixed lid canister filter. At 244 K, the effective release rate from the two filtered PVC pouches representing the ICL is calculated as:

　　　　ICL Release Rate = 7.70E-6 mole/s/mole fraction / 2 = 3.85E-6 mole/s/mole fraction

At 324.3 K, the effective release rate from the two filtered PVC pouches representing the ICL is calculated as:

　　　　ICL Release Rate = 1.28E-5 mole/s/mole fraction / 2 = 6.40E-6 mole/s/mole fraction

2.5.5.5   Confinement Layer Void Volumes

For this example, a void volume of 240 liters for the canister void is used as an additional margin of safety even though three 30-gallon drums occupy only approximately half of the volume of 55-gallon drums (see Table 2.5-2). The void volumes within the 30-gallon drum (i.e., outside the outer PVC pouch) and within the PVC pouches (ICLs) are each conservatively assumed to be 1 liter (see Table 2.5-2). Table 2.5-4 summarizes the various void volumes for Content Code ID 325B that will be used to calculate the FGGR limits (default values from Table 2.5-2).

Table 2.5-4 – Confinement Layer Void Volumes for Content Code ID 325B

Confinement Layer	Void Volume (L)
Innermost Confinement Layer (2 filtered PVC pouches)	1
30-Gallon Drum	1
Canister (Fixed lid containing up to three 30-gallon drums)	240
RH-TRU 72-B packaging IV	450

2.5.5.6 Calculational Methodology

The calculation methodology involves numerically solving the system of differential equations that describe the unsteady-state mass balances on flammable gas within each confinement volume in the RH-TRU 72-B package. The applicable equations are Equations 5, 8, 11, and 14. The FGGR that yields 5 volume percent (i.e., 0.05 mole fraction) within the ICL at the end of the shipping period is not known *a priori*. The rate is calculated through an iterative scheme as described below.

For the case of a container of Content Code ID 325B, there are four void volumes (ICL, 30-gallon drum, canister, and RH-TRU 72-B packaging IV) and the following four flammable gas mass balance differential equations in the system:

Innermost Void (Confinement) Volume (i = 1)

The hydrogen mass balance within the innermost void (confinement) volume (i = 1) is:

Equation 27

$$\frac{dX_1}{dt} = \frac{C_1}{V_1} - \frac{R_1 \ (X_1 - X_2)}{V_1}$$

Drum Void (Confinement) Volume (i = 2)

The hydrogen mass balance in the 30-gallon drum void volume (i = 2) is:

Equation 28

$$\frac{dX_2}{dt} = \frac{R_1 \ (X_1 - X_2)}{V_2} - \frac{R_2 \ (X_2 - X_3)}{V_2}$$

Canister Void (Confinement) Volume (i = 3)

The hydrogen mass balance in the canister void volume (i = 3) with three 30-gallon drums (i.e., generators such that $N_3 = 3$) within the canister is:

Equation 29

$$\frac{dX_3}{dt} = \frac{N_3 \ R_2 (X_2 - X_3)}{V_3} - \frac{R_3 (X_3 - X_4)}{V_3}$$

RH-TRU 72-B IV Void (Confinement) Volume (i = 4)

The hydrogen mass balance in the RH-TRU 72-B packaging IV void volume is:

Equation 30

$$\frac{dX_4}{dt} = \frac{R_3\,(X_3 - X_4)}{V_4}$$

where,

X_i	=	Mole fraction hydrogen in void (i.e., confinement) volume "i" (dimensionless)
R_i	=	Effective release rate of hydrogen across the confinement layer "i" (L/day)
V_i	=	Void volume within confinement layer "i" (L)
t	=	Time (days)
R	=	Gas law constant (0.08206 atm L mol^{-1} K^{-1})
T	=	Absolute temperature (294 K)
P	=	Absolute pressure (1 atm)
CG	=	Hydrogen gas generation rate per ICL (mol/s) within a 30-gallon drum
N_i	=	Number of generators in confinement volume "i".

Subscripts

i	=	Confinement layer "i"
1	=	Innermost confinement layer
2	=	30-gallon drum
3	=	Canister
4	=	RH-TRU 72-B packaging IV

and

$$C_1 = CG \times R \times T / P$$

To derive the steady-state concentrations, Equation 27 through Equation 29 are each equated to zero (as there is no accumulation of flammable gas), and the concentration of flammable gas outside the canister is set to zero (i.e., $X_4 = 0$) in Equation 29. The resulting system of algebraic equations is solved for the steady-state concentrations in the different confinement layers to arrive at the following:

The canister steady-state flammable gas concentration, $X_3(ss)$, is given as:

Equation 31

$$X_3(ss) = \frac{3\,C_1}{R_3}$$

The drum steady-state flammable gas concentration, $X_2(ss)$, is given as:

Equation 32

$$X_2(ss) = X_3(ss) + \frac{C_1}{R_2}$$

The ICL steady-state flammable gas concentration, $X_1(ss)$, is given as:

Equation 33

$$X_1(ss) = X_2(ss) + \frac{C_1}{R_1}$$

The steady-state concentrations are then used to define the initial state of the system (i.e., flammable gas mole fractions within each confinement volume) at the time the RH-TRU 72-B packaging is sealed for transport. An initial gas generation rate, CG (initial), is assumed. Equation 31 through Equation 33 are then solved to define the initial concentrations in the container and canister void volume at the time of sealing the RH-TRU 72-B packaging. The system of Equation 27 through Equation 30 is then solved to arrive at the ICL concentration (X_1) at the end of an assumed 60-day shipping period. Depending on the value of the ICL concentration, X_1, the FGGR, CG, is adjusted accordingly and the process repeated iteratively until X_1 is 0.05 at the end of an assumed 60-day shipping period.

The parameter values used in Equation 27 through Equation 33 are listed in Table 2.5-5. Steady-state concentrations calculated using Equation 31 through Equation 33 are listed in Table 2.5-6. The flammable gas concentrations in the various confinement volumes within the RH-TRU 72-B packaging at the end of the 60-day shipping period are listed in Table 2.5-7.

Table 2.5-5 – Parameter Values for Equation 27 through Equation 33

Symbol	Value at 244 K	Value at 324.3 K
R_1	6.66 L/day	14.68 L/day
R_2	4.52 L/day	9.86 L/day
R_3	113.8 L/day	249.0 L/day
V_1	1.0 L	1.0 L
V_2	1.0 L	1.0 L
V_3	240 L	240 L
V_4	450 L	450 L
N_3	3	3
C_1	7.715E-2 L day^{-1}	1.146E-1 L day^{-1}

Table 2.5-6 – Steady-State Flammable Gas Concentrations for Content Code ID 325B

Void Volume	Symbol	Mole Fraction at 244 K	Value at 324.3 K
Innermost Confinement Layer	$X_1(ss)$	0.03070	0.02081
30-Gallon Drum	$X_2(ss)$	0.01912	0.01300
Canister	$X_3(ss)$	0.00203	0.00138

Table 2.5-7 – Flammable Gas Concentrations at 60 Days for Content Code ID 325B

Void Volume	Symbol	Mole Fraction at 244 K	Value at 324.3 K
Innermost Confinement Layer	X_1	0.04999	0.05000
30-Gallon Drum	X_2	0.03846	0.04222
Canister	X_3	0.02152	0.03070
RH-TRU 72-B IV void	X_4	0.02021	0.02981

Based on this methodology the FGGR limits at the minimum and maximum temperatures were calculated to be:

At 244 K, FGGR = 3.701E-8 mole/s per drum

At 324.3 K, FGGR = 5.498E-8 mole/s per drum.

The lower FGGR value calculated at 244 K is the applicable FGGR limit for the drums assigned to Content Code ID 325B. Both FGGR values are used to determine the decay heat limits for Content Code ID 325B as shown in Section 2.5.6. As up to three drums may be packaged in each canister, the FGGR limit per canister is three times the FGGR limit for the drum.

2.5.6 Example Decay Heat Limit Calculation

2.5.6.1 Introduction

This section provides an example calculation of the decay heat limits for Content Code ID 325B. A copy of Content Code ID 325B is provided in Section 2.5.7.

2.5.6.2 Content Code ID 325B Flammable Gas Generation Rate Limits

As demonstrated in Section 2.5.5, the 5% limit on hydrogen concentration can be converted into FGGR limits. The FGGR limits can then in turn be converted into decay heat limits using the appropriate G value. The FGGR limits for Content Code ID 325B were calculated at 244 K and at 324.3 K in the example provided in Section 2.5.5 and are summarized in Table 2.5-8. The FGGR limits per canister are also listed in Table 2.5-8 in units of cm³/hour at the standard temperature and pressure (STP) of 0ºC and 1 atm. The units of cm³ (STP)/hour for the FGGR are those reported by the RadCalc program, which is used to establish the decay heat limits. This

section provides a specific example of how the FGGR limits are used to establish the decay heat limits for Content Code ID 325B.

Table 2.5-8 – Flammable Gas Generation Rate Limits for Content Code ID 325B

Temperature (K)	FGGR Limit per Drum (mole/sec)	FGGR Limit per Canister (mole/sec)	FGGR Limit per Canister (cm^3/hour at STP [0°C and 1 atm])
244	3.701E-08	1.110E-07	8.959
324.3	5.498E-08	1.649E-07	13.31

2.5.6.3   Effective G Value for Content Code ID 325B

Bounding G values of hydrogen for RH-TRU waste are presented in Appendix 2.2 of the RH-TRU Payload Appendices. Based on the materials listed in the chemical list for Content Code ID 325B, the two bounding materials are cellulose and polyethylene (PE). To establish the governing effective G value, the effective G values for each of these two materials are calculated at 244 K, 324.3 K, and at 324.7 K.

As discussed in Appendix 2.1 of the RH-TRU Payload Appendices, G values follow an Arrhenius-type function dependence on temperature based on the activation energy (E_a) for the material. The temperature-corrected effective G value at an absolute temperature T_2 is calculated through the following Arrhenius equation:

Equation 34

$$G_{eff}(T_2) = G_{eff}(T_1) \exp \{(E_a / R)[(T_2 - T_1)/(T_2 \ x \ T_1)]\}$$

> where:
>
> $G_{eff}(T_1)$ =   Effective G value at room temperature (i.e., 70°F) [the number of molecules of gas generated per 100 eV of energy (molecules/100 eV) for target material at room temperature]
>
> E_a =   Activation energy for target material (kcal/mol)
>
> R   =   Ideal gas constant (1.99 x 10^{-3} kcal/mole-K)
>
> T_2 =   Absolute average contents temperature (either 244 K, 324.3 K, or 324.7 K)
>
> T_1 =   Room temperature (70°F, 21°C, or 294 K).

Based on the G values at 70°F (294 K) and the activation energies for these two materials as listed in Table 2.2-1 of Appendix 2.2 of the RH-TRU Payload Appendices, the G values were calculated at 244 K and at 324.3 K using Equation 34 and are summarized in Table 2.5-9. The bounding material at 244 K and 324.3 K is PE. The bounding G values for Content Code ID 325B are listed in the last column of Table 2.5-9.

Table 2.5-9 – G Values for Cellulose and Polyethylene (Dose ≤0.012 watt*year)

Temperature (K)	Cellulose G Value	Polyethylene G Value	Bounding G Value for Content Code ID 325B
244	1.53	3.10	3.10
324.3	4.48	4.66	4.66

For containers of Content Code ID 325B that have met the >0.012 watt*year criteria, dose-dependent G values for alpha and beta radiations are not temperature corrected based on the results of the Matrix Depletion Program (MDP) testing as stated in Attachment A to Appendix 2.2. The dose-dependent G values based on the results of the MDP program at 244 K and at 324.7 K are summarized in Table 2.5-10. The bounding material at 244 K and 324.7 K is cellulose for alpha and beta radiation. The bounding G values for Content Code ID 325B are listed in the last column of Table 2.5-10.

Table 2.5-10 – G Values for Cellulose and Polyethylene (Dose >0.012 watt*year)

Temperature (K)	Cellulose G Value	Polyethylene G Value	Bounding G Value for Content Code ID 325B
244	1.09	0.64	1.09
324.7	1.09	0.64	1.09

Using Equation 34, the effective gamma radiation G value of 4.67 molecules/100 eV is calculated at 324.7 K when the dose >0.012 watt*year. Table 2.5-11 summarizes all the effective G values for Content Code ID 325B at the minimum (i.e., 244 K) and maximum (i.e. T_{ap}) temperatures.

Table 2.5-11 – Effective G Values for Content Code ID 325B

	Temperature (K)	α Radiation Flammable Gas G Value (molecules/ 100 eV)	β Radiation Flammable Gas G Value (molecules/ 100 eV)	γ Radiation Flammable Gas G Value (molecules/ 100 eV)
Dose ≤0.012 watt*year	244	2.54	3.10	3.10
	324.3	3.82	4.66	4.66
Dose >0.012 watt*year	244	1.09	1.09	3.10
	324.7	1.09	1.09	4.67

2.5.6.4 Isotopic Composition of the Waste (Source Data)

Knowledge of the isotopic composition is necessary to establish what percentage of the emitted energy is due to alpha, beta, or gamma emitters. The initial normalized isotopic composition for Content Code ID 325B is listed in Table 2.5-12. The waste assigned to Content Code ID 325B was packaged between 1990 and 1995. RH-TRU waste shipments are assumed to occur after 2005. Thus, the minimum decay time of 10 years was specified as an input parameter to the RadCalc program to perform radionuclide decay and in-growth calculations between the time period from waste generation to shipment date.

Table 2.5-12 – Initial Isotopic Activity Fractions for Content Code ID 325B

Isotope	Activity Fraction
Mn-54	2.965E-03
Fe-55	3.387E-03
Co-60	8.930E-05
Sr-89	3.265E-04
Sr-90	4.698E-02
Y-90	4.706E-02
Y-91	1.154E-03
Zr-95	2.625E-03
Nb-95	5.736E-03
Ru-106	8.109E-02
Rh-106	8.089E-02
Sn-123	2.449E-04
Sb-125	4.150E-03
Te-125m	1.724E-03
Te-127	2.855E-04
Te-127m	2.914E-04
Cs-134	2.508E-03
Cs-137	6.331E-02
Ba-137m	5.963E-02
Ce-144	1.469E-01
Pr-144	1.469E-01
Pr-144m	6.137E-04
Pm-147	9.043E-02
Sm-151	1.391E-03
Eu-154	2.219E-04
Eu-155	3.733E-03
U-234	3.825E-06
U-235	3.422E-07
U-238	5.059E-08
Pu-238	3.371E-04
Pu-239	9.610E-03
Pu-240	6.195E-03
Pu-241	1.886E-01
Am-241	4.076E-04
Cm-242	9.343E-05
Cm-244	1.985E-06
Total	**1.000E+00**

2.5.6.5 Container and Waste Data

<u>**Container Geometry**</u>

The selection of a container establishes the gamma curve model. Neither the RH-TRU canister nor the RH-TRU 72-B packaging is specifically included as a container within the RadCalc program. The option provided by RadCalc for a 6- by 6-foot liner with an internal volume of approximately 4,600 liters is conservatively used to represent the RH-TRU canister, which is much smaller in size.

<u>**Waste Density**</u>

The maximum mass, including packaging materials, in more than 600 waste drums assigned to Content Code ID 325B containing combustible or noncombustible waste is 196 pounds[8]. The waste volume is contained inside 30-gallon (113.6-liter) drums with a maximum of three drums placed inside the RH-TRU canister. The maximum waste density based on the heaviest drum is calculated to be:

Equation 35

$$\rho_{\max\ actual} = \frac{196\ lb\ (453.6\ g\ lb^{-1})}{113,600\ cm^3} = 0.783\ g\ cm^{-3}$$

Since this density is higher than the 0.6 g cm^{-3} minimum density that is valid for gamma curve fits in the RadCalc program, a waste density of 0.783 g cm^{-3} for Content Code ID 325B is used as input to the RadCalc program.

2.5.6.5.1 Calculational Results

The primary function of the RadCalc program[4,5,6] is to calculate the generation of hydrogen gas by radiolytic production in the waste matrix of radioactive wastes. The first step in the calculation of decay heat limits involves determining the activities of the radionuclides and daughters and the associated FGGR at the time of waste shipment based on the initial isotopic composition for Content Code ID 325B. The second step involves iterating on the total activity (or, equivalently, the decay heat) given the activity fractions from the first step until the applicable FGGR limit listed in Table 2.5-8 is obtained. The decay heat that produces the FGGR equal to the applicable FGGR limit in Table 2.5-8 then corresponds to the decay heat limit for the container at the appropriate temperature. Table 2.5-13 lists the calculated decay heat values for Content Code ID 325B at the minimum and maximum temperatures. For this content code, minimum decay heat values are obtained at the maximum temperature of 324.3 K if dose ≤0.012 watt*year. If the dose >0.012 watt*year, minimum decay heat values are obtained at the minimum temperature of 244 K. These values are thus conservatively assigned as the decay heat limits for Content Code ID 325B as indicated in Table 2.5-14.

Table 2.5-13 – Decay Heat Values at Minimum and Maximum Temperatures for Content Code ID 325B

	Temperature (K)	Decay Heat Limit per Drum (Watt)	Decay Heat Limit per Canister (Watt)
Dose ≤0.012 watt*year	244	0.1337	0.4011
	324.3	0.1321	0.3963
Dose >0.012 watt*year	244	0.2782	0.8347
	324.7	0.3607	1.0820

Table 2.5-14 – Decay Heat Limits for Content Code ID 325B

	Decay Heat Limit per Drum (Watt)	Decay Heat Limit per Canister (Watt)
Dose ≤0.012 watt*year	0.1321	0.3963
Dose >0.012 watt*year	0.2782	0.8347

2.5.7 Content Code ID 325B

The example Content Code ID 325B, along with the associated chemical list, that corresponds to the numerical examples presented in Section 2.5.5 and Section 2.5.6 is provided in this section.

CONTENT CODE: ID 325B

CONTENT DESCRIPTION: Solid Organic Waste

GENERATING SITE: Argonne National Laboratory-East (ANL-E)

STORAGE SITE: Idaho National Laboratory (INL)

WASTE DESCRIPTION: This waste consists primarily of a variety of combustible debris.

GENERATING SOURCE(S): This waste is generated at the Argonne National Laboratory-East (ANL-E) Alpha Gamma Hot Cell Facility (AGHCF) between November 1971 and November 1995 during the processing of irradiated and unirradiated fuel pins from various reactor programs at ANL-W [Experimental Breeder Reactor-II (EBR-II)] and other U.S. Department of Energy (DOE) reactors, such as the New Production Reactor at the Savannah River Site (SRS). The AGHCF is a hot-cell complex that includes office space, shielded gloveboxes, a hot cell under nitrogen atmosphere with work stations for remote manipulation of materials, and a Decontamination/Repair Area (DRA).

WASTE FORM: The waste consists of neoprene gloves and O-rings, polyethylene and polypropylene bottles; plastic tubing (including PVC, polyethylene, rubber, and styrene butadiene); PVC, polyurethane, and polyethylene bagging pouches; silicone and Teflon O-rings; paper products; cotton and synthetic rags; polyethylene and PVC sheeting; wood products (including masonite); neoprene, koroseal, and rubber gaskets; and a variety of plastics and cellulosics. Waste was contaminated primarily with fissile materials, mixed fission products (MFP), and activation products. The predominant radionuclides are: plutonium (Pu)-239, Pu-240, Pu-241, americium (Am)-241, uranium (U)-235, U-238, cesium (CS)-137, barium (Ba)-137m, strontium (Sr)-90, yttrium (Y)-90, cobalt (Co)-60, and iron (Fe)-55.

WASTE PACKAGING: The waste is packaged either in two 7.5-gallon metal cans or in one 5-gallon and one 10-gallon metal can. The metal cans are not considered layers of confinement because the lid of each can does not have a gasket, and there are holes drilled in the can sides to accommodate the placement of a lifting cable attachment. The metal cans are placed in a fiber drum pouch spreader, an inner PVC pouch with a HEPA filter vent, a polyethylene drum liner, an outer PVC pouch with a filter vent, and a 17H 30-gallon drum with a filter vent or an opening in the drum lid. The inner PVC pouch is placed inside a rigid polyethylene liner without a lid. The liner and its contents are then heat-sealed inside the outer PVC pouch. Up to three 30-gallon drums are placed in a fixed-lid RH-TRU canister.

METHOD(S) FOR ISOTOPIC DETERMINATION: The isotopic composition of the waste is determined from process loss calculations and fission product calculations and was recorded on the associated forms or in data management systems. Therefore, the isotopic composition of the waste need not be determined by direct analysis or measurement of the waste unless process information is not available.

RESIDUAL LIQUIDS: Liquid waste is prohibited in the drums except for residual amounts in well-drained containers. The total volume of residual liquid in a payload container shall be less than 1 volume percent of the payload container. Waste packaging procedures ensure that residual liquids are less than 1 volume percent of the payload container.

EXPLOSIVES/COMPRESSED GASES: Explosives and compressed gases in the payload containers are prohibited by waste packaging procedures.

PYROPHORICS: Sodium and NaK were passivated with alcohol and the alcohol absorbed into palletized clay and evaporated. Other pyrophorics such as Zircalloy were sorted to segregate from WIPP waste containers.

CORROSIVES: Corrosives are prohibited in the payload container. Etchant solutions were neutralized and absorbed in palletized clay rendering the solution noncorrosive prior to being a part of the waste. The physical form of the waste and the waste generating procedures ensure that the waste is in a nonreactive form.

CHEMICAL COMPATIBILITY: A chemical compatibility study has been performed on this content code, and all waste is chemically compatible for materials in greater than trace (>1% by weight) quantities. The chemicals found in this content code are restricted to the allowable chemical list in Table 4.3-1 of the RH-TRAMPAC.

G VALUE: The bounding G values for hydrogen and total gas for this content code are provided by cellulose and polyethylene, as determined from the chemical list for the content code. These G values are derived from the information presented in Appendix 2.2 of the RH-TRU Payload Appendices.

ADDITIONAL CRITERIA: The hydrogen diffusivity of the filter vent installed in the 30-gallon drum lid, if present, is equal to or greater than 3.70E-06 mol/s/mol fraction at 25ºC. The drum lid opening, if present, has an equivalent diameter equal to or greater than 0.3 in. Each bag filter vent has a minimum hydrogen diffusivity of 1.075E-05 mol/s/mol fraction at 25ºC.

MAXIMUM ALLOWABLE DECAY HEAT LIMITS: The maximum allowable decay heat limits are as follows:

Confinement Layer	Maximum Allowable Decay Heat Limits Fixed Lid Canister (watts)	
	Without Dose-Dependent G Values	With Dose-Dependent G Values (watt*year >0.012)
Drum	0.1321	0.2782
Canister	0.3963	0.8347

MAXIMUM ALLOWABLE HYDROGEN GENERATION RATES: The maximum allowable hydrogen generation rate limits are as follows:

Confinement Layer	Maximum Allowable Hydrogen Generation Rate Limits Fixed Lid Canister (moles/second)
Drum	3.701E-08
Canister	1.110E-07

IDAHO NATIONAL LABORATORY
CONTENT CODE ID 325
SOLID ORGANIC AND INORGANIC WASTE

MATERIALS AND CHEMICALS (>1% by weight)

CELLULOSICS
CLAY, PELLETIZED
COTTON
INORGANIC DEBRIS
KOROSEAL
NEOPRENE
PLASTIC
POLYETHYLENE
POLYPROPYLENE
POLYVINYL CHLORIDE (PVC)
POLYURETHANE
PAPER
RUBBER
SILICONE
STYRENE BUTADIENE
SYNTHETIC RAGS
TEFLON
WOOD (including masonite)

MATERIALS AND CHEMICALS (<1% by weight)

TOLUENE

This page intentionally left blank.

APPENDIX 3.1

**GAS GENERATION TEST PLAN FOR
REMOTE-HANDLED TRANSURANIC (RH-TRU) WASTE CONTAINERS**

This page intentionally left blank.

3.1   Gas Generation Test Plan for Remote-Handled Transuranic (RH-TRU) Waste Containers

3.1.1   Objectives of the Gas Generation Testing

All waste to be transported in the RH-TRU 72-B packaging shall comply with the 5% (by volume) limit on hydrogen concentration during transport. Appendix 2.5 of the RH-TRU Payload Appendices presents the compliance methodology for meeting this limit. The 5% (by volume) limit on the hydrogen concentration may be converted to limits on the flammable gas generation rate (FGGR) and decay heat for each content code. If it can be shown for a given waste container that one of these limits can be met, the hydrogen concentration will remain at or below 5% under transportation conditions. FGGR and decay heat limits determined in accordance with Appendix 2.5 of the RH-TRU Payload Appendices are specified in content codes approved by the WIPP RH-TRU Payload Engineer.

As shown in Figure 3.1-1, the 5% limit on hydrogen concentration and the associated FGGR and decay heat limits specified in a given content code are adjusted down when the container headspace concentration of flammable volatile organic compounds (VOCs) is greater than 500 parts per million. In this case, the limit on hydrogen concentration is less than 5% to account for the concentration of flammable VOCs. The resulting reduced allowable flammable gas concentration (AFGC) is converted to reduced limits on FGGR and decay heat for the content code.

Once a container is assigned to an approved content code and the "Compliance with FGGR limit" method is selected, the FGGR for the container must be determined (see Figure 3.1-1). The generalized procedure for determining the FGGR of a container by measuring/testing is provided in this appendix. The FGGR for the container can then be compared to the FGGR limit specified for the assigned content code. As described in Section 5.1 of the Remote-Handled Transuranic Waste Authorized Methods for Payload Control (RH-TRAMPAC)[1] for the compliance option using the FGGR limit, if the container meets the limit, it is eligible for shipment if all other transportation requirements are met. If the container does not meet the limit, it cannot be shipped and shall be segregated for repackaging or other mitigation measures.

3.1.2   Gas Generation Test Methodology

The following sections describe how compliance with the FGGR limit will be implemented for solid and solidified waste forms. Implementation of the requirements of this test plan shall be documented in site-specific procedures under a documented quality assurance (QA) program approved by the U.S. Department of Energy, Carlsbad Field Office.

---

[1] U.S. Department of Energy (DOE), *Remote-Handled Transuranic Waste Authorized Methods for Payload Control (RH-TRAMPAC)*, current revision, U.S. Department of Energy, Carlsbad Field Office, Carlsbad, New Mexico.

Container data package

Is waste described by an approved content code? — No → Request content code approval from WIPP RH-TRU Payload Engineer

↓ Yes

Site selects method of compliance*

Compliance with decay heat limit

Determine decay heat value for container (Section 5.1.4)

Is decay heat plus error ≤ decay heat limit for content code? — No

↓ Yes

Compliance with FGGR limit

Determine FGGR for container (Section 5.1.3)

Is FGGR ≤ FGGR limit for content code? — No → Mitigate/repackage container

↓ Yes

Compliance with flammable (gas/VOC) concentration limits demonstrated for container

115875.01000000 A2

Is flammable VOC concentration in headspace >500 ppm (Section 5.1.5)?

No → AFGC = 5%

Yes → AFGC = MLEL - Sum of flammable VOCs (Section 5.1.5)

Determine applicable shipping period

Calculate FGGR limits (Section 5.1.3)

Calculate decay heat limits (Section 5.1.4)

WIPP RH-TRU Payload Engineer approves content code

Re-evaluate container

AFGC   = Allowable flammable gas concentration
FGGR   = flammable gas generation rate
MLEL   = mixture lower explosive limit
ppm   = parts per million
RH-TRU = remote-handled transuranic
VOC   = volatile organic compound

* If decay heat limit is not defined for content code, compliance with FGGR limit must be evaluated.

Note: All section numbers refer to the RH-TRAMPAC

Figure 3.1-1 – Methodology for Compliance with Flammable (Gas/VOC) Concentration Limits

3.1.2.1 Demonstration of Compliance with FGGR Limit for Solid Waste Forms

For solid waste forms, the container headspace will be sampled and analyzed to determine the concentration of hydrogen. Sampling lines that communicate with the container headspace will be installed. Samples of the headspace gas will be withdrawn and analyzed using a gas chromatograph (GC) and/or a mass spectrometer (MS). The analytical results will be used to calculate the FGGR. The measured FGGR will be compared to the appropriate FGGR limit for the assigned content code.

<u>Steady-State Conditions</u>

At steady-state conditions (applicable to the majority of RH-TRU waste containers that are generated and/or stored in a vented condition over extended time periods before shipment), the rate of gas generation by radiolysis equals the release rate of gas across each layer of confinement. The measured hydrogen gas concentration in the container headspace is used to calculate the FGGR.

The FGGR of the container is calculated from the measured hydrogen gas concentration using the following relationship:

Equation 1

$$C_g = X_H \; x \; L_{CF}$$

> where,
>
> | | | |
> |---|---|---|
> | C_g | = | FGGR [mole/second (sec)] |
> | X_H | = | Measured concentration of hydrogen gas in the container headspace (mole fraction) |
> | L_{CF} | = | Diffusion characteristic of the container filter (mole/sec/mole fraction). |

The FGGR shall be compared to the FGGR limit specified in the assigned content code. The container shall be qualified for shipment only if the limit is met.

The above methodology can be implemented for an RH-TRU canister or individually for inner containers. In addition, closed systems where a container is enclosed in a gas generation testing vessel can be used to perform gas generation testing. In this case, the headspace of the gas generation testing vessel can be monitored for gas generation with periodic sampling. Gas concentrations in the enclosure will increase in time and can be related to gas generation rates of hydrogen.

<u>Unsteady-State Conditions</u>

For unsteady-state conditions (applicable if RH-TRU waste containers have been vented only for short time periods), the following methodology will be used to determine compliance with the FGGR limit.

The generation of flammable gas within the innermost confinement layer and subsequent transport across the various confinement layers of a container can be simulated by solving the differential equations that describe the unsteady-state mass balances on flammable gas within each confinement layer of the container. To account for the various packaging configurations and container conditions, a system of differential equations must be solved along with the

appropriate initial conditions that represent the initial state of a container. The system of differential equations describing the hydrogen mass balances within the various confinement volumes of a container are presented by Equations 5, 8, and 11 in Appendix 2.5 of the RH-TRU Payload Appendices. The hydrogen concentration outside the container during storage and after packaging is assumed to be zero. Thus, for example, if the container is an RH-TRU canister, the concentration term, X_{IV}, in Equation 11 in Appendix 2.5 of the RH-TRU Payload Appendices is set to zero.

The first step in applying the methodology is to establish the container history (i.e., dates of container packaging, venting, and sampling). At the time of packaging, all layers will have zero hydrogen concentrations that will continue to increase until steady-state concentration conditions exist. Next, the container headspace hydrogen gas concentration is obtained through measurement. The equations in Appendix 2.5 of the RH-TRU Payload Appendices are solved iteratively adjusting the FGGR until the predicted FGGR provides a headspace hydrogen gas concentration that matches the measured headspace hydrogen gas concentration. A validated software program can be used to apply this methodology to calculate the container hydrogen generation rate by measuring the hydrogen concentration in the container headspace. The resulting FGGR (corresponding to the container headspace hydrogen gas concentration) shall be compared to the FGGR limit specified in the assigned content code. The container shall be qualified for shipment only if the limit is met. The above methodology can be implemented for an RH-TRU canister or individually for inner containers.

3.1.2.2 Demonstration of Compliance with FGGR Limit for Solidified Waste Forms

The methods described in Section 3.1.2.1 (for solid waste forms) may be used to determine compliance with FGGR limits for solidified waste forms in addition to the methodology described below.

To determine the FGGR for a container of solidified waste, a small sample of the waste form can be analyzed for its gas generation properties. The FGGR for the container can then be determined based on the mass of waste in the container. For example, a sludge sample can be placed in a sealed test chamber of known volume. The concentration of hydrogen will be measured in the chamber after an elapsed period of time, and the following relationship will be used to calculate the FGGR for the sample:

Equation 2

$$C_{g,sample} = \frac{X\ P\ V_{chamber}}{R\ T\ \Delta t}$$

> where,
>
> $C_{g,sample}$ =   FGGR for sample (mol/sec)
>
> X =   Mole fraction hydrogen in the test chamber
>
> P =   Absolute ambient pressure (atm)
>
> $V_{chamber}$ =   Volume of the test chamber (L)
>
> R =   Gas law constant ($0.08206\ \text{atm L mol}^{-1}\ \text{K}^{-1}$)

T	=	Absolute ambient temperature (K)
Δt	=	Elapsed time (sec).

The FGGR for the container will be calculated using the following relationship:

Equation 3

$$C_{g,container} = C_{g,sample}\ \frac{m_{container}}{m_{sample}}$$

where,

$C_{g,container}$	=	FGGR for container (mol/sec)
$m_{container}$	=	Mass of waste in container (g)
m_{sample}	=	Mass of sample (g).

3.1.3 Data Needs and Interpretation

This section documents the data needs for the testing described in Section 3.1.2.1 and Section 3.1.2.2. For any sampling and analysis done as part of these procedures, the following information should be documented:

1. Content Code - This is the content code for the waste being tested, which provides a short description of the waste.

2. Container ID - The test container should be given an identification code, which should be recorded for each test.

3. Ambient Conditions - The temperature and pressure conditions should be recorded during the test period.

4. Duration of Testing - Testing should be continued until enough analytical data is available to calculate the FGGR.

5. Sampling - Gas samples shall be collected in documented air-tight containers with proper chain of custody forms for transmittal to the analytical laboratory.

6. Analytical Methods - Instruments and methods used for measuring gas concentrations should conform to standard analytical methods (e.g., GC or GC/MS). Instruments shall be calibrated with certified gas standards. Calibration data, including instrument error and precision, should be available for all testing done.

7. Data Reduction - Any formulae or mathematical analysis used to reduce the data obtained to derive the FGGR should be documented, checked, and approved by a qualified individual. Proper QA procedures should be followed and documented for any data reduction.

8. Interpretation of Results - The interpretation of results with respect to the test criteria should be documented by the test supervisor.

3.1.4   Analytical Requirements for Test Methods

The minimum data requirements for the test methods described in Section 3.1.2.1 and Section 3.1.2.2 are as follows:

- If a sample of the waste is tested (Section 3.1.2.2), the results should be reproducible with respect to the hydrogen generation potential of the waste.

- If the headspace hydrogen concentration of a container is the primary variable measured (Section 3.1.2.1), a sufficient number of data points should be obtained in order to determine a hydrogen generation rate. Data points should be obtained until the FGGR is shown to remain constant or decrease, or until the testing period equals or exceeds the time of the shipping period.

- If multiple containers assigned to a single content code require evaluation for FGGR limit compliance, a statistical subpopulation of these containers may be evaluated. Not all containers assigned to a single content code may have consistent gas generation properties. Therefore, the basis for defining a population of containers with consistent gas generation properties must be documented.

  Containers selected from the defined population for evaluation (i.e., the subpopulation) must be representative of the population with techniques such as random or stratified sampling used to avoid bias in container selection. The required subpopulation size may be calculated using the following equation (a form of the finite population correction formula for binomial distribution results)[2]:

Equation 4

$$n = \frac{n_0}{1 + \frac{(n_0 - 1)}{N}} = \frac{n_0 * N}{N + n_0 - 1}$$

where,

n_0 =   203, a conservative (upper limit) subpopulation size for ensuring the 95th percentile can be established with a ±0.03 precision level and 95% confidence for a finite population

n =   Required subpopulation size

N =   Size of represented population.

A 95% upper tolerance limit (UTL) of the FGGR shall be calculated for each subpopulation using the Bootstrap (Resampling) technique.[2]

As shown by the equation, the minimum number of required containers in the subpopulation depends on the represented population size. When used with Bootstrap (Resampling) technique with replication size of 1,000 or more, the equation is valid for a represented minimum population size of 20. However, for RH-TRU waste populations a

---

[2] Gatliffe, T., May 2006, "Determination of Minimum Sample Size for Statistical Sampling of Remote-Handled Transuranic (RH-TRU) Waste," Washington TRU Solutions LLC, Carlsbad, New Mexico.

minimum population size of 50 is specified (given the large percentage of containers that have to be sampled in smaller populations). Because the Bootstrap technique is independent of the population distribution form, the only requirement for the subpopulation is that it be representative of the population. Equation 4 ensures that the proportion of the population represented in the subpopulation increases as the population size decreases. As such, potential local distributional anomalies in smaller populations should be adequately represented in the selected subpopulation.

This page intentionally left blank.

APPENDIX 3.2

**SUMMARY OF FLAMMABILITY
ASSESSMENT METHODOLOGY PROGRAM**

This page intentionally left blank.

3.2   Summary of Flammability Assessment Methodology Program

3.2.1   Introduction

The Flammability Assessment Methodology Program (FAMP) was established to investigate the flammability of gas mixtures found in transuranic (TRU) waste containers. Central to the program was experimental testing and modeling to predict the gas mixture lower explosive limit (MLEL) of gases observed in TRU waste containers. Flammability testing was conducted by the National Institute for Occupational Safety and Health (NIOSH) Pittsburgh Research Laboratory (PRL), as described in Loehr et al., 1997.[1] The MLELs of the gas mixtures in the flammability tests were used to develop and evaluate models for predicting the flammability of TRU waste drum contents that could potentially have flammable gas/volatile organic compound (VOC) mixtures. A summary of the test design, equipment and procedures, and results is provided below.

3.2.2   Experimental Design

The experimental design focused on investigating classes of compounds, including nonflammable VOCs, to predict MLELs and to provide data that represent a variety of TRU waste gas mixtures for evaluating MLEL models. Table 3.2-1 lists the compounds (flammable VOCs, nonflammable VOCs, and flammable gases) observed in TRU waste containers and considered in the FAMP. Flammable VOCs were classified according to their chemical structural characteristics and lower explosive limit (LEL) group (Table 3.2-2). The functional groups considered were aromatics, ketones, alcohols, and alkanes/alkenes. The LEL groups were designated by LELs of 0.9% to 1.3%, 1.4% to 2.6%, and 5.6% to 6.7%. In general, there is a correlation between functional and LEL group. LEL groups were chosen as classifications for flammable VOCs by functional and LEL groups.

In addition to LEL groups as classifications for flammable VOCs, flammable gases and nonflammable VOCs were two additional classes of compounds considered in the experimental design. Test mixtures for flammability testing were determined based on the following factors:

- Presence or absence of a flammable VOC from one or more of the three LEL groups

- Presence or absence of hydrogen

- Presence or absence of a nonflammable VOC.

VOCs were selected to represent compound classes based on prevalence in TRU waste and on physical characteristics that facilitated testing.

---

[1] Loehr, C.A., S.M. Djordjevic, K.J. Liekhus, and M. J. Connolly (1997). Flammability Assessment Methodology Program Phase I: Final Report. INEEL/EXT-97-01073. Idaho National Engineering and Environmental Laboratory, Idaho Falls, Idaho.

Table 3.2-1 — Flammable and Nonflammable Volatile Organic Compounds and Flammable Gases Considered in the Flammability Assessment Methodology Program

Flammable VOCs	Nonflammable VOCs	Flammable Gases
Acetone	Bromoform	Hydrogen
Benzene	Carbon tetrachloride	Methane
1-Butanol	Chloroform	
Chlorobenzene	Formaldehyde	
Cyclohexane	Methylene chloride	
1,1-Dichloroethane	1,1,2,2-Tetrachloroethane	
1,2-Dichloroethane	Tetrachloroethene	
1,1-Dichloroethene	1,1,1-Trichloroethane	
Cis-1,2-Dichloroethene	Trichloroethene	
Ethyl benzene	1,1,2-Trichloro-1,2,2-trifluoroethane	
Ethyl ether		
Methanol		
Methyl ethyl ketone		
Methyl isobutyl ketone		
Toluene		
1,2,4-Trimethylbenzene		
1,3,5-Trimethylbenzene		
m-Xylene		
o-Xylene		
p-Xylene		

Table 3.2-2 — Classification of Flammable Volatile Organic Compounds

Flammable VOC	Structural Type	Functional Group Number	LEL (vol. %)	LEL Group Number
Acetone	Ketone	2	2.6	2
Benzene	Aromatic	1	1.3	1
1-Butanol	Alcohol	3	1.7	2
Chlorobenzene	Aromatic	1	1.3	1
Cyclohexane	Cycloalkane	-	1.3	1
1,1-Dichloroethane	Alkane	4	5.6	3
1,2-Dichloroethane	Alkane	4	~5	3
1,1-Dichloroethene	Alkene	4	6.5	3
cis-1,2-Dichloroethene	Alkene	4	5.6	3
Ethyl benzene	Aromatic	1	1.0	1
Ethyl ether	Ether	-	1.9	2
Methanol	Alcohol	3	6.7	3
Methyl ethyl ketone	Ketone	2	1.9	2
Methyl isobutyl ketone	Ketone	2	1.4	2
Toluene	Aromatic	1	1.2	1
1,2,4-Trimethylbenzene	Aromatic	1	0.9	1
1,3,5-Trimethylbenzene	Aromatic	1	1.0	1
o-Xylene	Aromatic	1	1.1	1
m-Xylene	Aromatic	1	1.1	1
p-Xylene	Aromatic	1	1.1	1

A full factorial design of the experimental factors plus a quarter replication and minus combinations that resulted in no gas in the mixture resulted in a test matrix of 38 gas mixtures. Replicate runs were included in the test matrix to assess the experimental error. All runs were performed in a random order to help ensure that experimental errors and factor effects were properly estimated and not confounded with experimental procedure trends and other possible experimental effects.

The experimental test mixtures consisted of hydrogen and four VOCs, including 1,2-dichloroethane, to represent chlorinated hydrocarbons and alkanes; methyl ethyl ketone (2-butanone) to represent oxygenated hydrocarbons and ketones; toluene to represent aromatic hydrocarbons; and carbon tetrachloride to represent nonflammable VOCs. These VOCs were chosen to represent the LEL and, thus, the functional groups, because they have sufficient vapor pressures to remain in the gas phase under conditions of standard temperature and pressure. Ethyl ether (an ether) and cyclohexane (a cycloalkane) were not included in the test mixtures

because they are not prevalent in TRU waste. The test mixtures contained equimolar amounts of the above constituents as shown in Table 3.2-3.

In planning the experiments, errors were anticipated for measuring the actual concentration of a mixture component injected into the test chamber, the component vapor pressure and associated temperature, and the actual final mixture pressure. The required overall data quality objective (DQO) was to maintain the error in the experimental MLEL result to less than 5%.

Table 3.2-3 — Experimental Test Mixtures and MLEL Results

Mixture No.	1,2 - Dichloroethane (vol. %)	Methyl ethyl ketone (vol. %)	Toluene (vol. %)	Hydrogen (vol. %)	Carbon tetrachloride (vol. %)	MLEL(%)
1	20	20	20	20	20	3.40±0.10
2	100	0	0	0	0	4.85±0.05
3	50	50	0	0	0	2.65±0.05
4	33	33	33	0	0	1.95+0.03
5	25	25	25	25	0	2.40±0.05
6	33	33	0	33	0	3.40±0.07
7	25	25	0	25	25	5.15±0.05
8	33	33	0	0	33	4.85±0.10
9	25	25	25	0	25	2.80±0.05
10	50	0	50	0	0	2.05±0.03
11	33	0	33	0	33	3.50±0.05
12	33	0	33	33	0	2.65±0.05
13	25	0	25	25	25	3.95±0.05
14	50	0	0	50	0	5.35±0.20
15	33	0	0	33	33	9.7±0.50
16	50	0	0	0	50	Not Determined
17	0	100	0	0	0	1.95±0.03
18	0	50	0	0	50	4.65±0.03
19	0	50	50	0	0	1.45±0.05
20	0	50	0	50	0	3.15±0.07
21	0	25	25	25	25	2.90±0.05
22	0	0	100	0	0	1.20±0.03
23	0	0	50	0	50	2.90±0.05
24	0	0	50	50	0	2.05±0.03
25	0	0	33	33	33	3.65±0.10
26	0	0	0	100	0	5.00±0.40
27	0	0	0	50	50	10.8±0.80
28	0	33	33	0	33	2.45±0.05
29	0	33	33	33	0	2.00±0.05
30	0	33	0	33	33	5.20±0.10

Mixture No.	1,2 - Dichloroethane (vol. %)	Methyl ethyl ketone (vol. %)	Toluene (vol. %)	Hydrogen (vol. %)	Carbon tetrachloride (vol. %)	MLEL(%)
31	0	0	0	0	100	Not Flammable
32	0	0	0	0	0	Not Applicable
33	33	0	33	0	33	3.45±0.10
34	0	33	33	0	33	2.35±0.05
35	33	0	0	33	33	10.1±0.50
36	0	33	0	33	33	5.20±0.07
37	0	0	0	0	0	Not Applicable
38	50	50	0	0	0	2.70±0.05
39	0	0	50	50	0	2.05±0.03
40	25	25	25	25	0	2.40±0.10

3.2.3 Flammability Testing Equipment and Procedures

A heavy-walled, stainless steel test chamber with an approximate volume of 19 liters was used for the gas mixture flammability tests. The chamber has been used extensively for dust and gas explosibility measurements. Such chambers are now the standard laboratory chambers for dust explosibility measurements[2], and are highly useful for gas explosibility measurements as well. They are considerably larger than the 5-liter spherical glass flasks specified in the American Society for Testing and Materials (ASTM) vapor flammability test procedure[3], but are consistent with the ASTM standard. The larger size of the chamber allowed for the potential use of stronger igniters to ensure the absence of ignition limitations when measuring flammability limits, and minimized wall effects on flammability. The questions of ignition limitations and wall effects are particularly important in testing halogenated VOCs. The equipment used objective pressure criteria for explosions rather that a purely visual and subjective criteria as in ASTM E681-94[3].

The chamber was equipped with viewing ports and various access ports for pressure and temperature sensors, electronic ignition, evacuation, gas admission, and VOC liquid injection. Ignition was attempted using a 41-joule energy spark, and the resulting pressure trace was monitored to determine flammability or nonflammability for each test. By using the test chamber, stronger ignition sources could be used to ensure the absence of ignition limitations when measuring flammability limits, and minimizing wall effects (i.e., heat losses) on flammability.

---

[2] American Society for Testing and Materials (ASTM) (1997) E1515-96. Standard Test Method for Minimum Explosible Concentration of Combustible Dusts, American Society for Testing and Materials, West Conshohocken, Pennsylvania.

[3] American Society for Testing and Materials (ASTM) (1994) E681-94. Standard Test Method for Concentration Limits of Flammability of Chemicals, American Society for Testing and Materials, West Conshohocken, Pennsylvania.

A computer-controlled data acquisition system was used to display the pressure, rate of pressure rise (dP/dt), and temperature data versus time. The partial pressures of the VOCs, hydrogen, and air were monitored using two Viatran pressure transducers for the explosion pressures and a Baratron pressure transducer for the component pressures. Chamber temperature was monitored by a Chromel-Alumel (type K) thermocouple.

The PRL measured the MLEL in dry air at a total pressure of 1 atm for the VOC mixtures. All testing used known amounts of the appropriate individual components. To ensure complete volatilization of the VOCs, each component was introduced under reduced pressure into the test chamber. Once the appropriate components were introduced into the chamber and pressures were checked to ensure proper component concentrations, the chamber was brought to atmospheric pressure using dry air. Once a uniform mixture was obtained, the test was started by energizing the appropriate ignition source and recording pressure and temperature. Ignition of the mixture was identified by the pressure rise of the test chamber vessel. A positive ignition was required for those test mixtures that contain a flammable gas.

This was accomplished by increasing the component concentrations, while maintaining the required component ratio, until the sample gave a positive ignition. The ignition source selected was of sufficient energy and duration as to avoid ignition limitations as discussed below.

An initial testing phase was completed prior to initiation of testing the 38 gas mixtures in order to verify and establish the following:

- *LEL of the individual components (hydrogen and VOCs)*. The LELs determined through the initial testing were compared to values previously determined at the PRL for hydrogen and taken from the literature for the VOCs.

- *Criterion (i.e., pressure rise) for a positive ignition*. Based on the preliminary testing and comparisons to earlier measurements, a pressure rise of 0.5 pounds per square inch (psi) was chosen as the LEL criterion.

- *Equipment performance*.

  - *An appropriate ignition source for flammability tests*. Preliminary tests on the LELs of toluene and methyl ethyl ketone had used a stored spark energy of 17 joules. The LELs were found to be in agreement with the reported values from closed flammability tubes. Despite the apparent adequacy of the spark energy used, it was determined to use an even more energetic spark of 41 joules for the test series to help ensure that the more difficult to ignite halogenated VOCs (e.g., 1,2-dichloroethane) and mixtures (those with 1,2-dichloroethane or carbon tetrachloride) would not be ignition limited. Switching to the higher capacitance spark did not reduce the LEL for methyl ethyl ketone. There was, therefore, no indication that the more energetic spark was "overdriving" the chamber mixture, nor was there any expectation that the actual thermal energy deposited in the chamber by the spark (about 1 joule) could possibly do so.

The following measurements were made during an experimental run:

- *Pressure Measurements*. Individual component partial pressure (VOCs, hydrogen, and air) and total chamber pressure were established before each test. The time

development of chamber pressure and rate of pressure rise in the chamber were recorded once the appropriate ignition source was energized. The pressure rise criterion, which was determined experimentally, was used to establish ignition of the test gas mixture. In addition to the pressure transducer used to measure component pressures (Baratron), two pressure transducers (Viatran) were used to measure the gas mixture explosion pressure.

- *Temperature measurements*. Test chamber temperature was monitored during each test using a Chromel-Alumel (type K) thermocouple and recoded as a function of time. The thermocouple was able to give qualitative data on flame propagation and temperature, but did not have the response time to allow the monitoring of the actual peak explosion temperature. Because the thermocouple was cemented in place inside the reaction chamber, it was considered impractical to recalibrate the temperature output on a regular basis. Therefore, the temperature output was treated as a relative rather than an absolute measurement, with more significance given to the measured explosion temperature rise than on the absolute initial starting temperature.

- *Concentration Measurements*. The partial pressure of all gases (VOCs, hydrogen, and air) was used to determine concentrations prior to running a test.

Prior to their use, instruments used in the flammability tests were checked against known standards. Pressure transducers with built in calibrations were checked daily.

3.2.4 Experimental Results

The lowest flammable concentration in air of all mixtures specified in the experimental design was determined in the 19-liter laboratory chamber using a strong spark ignition source. Except for 1,2-dichloroethane, the LELs of pure VOCs were within the narrow range of literature values cited by the PRL. The experimental LEL for 1,2-dichloroethane is below the range of values cited in the literature, but may be more accurate because a larger chamber was used in combination with a more energetic spark and it is know that the halogenated species are prone to exhibiting wall effects and ignition limitations. Experimental MLELs generally agreed with calculated values for the mixtures to within 10%.[1]

Partial pressures of the VOC and hydrogen components were used to determine test mixture composition and concentration in air for MLEL determinations. Mixture explosion pressure and temperature data were also measured during the experimental tests. Temperature rise measurements and visual observations of the flame propagation were found to correlate well with pressure rise measurements.[1] MLELs for the various test mixtures listed in Table 3.2-3 are based on pressure versus component concentration data plots.

The precision of the MLELs reported in Table 3.2-3 is based on the number of data points in the near vicinity of the LEL value, how close the data points are to the LEL, the effect of using a range of pressure rise criteria (0.5 ± 02 psi), and sensitivity of explosion pressures near the LEL.

The relative precision values form replicate runs, less than or equal to 5% of the LEL value, is consistent with the DQO identified in the FAMP Test Plan.[4]

The largest uncertainty in the MLEL determinations was due to a gradual increase in explosion pressure with hydrogen concentration and the dominance of hydrogen in some mixtures, particularly the hydrogen and carbon tetrachloride mixture, which combines the lightest, most diffusible molecule, hydrogen, with the heaviest VOC, carbon tetrachloride, selected for the experimental tests. The flammability of equimolar mixtures containing hydrogen is expected to be more influenced by hydrogen because of its diffusivity and reactivity as a fuel. This behavior is greatest when other mixture components are much heavier and slower than hydrogen, such as the halogenated components carbon tetrachloride and 1,2-dichloroethane. The other hydrogen-containing mixtures and the pure VOC mixtures (excluding hydrogen and carbon tetrachloride) show a sharp discontinuity at the flammability boundary and, therefore, have more well-defined MLEL and LEL values.[1]

3.2.5   Model Development, Evaluation, and Selection

The FAMP evaluated seven models for predicting MLELs for gas mixtures, including (a) the original method of Le Chatelier; (b) a modified Le Chatelier method based on accounting for the nonflammable VOC proportion in the mixture; (c) a group contribution factor (GCF) method, which accounts for the compound stoichiometry; (d) a GCF method that accounts only for flammable VOCs (Flammable Group method); (e) a group contribution method that uses experimental LELs as input; (f) predictions using the ASTM code, CHETAH; and (g) linear regression of test MLELs on proportions of compounds in the classifications used for flammability testing. In addition, the effects of imposing bias on relatively unbiased models were investigated.

Model predictions for the test mixtures were compared to MLELs determined in flammability testing. Statistics on measures of the degree of consistency of agreement between predicted and test MLELs were generated. An evaluation of the models was also performed using innermost layer concentrations for 532 drums characterized under the contact-handled TRU waste characterization program at the Idaho National Engineering and Environmental Laboratory and the Rocky Flats Environmental Technology Site.

In applying the models to actual drum data, it was found that some methods resulted in unrealistic MLELs. For instance, all methods except the Flammable Group method resulted in extremely high MLELs predicted for some drums. Based on the results of model evaluations and because of favorable results in the experimental-based evaluations, the Flammable Group model was selected as a conservative approach to determine the MLEL of a mixture of flammable VOCs and flammable gas.

---

[4] Connolly, M.J., S.M. Djordjevic, L. Evans, and C.A. Loehr (1997). Flammability Assessment Methodology Program Test Plan, Revision 0. INEL 96/0352. Idaho National Engineering and Environmental Laboratory, Idaho Falls, Idaho.

The Flammable Group method is based on an extension of the method presented in the American Institute of Chemical Engineers (AIChE) Procedure B: Method for Estimating Lower Flammability Limit of Pure Compounds in the Data Prediction Manual.[5] This method predicts the MLEL of a mixture based on knowledge of the chemical structure of each individual component in the mixture. The MLEL will be calculated by the following equation:

$$MLEL = \frac{100\%}{\sum f_i \, x \, GCF_i} \tag{1}$$

where,

$MLEL$ =   Mixture lower explosive limit (vol %)

f_i =   Fraction of flammable gas i in mixture on an air free and nonflammable VOC free basis (i.e., the concentration of flammable compound i divided by the sum of the concentrations of flammable VOCs and flammable gas).

GCF_i =   GCF for compound i.

The GCF for a compound is calculated by the following method:

$$GCF_i = \sum n_j * GF_j \tag{2}$$

where,

n_j =   Number of group type j in compound i

GF_j =   Group factor for group type j.

Table 3.2-4 contains the FAMP calculated group factor (GF) values for the various groups used to determine the GCF for a compound of interest. As an example, the GCF for methanol (CH_3OH) or structurally as

$$\begin{array}{c} H \\ | \\ H - C - OH \\ | \\ H \end{array}$$
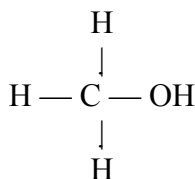
is calculated as 1 C group + 4 H groups + 1 O group or (9.10) + (4*2.17) + (-2.68) = 15.1. The GCF values for various flammable VOCs are listed in Table 3.2-5.

---

[5] American Institute of Chemical Engineers (1994), Procedure B: Method for Estimating Lower Flammability Limit of Pure Compounds in the Data Prediction Manual, American Institute of Chemical Engineers, New York, New York.

Table 3.2-4 — FAMP Group Factor (GF) Values

Group	Group Factor
C	9.10
H	2.17
H_2	20.0
O	-2.68
N	1.38
Cl	-4.38
C=C	14.07
F (Number of H atoms > Number of F atoms)	-4.18
F (Number of H atoms < Number of F atoms)	-2.55
I	17.5
S	10.9
P	9.6

Table 3.2-5 — Compound Group Contribution Factors

Compound	Group Contribution Factor (GCF)
Flammable VOCs	
Acetone	37.64
Benzene	82.53
1-Butanol	55.42
Chlorobenzene	75.98
Cyclohexane	80.64
1,1-Dichloroethane	18.12
1,2-Dichloroethane	18.12
1,1-Dichloroethene	9.65
cis-1,2-Dichloroethene	9.65
Ethyl benzene	109.41
Ethyl ether	55.42
Methanol	15.1
Methyl ethyl ketone	51.08
Methyl isobutyl ketone	77.96
Toluene	95.97
1,2,4-Trimethylbenzene	122.85
1,3,5-Trimethylbenzene	122.85
o-Xylene	109.41
m/p-Xylene	109.41
Flammable Gases	
Hydrogen	20
Methane	20

This page intentionally left blank.

APPENDIX 4.1

CHEMICAL COMPATIBILITY OF WASTE FORMS

This page intentionally left blank.

4.1   Chemical Compatibility of Waste Forms

4.1.1   Introduction

This appendix describes the method used for demonstrating chemical compatibility in a given waste canister of a given content code and among waste forms to simulate mixing of waste during hypothetical accident conditions.

4.1.2   Chemical Compatibility Analyses

The chemical compatibility analyses were performed using the methods described in the U.S. Environmental Protection Agency (EPA) document "A Method for Determining the Compatibility of Hazardous Wastes" (EPA-600/2-80-076).[1] Waste is considered "incompatible" if the potential exists for any of the following reactions:

- Explosion
- Heat generation
- Gas generation (flammable gases)
- Pressure build up (nonflammable gases)
- Toxic by-product generation
- Fire
- Violent polymerization
- Solubilization of toxic substances.

Note: Solubilization of toxic substances and toxic byproduct generation are not directly a concern for transportation of waste in the RH-TRU 72-B, but have been included for completeness.

Each generator and storage site has produced a comprehensive list of chemicals/materials present in an approved content code. The chemical components found in each waste generation process are determined by examining the process technology, by chemical analysis, or by process flow analysis. Under this system, all chemical inputs are accounted for, even though all of these components may not be part of the waste. For example, generator sites might include both acids and bases in their lists, even though the two groups have been neutralized prior to placement in a payload container.

The chemical concentration levels are reported as either ≥1 percent (by weight) or <1 percent (by weight). The list is divided into groups based on chemical properties and structure (e.g., acids, caustics, metals, etc.). Table 4.1-1 lists all the groups and their number designations. As noted in the table, the groups and examples listed are only for illustrative purposes, and do not necessarily represent components of waste materials in a payload. A listing of chemicals allowed in the waste in quantities >1% (weight) is provided in Section 4.3 of the Remote-Handled Transuranic Waste Authorized Methods for Payload Control (RH-TRAMPAC). As

---

[1] Hatayama, H.K., J.J. Chen, E.R. deVera, R.D. Stephens, and D.L. Storm, 1980, "A Method for Determining the Compatibility of Hazardous Wastes," EPA-600/2-80-076, U.S. Environmental Protection Agency, Cincinnati, Ohio.

specified by Section 4.3 of the RH-TRAMPAC, the total quantity of the trace chemicals/materials in the payload container is restricted to less than 5 weight percent.

Table 4.1-1 – EPA List of Chemical Groups and Materials[①]

Group Number	Group Name	Example
1	Acids, Mineral, Non-Oxidizing	Hydrochloric Acid
2	Acids, Mineral, Oxidizing	Nitric Acid (>1%)
3	Acids, Organic	Acetic Acid
4	Alcohols and Glycols	Methanol
5	Aldehydes	Formaldehyde
6	Amides	Acetamide
7	Amines, Aliphatic and Aromatic	Aniline
8	Azo Compounds, Diazo Compounds and Hydrazines	Hydrazine
9	Carbamates	Carbaryl
10	Caustics	Sodium Hydroxide
11	Cyanides	Potassium Cyanide
12	Dithiocarbamates	Maneb
13	Esters	Vinyl Acetate
14	Ethers	Tetrahydrofuran
15	Fluorides, Inorganic	Potassium Fluoride
16	Hydrocarbons, Aromatic	Toluene
17	Halogenated Organics	Carbon Tetrachloride
18	Isocyanates	Methyl Isocyanate
19	Ketones	Acetone
20	Mercaptans and other Organic Sulfides	Carbon Disulfide
21	Metals, Alkali and Alkaline Earth, Elemental	Metallic Sodium
22	Metals, other Elemental and Alloys in the form of Powders, Vapors or Sponges	Titanium
23	Metals, other Elemental and Alloys as Sheets, Rods, Moldings, Drops, etc.	Aluminum
24	Metals and Metal Compounds, Toxic	Beryllium
25	Nitrides	Sodium Nitride
26	Nitriles	Acetonitrile
27	Nitro Compounds	Dinitrobenzene
28	Hydrocarbons, Aliphatic, Unsaturated	Butadiene
29	Hydrocarbons, Aliphatic, Saturated	Cyclohexane
30	Peroxides and Hydroperoxides Organic	Acetyl Peroxide
31	Phenols, Cresols	Phenol
32	Organophosphates, Phosphothioates, and Phosphodithioates	Malathion
33	Sulfides, Inorganic	Zinc Sulfide
34	Epoxides	Epoxybutane

Group Number	Group Name	Example
101	Combustible and Flammable Materials, Miscellaneous	Cellulose
102	Explosives	Ammonium Nitrate
103	Polymerizable Compounds	Acrylonitrile
104	Oxidizing Agents, Strong	Hydrogen Peroxide
105	Reducing Agents, Strong	Metallic Sodium
106	Water and Mixtures Containing Water	Water
107	Water Reactive Substances	Sulfuric Acid (>70%)

① Modified from "A Method for Determining the Compatibility of Hazardous Wastes." [1]

NOTE: The chemical groups and materials listed in this table are a comprehensive listing of chemical compounds that may be incompatible. This is not meant to infer that all the listed chemical compounds and materials are present in TRU waste.

Interactions between compounds present in trace quantities (<1 percent by weight) and compounds present in concentrations ≥1 percent by weight do not pose an incompatibility problem for the following reasons:

- The trace chemicals reported by the sites are in concentrations well below the trace definition of less than 1 weight percent.

- The trace chemicals are usually dispersed in the waste, which further dilutes concentrations of these materials.

- Total trace chemicals within a payload container are limited to less than 5 weight percent.

- Trace chemicals that might be incompatible with materials/chemicals ≥1 weight percent would have reacted during the waste generating process prior to placement in payload containers.

- Because of restrictions imposed by the EPA on reporting of hazardous wastes, some chemicals are listed in trace quantities even if they have already reacted. Hazardous waste regulations as promulgated by the EPA[2] (known as the mixture rule) require that a mixture of any solid waste and a hazardous waste listed in 40 CFR Part 261, Subpart D be considered a hazardous waste subject to RCRA regulations. However, Subpart D does not list minimum concentrations for these listed wastes, with the result that any such mixtures must be considered hazardous waste even if the Subpart D constituent is at or below detection limits.

---

[2] U.S. Environmental Protection Agency, Title 40, Code of Federal Regulations, Part 261, Subpart D, U.S Environmental Protection Agency, Washington, D.C.

- The waste is either solidified and immobilized (solidified materials) or present in bulk form as a solid (solid materials). In almost all cases, any possible reactions take place before the waste is generated in its final form.

As specified by the RH-TRAMPAC, the total quantity of trace chemicals/materials is restricted to less than 5 weight percent total. Potential incompatibilities among compounds potentially present in quantities ≥1 percent weight have been analyzed for the payload using the list of allowable materials in Section 4.3 of the RH-TRAMPAC. The analysis assigned EPA chemical reactivity group numbers and names to each allowable constituent. The reactivity group numbers were assigned based on information provided in Hatayama, et al.[1] If the allowable material (or chemical) is a non-reactive inorganic material (not covered under the EPA reactivity group numbers), it was assigned a reactivity group number of "0" to reflect a complete analysis for all allowable materials (materials assigned a reactivity group number of "0" do not present a compatibility concern). The list of allowable materials and assigned reactivity group numbers is provided in Attachment A of this appendix.

The list of allowable materials and assigned reactivity group numbers was sorted by reactivity group number and then condensed to form a list of the represented reactivity groups (Attachment B of this appendix).

Using the list of represented reactivity groups, a hazardous waste compatibility chart was generated. The chart, which is provided in Attachment C, is a reduced version of the hazardous waste compatibility chart presented in Hatayama, et al.[1] The chart summarizes the potential types of reactions possible between each of the reactivity groups represented in the list of allowable materials. The reaction codes and consequences of the reactions are specified for each combination of two reactivity groups.

Using the hazardous waste compatibility chart, a list of potential chemical incompatibilities in the TRU waste was generated. The list, which is presented in Attachment D, also presents explanations of why the reaction associated with each of the potential chemical incompatibilities will not occur.

The results of the analysis demonstrate chemical compatibility among the list of allowable materials. Each content code is required to have an associated chemical list. Chemical incompatibilities do not exist in approved content codes. This has been ensured by a knowledge of the processes generating the wastes and the chemical compatibility analysis. The chemical constituents present in quantities ≥1% (weight) in the chemical list associated with each content code are evaluated for compliance with the list of allowable materials specified in Section 4.3 of the RH-TRAMPAC. Only content codes with chemical lists that have been evaluated by this process and determined to be compatible shall be approved for shipment in the package. As described in Section 4.3 of the RH-TRAMPAC, any change to the chemical list of an approved content code, as well as requests for additional waste forms, must be submitted to the WIPP RH-TRU Payload Engineer for evaluation for compliance with the list of allowable materials of the RH-TRAMPAC.

Attachment A
List of Allowable Materials and Associated Reactivity Groups

List of Allowable Materials and Associated Reactivity Groups

Allowable Chemical/Material[a]	Reactivity Group[b] Name	Number[c]
Absorbent polymers, organic	Combustible and flammable materials, miscellaneous	101
Absorbents/adsorbents (e.g., Celite®, diatomaceous earth, diatomite, Florco®, Oil-Dri®, perlite, vermiculite)	Other solidification materials and absorbents/adsorbents	0
Acids, inorganic	Acids, Mineral, Non-oxidizing	1
Acids, inorganic	Acids, Mineral, Oxidizing	2
Acids, organic	Acids, organic	3
Alcohols (e.g., butanol, ethanol, isopropanol, methanol)	Alcohols and Glycols	4
Alumina cement	Water reactive substance	107
Aquaset® products (for aqueous solutions)	Other solidification materials and absorbents/adsorbents	0
Aqueous sludges	Other solidification materials and absorbents/adsorbents	0
Aqueous solutions/water	Water and Mixtures containing water	106
Asbestos	Other Inorganics (non-reactive)	0
Ash (e.g., ash bottoms, fly ash, soot)	Other Inorganics (non-reactive)	0
Asphalt	Combustible and flammable materials, miscellaneous	101
Bakelite®	Combustible and flammable materials, miscellaneous	101
Batteries, dry (e.g., flashlight)	Metals, alkali and alkaline earth, elemental and alloys	21
Caustics	Caustics	10
Cellulose (e.g., Benelex®, cotton Conwed®, paper, rags, rayon, wood)	Combustible and flammable materials, miscellaneous	101
Cellulose acetate butyrate	Polymerizable compounds	103
Cellulose propionate	Polymerizable compounds	103
Ceramics (e.g., molds and crucibles)	Other Inorganics (non-reactive)	0
Chlorinated polyether	Ethers	14
Clays (e.g., bentonite)	Other Inorganics (non-reactive)	0
Concrete	Other solidification materials and absorbents/adsorbents	0
Detergents, solid (e.g., emulsifiers, surfactants)	Esters	13
Detergents, solid (e.g., emulsifiers, surfactants)	Hydrocarbons, aromatic	16
Detergents, solid (e.g., emulsifiers, surfactants)	Hydrocarbons, aliphatic unsaturated	28
Detergents, solid (e.g., emulsifiers, surfactants)	Organophosphates, phosphothioates, and phosphodithioates	32
Envirostone® (no organic emulsifiers allowed)	Other solidification materials and absorbents/adsorbents	0
Esters (e.g., ethyl acetate, polyethylene glycol ester)	Esters	13
Ethers (e.g., ethyl ether)	Ethers	14

Allowable Chemical/Material[a]	Reactivity Group[b]	
	Name	Number[c]
Fiberglass, inorganic	Other Inorganics (non-reactive)	0
Fiberglass, organic	Combustible and flammable materials, miscellaneous	101
Filter media, inorganic	Other Inorganics (non-reactive)	0
Filter media, organic	Combustible and flammable materials, miscellaneous	101
Firebrick	Other Inorganics (non-reactive)	0
Glass (e.g., borosilicate glass, labware, leaded glass, Raschig rings)	Other Inorganics (non-reactive)	0
Graphite (e.g., molds and crucibles)	Metals, other elemental, and alloy, as sheets, rods, moldings, vapors, or sponges	23
Greases, commercial brands	Combustible and flammable materials, miscellaneous	101
Grit	Other Inorganics (non-reactive)	0
Halogenated organics (e.g., bromoform; carbon tetrachloride; chlorobenzene; chloroform; 1,1-dichloroethane; 1,2-dichloroethane; 1,1-dichloroethylene; cis-1,2-dichloroethylene; methylene chloride; 1,1,2,2-tetrachloroethane; tetrachloroethylene; 1,1,1-trichloroethane; 1,1,2-trichloroethane; trichloroethylene; 1,1,2-trichloro-1,2,2-trifluoroethane	Halogenated Organics	17
Heel (e.g., ash heel; soot heel; firebrick heel; sand, slag, and crucible heel)	Other Inorganics (non-reactive)	0
Hydrocarbons, aliphatic (e.g., cyclohexane, n-paraffin hydrocarbons)	Hydrocarbon, aliphatic, unsaturated	28
Hydrocarbons, aliphatic (e.g., cyclohexane, n-paraffin hydrocarbons)	Hydrocarbon, aliphatic, saturated	29
Hydrocarbons, aromatic (e.g., benzene; ethyl benzene; toluene; 1,2,4-trimethylbenzene; 1,3,5-trimethylbenzene; xylene)	Hydrocarbons, aromatic	16
Insulation, inorganic	Other Inorganics (non-reactive)	0
Insulation, organic	Combustible and flammable materials, miscellaneous	101
Ketones (e.g., acetone, methyl ethyl ketone, methyl isobutyl ketone)	Ketones	19
Leaded rubber (e.g., gloves, aprons, sheet material)	Metals, Other elemental, and alloy, as sheets, rods, moldings, vapors, or sponges	23
Leaded rubber (e.g., gloves, aprons, sheet material)	Metals and metal compounds, toxic	24
Leaded rubber (e.g., gloves, aprons, sheet material)	Combusible and flammable materials, miscellaneous	101
Leather	Combustible and flammable materials, miscellaneous	101
Magnesia cement (e.g., Ramcote® cement)	Water reactive substance	107

| Allowable Chemical/Material[a] | Reactivity Group[b] | |
	Name	Number[c]
Magnesium alloy	Metals, Other elemental, and alloy, as sheets, rods, moldings, vapors, or sponges	23
Metal hydroxides	Other Inorganics (non-reactive)	0
Metal oxides (e.g., slag)	Other Inorganics (non-reactive)	0
Metals (e.g., aluminum, cadmium, copper, steel, tantalum, tungsten, zinc)	Metals, alkali and alkaline earth, elemental	21
Metals (e.g., aluminum, cadmium, copper, steel, tantalum, tungsten, zinc)	Metals, Other elemental and alloy in the form of powders, vapors, or sponges	22
Metals (e.g., aluminum, cadmium, copper, steel, tantalum, tungsten, zinc)	Metals, Other elemental, and alloy, as sheets, rods, moldings, vapors, or sponges	23
Metals (e.g., aluminum, cadmium, copper, steel, tantalum, tungsten, zinc)	Metals and metal compounds, toxic	24
Metals (e.g., aluminum, cadmium, copper, steel, tantalum, tungsten, zinc)	Reducing agents, strong	105
Nitrates (e.g., ammonium nitrate, sodium nitrate)	Oxidizing Agents, Strong	104
Oil (e.g., petroleum, mineral)	Combustible and flammable materials, miscellaneous	101
Organophosphates (e.g., tributyl phosphate, dibutyl phosphate, monobutyl phosphate)	Organophosphates, phosphothioates, and phosphodithioates	32
Paint, dry (e.g., floor/wall paint, ALARA)	Combustible and flammable materials, miscellaneous	101
Petroset® products (for aqueous solutions)	Other solidification materials and absorbents/adsorbents	0
Plastics [e.g., polycarbonate, polyethylene, polymethyl methacrylate (Plexiglas®, Lucite®), polysulfone, polytetrafluoroethylene (Teflon®), polyvinyl acetate, polyvinyl chloride (PVC), polyvinylidene chloride (saran)]	Combustible and flammable materials, miscellaneous	101
Polyamides (nylon)	Amides	6
Polyamides (nylon)	Combustible and flammable materials, miscellaneous	101
Polychlorotrifluoroethylene (e.g., Kel-F®)	Combustible and flammable materials, miscellaneous	101
Polyesters (e.g., Dacron®, Mylar®)	Esters	13
Polyesters (e.g., Dacron®, Mylar®)	Combustible and flammable materials, miscellaneous	101
Polyethylene glycol (e.g., Carbowax®)	Alcohols and Glycols	4
Polyethylene glycol (e.g., Carbowax®)	Combustible and flammable materials, miscellaneous	101
Polyimides	Hydrocarbons, aromatic	16
Polyphenyl methacrylate	Combustible and flammable materials, miscellaneous	101
Polypropylene (e.g., Ful-Flo® filters)	Combustible and flammable materials, miscellaneous	101

Allowable Chemical/Material[a]	Reactivity Group[b]	
	Name	Number[c]
Polyurethane	Combustible and flammable materials, miscellaneous	101
Polyvinyl alcohol	Alcohols and Glycols	4
Portland cement	Caustics	10
Portland cement	Water reactive substance	107
Resins (e.g., aniline-formaldehyde, melamine-formaldehyde, organic resins, phenol-formaldehyde, phenolic resins, urea-formaldehyde)	Aldehydes	5
Resins (e.g., aniline-formaldehyde, melamine-formaldehyde, organic resins, phenol-formaldehyde, phenolic resins, urea-formaldehyde)	Phenols and Creosols	31
Rubber, natural or synthetic [e.g., chlorosulfonated polyethylene (Hypalon®), ethylene-propylene rubber, EPDM, polybutadiene, polychloroprene (neoprene), polyisobutylene, polyisoprene, polystyrene, rubber hydrochloride (pliofilm®)]	Combustible and flammable materials, miscellaneous	101
Salts (e.g., calcium chloride, calcium fluoride, sodium chloride)	Other Inorganics (non-reactive)	0
Salts (e.g., calcium chloride, calcium fluoride, sodium chloride)	Fluorides, inorganic	15
Sand/soil, inorganic	Other Inorganics (non-reactive)	0
Sand/soil, organic	Combustible and flammable materials, miscellaneous	101
Trioctyl phosphine oxide	Organophosphates, phosphothioates, and phosphodithioates	32
Waxes, commercial brands	Combustible and flammable materials, miscellaneous	101
Other inorganic materials	Other Inorganics (non-reactive)	0

[a] Chemicals in **bold italic** have been assigned to more than one reactivity group.
[b] Reactivity group from Hatayama, H.K., J. J. Chen, E.R. deVera, R.D. Stephens, and D.L. Storm, 1980, "A Method for Determining the Compatibility of Hazardous Wastes," EPA-600/2-80-076, U.S. Environmental Protection Agency, Cincinnati, Ohio.
[c] Non-reactive inorganic materials or chemicals are assigned a reactivity group number of "0."

This page intentionally left blank.

Attachment B
List of Unique Reactivity Group Numbers in List of
Allowable Materials

List of Unique Reactivity Group Numbers in
List of Allowable Materials

Allowable Chemical/Material[a]	Reactivity Group[b]	
	Name	Number
Absorbents/adsorbents (e.g., Celite®, diatomaceous earth, diatomite, Florco®, Oil-Dri®, perlite, vermiculite)	Other solidification materials and absorbents/adsorbents	0
Acids, inorganic	Acids, Mineral, Non-oxidizing	1
Acids, inorganic	Acids, Mineral, Oxidizing	2
Acids, solid, organic	Acids, Organic	3
Polyethylene glycol (e.g., Carbowax®)	Alcohols and Glycols	4
Resins (e.g., aniline-formaldehyde, melamine-formaldehyde, organic resins, phenol-formaldehyde, phenolic resins, urea-formaldehyde)	Aldehydes	5
Polyamides (nylon)	Amides	6
Portland cement	Caustics	10
Esters (e.g., ethyl acetate, polyethylene glycol ester)	Esters	13
Ethers (e.g., ethyl ether)	Ethers	14
Salts (e.g., calcium chloride, calcium fluoride, sodium chloride)	Fluorides, inorganic	15
Hydrocarbons, aromatic (e.g., benzene; ethyl benzene; toluene; 1,2,4-trimethylbenzene; 1,3,5-trimethylbenzene; xylene)	Hydrocarbons, aromatic	16
Halogenated organics (e.g., bromoform; carbon tetrachloride; chlorobenzene; chloroform; 1,1-dichloroethane; 1,2-dichloroethane; 1,1-dichloroethylene; cis-1,2-dichloroethylene; methylene chloride; 1,1,2,2-tetrachloroethane; tetrachloroethylene; 1,1,1-trichloroethane; 1,1,2-trichloroethane; trichloroethylene; 1,1,2-trichloro-1,2,2-trifluoroethane)	Halogenated Organics	17
Ketones (e.g., acetone, methyl ethyl ketone, methyl isobutyl ketone)	Ketones	19
Batteries, dry (e.g., flashlight)	Metals, alkali and alkaline earth, elemental and alloys	21
Metals (e.g., aluminum, cadmium, copper, steel, tantalum, tungsten, zinc)	Metals, Other elemental and alloy in the form of powders, vapors, or sponges	22
Metals (e.g., aluminum, cadmium, copper, steel, tantalum, tungsten, zinc)	Metals, Other elemental, and alloy, as sheets, rods, moldings, vapors, or sponges	23
Leaded rubber (e.g., gloves, aprons, sheet material)	Metals and metal compounds, toxic	24
Hydrocarbons, aliphatic (e.g., cyclohexane, n-paraffin hydrocarbons)	Hydrocarbon, aliphatic, unsaturated	28
Hydrocarbons, aliphatic (e.g., cyclohexane, n-paraffin hydrocarbons)	Hydrocarbon, aliphatic, saturated	29

| Allowable Chemical/Material[a] | Reactivity Group[b] | |
	Name	Number
Resins (e.g., aniline-formaldehyde, melamine-formaldehyde, organic resins, phenol-formaldehyde, phenolic resins, urea-formaldehyde)	Phenols and Creosols	31
Organophosphates (e.g., tributyl phosphate, dibutyl phosphate, monobutyl phosphite)	Organophosphates, phosphothioates, and phosphodithioates	32
Asphalt	Combustible and flammable materials, miscellaneous	101
Cellulose acetate butyrate	Polymerizable compounds	103
Nitrates (e.g., ammonium nitrate, sodium nitrate)	Oxidizing Agents, Strong	104
Metals (e.g., aluminum, cadmium, copper, steel, tantalum, tungsten, zinc)	Reducing agents, strong	105
Aqueous solutions/water	Water and Mixtures containing water	106
Portland cement	Water reactive substances	107

[a] Chemicals in **bold italic** have been assigned to more than one reactivity group.
[b] Reactivity group from Hatayama, H.K., J.J. Chen, E.R. deVera, R.D. Stephens, and D.L. Storm, 1980, "A Method for Determining the Compatibility of Hazardous Wastes," EPA-600/2-80-076, U.S. Environmental Protection Agency, Cincinnati, Ohio.

This page intentionally left blank.

Attachment C
Waste Chemical Compatibility Chart

Waste Chemical Compatibility Chart

Legend:

E	=	Explosion
F	=	Fire
G	=	Innocuous and Non-Flammable Gas Generation
GF	=	Flammable Gas Generation
GT	=	Toxic Gas Generation
H	=	Heat Generation
P	=	Violent Polymerization
S	=	Solubilization of Toxic Substances

Source: Hatayama, H.K., J.J. Chen, E.R. deVera, R.D. Stephens, and D.L. Storm, "A Method for Determining the Compatibility of Hazardous Wastes," EPA-600/2-80-076, U.S. Environmental Protection Agency, Cincinnati, Ohio, 1980.

Group No.	Reactivity Group Name	1	2	3	4	5	6	10	13	14	15	16	17	19	21	22	23	24	28	29	31	32	101	103	104	105	106	107
1	Acids, Mineral, Non-Oxidizing	**1**																										
2	Acids, Mineral, Oxidizing		**2**																									
3	Acids, Organic		G, H	**3**																								
4	Alcohols and Glycols	H	H, F	H, P	**4**																							
5	Aldehydes	H, P	H, F	H, P		**5**																						
6	Amides	H	H, GT				**6**																					
10	Caustics	H	H	H		H		**10**																				
13	Esters	H	H, F				H		**13**																			
14	Ethers	H	H, F							**14**																		
15	Fluorides, Inorganic	GT	GT	GT							**15**																	
16	Hydrocarbons, Aromatic		H, F									**16**																
17	Halogenated Organics	H, GT	H, F, GT			H, GT	H						**17**															
19	Ketones	H	H, F				H							**19**														
21	Metals, Alkali and Alkaline Earth, Elemental	GF, H, F	GF, H, F	GF, H, F	GF, H, F	GF, H, F	GF, H	GF, H	GF, H				H, E	GF, H	**21**													
22	Metals, Other Elemental and Alloys as Powders, Vapors, or Sponges	GF, H, F	GF, H, F	GF				GF, H					H, E			**22**												
23	Metals, Other Elemental and Alloys as Sheets, Rods, Drops, Moldings, etc.	GF, H, F	GF, H, F					GF, H					H, F				**23**											
24	Metals and Metal Compounds, Toxic	S	S	S			S	S										**24**										
28	Hydrocarbons, Aliphatic, Unsaturated	H	H, F			H							H, E						**28**									
29	Hydrocarbons, Aliphatic, Saturated		H, F																	**29**								
31	Phenols and Creosols	H	H, F												GF, H						**31**							
32	Organophosphates, Phosphothioates, Phosphodithioates	H, GT	H, GT					H, E							H							**32**						
101	Combustible and Flammable Materials, Miscellaneous	H, G	H, F, GT												H, G, F								**101**					
103	Polymerizable Compounds	P, H	P, H	P, H				P, H							P, H	P, H	P, H	P, H			P, H			**103**				
104	Oxidizing Agents, Strong	H, GT		H, GT	H, F	H, F	H, F, GT	H, F	H, F			H, F	H, GT	H, F	H, F, E	H, F, E	H, F		H, F	H, F	H, F	H, F, GT	H, F, G	H, F, GT	**104**			
105	Reducing Agents, Strong	H, GF	H, F, GT	H, GF	H, GF, F	H, GF, F	H, GF		H, F				H, E	GF, H							GF, H	GT, GF, H	GF, H	H, P, GF	H, F, E	**105**		
106	Water and Mixtures Containing Water	H	H												GF, H	GF, H		S							GF, GT		**106**	
107	Water Reactive Substances	<----- Extremely Reactive ----- Do Not Mix with Any Chemical or Waste Material ----- Extremely Reactive ----->																										**107**
Reactivity Group Number		1	2	3	4	5	6	10	13	14	15	16	17	19	21	22	23	24	28	29	31	32	101	103	104	105	106	107

4.1-16

Attachment D
Potential Chemical Incompatibilities

Potential Chemical Incompatibilities

Combination of Reactivity Groups		Reaction Result (A x B)	Explanation of Potential Incompatibility
Group A	**Group B**		
1	4	Heat Generation	Reaction will not occur – Acids are neutralized and solidified/immobilized prior to shipping
1	5	Heat Generation	Reaction will not occur – Acids are neutralized and solidified/immobilized prior to shipping
1	5	Violent Polymerization	Reaction will not occur – Acids are neutralized and solidified/immobilized prior to shipping
1	6	Heat Generation	Reaction will not occur – Acids are neutralized and solidified/immobilized prior to shipping
1	10	Heat Generation	Reaction will not occur – Acids are neutralized and solidified/immobilized prior to shipping; Bases/caustic materials are neutralized and solidified/immobilized prior to shipping
1	13	Heat Generation	Reaction will not occur – Acids are neutralized and solidified/immobilized prior to shipping
1	14	Heat Generation	Reaction will not occur – Acids are neutralized and solidified/immobilized prior to shipping
1	15	Toxic Gas Generation	Reaction will not occur – Acids are neutralized and solidified/immobilized prior to shipping
1	17	Heat Generation	Reaction will not occur – Acids are neutralized and solidified/immobilized prior to shipping
1	17	Toxic Gas Generation	Reaction will not occur – Acids are neutralized and solidified/immobilized prior to shipping
1	19	Heat Generation	Reaction will not occur – Acids are neutralized and solidified/immobilized prior to shipping
1	21	Flammable Gas Generation	Reaction will not occur – Acids are neutralized and solidified/immobilized prior to shipping
1	21	Heat Generation	Reaction will not occur – Acids are neutralized and solidified/immobilized prior to shipping
1	21	Fire	Reaction will not occur – Acids are neutralized and solidified/immobilized prior to shipping
1	22	Flammable Gas Generation	Reaction will not occur – Acids are neutralized and solidified/immobilized prior to shipping
1	22	Heat Generation	Reaction will not occur – Acids are neutralized and solidified/immobilized prior to shipping
1	22	Fire	Reaction will not occur – Acids are neutralized and solidified/immobilized prior to shipping
1	23	Flammable Gas Generation	Reaction will not occur – Acids are neutralized and solidified/immobilized prior to shipping
1	23	Heat Generation	Reaction will not occur – Acids are neutralized and solidified/immobilized prior to shipping
1	23	Fire	Reaction will not occur – Acids are neutralized and solidified/immobilized prior to shipping

Combination of Reactivity Groups		Reaction Result (A x B)	Explanation of Potential Incompatibility
Group A	Group B		
1	24	Solubilization of Toxic Substances	Reaction will not occur – Acids are neutralized and solidified/immobilized prior to shipping Additionally, any solubilization of toxic substances will not affect transportation of wastes
1	28	Heat Generation	Reaction will not occur – Acids are neutralized and solidified/immobilized prior to shipping
1	31	Heat Generation	Reaction will not occur – Acids are neutralized and solidified/immobilized prior to shipping
1	32	Heat Generation	Reaction will not occur – Acids are neutralized and solidified/immobilized prior to shipping
1	32	Toxic Gas Generation	Reaction will not occur – Acids are neutralized and solidified/immobilized prior to shipping
1	101	Heat Generation	Reaction will not occur – Acids are neutralized and solidified/immobilized prior to shipping
1	101	Innocuous and Non-Flammable Gas Generation	Reaction will not occur – Acids are neutralized and solidified/immobilized prior to shipping
1	103	Violent Polymerization	Reaction will not occur – Acids are neutralized and solidified/immobilized prior to shipping
1	103	Heat Generation	Reaction will not occur – Acids are neutralized and solidified/immobilized prior to shipping
1	104	Heat Generation	Reaction will not occur – Acids are neutralized and solidified/immobilized prior to shipping; oxidizing agents are reacted prior to being placed in the waste/shipped
1	104	Toxic Gas Generation	Reaction will not occur – Acids are neutralized and solidified/immobilized prior to shipping; oxidizing agents are reacted prior to being placed in the waste/shipped
1	105	Heat Generation	Reaction will not occur – Acids are neutralized and solidified/immobilized prior to shipping; reducing agents are reacted prior to being placed in the waste/shipped
1	105	Flammable Gas Generation	Reaction will not occur – Acids are neutralized and solidified/immobilized prior to shipping; reducing agents are reacted prior to being placed in the waste/shipped
1	106	Heat Generation	Reaction will not occur – Acids are neutralized and solidified/immobilized prior to shipping; residual liquid content is limited to less than 1% of waste volume

Combination of Reactivity Groups		Reaction Result (A x B)	Explanation of Potential Incompatibility
Group A	**Group B**		
1	107	Highly Reactive	Reaction will not occur – Acids are neutralized and solidified/immobilized prior to shipping; residual liquid content is limited to less than 1% of waste volume; water reactive substances are reacted prior to being placed in the waste/shipped. Lime in Portland cement is most common water reactive substance expected in the waste. Portland cement is used as an absorbent and solidification agent for the wastes.
2	3	Innocuous and Non-Flammable Gas Generation	Reaction will not occur – Acids are neutralized and solidified/immobilized prior to shipping
2	3	Heat Generation	Reaction will not occur – Acids are neutralized and solidified/immobilized prior to shipping
2	4	Heat Generation	Reaction will not occur – Acids are neutralized and solidified/immobilized prior to shipping
2	4	Fire	Reaction will not occur – Acids are neutralized and solidified/immobilized prior to shipping
2	5	Heat Generation	Reaction will not occur – Acids are neutralized and solidified/immobilized prior to shipping
2	5	Fire	Reaction will not occur – Acids are neutralized and solidified/immobilized prior to shipping
2	6	Heat Generation	Reaction will not occur – Acids are neutralized and solidified/immobilized prior to shipping
2	6	Toxic Gas Generation	Reaction will not occur – Acids are neutralized and solidified/immobilized prior to shipping
2	10	Heat Generation	Reaction will not occur – Acids are neutralized and solidified/immobilized prior to shipping; Bases/caustic materials are neutralized and solidified/immobilized prior to shipping
2	13	Heat Generation	Reaction will not occur – Acids are neutralized and solidified/immobilized prior to shipping
2	13	Fire	Reaction will not occur – Acids are neutralized and solidified/immobilized prior to shipping
2	14	Heat Generation	Reaction will not occur – Acids are neutralized and solidified/immobilized prior to shipping
2	14	Fire	Reaction will not occur – Acids are neutralized and solidified/immobilized prior to shipping
2	15	Toxic Gas Generation	Reaction will not occur – Acids are neutralized and solidified/immobilized prior to shipping
2	16	Heat Generation	Reaction will not occur – Acids are neutralized and solidified/immobilized prior to shipping
2	16	Fire	Reaction will not occur – Acids are neutralized and solidified/immobilized prior to shipping
2	17	Heat Generation	Reaction will not occur – Acids are neutralized and solidified/immobilized prior to shipping

Combination of Reactivity Groups		Reaction Result	Explanation of Potential Incompatibility
Group A	Group B	(A x B)	
2	17	Fire	Reaction will not occur – Acids are neutralized and solidified/immobilized prior to shipping
2	17	Toxic Gas Generation	Reaction will not occur – Acids are neutralized and solidified/immobilized prior to shipping
2	19	Heat Generation	Reaction will not occur – Acids are neutralized and solidified/immobilized prior to shipping
2	19	Fire	Reaction will not occur – Acids are neutralized and solidified/immobilized prior to shipping
2	21	Flammable Gas Generation	Reaction will not occur – Acids are neutralized and solidified/immobilized prior to shipping
2	21	Heat Generation	Reaction will not occur – Acids are neutralized and solidified/immobilized prior to shipping
2	21	Fire	Reaction will not occur – Acids are neutralized and solidified/immobilized prior to shipping
2	22	Flammable Gas Generation	Reaction will not occur – Acids are neutralized and solidified/immobilized prior to shipping
2	22	Heat Generation	Reaction will not occur – Acids are neutralized and solidified/immobilized prior to shipping
2	22	Fire	Reaction will not occur – Acids are neutralized and solidified/immobilized prior to shipping
2	23	Flammable Gas Generation	Reaction will not occur – Acids are neutralized and solidified/immobilized prior to shipping
2	23	Heat Generation	Reaction will not occur – Acids are neutralized and solidified/immobilized prior to shipping
2	23	Fire	Reaction will not occur – Acids are neutralized and solidified/immobilized prior to shipping
2	24	Solubilization of Toxic Substances	Reaction will not occur – Acids are neutralized and solidified/immobilized prior to shipping Additionally, any solubilization of toxic substances will not affect transportation of wastes
2	28	Heat Generation	Reaction will not occur – Acids are neutralized and solidified/immobilized prior to shipping
2	28	Fire	Reaction will not occur – Acids are neutralized and solidified/immobilized prior to shipping
2	29	Heat Generation	Reaction will not occur – Acids are neutralized and solidified/immobilized prior to shipping
2	29	Fire	Reaction will not occur – Acids are neutralized and solidified/immobilized prior to shipping
2	31	Heat Generation	Reaction will not occur – Acids are neutralized and solidified/immobilized prior to shipping
2	31	Fire	Reaction will not occur – Acids are neutralized and solidified/immobilized prior to shipping
2	32	Heat Generation	Reaction will not occur – Acids are neutralized and solidified/immobilized prior to shipping
2	32	Toxic Gas Generation	Reaction will not occur – Acids are neutralized and solidified/immobilized prior to shipping

| Combination of Reactivity Groups | | Reaction Result | Explanation of Potential Incompatibility |
Group A	Group B	(A x B)	
2	101	Heat Generation	Reaction will not occur – Acids are neutralized and solidified/immobilized prior to shipping
2	101	Fire	Reaction will not occur – Acids are neutralized and solidified/immobilized prior to shipping
2	101	Toxic Gas Generation	Reaction will not occur – Acids are neutralized and solidified/immobilized prior to shipping
2	103	Violent Polymerization	Reaction will not occur – Acids are neutralized and solidified/immobilized prior to shipping
2	103	Heat Generation	Reaction will not occur – Acids are neutralized and solidified/immobilized prior to shipping
2	105	Heat Generation	Reaction will not occur – Acids are neutralized and solidified/immobilized prior to shipping; reducing agents are reacted prior to being placed in the waste/shipped
2	105	Fire	Reaction will not occur – Acids are neutralized and solidified/immobilized prior to shipping; reducing agents are reacted prior to being placed in the waste/shipped
2	105	Toxic Gas Generation	Reaction will not occur – Acids are neutralized and solidified/immobilized prior to shipping; reducing agents are reacted prior to being placed in the waste/shipped
2	106	Heat Generation	Reaction will not occur – Acids are neutralized and solidified/immobilized prior to shipping; residual liquid content is limited to less than 1% of waste volume
2	107	Highly Reactive	Reaction will not occur – Acids are neutralized and solidified/immobilized prior to shipping; residual liquid content is limited to less than 1% of waste volume; water reactive substances are reacted prior to being placed in the waste/shipped. Lime in Portland cement is most common water reactive substance expected in the waste. Portland cement is used as an absorbent and solidification agent for the wastes.
3	4	Heat Generation	Reaction will not occur – Acids are neutralized and solidified/immobilized prior to shipping
3	4	Violent Polymerization	Reaction will not occur – Acids are neutralized and solidified/immobilized prior to shipping
3	5	Heat Generation	Reaction will not occur – Acids are neutralized and solidified/immobilized prior to shipping
3	5	Violent Polymerization	Reaction will not occur – Acids are neutralized and solidified/immobilized prior to shipping
3	10	Heat Generation	Reaction will not occur – Acids are neutralized and solidified/immobilized prior to shipping; Bases/caustic materials are neutralized and solidified/immobilized prior to shipping

Combination of Reactivity Groups		Reaction Result	Explanation of Potential Incompatibility
Group A	Group B	(A x B)	
3	15	Toxic Gas Generation	Reaction will not occur – Acids are neutralized and solidified/immobilized prior to shipping
3	21	Flammable Gas Generation	Reaction will not occur – Acids are neutralized and solidified/immobilized prior to shipping
3	21	Heat Generation	Reaction will not occur – Acids are neutralized and solidified/immobilized prior to shipping
3	21	Fire	Reaction will not occur – Acids are neutralized and solidified/immobilized prior to shipping
3	22	Flammable Gas Generation	Reaction will not occur – Acids are neutralized and solidified/immobilized prior to shipping
3	24	Solubilization of Toxic Substances	Reaction will not occur – Acids are neutralized and solidified/immobilized prior to shipping Additionally, any solubilization of toxic substances will not affect transportation of wastes
3	103	Violent Polymerization	Reaction will not occur – Acids are neutralized and solidified/immobilized prior to shipping
3	103	Heat Generation	Reaction will not occur – Acids are neutralized and solidified/immobilized prior to shipping
3	104	Heat Generation	Reaction will not occur – Acids are neutralized and solidified/immobilized prior to shipping; oxidizing agents are reacted prior to being placed in the waste/shipped
3	104	Toxic Gas Generation	Reaction will not occur – Acids are neutralized and solidified/immobilized prior to shipping; oxidizing agents are reacted prior to being placed in the waste/shipped
3	105	Heat Generation	Reaction will not occur – Acids are neutralized and solidified/immobilized prior to shipping; reducing agents are reacted prior to being placed in the waste/shipped
3	105	Flammable Gas Generation	Reaction will not occur – Acids are neutralized and solidified/immobilized prior to shipping; reducing agents are reacted prior to being placed in the waste/shipped
3	107	Highly Reactive	Reaction will not occur – Acids are neutralized and solidified/immobilized prior to shipping; residual liquid content is limited to less than 1% of waste volume; water reactive substances are reacted prior to being placed in the waste/shipped. Lime in Portland cement is most common water reactive substance expected in the waste. Portland cement is used as an absorbent and solidification agent for the wastes.
4	21	Flammable Gas Generation	Reaction will not occur – Alcohols and Glycols are solidified/immobilized prior to shipping

Combination of Reactivity Groups		Reaction Result (A x B)	Explanation of Potential Incompatibility
Group A	Group B		
4	21	Heat Generation	Reaction will not occur – Alcohols and Glycols are solidified/immobilized prior to shipping
4	21	Fire	Reaction will not occur – Alcohols and Glycols are solidified/immobilized prior to shipping
4	104	Heat Generation	Reaction will not occur – Alcohols and Glycols are solidified/immobilized prior to shipping; oxidizing agents are reacted prior to being placed in the waste/shipped
4	104	Fire	Reaction will not occur – Alcohols and Glycols are solidified/immobilized prior to shipping; oxidizing agents are reacted prior to being placed in the waste/shipped
4	105	Heat Generation	Reaction will not occur – Alcohols and Glycols are solidified/immobilized prior to shipping; reducing agents are reacted prior to being placed in the waste/shipped
4	105	Flammable Gas Generation	Reaction will not occur – Alcohols and Glycols are solidified/immobilized prior to shipping; reducing agents are reacted prior to being placed in the waste/shipped
4	105	Fire	Reaction will not occur – Alcohols and Glycols are solidified/immobilized prior to shipping; reducing agents are reacted prior to being placed in the waste/shipped
4	107	Highly Reactive	Reaction will not occur – Alcohols and Glycols are solidified/immobilized prior to shipping; residual liquid content is limited to less than 1% of waste volume; water reactive substances are reacted prior to being placed in the waste/shipped. Lime in Portland cement is most common water reactive substance expected in the waste. Portland cement is used as an absorbent and solidification agent for the wastes.
5	10	Heat Generation	Reaction will not occur – Aldehydes are solidified/immobilized prior to shipping; bases/caustic materials are neutralized and solidified/immobilized prior to shipping
5	21	Flammable Gas Generation	Reaction will not occur – Aldehydes are solidified/immobilized prior to shipping
5	21	Heat Generation	Reaction will not occur – Aldehydes are solidified/immobilized prior to shipping
5	21	Fire	Reaction will not occur – Aldehydes are solidified/immobilized prior to shipping
5	28	Heat Generation	Reaction will not occur – Aldehydes are solidified/immobilized prior to shipping

Combination of Reactivity Groups		Reaction Result (A x B)	Explanation of Potential Incompatibility
Group A	**Group B**		
5	104	Heat Generation	Reaction will not occur – Aldehydes are solidified/immobilized prior to shipping; oxidizing agents are reacted prior to being placed in the waste/shipped
5	104	Fire	Reaction will not occur – Aldehydes are solidified/immobilized prior to shipping; oxidizing agents are reacted prior to being placed in the waste/shipped
5	105	Heat Generation	Reaction will not occur – Aldehydes are solidified/immobilized prior to shipping; reducing agents are reacted prior to being placed in the waste/shipped
5	105	Flammable Gas Generation	Reaction will not occur – Aldehydes are solidified/immobilized prior to shipping; reducing agents are reacted prior to being placed in the waste/shipped
5	105	Fire	Reaction will not occur – Aldehydes are solidified/immobilized prior to shipping; reducing agents are reacted prior to being placed in the waste/shipped
5	107	Highly Reactive	Reaction will not occur – Aldehydes are solidified/immobilized prior to shipping; residual liquid content is limited to less than 1% of waste volume; water reactive substances are reacted prior to being placed in the waste/shipped. Lime in Portland cement is most common water reactive substance expected in the waste. Portland cement is used as an absorbent and solidification agent for the wastes.
6	17	Heat Generation	Reaction will not occur – Amides are solidified/immobilized prior to shipping
6	17	Toxic Gas Generation	Reaction will not occur – Amides are solidified/immobilized prior to shipping
6	21	Flammable Gas Generation	Reaction will not occur – Amides are solidified/immobilized prior to shipping
6	21	Heat Generation	Reaction will not occur – Amides are solidified/immobilized prior to shipping
6	24	Solubilization of Toxic Substances	Reaction will not occur – Amides are solidified/immobilized prior to shipping Additionally, any solubilization of toxic substances will not affect transportation of wastes
6	104	Heat Generation	Reaction will not occur – Amides are solidified/immobilized prior to shipping; oxidizing agents are reacted prior to being placed in the waste/shipped

Combination of Reactivity Groups		Reaction Result	Explanation of Potential Incompatibility
Group A	Group B	(A x B)	
6	104	Fire	Reaction will not occur – Amides are solidified/immobilized prior to shipping; oxidizing agents are reacted prior to being placed in the waste/shipped
6	104	Toxic Gas Generation	Reaction will not occur – Amides are solidified/immobilized prior to shipping; oxidizing agents are reacted prior to being placed in the waste/shipped
6	105	Heat Generation	Reaction will not occur – Amides are solidified/immobilized prior to shipping; reducing agents are reacted prior to being placed in the waste/shipped
6	105	Flammable Gas Generation	Reaction will not occur – Amides are solidified/immobilized prior to shipping; reducing agents are reacted prior to being placed in the waste/shipped
6	107	Highly Reactive	Reaction will not occur – Amides are solidified/immobilized prior to shipping; residual liquid content is limited to less than 1% of waste volume; water reactive substances are reacted prior to being placed in the waste/shipped. Lime in Portland cement is most common water reactive substance expected in the waste. Portland cement is used as an absorbent and solidification agent for the wastes.
10	13	Heat Generation	Reaction will not occur – Caustics/bases are neutralized and solidified/immobilized prior to shipping
10	17	Heat Generation	Reaction will not occur – Caustics/bases are neutralized and solidified/immobilized prior to shipping
10	19	Heat Generation	Reaction will not occur – Caustics/bases are neutralized and solidified/immobilized prior to shipping
10	21	Flammable Gas Generation	Reaction will not occur – Caustics/bases are neutralized and solidified/immobilized prior to shipping
10	21	Heat Generation	Reaction will not occur – Caustics/bases are neutralized and solidified/immobilized prior to shipping
10	22	Flammable Gas Generation	Reaction will not occur – Caustics/bases are neutralized and solidified/immobilized prior to shipping
10	22	Heat Generation	Reaction will not occur – Caustics/bases are neutralized and solidified/immobilized prior to shipping

Combination of Reactivity Groups		Reaction Result (A x B)	Explanation of Potential Incompatibility
Group A	Group B		
10	23	Flammable Gas Generation	Reaction will not occur – Caustics/bases are neutralized and solidified/immobilized prior to shipping
10	23	Heat Generation	Reaction will not occur – Caustics/bases are neutralized and solidified/immobilized prior to shipping
10	24	Solubilization of Toxic Substances	Reaction will not occur – Caustics/bases are neutralized and solidified/immobilized prior to shipping; Additionally, any solubilization of toxic substances will not affect transportation of wastes
10	32	Heat Generation	Reaction will not occur – Caustics/bases are neutralized and solidified/immobilized prior to shipping
10	32	Explosion	Reaction will not occur – Caustics/bases are neutralized and solidified/immobilized prior to shipping
10	103	Violent Polymerization	Reaction will not occur – Caustics/bases are neutralized and solidified/immobilized prior to shipping
10	103	Heat Generation	Reaction will not occur – Caustics/bases are neutralized and solidified/immobilized prior to shipping
10	107	Highly Reactive	Reaction will not occur – Caustics/bases are neutralized and solidified/immobilized prior to shipping; residual liquid content is limited to less than 1% of waste volume; water reactive substances are reacted prior to being placed in the waste/shipped. Lime in Portland cement is most common water reactive substance expected in the waste. Portland cement is used as an absorbent and solidification agent for the wastes.
13	21	Flammable Gas Generation	Reaction will not occur – Esters are solidified/immobilized prior to shipping
13	21	Heat Generation	Reaction will not occur – Esters are solidified/immobilized prior to shipping
13	104	Heat Generation	Reaction will not occur – Esters are solidified/immobilized prior to shipping; oxidizing agents are reacted prior to being placed in the waste/shipped
13	104	Fire	Reaction will not occur – Esters are solidified/immobilized prior to shipping; oxidizing agents are reacted prior to being placed in the waste/shipped

Combination of Reactivity Groups		Reaction Result (A x B)	Explanation of Potential Incompatibility
Group A	Group B		
13	105	Heat Generation	Reaction will not occur – Esters are solidified/immobilized prior to shipping; reducing agents are reacted prior to being placed in the waste/shipped
13	105	Fire	Reaction will not occur – Esters are solidified/immobilized prior to shipping; reducing agents are reacted prior to being placed in the waste/shipped
13	107	Highly Reactive	Reaction will not occur – Esters are solidified/immobilized prior to shipping; residual liquid content is limited to less than 1% of waste volume; water reactive substances are reacted prior to being placed in the waste/shipped. Lime in Portland cement is most common water reactive substance expected in the waste. Portland cement is used as an absorbent and solidification agent for the wastes.
14	104	Heat Generation	Reaction will not occur – Ethers are solidified / immobilized prior to shipping. Oxidizing agents are reacted prior to being placed in the waste/shipped.
14	104	Fire	Reaction will not occur – Ethers are solidified / immobilized prior to shipping. Oxidizing agents are reacted prior to being placed in the waste/shipped.
14	107	Highly Reactive	Reaction will not occur – Ethers are solidified / immobilized prior to shipping. Residual liquid content is limited to less than 1% of waste volume; water reactive substances are reacted prior to being placed in the waste/shipped. Lime in Portland cement is most common water reactive substance expected in the waste. Portland cement is used as an absorbent and solidification agent for the wastes.
15	107	Highly Reactive	Reaction will not occur – Salts are reacted during use and processing; residual liquid content is limited to less than 1% of waste volume; water reactive substances are reacted prior to being placed in the waste/shipped. Lime in Portland cement is most common water reactive substance expected in the waste. Portland cement is used as an absorbent and solidification agent for the wastes.
16	104	Heat Generation	Reaction will not occur – Aromatic hydrocarbons are solidified/immobilized prior to shipping. Oxidizing agents are reacted prior to being placed in the waste/shipped.

Combination of Reactivity Groups		Reaction Result	Explanation of Potential Incompatibility
Group A	Group B	(A x B)	
16	104	Fire	Reaction will not occur – Aromatic hydrocarbons are solidified/immobilized prior to shipping. Oxidizing agents are reacted prior to being placed in the waste/shipped.
16	107	Highly Reactive	Reaction will not occur – Aromatic hydrocarbons are solidified/immobilized prior to shipping. Residual liquid content is limited to less than 1% of waste volume; water reactive substances are reacted prior to being placed in the waste/shipped. Lime in Portland cement is most common water reactive substance expected in the waste. Portland cement is used as an absorbent and solidification agent for the wastes.
17	21	Heat Generation	Reaction will not occur – Halogenated organics are solidified/immobilized prior to shipping
17	21	Explosion	Reaction will not occur – Halogenated organics are solidified/immobilized prior to shipping
17	22	Heat Generation	Reaction will not occur – Halogenated organics are solidified/immobilized prior to shipping
17	22	Explosion	Reaction will not occur – Halogenated organics are solidified/immobilized prior to shipping
17	23	Heat Generation	Reaction will not occur – Halogenated organics are solidified/immobilized prior to shipping
17	23	Fire	Reaction will not occur – Halogenated organics are solidified/immobilized prior to shipping
17	104	Heat Generation	Reaction will not occur – Halogenated organics are solidified/immobilized prior to shipping; oxidizing agents are reacted prior to being placed in the waste/shipped
17	104	Toxic Gas Generation	Reaction will not occur – Halogenated organics are solidified/immobilized prior to shipping; oxidizing agents are reacted prior to being placed in the waste/shipped
17	105	Heat Generation	Reaction will not occur – Halogenated organics are solidified/immobilized prior to shipping; reducing agents are reacted prior to being placed in the waste/shipped
17	105	Explosion	Reaction will not occur – Halogenated organics are solidified/immobilized prior to shipping; reducing agents are reacted prior to being placed in the waste/shipped

Combination of Reactivity Groups		Reaction Result	Explanation of Potential Incompatibility
Group A	Group B	(A x B)	
17	107	Highly Reactive	Reaction will not occur – Halogenated organics are solidified/immobilized prior to shipping; residual liquid content is limited to less than 1% of waste volume; water reactive substances are reacted prior to being placed in the waste/shipped. Lime in Portland cement is most common water reactive substance expected in the waste. Portland cement is used as an absorbent and solidification agent for the wastes.
19	21	Flammable Gas Generation	Reaction will not occur – Ketones are solidified/immobilized prior to shipping
19	21	Heat Generation	Reaction will not occur – Ketones are solidified/immobilized prior to shipping
19	104	Heat Generation	Reaction will not occur –Ketones are solidified/immobilized prior to shipping; oxidizing agents are reacted prior to being placed in the waste/shipped
19	104	Fire	Reaction will not occur –Ketones are solidified/immobilized prior to shipping; oxidizing agents are reacted prior to being placed in the waste/shipped
19	105	Flammable Gas Generation	Reaction will not occur –Ketones are solidified/immobilized prior to shipping; reducing agents are reacted prior to being placed in the waste/shipped
19	105	Heat Generation	Reaction will not occur –Ketones are solidified/immobilized prior to shipping; reducing agents are reacted prior to being placed in the waste/shipped
19	107	Highly Reactive	Reaction will not occur – Ketones are solidified/immobilized prior to shipping; residual liquid content is limited to less than 1% of waste volume; water reactive substances are reacted prior to being placed in the waste/shipped. Lime in Portland cement is most common water reactive substance expected in the waste. Portland cement is used as an absorbent and solidification agent for the wastes.
21	31	Flammable Gas Generation	Reaction will not occur – Phenols and Creosols are solidified/immobilized prior to shipping; metals are typically in oxide form
21	31	Heat Generation	Reaction will not occur – Phenols and Creosols are solidified/immobilized prior to shipping; metals are typically in oxide form

| Combination of Reactivity Groups | | Reaction Result | |
Group A	Group B	(A x B)	Explanation of Potential Incompatibility
21	32	Heat Generation	Reaction will not occur – Organophosphates are solidified/immobilized prior to shipping; metals are typically in oxide form
21	101	Heat Generation	Reaction will not occur – Combustible materials are dry; residual liquid content is limited to less than 1% of waste volume; metals are typically in oxide form
21	101	Innocuous and Non-Flammable Gas Generation	Reaction will not occur – Combustible materials are dry; residual liquid content is limited to less than 1% of waste volume; metals are typically in oxide form
21	101	Fire	Reaction will not occur – Combustible materials are dry; residual liquid content is limited to less than 1% of waste volume; metals are typically in oxide form
21	103	Violent Polymerization	Reaction will not occur – Polymerizable compounds are reacted or immobilized/solidified prior to shipping; metals are typically in oxide form
21	103	Heat Generation	Reaction will not occur – Polymerizable compounds are reacted or immobilized/solidified prior to shipping; metals are typically in oxide form
21	104	Heat Generation	Reaction will not occur –Oxidizing agents are reacted prior to being placed in the waste/shipped; metals are typically in oxide form
21	104	Fire	Reaction will not occur –Oxidizing agents are reacted prior to being placed in the waste/shipped; metals are typically in oxide form
21	104	Explosion	Reaction will not occur –Oxidizing agents are reacted prior to being placed in the waste/shipped; metals are typically in oxide form
21	106	Flammable Gas Generation	Reaction will not occur – Residual liquids are limited to less than 1% of waste volume; metals are typically in oxide form
21	106	Heat Generation	Reaction will not occur – Residual liquids are limited to less than 1% of waste volume; metals are typically in oxide form
21	107	Highly Reactive	Reaction will not occur – Metals are typically in oxide form; water reactive substances are reacted prior to being placed in the waste/shipped. Lime in Portland cement is most common water reactive substance expected in the waste. Portland cement is used as an absorbent and solidification agent for the wastes.
22	28	Heat Generation	Reaction will not occur – Unsaturated aliphatic hydrocarbons are solidified/immobilized prior to shipping
22	28	Explosion	Reaction will not occur – Unsaturated aliphatic hydrocarbons are solidified/immobilized prior to shipping

Combination of Reactivity Groups		Reaction Result (A x B)	Explanation of Potential Incompatibility
Group A	Group B		
22	103	Violent Polymerization	Reaction will not occur – Polymerizable compounds are reacted or immobilized/solidified prior to shipping
22	103	Heat Generation	Reaction will not occur – Polymerizable compounds are reacted or immobilized/solidified prior to shipping
22	104	Heat Generation	Reaction will not occur – Oxidizing agents are reacted prior to being placed in the waste/shipped
22	104	Fire	Reaction will not occur – Oxidizing agents are reacted prior to being placed in the waste/shipped
22	104	Explosion	Reaction will not occur – Oxidizing agents are reacted prior to being placed in the waste/shipped
22	106	Flammable Gas Generation	Reaction will not occur – Residual liquids are limited to less than 1% of waste volume; water reactive metals are reacted prior to shipping
22	106	Heat Generation	Reaction will not occur – Residual liquids are limited to less than 1% of waste volume; water reactive metals are reacted prior to shipping
22	107	Highly Reactive	Reaction will not occur –Water reactive substances are reacted prior to being placed in the waste/shipped. Lime in Portland cement is most common water reactive substance expected in the waste. Portland cement is used as an absorbent and solidification agent for the wastes.
23	103	Violent Polymerization	Reaction will not occur – Polymerizable compounds are reacted or immobilized/solidified prior to shipping
23	103	Heat Generation	Reaction will not occur – Polymerizable compounds are reacted or immobilized/solidified prior to shipping
23	104	Heat Generation	Reaction will not occur – Oxidizing agents are reacted prior to being placed in the waste/shipped
23	104	Fire	Reaction will not occur – Oxidizing agents are reacted prior to being placed in the waste/shipped
23	107	Highly Reactive	Reaction will not occur –Water reactive substances are reacted prior to being placed in the waste/shipped. Lime in Portland cement is most common water reactive substance expected in the waste. Portland cement is used as an absorbent and solidification agent for the wastes.
24	103	Violent Polymerization	Reaction will not occur – Polymerizable compounds are reacted or immobilized/solidified prior to shipping
24	103	Heat Generation	Reaction will not occur – Polymerizable compounds are reacted or immobilized/solidified prior to shipping
24	106	Solubilization of Toxic Substances	Reaction will not occur – Residual liquid content is limited to less than 1% of waste volume; Additionally, any solubilization of toxic substances will not affect transportation of wastes

Combination of Reactivity Groups		Reaction Result (A x B)	Explanation of Potential Incompatibility
Group A	Group B		
24	107	Highly Reactive	Reaction will not occur – Water reactive substances are reacted prior to being placed in the waste/shipped. Lime in Portland cement is most common water reactive substance expected in the waste. Portland cement is used as an absorbent and solidification agent for the wastes.
28	104	Heat Generation	Reaction will not occur – Unsaturated aliphatic hydrocarbons are immobilized/solidified prior to shipping; oxidizing agents are reacted prior to being placed in the waste/shipped
28	104	Fire	Reaction will not occur – Unsaturated aliphatic hydrocarbons are immobilized/solidified prior to shipping; oxidizing agents are reacted prior to being placed in the waste/shipped
28	107	Highly Reactive	Reaction will not occur – Unsaturated aliphatic hydrocarbons are immobilized/solidified prior to shipping; residual liquid content is limited to less than 1% of waste volume; water reactive substances are reacted prior to being placed in the waste/shipped. Lime in Portland cement is most common water reactive substance expected in the waste. Portland cement is used as an absorbent and solidification agent for the wastes.
29	104	Heat Generation	Reaction will not occur – Saturated aliphatic hydrocarbons are immobilized/solidified prior to shipping; oxidizing agents are reacted prior to being placed in the waste/shipped
29	104	Fire	Reaction will not occur – Saturated aliphatic hydrocarbons are immobilized/solidified prior to shipping; oxidizing agents are reacted prior to being placed in the waste/shipped
29	107	Highly Reactive	Reaction will not occur – Saturated aliphatic hydrocarbons are immobilized/solidified prior to shipping; residual liquid content is limited to less than 1% of waste volume; water reactive substances are reacted prior to being placed in the waste/shipped. Lime in Portland cement is most common water reactive substance expected in the waste. Portland cement is used as an absorbent and solidification agent for the wastes.

Combination of Reactivity Groups		Reaction Result (A x B)	Explanation of Potential Incompatibility
Group A	Group B		
31	103	Violent Polymerization	Reaction will not occur – Polymerizable compounds are reacted or immobilized/solidified prior to shipping; phenols and creosols are immobilized/solidified prior to shipping
31	103	Heat Generation	Reaction will not occur – Polymerizable compounds are reacted or immobilized/solidified prior to shipping; phenols and creosols are immobilized/solidified prior to shipping
31	104	Heat Generation	Reaction will not occur – Phenols and creosols are immobilized/solidified prior to shipping; oxidizing agents are reacted prior to being placed in the waste/shipped
31	104	Fire	Reaction will not occur – Phenols and creosols are immobilized/solidified prior to shipping; oxidizing agents are reacted prior to being placed in the waste/shipped
31	105	Flammable Gas Generation	Reaction will not occur – Phenols and creosols are immobilized/solidified prior to shipping; reducing agents are reacted prior to being placed in the waste/shipped
31	105	Heat Generation	Reaction will not occur – Phenols and creosols are immobilized/solidified prior to shipping; reducing agents are reacted prior to being placed in the waste/shipped
31	107	Highly Reactive	Reaction will not occur – Phenols and creosols are immobilized/solidified prior to shipping; residual liquid content is limited to less than 1% of waste volume; water reactive substances are reacted prior to being placed in the waste/shipped. Lime in Portland cement is most common water reactive substance expected in the waste. Portland cement is used as an absorbent and solidification agent for the wastes.
32	104	Heat Generation	Reaction will not occur – Organophosphates are immobilized/solidified prior to shipping; oxidizing agents are reacted prior to being placed in the waste/shipped
32	104	Fire	Reaction will not occur – Organophosphates are immobilized/solidified prior to shipping; oxidizing agents are reacted prior to being placed in the waste/shipped
32	104	Toxic Gas Generation	Reaction will not occur – Organophosphates are immobilized/solidified prior to shipping; oxidizing agents are reacted prior to being placed in the waste/shipped

Combination of Reactivity Groups		Reaction Result	Explanation of Potential Incompatibility
Group A	Group B	(A x B)	
32	105	Toxic Gas Generation	Reaction will not occur – Organophosphates are immobilized/solidified prior to shipping; reducing agents are reacted prior to being placed in the waste/shipped
32	105	Flammable Gas Generation	Reaction will not occur – Organophosphates are immobilized/solidified prior to shipping; reducing agents are reacted prior to being placed in the waste/shipped
32	105	Heat Generation	Reaction will not occur – Organophosphates are immobilized/solidified prior to shipping; reducing agents are reacted prior to being placed in the waste/shipped
32	107	Highly Reactive	Reaction will not occur – Organophosphates are immobilized/solidified prior to shipping; residual liquid content is limited to less than 1% of waste volume; water reactive substances are reacted prior to being placed in the waste/shipped. Lime in Portland cement is most common water reactive substance expected in the waste. Portland cement is used as an absorbent and solidification agent for the wastes.
101	104	Heat Generation	Reaction will not occur – Combustible materials are dry; oxidizing agents are reacted prior to being placed in the waste/shipped
101	104	Fire	Reaction will not occur – Combustible materials are dry; oxidizing agents are reacted prior to being placed in the waste/shipped
101	104	Innocuous and Non-Flammable Gas Generation	Reaction will not occur – Combustible materials are dry; oxidizing agents are reacted prior to being placed in the waste/shipped
101	105	Flammable Gas Generation	Reaction will not occur – Combustible materials are dry; reducing agents are reacted prior to being placed in the waste/shipped
101	105	Heat Generation	Reaction will not occur – Combustible materials are dry; reducing agents are reacted prior to being placed in the waste/shipped
101	107	Highly Reactive	Reaction will not occur – Combustible materials are dry; residual liquid content is limited to less than 1% of waste volume; water reactive substances are reacted prior to being placed in the waste/shipped. Lime in Portland cement is most common water reactive substance expected in the waste. Portland cement is used as an absorbent and solidification agent for the wastes.

Combination of Reactivity Groups		Reaction Result (A x B)	Explanation of Potential Incompatibility
Group A	Group B		
103	104	Heat Generation	Reaction will not occur – Polymerizable compounds are reacted or immobilized/solidified prior to shipping; oxidizing agents are reacted prior to being placed in the waste/shipped
103	104	Fire	Reaction will not occur – Polymerizable compounds are reacted or immobilized/solidified prior to shipping; oxidizing agents are reacted prior to being placed in the waste/shipped
103	104	Toxic Gas Generation	Reaction will not occur – Polymerizable compounds are reacted or immobilized/solidified prior to shipping; oxidizing agents are reacted prior to being placed in the waste/shipped
103	105	Heat Generation	Reaction will not occur – Polymerizable compounds are reacted or immobilized/solidified prior to shipping; reducing agents are reacted prior to being placed in the waste/shipped
103	105	Violent Polymerization	Reaction will not occur – Polymerizable compounds are reacted or immobilized/solidified prior to shipping; reducing agents are reacted prior to being placed in the waste/shipped
103	105	Flammable Gas Generation	Reaction will not occur – Polymerizable compounds are reacted or immobilized/solidified prior to shipping; reducing agents are reacted prior to being placed in the waste/shipped
103	107	Highly Reactive	Reaction will not occur – Polymerizable compounds are reacted or immobilized/solidified prior to shipping; residual liquid content is limited to less than 1% of waste volume; water reactive substances are reacted prior to being placed in the waste/shipped. Lime in Portland cement is most common water reactive substance expected in the waste. Portland cement is used as an absorbent and solidification agent for the wastes.
104	105	Heat Generation	Reaction will not occur – Oxidizing agents are reacted prior to being placed in the waste/shipped; reducing agents are reacted prior to being placed in the waste/shipped
104	105	Fire	Reaction will not occur – Oxidizing agents are reacted prior to being placed in the waste/shipped; reducing agents are reacted prior to being placed in the waste/shipped
104	105	Explosion	Reaction will not occur – Oxidizing agents are reacted prior to being placed in the waste/shipped; reducing agents are reacted prior to being placed in the waste/shipped

Combination of Reactivity Groups		Reaction Result	Explanation of Potential Incompatibility
Group A	Group B	(A x B)	
104	107	Highly Reactive	Reaction will not occur – Oxidizing agents are reacted prior to being placed in the waste/shipped; residual liquid content is limited to less than 1% of waste volume; water reactive substances are reacted prior to being placed in the waste/shipped. Lime in Portland cement is most common water reactive substance expected in the waste. Portland cement is used as an absorbent and solidification agent for the wastes.
105	106	Flammable Gas Generation	Reaction will not occur – Reducing agents are reacted prior to being placed in the waste/shipped; residual liquid content is limited to less than 1% of waste volume
105	106	Toxic Gas Generation	Reaction will not occur – Reducing agents are reacted prior to being placed in the waste/shipped; residual liquid content is limited to less than 1% of waste volume
105	107	Highly Reactive	Reaction will not occur – Reducing agents are reacted prior to being placed in the waste/shipped; residual liquid content is limited to less than 1% of waste volume; water reactive substances are reacted prior to being placed in the waste/shipped. Lime in Portland cement is most common water reactive substance expected in the waste. Portland cement is used as an absorbent and solidification agent for the wastes.
106	107	Highly Reactive	Reaction will not occur – Residual liquid content is limited to less than 1% of waste volume; water reactive substances are reacted prior to being placed in the waste/shipped. Lime in Portland cement is most common water reactive substance expected in the waste. Portland cement is used as an absorbent and solidification agent for the wastes.

This page intentionally left blank.

APPENDIX 4.2

FREE HALIDES IN THE RH-TRU 72-B PAYLOAD – SOURCE TERM AND RELEASE RATE ESTIMATES

This page intentionally left blank.

4.2   Free Halides in the RH-TRU 72-B Payload – Source Term and Release Rate Estimates

4.2.1   Summary

An evaluation of source terms for halides has demonstrated that very small amounts of halides are available for chemical reaction to cause stress corrosion cracking (SCC) of the inner vessel (IV) of RH-TRU 72-B. This is substantiated with sampling data from actual waste drums and radiolysis experiments conducted on contact-handled transuranic (CH-TRU) waste materials. Extensive sampling programs of both retrievably stored and newly generated CH-TRU waste did not detect hydrogen chloride (HCl) gas in the headspace of any of the payload containers. Experiments designed to simulate alpha and gamma radiolysis of actual bagging and CH-TRU waste materials from generator sites demonstrated HCl gas generation to be very low.

These observations support the conclusions that alpha or gamma radiolysis of actual waste produces little or no HCl gas. Any small quantities of HCl gas produced are likely either to dissolve readily in any absorbed water or moisture present in the waste, or to react with the waste contents or payload containers. This will retard the release of HCl gas from the payload containers, precluding the possibility of stress corrosion cracking of the IV.

4.2.2   Introduction

The production of free halides from radiolysis of the payload materials can potentially cause SCC of the RH-TRU 72-B. The primary material of construction used for the IV and the outer containment (OC) of the RH-TRU 72-B is Type 304 stainless steel (austenitic). This material may be susceptible in the sensitized condition to SCC in the presence of chloride contamination. However, Tokiwai et al.[1], have shown 304 stainless steel to be resistant to SCC at temperatures below 55°C, even for heavily sensitized material at stresses near yield, for maximum allowable levels of NaCl concentration and relative humidities. Normal operating temperatures of the cavity headspace or RH-TRU 72-B walls are not expected to exceed 55ºC. The following discussion will provide an analysis of the source terms for the halides and their potential to reach the IV.

4.2.3   Source Terms for Chlorides and Fluorides in Waste Material

The contaminants of concern are hydrogen chloride (HCl) and hydrogen fluoride (HF), which could originate from the radiolysis of polyvinyl chloride or halogenated organics.

4.2.3.1   Potential for Fluoride Production in Waste

Compounds containing fluorides considered as potential sources for HF gas have not been identified in the remote-handled (RH)-TRU materials in significant amounts. Only Teflon

---

[1] Tokiwai, M., H. Kimiura, and H. Kusangi, 1985, <u>Corrosion Science</u>, Vol. 25, No. 89, pp. 837-844.

occurs in the waste, and this does not produce HF from radiolysis (Appendix 2.1 of the RH-TRU Payload Appendices).

4.2.3.2   Potential for Chloride Production in Waste

The potential for chloride production in the payload materials comes primarily from radiolysis of the chlorinated compounds. Volatile organic compounds (VOCs) capable of generating HCl are not present in sufficient amounts in the waste to be of concern for SCC. Appendix 4.4 of the RH-TRU Payload Appendices discusses the source terms and release rates of VOCs. The only other compound present in the waste with a potential for HCl production is polyvinyl chloride (PVC).

Experimental evidence has shown average G(HCl) (moles of HCl in the gas or liquid state released per 100 eV of energy absorbed) values for radiolysis of commercial grades of plasticized stabilized PVC to be quite small (see Appendix 2.2 of the RH-TRU Payload Appendices). Table 4.2-1 summarizes the available data on generation of HCl from radiolysis of PVC. Three independent experiments of gamma radiolysis on actual waste and packaging material from three U.S. DOE sites demonstrated that very little or no HCl was produced. For the two gamma radiolysis experiments cited in Table 4.2-1 that measured detectable G(HCl), the quantitative measurement was made by titration of acidity in samples with a weak base. No direct evidence of HCl gas was reported in these experiments other than a qualitative indication of Cl$^-$.[2]

In conclusion, radiolytic activity within the payload containers of RH-TRU waste will not result in the generation of any substantial amounts of HCl gas. The source term for HCl gas itself (without any consideration of transport to the IV) is expected to be insignificant in payload containers transported in the RH-TRU 72-B.

4.2.3.3   Gas Sampling of CH-TRU Waste Drums

Sampling programs at Idaho National Engineering Laboratory (INEL)[3] and Rocky Flats Plant[4] did not detect HF or HCl gas in the headspace of any of the 249 drums of retrievably stored and newly generated contact-handled (CH)-TRU waste that were sampled. In addition to drum headspace sampling, twenty-two drums of retrievably stored and newly generated waste were sampled for gases within successive layers of confinement up to the innermost layer with the waste. In all cases, HF or HCl were never detected in any layers of confinement.

---

[2] Kazanjian, A.R, and A.K. Brown, December 1969, "Radiation Chemistry of Materials Used in Plutonium Processing," The Dow Chemical Company, Rocky Flats Division, RFP-1376.

[3] Clements, T.L., Jr., and D.E. Kudera, September 1985, "TRU Waste Sampling Program: Volume I, Waste Characterization," EGG-WM-6503, EG&G Idaho, Inc., Idaho Falls, Idaho.

[4] Roggenthen, D.K., T.L. McFeeters, and R.A. Nieweg, March 1989, "Waste Drum Gas Generation Sampling Program at Rocky Flats During FY 1988," RFP-4311.

Table 4.2-1 — G(HCl) Values for Plasticized Polyvinyl Chloride Materials in CH TRU Waste

	Irradiation	G(HCl)
Average G(HCl) for Plasticized PVC	α,γ	0.64[a]
Values for Materials used at U.S. DOE site		
PVC bagout bag (Los Alamos National Laboratory)[b]	α	~0[c]
Nine samples of PVC bag material (Rocky Flats Plant)[d]	γ	0.21[e]
Samples of PVC bagout material (Rocky Flats Plant)[f]	α	0
Samples of PVC gloves (Los Alamos National Laboratory)[g]	γ	0
Samples of PVC bags (Savannah River Plant)[h]	γ	<0.01[i]

[a]   Average of 27 literature values for plasticized PVC (Appendix 2.2 of the RH-TRU Payload Appendices).

[b]   Zerwekh, A., 1979, "Gas Generation from Radiolytic Attack of TRU- Contaminated Hydrogeneous Waste," Los Alamos National Laboratory, LA- 7674-MS, June 1979.

[c]   Mass spectrometric analysis of gases did not detect any Cl^- or HCl. Wet chemistry analysis of material inside glass reaction vessel yielded 0.06% Cl^-.

[d]   Kazanjian, A.R, and A.K. Brown, "Radiation Chemistry of Materials Used in Plutonium Processing," The Dow Chemical Company, Rocky Flats Division, RFP-1376, December 1969.

[e]   Tubes of irradiated PVC were opened under water, shaken, and titrated with NaOH. The presence of chlorides in solution was identified qualitatively. Only acid content (not Cl^-) was measured quantitatively. Acid concentration in water could be due to CO_2 dissolved from atmosphere.

[f]   Kazanjian, A. R, "Radiolytic Gas Generation in Plutonium Contaminated Waste Materials," Rockwell International, Rocky Flats Plant, RFP-2469, October 1976.

[g]   Kosiewicz, S.T., "Gas Generation from Organic Transuranic Wastes. I. Alpha Radiolysis at Atmospheric Pressure," Nuclear Technology 54, pp. 92-99, 1981.

[h]   Hobbs, David, Personal Communication, Savannah River Plant, Feb. 1989.

[i]   Personal communication for ongoing experiments.

The RH-TRU waste is very similar to the CH-TRU waste with respect to the non-radioactive materials that constitute the waste. For example, PVC materials are generated as both CH-TRU and RH-TRU waste. However, the CH-TRU wastes are contaminated to a much greater extent with alpha-emitting radionuclides than the RH-TRU waste. The predominant radionuclides present in the RH-TRU wastes primarily emit beta and gamma radiation. As shown in Table 4.2-1, the values for G (HCl) are consistently low for both alpha and gamma radiolysis experiments.

4.2.4 Mechanisms for Retardation of Chlorides Inside Payload Containers

Production of chlorides by radiolysis of waste materials in payload containers does not necessarily imply the presence of a gaseous phase. Some of the radiolysis experiments did not observe HCl gas in the void space of the experimental apparatus but did measure chlorides after washing of the interior of the reaction vessel.[5] This suggests the existence of mechanisms that can retard the release of gaseous HCl.

4.2.4.1 Solubility of HCl in Water

The presence of any free HCl that is produced in a payload container will be controlled in the headspace by the high solubility of HCl gas in water. Transfer of HCl gas to the aqueous phase occurs with very little resistance in the liquid phase and with very little back pressure of the gas.[6] For small quantities of HCl gas produced in the payload containers, the moisture content of the waste materials would probably be sufficient to absorb the gas generated.

The partial pressures of gaseous HCl over aqueous solutions of HCl are extremely small even at appreciable concentrations of HCl, due to its high solubility.[6] Table 4.2-2 provides the partial pressure of HCl above HCl aqueous solutions over a wide range of temperatures.[7] The partial pressures reported in the normal operating ranges of the RH-TRU 72-B would minimize the possibility of HCl being present as a gaseous phase.

Waste types to be transported in payload containers contain varying amounts of adsorbed/absorbed water as a by-product of processes (without the presence of free liquids) in addition to water vapor from atmospheric humidity inside the layers of confinement. Although water vapor was not quantitatively measured in the headspaces of the drums examined at RFP as part of the TRU waste sampling program,[3] water was noted in all gas samples.[8] Hence it is probable that any HCl produced would dissolve within the drums. It should be noted that anhydrous HCl is noncorrosive to 304 stainless steel.[9] Therefore, sufficient moisture exists in the form of adsorbed/absorbed water in layers of containment in payload containers to depress the vapor pressure of any HCl that may be present.

---

[5] Zerwekh, A., 1979, "Gas Generation from Radiolytic Attack of TRU- Contaminated Hydrogeneous Waste," Los Alamos National Laboratory, LA- 7674-MS, June 1979.

[6] Treybal, R.E., 1980, Mass Transfer Operations, McGraw-Hill Book Company, New York, New York.

[7] Perry, C.H., and D. Green, Eds., 1984, Chemical Engineers Handbook, McGraw-Hill Book Company, New York.

[8] Simmons, Bill, Rocky Flats Plant Personal Communications, 1988.

[9] Kirk, R.E., and D.F. Othmer, Eds., 1966, Encyclopedia of Chemical Technology, Vol. 11, John Wiley and Sons, New York.

4.2.5 Conclusion

In assessing the potential for stress corrosion cracking, it is apparent that the nature of the waste and the conditions under which the waste will be transported, should preclude the possibility of producing significant quantities of free HCl gas in the payload containers. Alpha or gamma radiolysis of PVC does not produce appreciable amounts of HCl gas, and any small quantities of the gas generated are likely to be retained in the payload containers, thereby limiting transport to the IV cavity.

Table 4.2-2— Partial Pressures of HCl Over Aqueous Solutions of HCl mmHg°Ca,b

%HCL	A	B	0°	5°	10°	15°	20°	25°	30°	35°	40°	45°	50°	60°	70°	80°
2	11.8037	4736	-----	----	0.0000117	0.000023	0.000044	0.000084	0.000151	0.000275	0.00047	0.00083	0.00140	0.00380	0.0100	0
4	11.6400	4471	0.000018	0.000036	0.000069	0.000131	0.00024	0.00044	0.00077	0.00134	0.0023	0.00385	0.0064	0.0165	0.0405	0
6	11.2144	4202	0.000066	0.000125	0.000234	0.000425	0.00076	0.00131	0.00225	0.0038	0.0062	0.0102	0.163	0.040	0.094	0
8	11.0406	4042	0.000118	0.000323	0.000583	0.00104	0.00178	0.0031	0.00515	0.0085	0.0136	0.022	0.0344	0.081	0.183	0
10	10.9311	3908	0.00042	0.00075	0.00134	0.00232	0.00395	0.0067	0.0111	0.0178	0.0282	0.045	0.069	0.157	0.35	0
12	10.7900	3765	0.00099	0.00175	0.00305	0.0052	0.0088	0.0145	0.0234	0.037	0.058	0.091	0.136	0.305	0.66	1
14	10.6954	3636	0.0024	0.00415	0.0071	0.0118	0.0196	0.0316	0.050	0.078	0.121	0.185	0.275	0.60	1.25	2
16	10.6261	3516	0.0056	0.0095	0.0016	0.0265	0.0428	0.0685	0.106	0.163	0.247	0.375	0.55	1.17	2.40	4
18	10.4957	3376	0.0135	0.0225	0.037	0.060	0.095	0.148	0.228	0.345	0.515	0.77	1.11	2.3	4.55	8
20	10.3833	3245	0.0316	0.052	0.084	0.132	0.205	0.32	0.48	0.72	1.06	1.55	2.21	4.4	8.5	15
22	10.3172	3125	0.0734	0.119	0.187	0.294	0.45	0.68	1.02	1.50	2.18	3.14	4.42	8.6	16.3	29
24	10.2185	2995	0.175	0.277	0.43	0.66	1.00	1.49	2.17	3.14	4.5	6.4	8.9	16.9	31.0	54
26	10.1303	2870	0.41	0.64	0.98	1.47	2.17	3.20	4.56	6.50	9.2	12.7	17.5	32.5	58.5	100
28	10.0115	2732	1.0	1.52	2.27	3.36	4.90	7.05	9.90	13.8	19.1	26.4	35.7	64	112	188
30	9.8763	2593	2.4	3.57	5.23	7.60	10.6	15.1	21.0	28.6	39.4	53	71	124	208	340
32	9.7523	2457	5.7	8.3	11.8	16.8	23.5	32.5	44.5	60.0	81	107	141	238	390	623
34	9.6061	2316	13.1	18.8	26.4	36.8	50.5	68.5	92	122	161	211	273	450	720	
36	9.5262	2229	29.0	41.0	56.4	78	105.5	142	188	246	322	416	535	860		
38	9.4670	2094	63.0	87.0	117	158	210	277	360	465	598	758	955			
40	9.2156	1939	130	176	233	307	399	515	627	830						
42	8.9925	1800	253	332	430	560	709	900								
44	8.8621	1681	510	655	840											
46	----	----	940													

[a]Perry, C.H., and D. Green, Eds., 1984 Chemical Engineers Handbook, McGraw Hill Book Company, New York, New York.

[b]$Log_{10}pmm = A - B/T$, which, however, agrees only approximately with the table. The table is more nearly correct.

APPENDIX 4.3

PAYLOAD COMPATIBILITY WITH BUTYL RUBBER O-RING SEALS

This page intentionally left blank.

4.3   Payload Compatibility with Butyl Rubber O-Ring Seals

4.3.1   Summary

Payload materials and chemicals in the RH-TRU 72-B packaging do not present an incompatibility concern with respect to the butyl rubber O-rings. Chemicals that are of concern with regard to incompatibility are not present in the waste in any significant amounts. Strong oxidizing acids are neutralized or basified prior to being generated as remote-handled transuranic (RH-TRU) waste. Organic solvents of concern that are present in residual amounts in the payload containers are usually bound or sorbed with the waste materials.

4.3.2   Introduction

This appendix evaluates the compatibility of the payload materials with the butyl rubber O-rings of the RH-TRU 72-B packaging. Chemicals that are reported as potentially incompatible with the butyl rubber O-rings (for liquid immersion or in saturated vapors) include the following:

- Concentrated oxidizing acids, (e.g., nitric acid)

- Aromatic hydrocarbons, (e.g., xylene and toluene)

- Halogenated organic solvents, (e.g., 1,1,2-trichloro-1,2,2-trifluoroethane [Freon-113], methylene chloride, carbon tetrachloride, and 1,1,1-trichloroethane).

4.3.3   Restrictions on Acids

The payload materials do not contain any free liquid acids, because the waste is in a solid form or is solidified. Acidic components from process operations, if present, are neutralized or basified before being generated as RH-TRU waste. Strong (concentrated) acids are prohibited through restrictions on corrosives.

4.3.4   Restrictions on Aromatic Hydrocarbons

Aromatic hydrocarbons (e.g., xylene) are also flammable and are restricted to the mixture lower explosive limit for the total flammable (gas/volatile organic compound) mixture as described in the Remote-Handled Transuranic Waste Authorized Methods for Payload Control (RH-TRAMPAC)[1] and Appendix 3.2 of the RH-TRU Payload Appendices. While this is an upper limit, process operations limit the presence and release of these hydrocarbons:

- Very few waste streams use flammable organic solvents at the sites, limiting the number of content codes that could contain these compounds.

---

[1] U.S. Department of Energy (DOE), *Remote-Handled Transuranic Waste Authorized Methods for Payload Control (RH-TRAMPAC)*, current revision, U.S. Department of Energy, Carlsbad Field Office, Carlsbad, New Mexico.

- Permeabilities of the aromatic hydrocarbons through any plastic bags used as confinement layers are extremely high.[2] Residual amounts of these compounds should escape from any bags before the waste is emplaced in the payload container.

- Analysis of solidified aqueous inorganic materials with ppm levels of aromatic hydrocarbons in the waste (Appendix 4.4 of the RH-TRU Payload Appendices) did not have any detectable levels in the headspace above the waste.

This class of compounds is therefore not an incompatibility concern for the payload materials and the package.

4.3.5   Restrictions on Halogenated Organic Solvents

Some of the organic solvents that are incompatible with butyl rubber are used in operations at the sites. Appendix 4.4 of the RH-TRU Payload Appendices evaluates the sources and release of these from the payload materials. Typically, RH-TRU waste is packaged in drums inside the RH-TRU waste canister, which further retards any potential release of organic solvents into the RH-TRU 72-B cavity. In view of these factors, the sealing properties of the butyl O-rings in the RH-TRU 72-B will not be affected by the payload materials.

4.3.6   Conclusions

In summary, the payload waste materials in the RH-TRU 72-B packaging do not present an incompatibility concern with respect to the butyl rubber O-rings. Chemicals that are of concern are not present in the RH-TRU waste in any significant amounts. Residual amounts of any solvents present are not expected to accumulate in any appreciable amounts in the RH-TRU 72-B cavity. These low concentrations are not sufficient to degrade the material properties of the butyl rubber O-rings and affect the sealing properties.

---

[2] Brandrup, J., and Immergut, E. H., eds., "Permeability Coefficients and Transmission Rates," Polymer Handbook, (Interscience Publishers, New York, 1966).

APPENDIX 4.4

VOLATILE ORGANIC COMPOUNDS (VOC) IN THE RH-TRU 72-B PAYLOAD – SOURCE TERM AND RELEASE RATE ESTIMATES

This page intentionally left blank.

4.4   Volatile Organic Compounds (VOC) in the RH-TRU 72-B Payload – Source Term and Release Rate Estimates

4.4.1   Introduction

Volatile organic compounds (VOC) are used by some of the U.S. Department of Energy (DOE) sites as part of their process operations. The presence of VOCs in the RH-TRU 72-B packaging, and their possible release into the inner vessel (IV) cavity during transport, could be of concern for two reasons: (1) potential damage to the butyl rubber O-ring seals due to interaction with the VOC vapors that could diffuse from the payload container, and (2) contribution to the overall pressure in the IV cavity by the vapor pressure that might be exerted by these chemicals. This appendix evaluates these concerns by an analysis of the process knowledge of the remote-handled transuranic (RH-TRU) waste generation processes.

4.4.2   Source Term of VOCS in Different Waste Types

VOCs are those organic compounds that exert appreciable vapor pressures at normal temperatures. Examples are halogenated compounds like 1,1,1-trichloroethane and methylene chloride and lower molecular weight alcohols (e.g., methanol). Some of these compounds are used at the DOE sites as industrial solvents and in decontamination operations. The potential of these volatiles being present in the payload of the RH-TRU 72-B packaging is of concern for the following reasons:

- The vapor pressure exerted by the volatiles may contribute to the total pressure in the RH-TRU 72-B cavity.

- Some of the organic solvents could potentially cause damage to the butyl rubber O-rings in the package during transport.

Hence, evaluation of the VOCs with respect to the payload and the package is necessary in order to ensure safe transport of the RH-TRU 72-B packaging. The following discussion demonstrates that the potential for VOCs being present in the waste and being released into the RH-TRU 72-B cavity is very small, and not a concern for transportation.

In general, the processes that generate RH-TRU wastes do not utilize significant amounts of the VOCs. Small amounts of carbon tetrachloride, 1,1,1-trichloroethane, freon-113, and methylene chloride may be used in the examination of metallographic fuel samples. In the case of contact-handled transuranic (CH-TRU) wastes, the use of VOCs was primarily as degreasing and cleaning agents in machining and lathe operations for the production of plutonium metal components. This is not true in the case of RH-TRU waste. RH-TRU materials are usually confined to operations that can be performed remotely in shielded glove boxes. These operations are typically limited bench-scale research and development activities and usually do not involve the use of halogenated VOCs.

Most of the RH-TRU waste has been in storage for a considerable period of time and will be repackaged prior to transport. Examples are the sludge and solid waste from Oak Ridge National Laboratory (ORNL). Any VOCs that were present in the original waste are likely to be present in the final waste configuration only in very small amounts. In addition, the sludge waste from

ORNL will be processed such that any VOCs present would be reduced to insignificant amounts in the final waste form.

A similar evaluation of the source term and release rates of VOCs for the TRUPACT-II and HalfPACT payloads (CH-TRU waste) was performed and presented in Appendix 6.4 of the CH-TRU Payload Appendices[1]. For TRUPACT-II and HalfPACT payloads, it was shown that, based on the source term and release estimates for the VOCs, release of these VOCs into the package is not a concern for transportation. A discussion of the payloads of the RH-TRU 72-B packaging (RH-TRU waste) and the TRUPACT-II and HalfPACT packages (CH-TRU waste) is presented here for comparative purposes.

CH-TRU waste has a category of waste (Waste Type IV - Solidified Organics) that could potentially have VOCs in greater than trace amounts in the waste. As detailed in the Contact-Handled Transuranic Waste Authorized Methods for Payload Control (CH-TRAMPAC)[2], this waste type was restricted from being a part of the TRUPACT-II or HalfPACT payload unless it was shown by actual testing that waste containers in this category were safe for transportation. RH-TRU waste is not expected to contain any solidified organics or VOCs in any appreciable amounts. As stated earlier, the use of VOCs in process operations (as solvents, degreasing agents, etc.) is less applicable to RH-TRU waste than it is to CH-TRU waste. With respect to the payload configuration, there is only the equivalent of three drums per shipment of RH-TRU waste as opposed to 14 or 7 drums of CH-TRU waste in the TRUPACT-II or HalfPACT, respectively, which limits the source term of the VOCs in the RH-TRU 72-B packaging. The configuration for a majority of the payload involves placing three drums in an RH-TRU waste canister. Both the drums and the RH-TRU waste canister are vented with filters, thereby minimizing the release of any VOCs into the RH-TRU 72-B cavity. As shown in Appendix 6.4 of the RH-TRU Payload Appendices[1], both the source term and release rates of VOCs into the packaging cavity are very small and are not a concern for transportation. In view of the above-mentioned factors, the presence of VOCs in the RH-TRU 72-B cavity is less of a concern for RH-TRU waste than it is for the CH-TRU waste.

The type of processes generating the RH-TRU wastes to be transported in the RH-TRU 72-B packaging and the payload configuration in the RH-TRU 72-B packaging are expected to preclude the presence of VOCs in any significant amounts. Similarly, as discussed in Appendix 4.3 of the RH-TRU Payload Appendices, the limits on the chemicals in the waste assure compatibility of the O-rings with the waste materials.

---

[1] U.S. Department of Energy (DOE), *CH-TRU Payload Appendices*, current revision, U.S. Department of Energy, Carlsbad Field Office, Carlsbad, New Mexico.

[2] U.S. Department of Energy (DOE), *Contact-Handled Transuranic Waste Authorized Methods for Payload Control (CH-TRAMPAC)*, current revision, U.S. Department of Energy, Carlsbad Field Office, Carlsbad, New Mexico.

APPENDIX 4.5

BIOLOGICAL ACTIVITY ASSESSMENT

This page intentionally left blank.

4.5   Biological Activity Assessment

4.5.1   Summary

This appendix addresses the impact of biological activity within the waste on shipments in the RH-TRU 72-B packaging. The primary concerns in this regard are the possible generation of gases by biotic processes that might contribute to the build up of pressure in the inner vessel (IV) cavity and/or produce potentially flammable gases. An analysis of the waste forms and their environment shows that biological activity will be minimal and will have little impact on the RH-TRU 72-B packaging during a potential shipping period of up to 60-days. Gas production by microbial processes is not a concern for transport of remote-handled transuranic (RH-TRU) waste in the RH-TRU 72-B packaging.

4.5.2   Introduction

Some of the RH-TRU waste forms and the packaging inside the payload containers (polyethylene [PE] and polyvinyl chloride [PVC] bags in drums) are organic in nature. The potential for microbial activity exists if a suitable environment exists for the degradation of these organics. As will be shown in the following sections, the waste environment during transport is not conducive for microbial proliferation.

4.5.3   Types of Biological Activity

There are different types of microorganisms to be considered in the degradation of RH-TRU waste. Aerobic microorganisms, which produce carbon dioxide (CO_2) and water (H_2O), require oxygen for growth.[1] Anaerobic microorganisms, which can produce CO_2 and hydrogen (H_2, predominantly as an intermediate) or methane (CH_4), as well as other products, degrade materials in anoxic (oxygen-free) environments.[1] Facultative anaerobes can live with or without oxygen. Obligate anaerobes, on the other hand, cannot tolerate any oxygen and will only grow in strict anoxic environments. Microorganisms most likely to be found in waste products include bacteria and fungi. Bacteria utilize only the surface of a material and can be either aerobic or anaerobic. Fungi can access the matrix of the material but are generally only found in aerobic environments. Microorganisms can also be classified based on the optimum temperature they require for growth. Mesophiles have an optimum temperature for growth between 20 and 55 °C, while thermophiles grow best at temperatures above 50 °C.

4.5.4   Waste Forms--Implications of Substrate and Nutrient Availability

Among the waste materials to be transported in the RH-TRU 72-B packaging, only the cellulosics materials (solid organics) can potentially serve as substrate for the microorganisms. Materials made of rubber and plastic are more resistant to microbial actions. The contribution of these compounds to the total gas generated will be negligible, (especially over the shipping

---

[1]Atlas, R. M., 1984, "Microbiology: Fundamentals and Applications," Macmillan Publishing Company, New York , New York.

period of 60 days) primarily because of their inert nature. Evidence of this is present from sampling studies done of similar waste forms of contact-handled transuranic (CH-TRU) waste (see Appendix 5.3 of the CH-TRU Payload Appendices[2]). With respect to biological activity within the waste, CH-TRU waste and RH-TRU waste can be expected to behave similarly (for those wastes that have similar constituents or substrates). Evidence from stored drums (in retrievable storage for periods up to 15 years) that were opened up as part of a sampling program shows little or no degradation of the packaging materials (see Appendix 5.3 of the CH-TRU Payload Appendices[2]). Even under conditions designed to promote microbial proliferation, these compounds degrade very slowly, if at all. Similarly, the solidified inorganic sludges should not exhibit any significant microbial gas generation due to their relatively high alkalinity (pH = 10-12), which would be hostile for most common microorganisms. This aspect is discussed further in the next section on environmental factors affecting microbial growth.

Examples of cellulosic materials that could be present in the RH-TRU 72-B payload are cotton, Kimwipes, and paper. Cellulose is a polymer composed of chains of glucose monomers. Biodegradation of cellulose requires the hydrolysis of the polymer into the monomer units. Biological depolymerization is a slow process that can significantly inhibit fermentation rates. Even though there are organisms that can degrade cellulose under different conditions, it is a complex process requiring very specific enzymes. Wood will also be present in TRU waste but is degraded at a much slower rate than cellulose in the form of cotton. Wood contains lignin which is much more resistant to microbial attack than cellulose. In addition, bacterial action is a strong function of surface area and substrate availability. The bulk form and segregated nature of the TRU waste creates conditions that are not very conducive to high microbial metabolic activities, especially during a limited period of 60 days. As shown in subsequent sections, the waste environment is such that, even for stored waste, the relatively long time period in itself is not sufficient to promote active microbial growth.

The availability of the nutrients, nitrogen and phosphorus, is another factor that can severely limit the extent of microbial activity in the RH-TRU 72-B payload. The dry weight of a bacterial cell typically contains 14% nitrogen and 3% phosphorus.[3] While some of the waste forms do contain sources of nitrogen, phosphorus is limiting in most cases. Even where sources of nitrogen are present, the waste form environments are far from optimum for bacterial growth. An example is inorganic sludges which contain nitrates but are lacking in carbon substrates, and which are basified to a pH of 10-12. In other words, even without any consideration of the non-ideal environmental conditions of the RH-TRU 72-B payload, substrate and nutrient limitations by themselves will maintain microbial activity at minimal levels in the packaging.

4.5.5 Environmental Factors Affecting Microbial Activity in the Payload

Environmental factors such as temperature, pH, Eh, oxygen, moisture content, and water availability are very important in determining the rates (kinetics) and feasibility (thermodynamic

---

[2] U.S. Department of Energy (DOE), "CH-TRU Payload Appendices," current revision, NRC Docket No. 71-9218, U.S. Department of Energy, Carlsbad Field Office, Carlsbad, New Mexico.

[3] Bailey, J. E., and D.F. Ollis, 1977, "Biochemical Engineering Fundamentals," McGraw Hill Book Company, New York , New York.

aspects) of microbial activity. For the RH-TRU 72-B payload, almost all of these environmental variables are either suboptimal or hostile for microbial activity. Each of these is considered in detail below.

4.5.5.1 pH and Temperature

The pH is an important factor to consider in the microbial degradation of RH-TRU waste. Typically, bacteria will be most active at neutral pHs. The sludges to be transported in the RH-TRU 72-B packaging are fairly basic (pH of 10-12), which will inhibit the activity of most bacteria and fungi. In addition, these sludges are lacking in carbon substrates. Specific organism groups like the methanogens (methane producers) also have sensitive pH ranges for growth.[2] Even under carefully controlled laboratory conditions, methanogenesis has a very long start-up phase and a fairly unstable operating phase. Establishment of an active population of methanogens is therefore unlikely in the RH-TRU 72-B packaging during the shipping period.

As mentioned in Section 4.5.3, microorganisms can be classified based on the optimum temperature they require for growth. Methanogens, for example, have an optimum temperature range between 90 to 100°F. Anaerobic digestion units (aimed at digesting sewage sludge and the production of methane) are usually provided with external heat exchangers to maintain optimum temperatures for methanogenesis.[3] These constant and optimal conditions are not likely to exist even for waste that has been stored for long periods of time. Fluctuations in the temperature also prevent the establishment of a stable microbial population in the waste containers.

4.5.5.2 Eh and Oxygen Availability

Eh (the redox potential) is an indication of whether an environment is oxidizing or reducing. Many microorganisms have strict Eh requirements for growth. Methanogens, for example, require a very reducing environment in which the Eh must be less than -200 mV.[4] They are obligate anaerobes and cannot tolerate even small amounts of oxygen. It is very unlikely that any significant quantities of methane will be produced during transport of RH-TRU waste. Methanogenesis from cellulose requires a complex set of organisms and conditions to be successful and is easily upset if favorable conditions are not maintained. The production of methane requires not only the depletion of oxygen but also the reduction of nitrates and sulfates.[3] Even in a process plant under optimum conditions, it is difficult to produce methane from cellulose. Even experiments done under controlled laboratory conditions showed no methane generation, with CO_2 being the major gaseous product.[5] (These experiments are not applicable to the transport conditions of the RH-TRU 72-B packaging - a bacterial inoculum was added to synthetic waste along with required nutrients in these experiments.) Radiolytic production of oxygen, even in trace quantities, would act as an inhibitor of anaerobic activity. In addition, the requirement of having a filter vent on all the waste containers before transport provides a means of communication with the environment, further destabilizing a constant environment even for the stored waste.

---

[4]Weiss, A. J., R. L. Tate III, and P. Colombo, 1982, "Assessment of Microbial Processes on Gas Production at Radioactive Low-Level Waste Disposal Sites," BNL-51557, Brookhaven National Laboratories, Brookhaven, New York.

[5]Molecke, M. A., 1979, "Gas Generation from Transuranic Waste Degradation: Data Summary and Interpretation," SAND79-1245, Sandia National Laboratories, Albuquerque, New Mexico.

4.5.5.3 Moisture Content and Water Availability

One of the prime requirements for microbial proliferation is the availability of sufficient amounts of water. Approximately 80% of a bacterial cell mass is water. Microbial activity can be sustained even at relative humidities below the saturation value, but metabolic activities under these conditions will be very slow. Hence, microbial gas generation rates in short time periods (like the 60-day shipping period) will be insignificant. As pointed out earlier, even if some of the content codes have pockets of damp waste, other requirements for biological activity (substrate, nutrients, suitable pH and Eh conditions) will not necessarily be present in these areas.

4.5.5.4 Radiation Effects on the Microorganisms

An additional factor that contributes to making the microbial environment non-ideal in the RH-TRU 72-B packaging is the radiation from the payload, which can result in the death of a portion of the microbial population. Radiation effects can potentially compound the existing hostile environment for the microorganisms in the payload.

4.5.6 Source Term of the Microorganisms

The waste packaging configuration in the payload containers restricts the source term for the microorganisms. While an initial microbial inoculum may be present in the waste, the filter vents on the waste containers have a filtering efficiency of ≥99.5%, with 0.3 to 0.5 micron particles, DOP (dioctyl phthalate) smoke (Section 2.4 of the Remote-Handled Transuranic Waste Authorized Methods for Payload Control [RH-TRAMPAC][6]). Typical dimensions of bacteria are between 0.5 to 3 microns.[3] This means that the filter vents would act as effective bacterial filters (though not 100%) to prevent continuous contamination of the waste with microorganisms.

4.5.7 Conclusions

The nature and configuration of the payload for the RH-TRU 72-B packaging are such that biological activity will be minimal and of very little concern during the 60-day shipping period. The environment in the IV cavity will be suboptimal or hostile for the growth of most microorganisms due to the segregation of the waste and essential nutrients and the limitations of usable substrate, nitrogen and phosphorus sources. The following factors support this statement:

1. Cellulose, which is the most likely waste product to be degraded by bacteria, is degraded by a complex process that requires a specific set of organisms. Some of these organisms may be present in the waste, but may not be in a sufficient quantity to contribute to the overall gas generation.

2. The proper nutrients (primarily nitrogen and phosphorus) must be present in order for the microorganisms to degrade any material. Nitrogen from the air cannot be efficiently utilized by microorganisms; it must come from a source such as nitrate.

---

[6] U.S. Department of Energy, "Remote Handled Transuranic Waste Authorized Methods for Payload Control (RH-TRAMPAC)," current revision, U.S. Department of Energy, Carlsbad, New Mexico.

Sufficient phosphorus, however, is very likely to be missing or limiting in many drums.

3.   It is very unlikely that methane would be produced during transportation of the waste for several reasons:

   -   The environment for methanogenesis must be very reducing (no oxygen)

   -   Very specific microorganisms are required, which exist in narrow ranges of suitable environments, and

   -   The process can be self-poisoning if intermediates produced are not controlled or neutralized.

4.   Although hydrogen may be produced during intermediate steps in anaerobic processes, it is very unlikely that it will be present as a final product. It is used as a reducing agent almost as quickly as it is produced.

5.   Another factor limiting bacterial degradation is substrate surface area. The cellulosic materials that are put into bags are in a very bulky form that is not easily accessible to surface-decomposing bacteria.

6.   Any aerobic decomposition will result in insignificant pressure changes due to the simultaneous consumption of oxygen with the production of carbon dioxide.

7.   Even retrievably stored waste does not provide the necessary conditions for continuous and prolonged microbial activity. Fluctuations in environmental variables like the temperature and oxygen availability (due to the filter vent) act to prevent anaerobic biological activity at any significant level. Evidence from sampling programs shows very little deterioration of the packaging materials even after years of storage. In addition, limitations in substrate and nutrient availability and segregation of these nutrients apply to retrievably stored waste as well.

This page intentionally left blank.

APPENDIX 4.6

**THERMAL STABILITY OF PAYLOAD MATERIALS AT TRANSPORT
TEMPERATURES**

This page intentionally left blank.

4.6   Thermal Stability of Payload Materials at Transport Temperatures

This appendix describes the thermal stability of payload materials, demonstrating that thermal degradation will be minimal for payload materials during transport in the RH-TRU 72-B packaging.

4.6.1   Introduction

The thermal stability of the payload materials is addressed for the wastes inside RH-TRU canisters.

Inorganic payload materials will be thermally inert, with the possible exception of small amounts of gases adsorbed on the surfaces, most of which will be water vapor. The pressure calculations performed in the RH-TRU 72-B Safety Analysis Report (SAR) assume saturated water vapor is present in all cases.

Organic materials meet transport requirements by demonstrating compliance with a limit on the hydrogen generation rate (Option 1) or a limit on the decay heat (Option 2) for a given content code, depending on the chemical makeup and decay heat of the wastes. Thermal stability of payload materials is addressed in terms of the threshold decomposition temperatures. The effect of irradiation on the materials at the lowest threshold decomposition temperature is shown to be negligible.

Plasticizers added to polymers to increase flexibility are typically less thermally or chemically stable than the polymers.[1] However, the vapor pressures of most common plasticizers (e.g., phthalates, sebacates, and other esters) are only 1 millimeter of mercury at 160 degrees Fahrenheit (^{o}F) (71 degrees Celsius [^{o}C]) or above[2] and can be ignored in pressure calculations.

Oxidation is the major degradation process for polymers heated in the presence of oxygen. In a sealed system, oxygen typically is depleted at a rate faster than the rate of formation of oxygen-containing gases such as carbon dioxide or carbon monoxide, leading to a net pressure decrease.

4.6.2   Threshold Decomposition Temperatures for Plastics and Other Polymers

Waste material and packaging components may be a combination of cellulosics, plastics, and rubber. Representative materials from each of these categories were studied to determine threshold decomposition temperatures.[3] The temperature at which a material loses weight, not including drying, is the threshold decomposition temperature. Gas generation from thermal decomposition was measured by pressure increases in sealed containers over long periods of time. Experiments were performed in aerobic and anaerobic atmospheres.

---

[1] Deanin, R. D., 1972, Polymer Structure, Properties and Applications, Chaners Books, Boston, Massachusetts.

[2] AIP Handbook, 1963, American Institute of Physics Handbook, Second Edition, McGraw-Hill Book Company, New York, New York.

[3] Kosiewicz, S. "Cellulose Thermally Decomposes at 70ºC," *Thermochimica Acta*, Vol. 40, pp 319-326, 1980.

The threshold decomposition temperature for materials in air is shown in Table 4.6-1. Pylox gloves (polyvinyl chloride) have the lowest threshold decomposition temperature of 302ºF (150ºC). Results of anaerobic experiments and experiments with potential catalysts that may be present in the waste yielded no significant lowering of the threshold decomposition temperatures.

Table 4.6-1 – Threshold Decomposition Temperatures in Air

Material	Temperature (°C)
Cellulosics[①]	
Scott utility wipes	185
Kleenex tissues	185
Diaper paper (PE-backed)	190-185
Cloth (cotton twill)	185
T-shirt (cotton)	185-190
Cheesecloth	205
Wood	175
Fiberboard	185-190
Plastics	
Pylox gloves (PVC)	150
Tygon tubing (PVC)	175
Polyethylene	210
Polypropylene	195-200
Lucite [poly(methyl methacrylate)]	170-175
Teflon [poly(fluoroethylene)]	430-435
Rubbers	
Hypalon	165
Neoprene	175-180
Durasol/neosol	180
Latex	195
Bitumen[②]	275

Source: Kosiewicz, S. "Cellulose Thermally Decomposes at 70ºC," Thermochimica Acta, Vol. 40, pp 319-326, 1980.

[①] Water loss observed at 40-110°C.

[②] Not a rubber material.

The generation of gas through thermal decomposition of the waste materials did not occur at temperatures lower than 302ºF (150ºC).

4.6.3 Effect of Radiation on Thermal Properties of Materials

Radiation chemically changes materials and can affect their thermal properties. For example, for an absorbed dose of 500 millirad in vacuum, the melting point of polyethylene was decreased about 9°F (5°C).[4]

Polyethylene films irradiated in vacuum or under a nitrogen atmosphere were subsequently heated in the presence of oxygen at 230°F (110°C). The weight change between unirradiated and irradiated polyethylene films (exposure times up to 1150 hours) was compared.[5] The major difference between irradiated and unirradiated materials was that the irradiated materials began to absorb oxygen and increase in weight after 50 hours without antioxidant, or after 500 hours with antioxidant.

The rate of weight loss versus temperature of polyethylene was measured for samples irradiated in air and then heated in air.[6] Thermal degradation was detectable above about 302°F (150°C), with only minor differences found between irradiated and unirradiated materials.

The conclusions reached are that while there are measurable differences in the thermal properties of polymers when they are irradiated, the effects are relatively small even near 392°F (200°C), and can be neglected for temperatures less than or equal to 302°F (150°C).

4.6.4 Conclusions

The generation of gases through thermal degradation of the waste materials up to 302°F (150°C) will be negligible. Since the organic (paper) waste payloads with a 50-watt thermal limit authorized for shipment in the RH-TRU 72-B package will not approach the 302ºF (150ºC) temperature during normal conditions of transport, the conclusion reached is that the generation of gases through thermal degradation of the waste materials will be negligible.

---

[4] Black, R. M., and A. Charlesby, 1959, "The Oxidation of Irradiated Polyethylene-II Thermal Oxidation," Inter. J. Appl. Radiat. Isotopes 7, pp. 134-140.

[5] Kato, K., et al., 1981, "Structural Changes and Melting Behavior of Gamma-Irradiated Polyethylene," Jap. J. Appl. Phys. 20, pp. 691-697.

[6] Igarashi, S., 1964, "Thermogravimetric Analysis of the Effect of Ionizing Radiation on Thermal Stability of Polyethylene," J. Appl. Polym. Sci., Vol. 8, pp 1455 - 1464.

This page intentionally left blank.

APPENDIX 5.1

DESCRIPTION OF NEUTRON SHIELDED CANISTER

This page intentionally left blank.

5.1 Description of Neutron Shielded Canister

5.1.1 Introduction

The neutron shielded canister is an augmentation of the removable lid canister available in two configurations, NS15 and NS30, which incorporates internal neutron shielding components that provide two levels of supplemental neutron shielding for approximately 15- and 30-gallon inner containers (drums), respectively. It is designed to be used for the shipment of specific transuranic waste forms in the RH-TRU 72-B package. Drawing X-106-503-SNP in Appendix 1.3.1 of the RH-TRU 72-B SAR[1] and Section 2.8 of the *Remote-Handled Transuranic Waste Authorized Methods for Payload Control* (RH-TRAMPAC)[2] delineate the materials of construction, sizes, and other dimensional specifications for the neutron shielded canister.

The neutron shielded canister is intended for the shipment of transuranic waste forms with high neutron source terms in the RH-TRU 72-B. The RH-TRU 72-B package can accommodate one neutron shielded canister. As configured for shipment, the neutron shielded canister payload assembly remains conservatively within the previously established design and certification bases and limits of the RH-TRU 72-B package for payload weight and decay heat. Limits on neutron shielded canister activity and fissile content are also set consistent with previously implemented and accepted analytic approaches.

This appendix describes the structural, thermal, shielding, and criticality basis of the neutron shielded canister payload.

5.1.2 Description

As illustrated in Figure 5.1-1, the NS30 neutron shielded canister is a 26-inch diameter, 120½-inch tall removable lid canister with a high-density polyethylene (HDPE) neutron shield insert, weighing approximately 1,660 pounds empty and having a maximum gross weight of 3,100 pounds. It is designed to carry three approximately 30-gallon steel payload drums with internal lever-lock closures, where each drum and its contents are limited to approximately 480 pounds. The NS30 neutron shielded canister incorporates the NS30 neutron shield insert which consists of HDPE top and bottom end caps (nominally 5 inches thick) with an integral open-cell urethane filter/gasket and a 24-inch outside diameter cylindrical pipe body (nominally 1.454 inches thick). The minimum thickness of HDPE neutron shielding provided by the body is 1.412 inches. As illustrated in Figure 5.1-2, the NS15 neutron shielded canister is essentially identical to the NS30 with appropriate modification to accommodate a thicker 24-inch outside diameter cylindrical pipe body (nominally 3.387 inches thick) with 3.288 inches minimum thickness and an approximate tare weight of 2,070 pounds and maximum gross weight of 3,100 pounds. The NS15 is designed to carry three approximately 15-gallon steel payload drums with internal lever-lock closures, where each drum and its contents are limited to approximately 337 pounds.

---

[1] U.S. Department of Energy (DOE), *RH-TRU 72-B Package Safety Analysis Report*, USNRC Certificate of Compliance 71-9212, U.S. Department of Energy, Carlsbad Field Office, Carlsbad, New Mexico.

[2] U.S. Department of Energy (DOE), *Remote-Handled Transuranic Waste Authorized Methods for Payload Control* (RH-TRAMPAC), U.S. Department of Energy, Carlsbad Field Office, Carlsbad, New Mexico.

Both the NS30 and NS15 neutron shielded canisters incorporate HDPE end caps that are slip-fit into the HDPE pipe body. The end caps are engaged and remain captured within the pipe body through a 2-inch deep end cap step and the limited (1/2-inch maximum) axial geometric clearance of the shield assembly within the surrounding canister structure. An optional, up to 1-inch thick, 24-inch diameter disc of CDX grade plywood may be located above the top end cap or below the bottom end cap to ensure the maximum axial clearance is maintained. Both end caps incorporate lifting D-rings utilized to facilitate handling during remote operations. In addition to the respective payload drums, the neutron shielded canisters may optionally contain a mesh "bag" used to facilitate remote installation of each payload drum into the shield insert assembly. The neutron shielded canister must be installed with a filter vent; Section 2.4 of the RH-TRAMPAC provides the minimum specification for the neutron shielded canister filter vent.

An isometric rendering of the NS30 neutron shielded canister (without payload drums) illustrating the installed end caps and gasket configuration is provided in Figure 5.1-3.
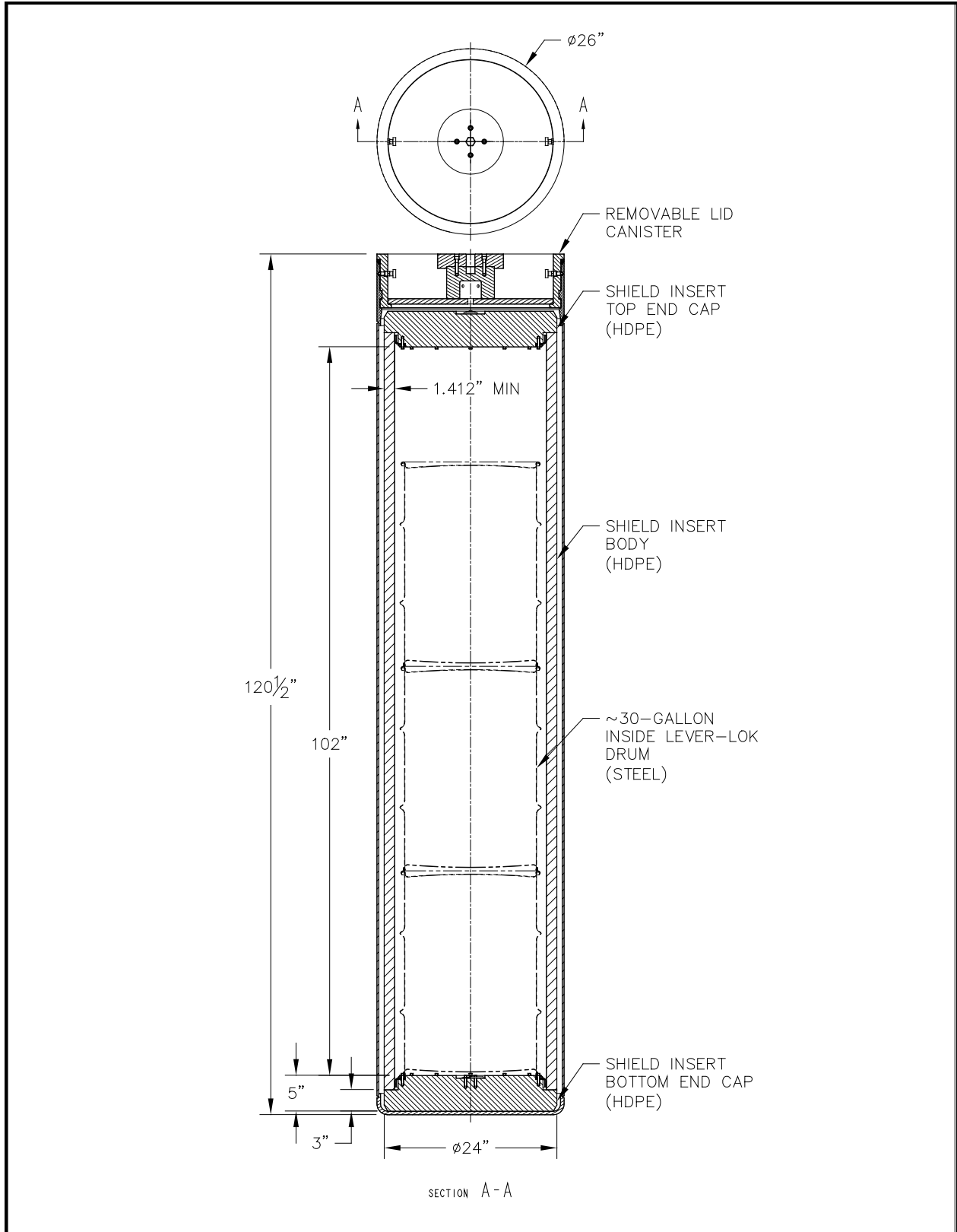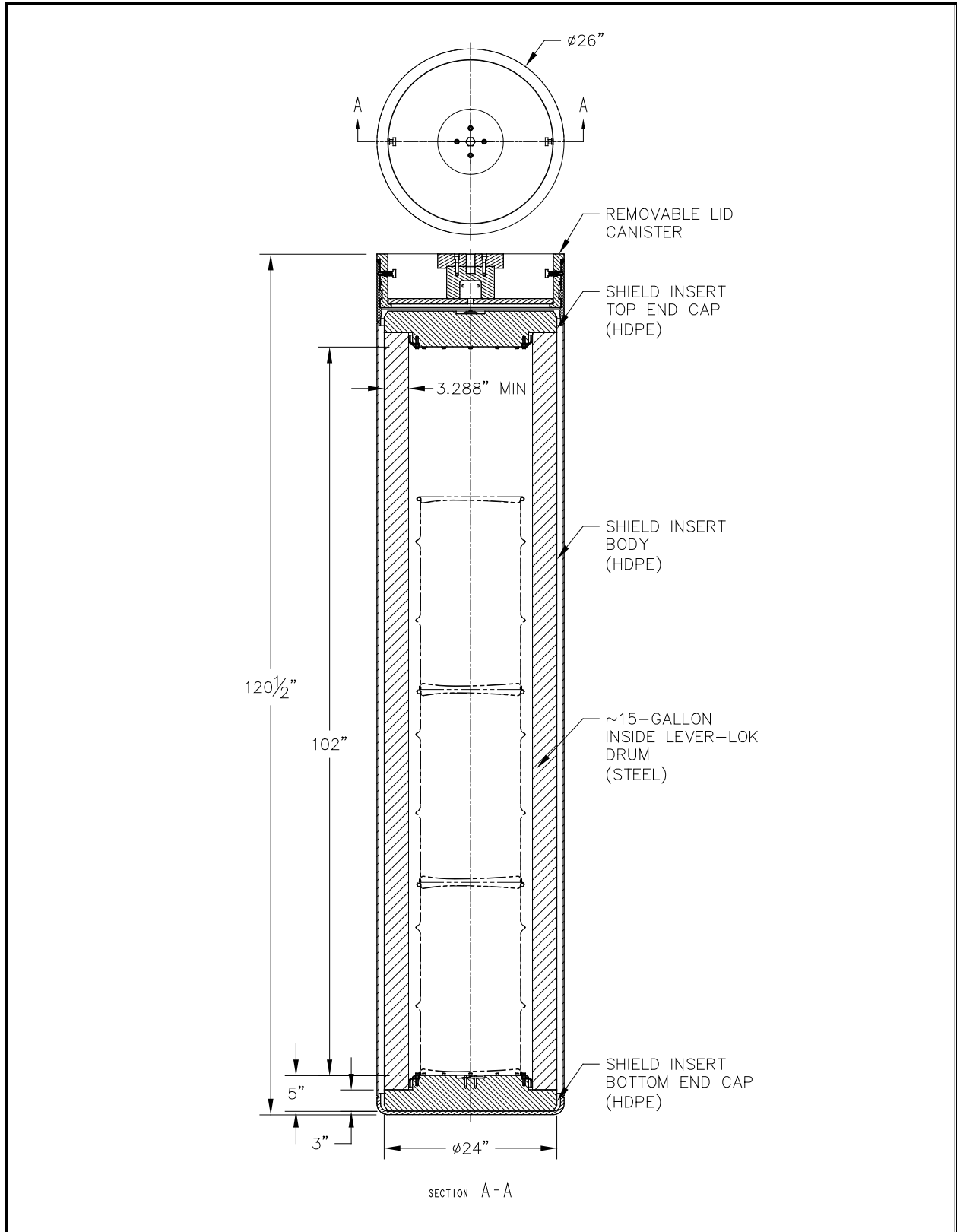
Figure 5.1-1 – Neutron Shielded Canister, NS30

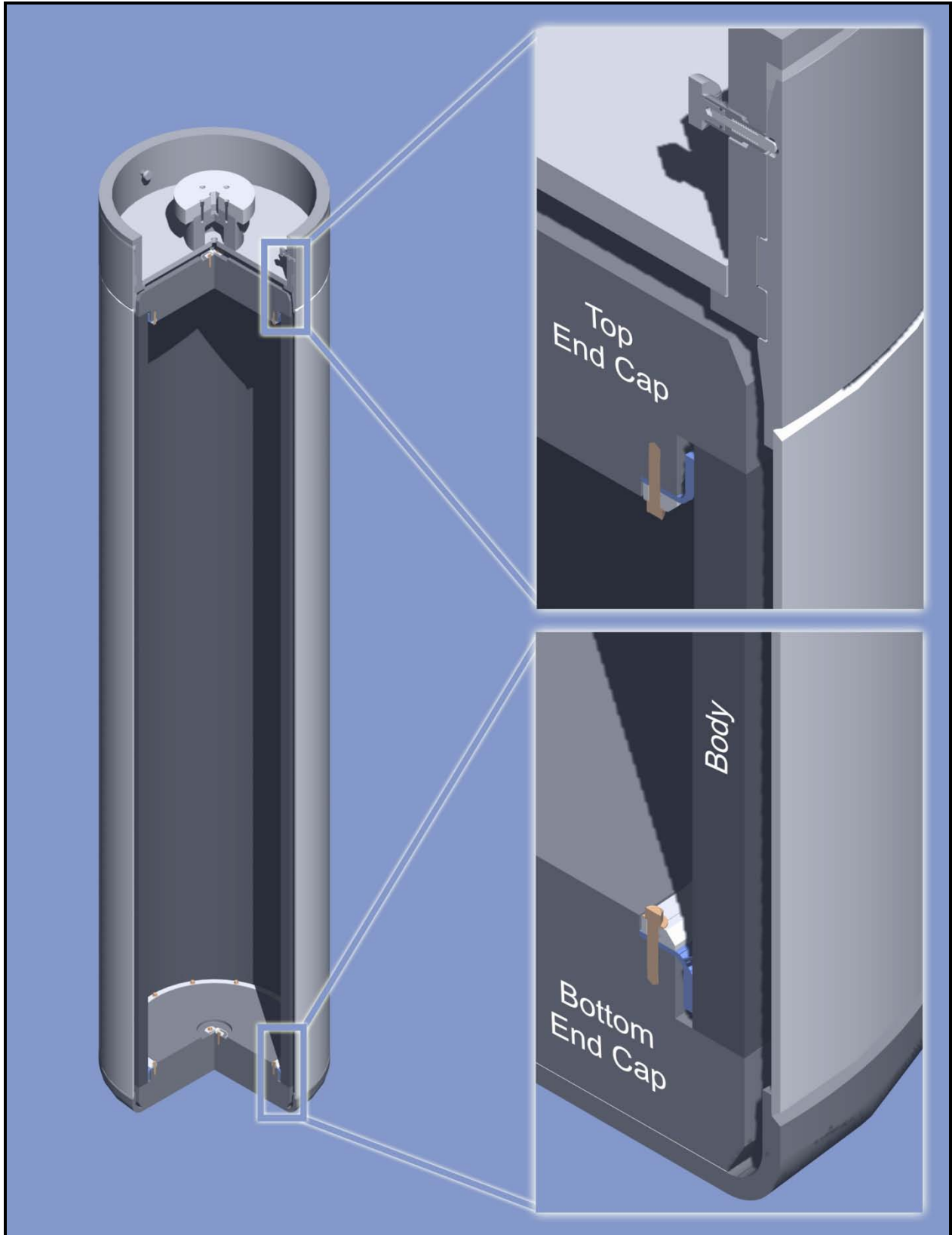**Figure 5.1-2** – Neutron Shielded Canister, NS15

Figure 5.1-3 – NS30 Isometric

5.1.3 Structural Evaluation

Based on the following paragraphs, the neutron shielded canister payload configuration is, from a RH-TRU 72-B packaging perspective, bounded by previous certification analyses and testing for the RH-TRU 72-B package as currently presented in the RH-TRU 72-B SAR. Therefore, the following structural evaluations are specific to determining the response of the neutron shielded canister and associated shield insert components when subject to transport and accident conditions when transported in the RH-TRU 72-B package.

5.1.3.1 Structural Evaluation for Normal Conditions of Transport

Under normal conditions of transport (NCT), the neutron shielded canister maintains gross confinement and primary shielding integrity. As discussed in Section 5.1.3.2, *Structural Evaluation for Hypothetical Accident Conditions*, gross confinement and primary shielding integrity has been demonstrated for hypothetical accident conditions (HAC) with less than ¼% (by weight) loss of the fine particulate releasable source term, minimal degradation of the shield insert components, and no loss of engagement of the shield insert end caps and body. Because HAC bounds NCT, demonstrations specific to NCT are not necessary.

5.1.3.2 Structural Evaluation for Hypothetical Accident Conditions

Under HAC, the neutron shielded canister confines greater than 99-¾% (by weight) of its contents within its shielded boundary. To demonstrate confinement and shielding integrity of the neutron shielded canister, a full-scale test program was conducted.[3] Since gross confinement integrity was maintained, and the shielding material did not reconfigure and was minimally degraded during HAC testing, NCT is bounded by the HAC test program.

The NS30 neutron shielded canister was assembled and installed within a test fixture fitted with end and side impact limiters and an internal lid flange and two centralizing rings that imposed g-forces and boundary conditions that conservatively replicated the RH-TRU 72-B packaging. The test fixture and two NS30 neutron shielded canisters were each subjected to two 30-foot free drops onto a flat, essentially unyielding, horizontal surface: a vertical end drop and a horizontal side drop with the test fixture at ambient conditions and the canister and shield insert components at cold (<-20 °F) and hot (>150 °F) conditions. At the conclusion of the second 30-foot free drop for both cold and hot conditions, each NS30 neutron shielded canister was removed from the test fixture and disassembled to verify that the shield insert end caps were engaged with the shield insert body, to ascertain any permanent deformation to the canister and shield insert components, and to determine whether any of the releasable source term (5 pounds of fine particulate sand in each of three inner 30-gallon drum payload container) was released.

To conservatively test to the maximum allowable payload weight of 3,100 pounds within a RH-TRU 72-B packaging, each NS30 neutron shielded canister test article utilized three 30-gallon steel drum (approximately 35 pounds empty) filled with 478 pounds of concrete on average and 5 pounds of sand, for a total average contents weight of 1,538 pounds. Combined with the NS30 canister test article tare weights, the average total gross weight of the loaded canisters was 3,205 pounds (105 pounds over the total gross weight limit).

---

[3] Engineering Report 7953-R-027, *30-foot Free Drop Post-Test Summary Report for the NS30 Neutron Shielded Canister*, Revision 0, Petersen Incorporated, November 2009.

5.1.3.2.1 Technical Basis for the Tests

The following sections supply the technical basis for the chosen free drop test orientations and sequences, the use of a test fixture as a surrogate to the RH-TRU 72-B packaging, the physical testing of the NS30 neutron shielded canister to bound both the NS30 and NS15 neutron shielded canister designs, and the free drop test temperatures and pressures.

5.1.3.2.1.1 Justification for Drop Orientations

A graphical representation of the data provided in Table 2.10.3-11 and Table 2.10.3-12 of the RH-TRU 72-B SAR is shown in Figure 5.1-4.   As summarized in Table 2.10.3-10 of the RH-TRU 72-B SAR, the largest impact acceleration occurs during an end drop (90°) orientation at -20 °F with a magnitude of 89.7g (essentially equivalent to acceleration of 90.7g at the 85° from horizontal impact orientation). Under cold conditions, the side drop (0°) orientation produces an impact acceleration of 81.2g. A similar response, although at a lower magnitude, is observed under hot (140 °F) conditions subject to the end and side drop orientations. At both temperature extremes for the RH-TRU 72-B impact limiters, the end and side drop orientations produce greater impact accelerations when compared to the intermediate impact orientation angles.

Due to the objective of the drop tests to determine the response of the neutron shielded canister (particularly the NS30 shield insert), which is effectively supported in all directions by the RH-TRU 72-B inner vessel (IV) and canister interfaces, drop testing at intermediate impact orientations between 0° and 90° and at the corresponding lower impact accelerations is not bounding. The interaction between internal drum payload containers and the shield insert body/end caps is maximized, along with the potential for damage to the neutron shield components, when impact accelerations are maximized. Intermediate impact angles simply distribute the interaction forces at lower g-levels between the payload and the shield insert body and end caps, whereas the 0° and 90° impact orientations maximize the impact accelerations and localized bearing forces in a manner to maximize the potential for shield damage. As such, side and end drop test orientations are bounding for the design.

The requirements of 10 CFR §71.73(c)(1) are satisfied as the drop test orientations are associated with positions for which maximum damage to the neutron shielded canister is expected.
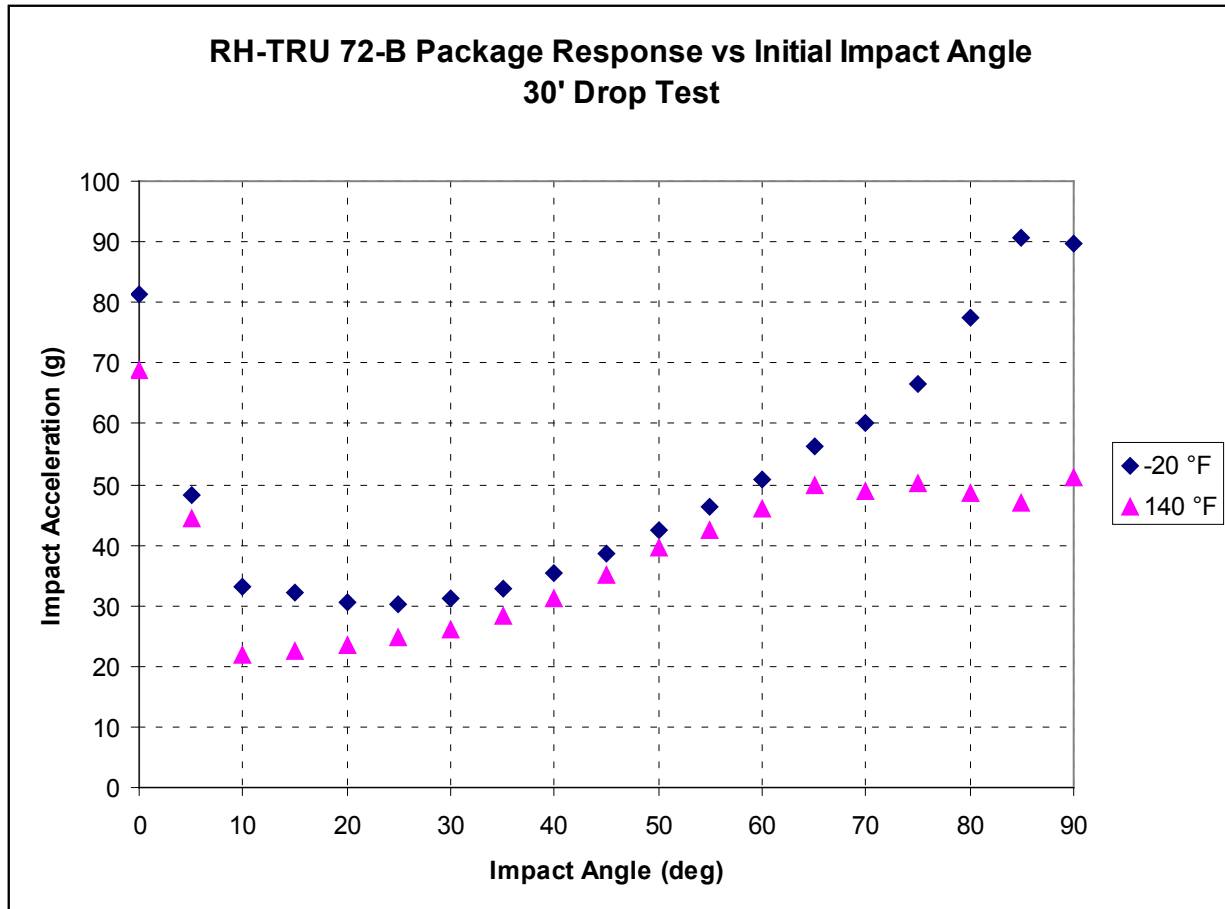
Figure 5.1-4 – RH-TRU 72-B Impact Acceleration Dependency on Impact Angle and Temperature

5.1.3.2.1.2 Justification for Testing Only the NS30 in a 72-B Surrogate Test Fixture

Due to the maximum gross weight limit of the NS30 and NS15 neutron shielded canisters being 3,100 pounds and significantly lower than the 8,000-pound payload capacity authorized for the RH-TRU 72-B packaging, the packaging response to a neutron shielded canister payload is bounded by the current packaging design and analysis. The use of the neutron shielded canister test fixture provided structural interfaces equivalent to the RH-TRU 72-B IV and generated impact accelerations that are conservatively in excess of the RH-TRU 72-B packaging. As such, the neutron shielded canister test fixture represented an appropriately bounding surrogate to testing the NS30 neutron shielded canister in an actual RH-TRU 72-B packaging. The test fixture was designed to be dropped with its impact limiters at nominal ambient temperature conditions while the NS30 neutron shielded canister payload was heated and cooled to the appropriate hot and cold canister test temperatures. The test fixture was designed to impart impact accelerations to the heated and/or cooled NS30 neutron shielded canister that were at least 150% of the maximum accelerations in an actual RH-TRU 72-B packaging.

Testing only the NS30 neutron shielded canister as a bounding surrogate for both the NS30 and NS15 neutron shielded canisters was appropriate because the gross weight of both canister designs is the same, the payload capacity of the NS30 is greater than that of the NS15, and the NS30 has less than half the body sidewall thickness. The end cap thickness of both the NS30 and NS15 designs is the same. The NS30 is therefore subjected to payload interaction (i.e., secondary impact) loads and primary impact acceleration based stresses that are greater than that for the NS15. As such, the NS30 neutron shielded canister was tested to qualify both designs.

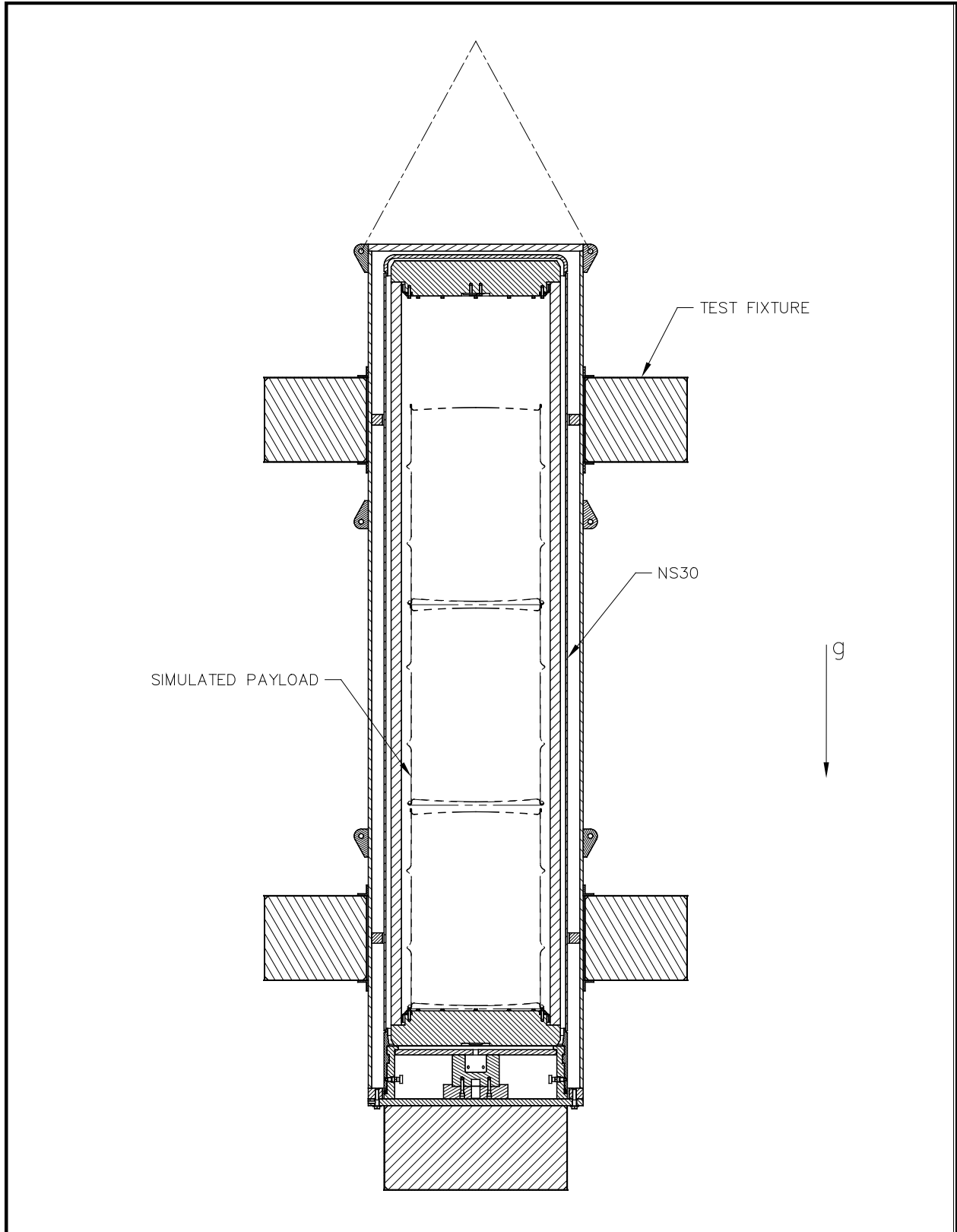The test configuration and orientations are illustrated in Figure 5.1-5 and Figure 5.1-6.
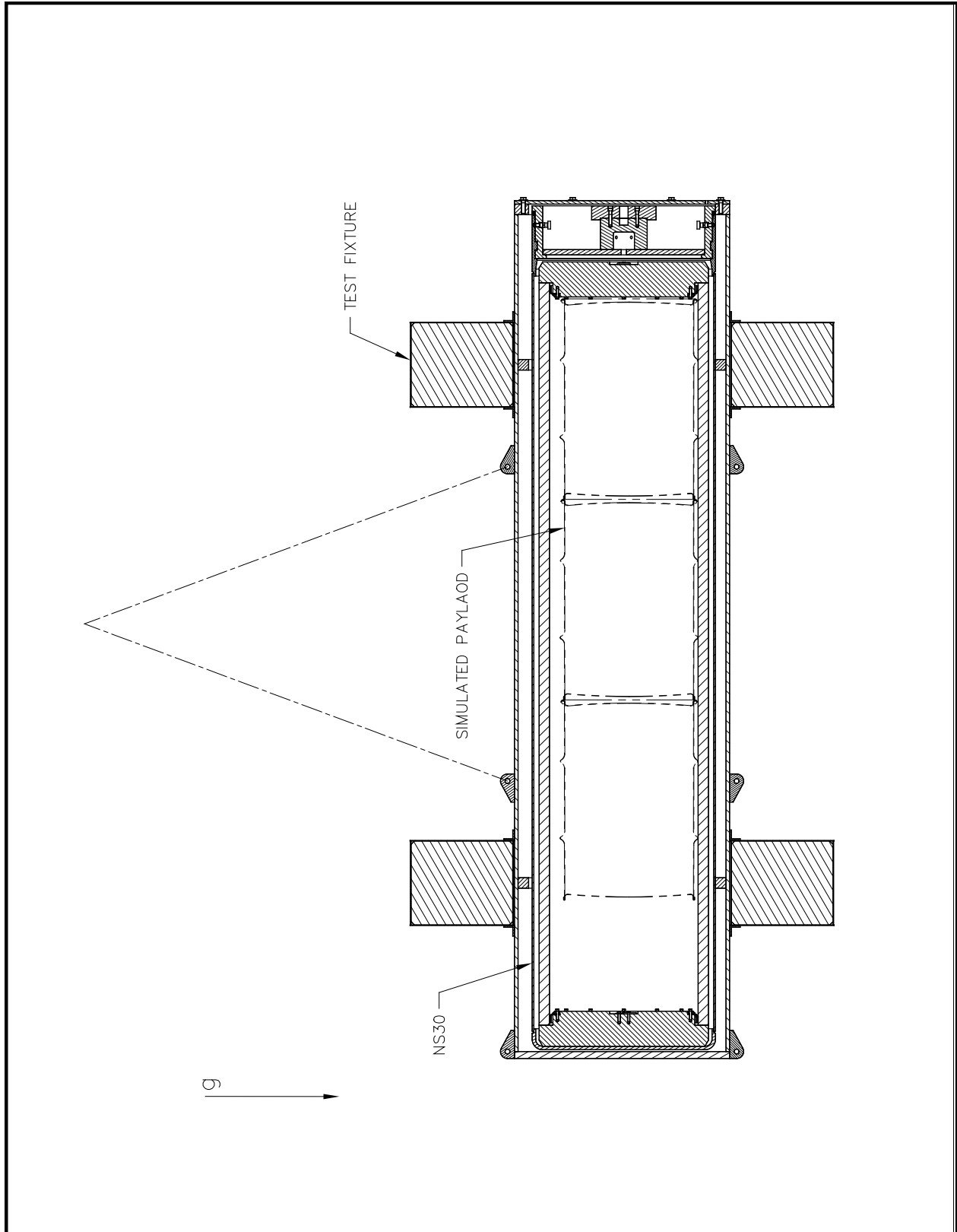
Figure 5.1-5 – End Drop Test Configuration

Figure 5.1-6 – Side Drop Test Configuration

5.1.3.2.1.3   Justification for Test Temperatures

The neutron shielded canister test fixture was tested at ambient temperature, but designed with impact limiters that at ambient temperature induce impact accelerations that are significantly in excess of those for the RH-TRU 72-B package with impact limiters at either hot or cold temperature conditions. To evaluate the response of the NS30 neutron shielded canister at hot and cold temperature conditions subject to the bounding impact accelerations induced by the test fixture, the NS30 was prepared and conditioned as discussed below. One NS30 neutron shielded canister was tested under cold conditions and one NS30 neutron shielded canister was tested under hot conditions.

5.1.3.2.1.3.1   Cold

The temperature of the NS30 neutron shielded canister components at the time of both the end and side drop tests was less than or equal to -20 °F, consistent with a thermal case of no internal decay heat and an ambient air temperature of -20 °F as prescribed in 10 CFR §71.73(b). In addition to the prescribed drop test temperatures, the evaluation of the effect of cold temperatures on the nil-ductility of the HDPE neutron shield insert body and end caps was performed. A maximum scratch/gouge criterion of ¼ inch depth was validated by inducing a ¼ inch deep circumferential v-groove (60° included angle) by routing/machining around the midline circumference of the body pipe. Additionally, a similar groove was routed/machined across the outer or upper midline face of the top end cap. Both the body pipe and top end cap had a v-groove of ¼ inch minimum depth at locations expected to experience the maximum bending and associated tensile stress that could propagate a material flaw. The absence of flaw propagation that induced shield failure validated the scratch/gouge criteria and demonstrated that the HDPE material does not exhibit a nil-ductility response due to the -20 °F temperature and associated drop test induced stress.

5.1.3.2.1.3.2   Hot

The temperature of the NS30 neutron shielded canister components at the time of both the end and side drop tests was greater than or equal to 150 °F, consistent with a thermal case of 50 watts internal decay heat and an ambient air temperature of 100 °F as prescribed in 10 CFR §71.73(b). Section 5.1.4.1, *Thermal Evaluation for Normal Conditions of Transport*, demonstrates that the maximum temperature for both the NS15 and NS30 neutron shield HDPE components under NCT conditions (with insolation) are 141 °F and 137 °F, respectively. Testing at a minimum of 150 °F conservatively bounded the authorized contents and temperatures of the canister components having material properties with a marked sensitivity to elevated temperature conditions.

5.1.3.2.1.4   Justification for Test Pressure

These NS30 and NS15 neutron shielded canisters are vented and not subject to differential pressures; hence, internal pressurization of the neutron shielded canister test fixture was not applicable.

5.1.3.2.2 Cold End and Side Drop Results

The cold end drop was performed using a neutron shielded canister test fixture that was fitted at one end with a 20 pound per cubic foot (pcf) rigid urethane foam impact limiter to conservatively simulate a cold end impact deceleration acting on the RH-TRU 72-B package of 89.70*g*. The NS30 neutron shielded canister, with its three 30-gallon drum simulated contents, was oriented in a lid down configuration such that maximum impact deceleration, payload rebound, and secondary impact was focused on the shield insert end cap and associated pipe body interface. Given the circumferentially uniform 5/8-inch residual end impact limiter deformation, the test fixture experienced an impact deceleration estimated with constant resistance as a function of the drop height and end limiter deformation (360 in./0.625 in.) of 576*g* with 375*g* average deceleration measured by two piezoelectric accelerometers attached to the test fixture outer shell near the impact location.

The subsequent cold side drop was performed utilizing the same test fixture and NS30 test article, impacting two 16 pcf rigid urethane foam impact limiters to conservatively simulate a cold side drop impact deceleration acting on the RH-TRU 72-B package of 81.20*g*. The NS30 neutron shielded canister and contents were oriented in a horizontal configuration such that maximum impact deceleration, payload rebound, and secondary impact was focused on the shield insert body and canister shell as simply supported by the package inner vessel centering rings. Given the 1-5/8-inch residual side impact limiter deformations, the test fixture experienced an impact deceleration estimated with constant resistance as a function of the drop height and end limiter deformation (360 in./1.625 in.) of 221*g* with 136*g* average deceleration measured by two piezoelectric accelerometers attached to the test fixture outer shell near the impact locations.

Observed deformations and measured decelerations demonstrate that the test fixture conservatively simulated the RH-TRU 72-B by inducing impact decelerations in both the cold end and side drop orientations that were in excess of the maximum decelerations that would have been experienced by testing with an RH-TRU 72-B package.

The top end cap and the body pipe components, manufactured from pipe grade extra high molecular weight HDPE, were tested at -20 °F with induced flaws in the form of ¼-inch deep 60° v-notch grooves machined across the outer face of the top end cap and circumferentially about the mid-line of the body pipe outside diameter. The flaws were located in areas of maximum bending-induced tensile stress to ensure acceptable material performance, as evidenced by no propagation of the flaws and/or a ductile response of the plastic components at low temperature. A maximum thickness CDX plywood spacer was additionally installed above the top end cap (and below the canister lid) to achieve an axial spacing that was greater than the ½-inch maximum allowed. The axial gap was initially maximized and the gap increased through crushing of the spacer during the end drop to conservatively determine whether the top and bottom end caps remained engaged with the body pipe and shield streaming paths precluded. The open-cell urethane foam debris gaskets experienced cut damage from interaction between the end caps and body pipe, but the end caps remained engaged with the body pipe and no release of the fine particulate sand was observed outside of the shield components after the cold end and side drop tests. Impact dents and gouges were observed in both the end caps and body pipe interior surfaces due to interaction with the payload drums and on exterior surfaces due to interaction with the surrounding canister features, but no dent or gouge exceeded ¼-inch maximum depth which is the defined scratch and gouge criteria.

Post-drop damage to the canister lid and body were minor with the only location of observed deformation being the interface between the canister shell and the internal centering rings in the test fixture. The canister lid was unaffected by the drop as it was easily unlocked, rotated, and removed for inspection after the drop tests using the standard manual operating techniques.

Figure 5.1-7 illustrates the drop-induced deformation of the test fixture end and side impact limiters. Figure 5.1-8 illustrates the deformation of the plywood spacer and end cap gasket damage. Figure 5.1-9 illustrates that there was no propagation of the induced v-notch defects in either the top end cap or body pipe at cold temperature. The engagement of the top end bottom end caps with the pipe body to preclude streaming paths out of the shield components is shown in Figure 5.1-10. The most aggressive external and internal dents and gouges experienced by the body pipe are shown in Figure 5.1-11. The condition of the canister lid and body is illustrated in Figure 5.1-12.

Figure 5.1-7 – Cold End and Side Drop Impact Limiter Deformation

Figure 5.1-8 –Cold Drop Damage to the Spacer and End Cap Gasket
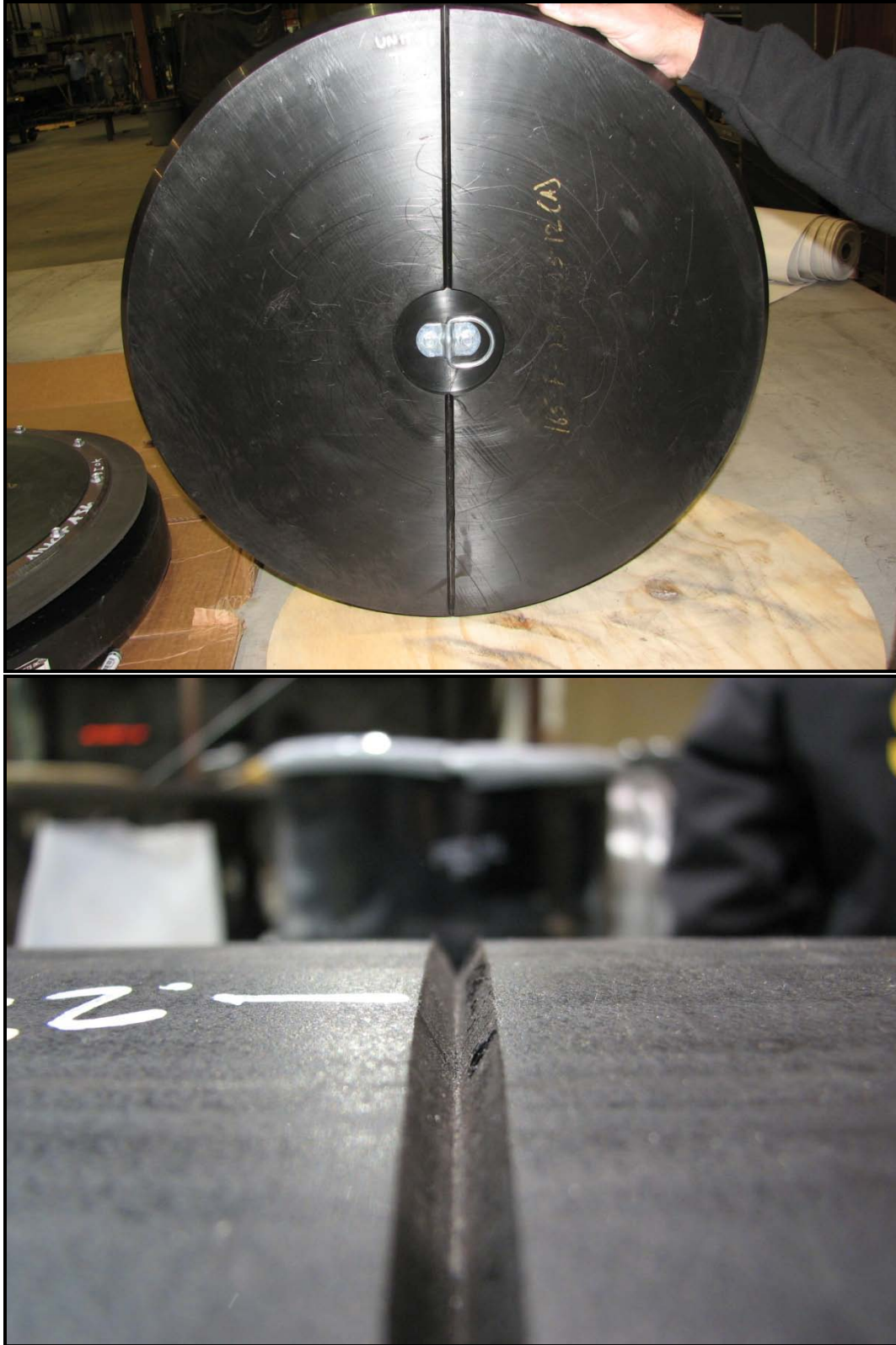
Figure 5.1-9 – Cold Drop End Cap and Body Pipe Groove V-notch Defects

Figure 5.1-10 – Cold Drop End Cap and Body Pipe Engagement
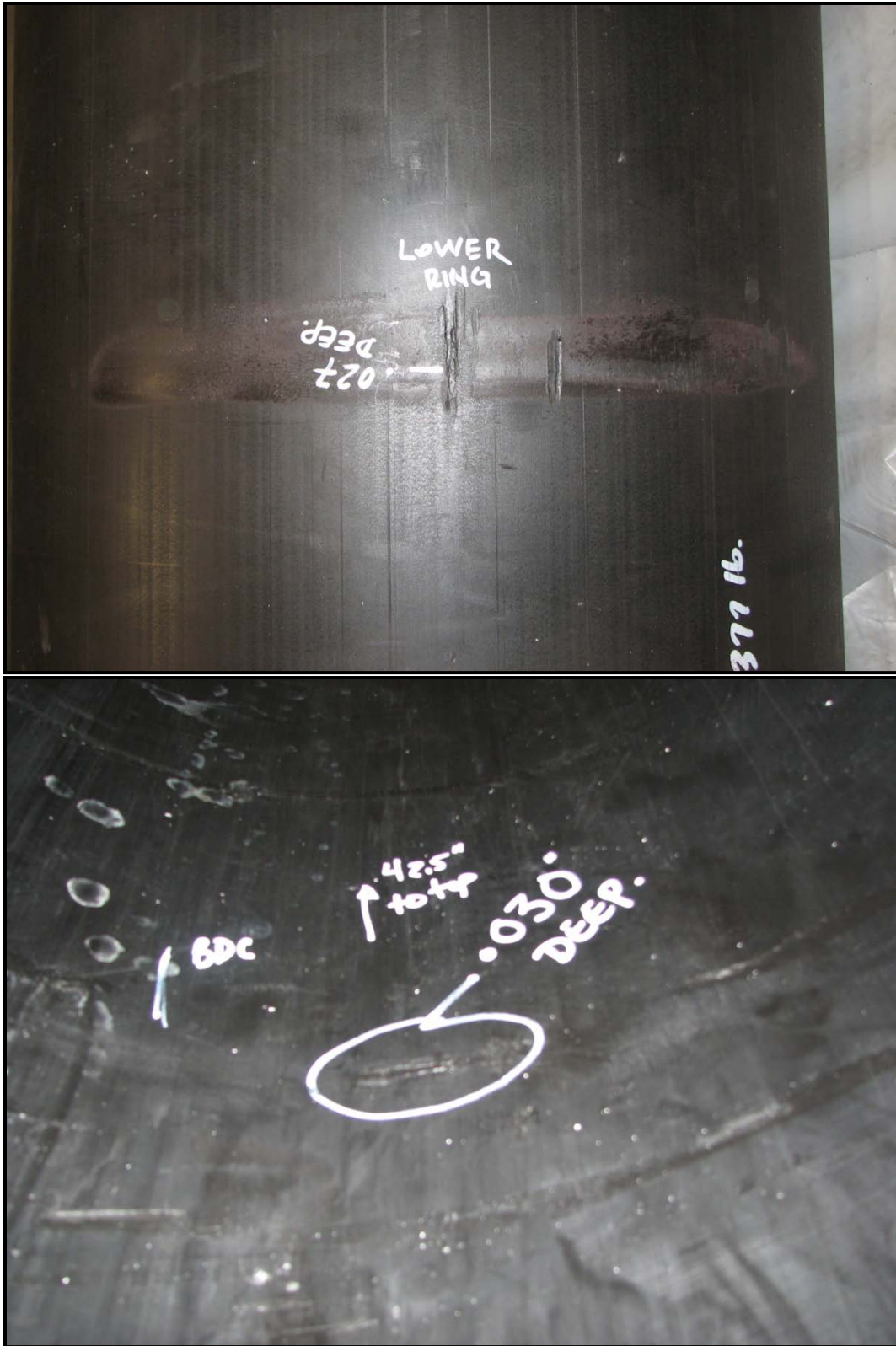
Figure 5.1-11 – Cold Drop Body Pipe Dents and Gouges

Figure 5.1-12 – Cold Drop Canister Metallic Component Deformations

5.1.3.2.3 Hot End and Side Drop Results

The hot end drop was performed using a neutron shielded canister test fixture that was fitted at one end with a new 20 pcf rigid urethane foam impact limiter to conservatively simulate a hot end impact deceleration acting on the RH-TRU 72-B package of 51.10*g*. The NS30 neutron shielded canister, with its three 30-gallon drum simulated contents, was oriented in a lid down configuration such that maximum impact deceleration, payload rebound, and secondary impact was focused on the shield insert end cap and associated pipe body interface. Given the circumferentially uniform 5/8-inch residual end impact limiter deformation, the test fixture experienced an impact deceleration estimated with constant resistance as a function of the drop height and end limiter deformation (360 in./0.625 in.) of 576*g* with 382*g* average deceleration measured by two piezoelectric accelerometers attached to the test fixture outer shell near the impact location.

The subsequent hot side drop was performed utilizing the same test fixture and NS30 test article, impacting two 16 pcf rigid urethane foam impact limiters (on the side opposite the cold side drop test) to conservatively simulate a hot side drop impact deceleration acting on the RH-TRU 72-B package of 68.90*g*. The NS30 neutron shielded canister and contents were oriented in a horizontal configuration such that maximum impact deceleration, payload rebound, and secondary impact was focused on the shield insert body and canister shell as simply supported by the package inner vessel centering rings. Given the 1-5/8-inch residual side impact limiter deformations, the test fixture experienced an impact deceleration estimated with constant resistance as a function of the drop height and end limiter deformation (360 in./1.625 in.) of 221*g* with 204*g* average deceleration measured by two piezoelectric accelerometers attached to the test fixture outer shell near the impact locations.

Observed deformations and measured decelerations demonstrate that the test fixture conservatively simulated the RH-TRU 72-B by inducing impact decelerations in both the hot end and side drop orientations that were in excess of the maximum decelerations that would have been experienced by testing with an RH-TRU 72-B package.

The top end cap and the body pipe components were not tested with induced flaws at 150 °F due to the enhanced ductility of HDPE at elevated temperature and no corresponding concerns regarding flaw propagation. A maximum thickness CDX plywood spacer was again installed above the top end cap (and below the canister lid) to achieve an axial spacing that was greater than the ½-inch maximum allowed. The axial gap was initially maximized and the gap increased through crushing of the spacer during the end drop to conservatively determine whether the top and bottom end caps remained engaged with the body pipe and shield streaming paths precluded. The open-cell urethane foam debris gaskets experienced cut damage from interaction between the end caps and body pipe, but the end caps remained engaged with the body pipe. However, likely due to a momentary loss of contact between the debris gasket and the body pipe, a small release of the fine particulate sand was observed outside of the shield components after the hot end and side drop tests. The total release of fine particulate beyond the shield insert boundary was meticulously collected and weighed at 0.035 pounds, or 0.23% of the total 15 pounds of releasable source term available in the three internal payload drums. Impact dents and gouges were again observed in both the end caps and body pipe interior surfaces due to interaction with the payload drums and on exterior surfaces due to interaction with the surrounding canister features, but no dent or gouge exceeded ¼-inch maximum depth, which is the defined scratch and gouge criteria.

Post-drop damage to the canister lid and body were again minor with only location of observed deformation being the interface between the canister shell and the internal centering rings in the test fixture. The canister shell deformation was larger under the hot drop than the cold drop conditions with the maximum dent depth being 7/8-inch. The canister lid was unaffected by the drop as it was easily unlocked, rotated, and removed for inspection after the drop tests using the standard manual operating techniques.

Figure 5.1-13 illustrates the drop-induced deformation of the test fixture end and side impact limiters. Figure 5.1-14 illustrates the deformation of the plywood spacer and end cap gasket damage. Figure 5.1-15 illustrates the location and presence of the fine particulate sand that was released beyond the shield insert boundary, but retained inside the overall canister boundary. The engagement of the top end bottom end caps with the pipe body to preclude streaming paths out of the shield components is shown in Figure 5.1-16. The most aggressive external and internal dents and gouges experienced by the body pipe are shown in Figure 5.1-17. The condition of the canister lid and body is illustrated in Figure 5.1-18.

Figure 5.1-13 – Hot End and Side Drop Impact Limiter Deformation

Figure 5.1-14 – Hot Drop Damage to the Spacer and End Cap Gasket

Figure 5.1-15 – Hot Drop Induced Presence of Released Fine Particulate

Figure 5.1-16 – Hot Drop End Cap and Body Pipe Engagement

Figure 5.1-17 – Hot Drop Body Pipe Dents and Gouges

Figure 5.1-18 – Hot Drop Canister Metallic Component Deformations

5.1.3.2.4 Summary of Testing

Key test observations include the following:

1. Post-test visual inspection of the interior and exterior surfaces of the three neutron shielded canisters shield insert components indicated no significant global or localized deformation or damage to the neutron shielding that exceeded ¼-inch depth. The internal localized deformations were due to impact with the solid, concrete-filled rolling hoops in the 30-gallon test payload drums and the external localized deformation were due to impact with the deformed canister shell at the IV centering ring locations. Localized deformations under the "hot" conditions were, as expected, greater than under "cold" conditions. There was no propagation of the ¼-inch depth v-notch groove defects machined into the body pipe and upper end cap indicating acceptable material ductility at -20 ºF. The as-tested gross weights of the canisters were approximately 100 pounds greater than the allowed total gross weight of 3,100 pounds.
2. Post-test visual inspection of the test fixture that was a surrogate for the RH-TRU 72-B revealed no localized deformations or other evidence that would indicate a 3,100 pound canister payload would compromise the authorized RH-TRU 72-B payload weight limit of 8,000 pounds based on analysis.
3. Post-test evaluation of the debris gasket indicated that, although damaged due to relative movement and impact between the shield end caps and body pipe, only a minor (0.23% by weight maximum) release of the simulated waste small particulate was measured. Note: A bounding contents release beyond the shield insert components is accounted for in the shielding analysis summarized in Section 5.1.5, *Shielding Evaluation*.

5.1.4 Thermal Evaluation

The thermal analysis[4] models of the RH-TRU 72-B packaging were developed using the computer programs Thermal Desktop[5] and SINDA/FLUINT[6]. The thermal models of the NS15 and NS30 neutron shielded canisters within the RH-TRU 72-B packaging are a composite of newly generated 'solids' models of the neutron shielded canisters and the waste contents and the current lumped parameter finite difference model of the RH-TRU 72-B packaging. Using a feature of the SINDA/FLUINT computer program, these 'submodels' are combined into a single thermal model and solved simultaneously to generate a unified thermal solution. Complete details of the packaging and impact limiter modeling are provided in the RH-TRU 72-B SAR and summarized in the shielded canister calculation package along with complete modeling details for the neutron shielded canister and waste contents model.[1,4]

With the exception of the payload definition and the thickness of the HDPE used for shielding, identical modeling approaches were used for the thermal models for the NS15 and NS30 canisters. The nominal canister and shield insert geometries were as given in the RH-TRU 72-B SAR drawing X-106-503-SNP. The NS15 canister is assumed to package three (3) 16-gallon inner containers while the NS30 canister is assumed to package three (3) 30-gallon inner containers (drums) containing two (2) 8-gallon waste containers each. The heat transfer between the various components within the shielded canisters is via radiation and conduction. All void spaces within the canister and packaging cavity are assumed to be filled with air at atmospheric pressure. A paper based waste stream with the effective conductivity of air is assumed for the payload with a maximum decay heat loading of 50 watts for both canister configurations. The decay heat is assumed to be equally distributed within the waste volume on a volumetric basis. These modeling approaches are equivalent to those used in the RH-TRU 72-B SAR.

Radial heat transfer between the HDPE shield insert components and the canister shell wall is simulated as conduction and radiation across the nominal 0.75-inch gap between the components. The use of a uniform radial gap is appropriate for NCT and HAC evaluations even though the RH-TRU 72-B package is transported horizontally since the increase in the radial gap on one side of the HPDE insert will be offset by a corresponding smaller gap on the opposing side. In addition, ignoring the narrow line contact that will exist for the horizontal package orientation will yield conservative temperature estimates for NCT conditions, while the bounding temperature achieved under HAC conditions can be conservatively estimated by assuming the inner surface reaches a temperature equivalent to that achieved by the outer surface.

Axial heat transfer between the HDPE shield insert components and the base and lid ends of the canister is modeled as conduction and radiation across 0.125-inch and 0.375-inch gaps, respectively. The HDPE insert is conservatively assumed to have shifted forwarded slightly under horizontal transportation from its vertical loading position. Maintaining a tight contact between the bases of the insert and canister shell will yield lower NCT temperatures for the insert and payload and lower HAC temperatures for the base of the canister shell since the

---

[4] G. J. Banken, *Thermal Analysis of RH Shielded Canisters in RH-TRU 72B Cask*, 01937.01.M0005.01-04, Rev. 2, AREVA Federal Services LLC, Tacoma, WA, February 2011.

[5] Thermal Desktop®, Version 5.1, Cullimore & Ring Technologies, Inc., Littleton, CO, 2007.

[6] SINDA/FLUINT, Systems Improved Numerical Differencing Analyzer and Fluid Integrator, Version 5.1, Cullimore & Ring Technologies, Inc., Littleton, CO, 2007.

thermal mass of the HDPE insert will not be as closely coupled to help absorb the heat flux during the fire event.

5.1.4.1 Thermal Evaluation for Normal Conditions of Transport

Three ambient conditions are evaluated for NCT conditions: NCT Hot (i.e., 100 ºF with steady-state modeling of regulatory solar averaged over 12 hours and credit for self shading), NCT Hot, No Solar (i.e., 100 ºF with no insolation loading), and NCT Hot Alternate (i.e., 100 ºF with transient modeling of regulatory solar applied in a "12 hours on/12 hours off" fashion and with no credit for self shading). Table 5.1-1 presents the resulting package temperatures for the first two evaluated conditions and for the transportation of the NS15 shielded canister, while Table 5.1-2 presents the same type of results for the NS30 shielded canister. The temperature levels achieved under NCT conditions demonstrate that all of the component temperatures for the NS15 and NS30 canister configurations are within their respective limits. Further, the computed temperatures for the RH-TRU 72-B packaging components are essentially the same as those predicted in the RH-TRU 72-B SAR for similar ambient conditions. Due to the insignificant temperature difference and the analysis assumption crediting only void space exterior to the canister, the bounding pressure analysis and wattages presented in Section 3.4.4.3, *Maximum Pressure for Normal Conditions of Transport*, of the RH-TRU 72-B SAR are applicable to the NS15 and NS30 canister configurations. Thus, the NS15 and NS30 neutron shielded canisters will not impact the safety basis of the RH-TRU 72-B packaging.

The sensitivity of the NCT results to the insolation modeling approach was evaluated via the third ambient condition described. Unlike the steady-state modeling approached used for the Table 5.1-1 and Table 5.1-2 evaluations, no credit is taken for self shading of the surfaces on the lower half of the horizontal cask. Instead, the 10 CFR §71.71(c)(1) specified 12-hour average insolation boundary condition of 122.92 Btu/hr-ft^2 for the curved surfaces and 61.46 Btu/hr-ft^2 for the vertical surfaces are applied in a transient "12 hours on/12 hours off" model. Table 5.1-3 presents a summary comparison of the results versus those presented in the Table 5.1-1 and Table 5.1-2 for steady-state modeling with credit for self shading. As expected, without credit for self shading, the 2-D axisymmetric model of the cask yields higher peak cask component temperatures. However, the 9 to 16 ºF increase in the cask structural component temperatures is insignificant in comparison with the available thermal margin for each component. The associated increase in the shielded canister insert and waste centerline temperatures is between 5 to 9 ºF. All component temperatures remain within the NCT allowable temperature limits under either modeling approach for insolation.

5.1.4.2 Thermal Evaluation for Hypothetical Accident Conditions

The RH-TRU 72-B SAR describes the initial conditions and the expected level of damage sustained by the RH-TRU 72-B package from the 10 CFR 71.73 prescribed free and puncture drops. As the total gross weight of the loaded NS15 or NS30 shielded canisters is 3,100 pounds and a factor of approximately 2.6 less than the 8,000-pound removable or fixed lid standard payload canister, the expected level of package damage would be less with an NS15 or NS30 shielded canister payload. Free drop testing of an NS30 shielded canister, which structurally bounds the NS15 shielded canister, in a RH-TRU 72-B surrogate test fixture demonstrated that no significant damage is sustained by the shield insert as a result of the free drop.[3] Therefore, the

analytical models of the shielded canister geometry used for the HAC evaluation are the same as the NCT models described above.

Table 5.1-4 and Table 5.1-5 present the predicted maximum temperatures for NS15 and NS30 shielded canister configurations, respectively, under HAC conditions. The results show that all component temperatures remain with allowable limits. The peak temperature of the HDPE shield inserts is seen to remain below the design limit, based on the vicat softening temperature of 256 ºF, for both configurations. Further, the fact that the canister shell also remains below this temperature level demonstrates that the HDPE temperature limit would not have been exceeded even if direct contact existed between the components. Also, the computed temperatures for the RH-TRU 72-B packaging components are essentially the same as those predicted in the RH-TRU 72-B SAR under HAC. Thus, the NS15 and NS30 neutron shielded canisters will not impact the safety basis of the RH-TRU 72-B packaging.

Similar to the NCT evaluation, the sensitivity of the HAC evaluations to the insolation modeling approach (see above) was evaluated. The method of modeling the insolation loads on the cask has no effect on the peak fire related temperatures since the effects of insolation are ignored prior to and during the 30-minute fire event. Table 5.1-6 presents a summary comparison of the post-fire peak temperature results obtained using a transient "12 hours on/12 hours off" model with no credit for self shading versus those obtained using a steady-state modeling approach with 12-hour averaged insolation levels and credit for self shading. With the exception of the waste centerline temperature, the peak component temperature achieved during the HAC event remain unchanged from those presented in Table 5.1-4 and Table 5.1-5.

As seen with the NCT evaluations, the 2-D axisymmetric model of the cask yields higher predicted peak post-fire component temperatures when no credit is taken for self shading. The level of difference yielded by the two modeling methodologies is similar to those seen for the NCT evaluations, with a 9 to 18 ºF increase in the cask structural component temperatures resulting if no credit for self shading is taken. Again, this level of temperature increase is insignificant in comparison with the available thermal margin for each component. The associated increase in the shielded canister insert and waste centerline temperatures is between 5 to 9 ºF. All component temperatures remain within the HAC allowable temperature limits under either modeling approach for insolation.

Table 5.1-1 – NCT Hot Temperatures with 50 Watts Decay Heat for NS15

Location/Component	Temperature (ºF)		
	NCT With Insolation	NCT Without Insolation	Allowable Temperature
Waste Centerline	247	225	①
NS15 Shield Insert	141	119	256
Canister Shell	133	111	2,600②
IV Shell	128	105	800③
IV Void Space Bulk Avg	127	104	N/A
OC Inner Shell	126	103	800③
OC Lead Shield	126	103	620
OC Outer Shell	126	103	800③
OC Thermal Shield	125	103	185④
OC Upper Ring Forging	125	102	800③
IV O-Ring Seal	125	103	225
OC O-Ring Seal	125	102	225
IV Lid	125	103	800③
OC Lid	125	103	800③
Impact Limiter Foam	132	104	300
Impact Limiter Shell	133	105	185④

Notes:

① The temperature limit for the waste material is discussed in Appendix 4.6 of the *RH-TRU Payload Appendices*.

② Temperature limit based on the minimum melting temperature for stainless steel or carbon steel.

③ Temperature limit based on the ASME B&PV Code.

④ Temperature limit based on the maximum accessible surface temperature for exclusive use shipments per 10 CFR 71.43(g).

Table 5.1-2 – NCT Hot Temperatures with 50 Watts Decay Heat for NS30

Location/Component	Temperature (ºF)		
	NCT With Insolation	NCT Without Insolation	Allowable Temperature
Waste Centerline	234	214	①
NS30 Shield Insert	137	115	256
Canister Shell	132	110	2,600②
IV Shell	128	105	800③
IV Void Space Bulk Avg	127	104	N/A
OC Inner Shell	126	103	800③
OC Lead Shield	126	103	620
OC Outer Shell	126	103	800③
OC Thermal Shield	125	103	185④
OC Upper Ring Forging	125	103	800③
IV O-Ring Seal	126	103	225
OC O-Ring Seal	125	103	225
IV Lid	126	103	800③
OC Lid	125	103	800③
Impact Limiter Foam	132	104	300
Impact Limiter Shell	133	105	185④

Notes:

① The temperature limit for the waste material is discussed in Appendix 4.6 of the *RH-TRU Payload Appendices*.

② Temperature limit based on the minimum melting temperature for stainless steel or carbon steel.

③ Temperature limit based on the ASME B&PV Code.

④ Temperature limit based on the maximum accessible surface temperature for exclusive use shipments per 10 CFR 71.43(g).

Table 5.1-3 – NCT Thermal Sensitivity to Insolation Modeling Methodology

Location / Component	Temperature (ºF)[1]			
	NS15		NS30	
	NCT With 12 Hr Averaged Insolation[2]	12 Hr On/Off Transient Cycle[3]	NCT With 12 Hr Averaged Insolation[2]	12 Hr On/Off Transient Cycle[3]
Waste Centerline	247	252	234	241
NSXX Shield Insert	141	149 Max 143 Avg	137	146 Max 142 Avg
Canister Shell	133	143 Max 140 Avg[4]	132	143 Max 140 Avg[4]
IV Shell	128	141 Max 135 Avg[4]	128	141 Max 135 Avg[4]
IV Void Space Bulk Avg	127	142	127	142
OC Inner Shell	126	142	126	142
OC Lead Shield	126	142	126	142
OC Outer Shell	126	142 Max 132 Avg[4]	126	142 Max 132 Avg[4]
OC Thermal Shield	125	146	125	146
OC Upper Ring Forging	125	135	125	135
IV O-Ring Seal	125	134	126	134
OC O-Ring Seal	125	134	125	134
IV Lid	125	135	126	135
OC Lid	125	134	125	134
Impact Limiter Foam	132	150 Max 133 Avg	132	150 Max 133 Avg
Impact Limiter Shell	133	158	133	158

Notes:

[1] Temperatures assume a total payload decay heat loading of 50 W.

[2] Steady-state modeling that includes credit for self-shading of lower half of horizontal cask.

[3] Modeling ignores self-shading of lower half of horizontal cask. Insolation applied equally around entire circumference of cask body.

[4] Average of maximum temperatures over a 24 hour period.

Table 5.1-4 – HAC Temperatures with 50 Watts Decay Heat for NS15

Location/Component	Temperature (ºF)			
	End of Fire	Peak	Post-Fire Steady-State	Allowable Temperature
Waste Centerline	225	244	244	①
NS15 Shield Insert	119	189	138	256
Canister Shell	113	229	130	2,600②
IV Shell	151	323	125	800③
IV Void Space Bulk Avg	284	406	124	N/A
OC Inner Shell	416	488	123	800③
OC Lead Shield	527	544	123	620
OC Outer Shell	605	606	123	800③
OC Thermal Shield	1,231	1,231	123	2,600②
OC Upper Ring Forging	105	166	123	800③
IV O-Ring Seal	103	149	123	360/225
OC O-Ring Seal	107	149	123	360/225
IV Lid	105	159	123	800③
OC Lid	106	150	123	800③
Impact Limiter Foam	N/A	N/A	N/A	N/A④
Impact Limiter Shell	1,427	1,427	131	2,600②

Notes:

① The temperature limit for the waste material is discussed in Appendix 4.6 of the *RH-TRU Payload Appendices*.

② Temperature limit based on the minimum melting temperature for stainless steel or carbon steel.

③ Temperature limit based on the ASME B&PV Code.

④ No temperature limit exists for the impact limiter foam under HAC since failure of the foam via thermal decomposition provides a principle thermal protection mechanism under elevated temperature conditions. Foam at temperatures greater than 670 ºF is assumed to be charred.[7]

---

[7] Williamson, C., and Iams, Z., *Thermal Assault and Polyurethane Foam - Evaluating Protective Mechanisms*, General Plastics Manufacturing Company, Tacoma, WA, presented at PATRAM International Symposium, Berlin, Germany, 2004.

Table 5.1-5 – HAC Temperatures with 50 Watts Decay Heat for NS30

Location/Component	Temperature (ºF)			
	End of Fire	Peak	Post-Fire Steady-State	Allowable Temperature
Waste Centerline	214	232	232	①
NS30 Shield Insert	115	206	135	256
Canister Shell	113	232	129	2,600②
IV Shell	151	323	125	800③
IV Void Space Bulk Avg	284	406	124	N/A
OC Inner Shell	416	488	123	800③
OC Lead Shield	527	544	123	620
OC Outer Shell	605	606	123	800③
OC Thermal Shield	1,231	1,231	123	2,600②
OC Upper Ring Forging	105	160	123	800③
IV O-Ring Seal	107	149	123	360/225
OC O-Ring Seal	104	149	123	360/225
IV Lid	109	160	123	800③
OC Lid	107	151	123	800③
Impact Limiter Foam	N/A	N/A	N/A	N/A④
Impact Limiter Shell	1,427	1,427	131	2,600②

Notes:

① The temperature limit for the waste material is discussed in Appendix 4.6 of the *RH-TRU Payload Appendices*.

② Temperature limit based on the minimum melting temperature for stainless steel or carbon steel.

③ Temperature limit based on the ASME B&PV Code.

④ No temperature limit exists for the impact limiter foam under HAC since failure of the foam via thermal decomposition provides a principle thermal protection mechanism under elevated temperature conditions. Foam at temperatures greater than 670 ºF is assumed to be charred.[7]

Table 5.1-6 – HAC Post-fire Thermal Sensitivity to Insolation Modeling Methodology

Location / Component	Post-Fire Peak Temperature (ºF)①			
	NS15		NS30	
	HAC With 12 Hr Averaged Insolation②	12 Hr On/Off Transient Cycle③	HAC With 12 Hr Averaged Insolation②	12 Hr On/Off Transient Cycle③
Waste Centerline	244	249	232	238
NSXX Shield Insert	138	146 Max 140 Avg	135	144 Max 139 Avg
Canister Shell	130	141 Max 138 Avg④	129	141 Max 137 Avg④
IV Shell	125	140 Max 131 Avg④	125	140 Max 131 Avg④
IV Void Space Bulk Avg	124	141	124	141
OC Inner Shell	123	141	123	141
OC Lead Shield	123	141	123	141
OC Outer Shell	123	141 Max 129 Avg④	123	141 Max 129 Avg④
OC Thermal Shield	123	146	123	146
OC Upper Ring Forging	123	133	123	133
IV O-Ring Seal	123	132	123	132
OC O-Ring Seal	123	131	123	132
IV Lid	123	133	123	133
OC Lid	123	132	123	132
Impact Limiter Foam	N/A	N/A	N/A	N/A
Impact Limiter Shell	131	156	131	156

Notes:

① Temperatures assume a total payload decay heat loading of 50 W.

② Steady-state modeling that includes credit for self-shading of lower half of horizontal cask.

③ Modeling ignores self-shading of lower half of horizontal cask. Insolation applied equally around entire circumference of cask body.

④ Average of maximum temperatures over a 24 hour period.

5.1.5 Shielding Evaluation

Consistent with the methodology and isotopes used in the RH-TRU 72-B SAR,[1] a shielding evaluation[8] was performed to determine the activity limit for each isotope of interest that results in a dose rate of 1,000 mrem/hr at a distance of 1 meter from the package surface subsequent to an accident. MCNP v1.40[9] was used for the neutron analysis, and a simple point-kernel approach was used for the gamma analysis.

The evaluation was concerned only with HAC dose rates. Under NCT, the dose rates will be determined by measurement.

Although HAC free drop testing determined that less than 0.23% of the releasable source term could reconfigure outside of the shield during an accident, the shielding analyses conservatively assumed more than 8 times that value would reconfigure outside of the shield insert components to a point source on the inner surface of the waste canister shell. As such, 98% of the waste was assumed to reconfigure into a point source against the inner surface of the shield insert body pipe with the remaining 2% at the same axial elevation against the inner surface of the canister cylindrical shell. Treating the source as point sources conservatively neglected self-shielding effects.

Under HAC, the 72-B package dose rate at 1-m in the radial direction is more limiting than the dose rate at 1-m in the axial direction. Because of the impact limiters, the distance from the point source to the dose location is significantly farther at the ends compared to the sides, yet the axial and radial neutron shielding is comparable in both directions. Therefore, the maximum side dose rate at 1-m bounds the maximum end dose rate at the same distance from the package surface.

The 72-B cask geometry in the MCNP models is the same as in the baseline RH-TRU 72-B SAR neutron shielding analysis. The input file listed in Section 5.5.7 of the 72-B SAR is used as the basis for the geometry.[1] The NS30 and NS15 neutron shielded canister models are based upon the dimensions in Drawing X-106-503-SNP, conservatively accounting for minimum tolerance shield thicknesses and maximum damage due to HAC drops. The NS15 neutron shield insert body pipe is modeled as 3.038-inch thick versus the 3.387-inch thick nominal. The NS30 neutron shield insert body pipe is modeled as 1.162-inch thick versus the 1.454-inch thick nominal.

The shield insert and canister shell are conservatively assumed to translate radially to the inner surface of the IV, neglecting the offset spacing provided by the IV centering rings and flange, with no radial gaps or spacing between components.

The gamma point-kernel models are simplified and neglect attenuation in the polyethylene, although distance credit is taken for the polyethylene. Also, the outer steel layer in the gamma models is 1.635-in thick rather than the 1.625-in thick used in the neutron models. The actual value is 1.635-in, so using 1.625-in for the neutron models is conservative and is consistent with the baseline 72-B SAR neutron analysis. The distances from the primary and secondary sources to the 1-meter detector were 45.011 inches and 43.849 inches, respectively, for the NS30 case. The

---

[8] R. J. Migliore and B. A. Day, *72-B with NS15 and NS30 Shielded Canister Shielding Analysis*, 01937.01.M005-03, Rev. 0, AREVA Federal Services LLC, Tacoma, WA, January 2010.

[9] MCNP5, *MCNP – A General Monte Carlo N-Particle Transport Code, Version 5; Volume II: User's Guide*, LA-CP-03-0245, Los Alamos National Laboratory, April 2003; MCNP5 is distributed by the Radiation Safety Information Computational Center (www-rsicc.ornl.gov), Release C00730MNYCP00 (Version 1.40, Windows PC).

distances from the primary and secondary sources to the 1-meter detector were 46.887 inches and 43.849 inches, respectively, for the NS15 case.

For isotopes that are both gamma and neutron emitters, the total activity limit is determined by combining the gamma (A_G) and neutron (A_N) activity results using the following equation:

$$A_{GN} = \frac{1}{\dfrac{1}{A_G} + \dfrac{1}{A_N}}$$

where the combined limit is determined for both the radial and axial configurations. The radial and axial limits are then compared to determine the limiting activity for each radionuclide.

Once the most restrictive combined neutron and gamma activities A_{GN} are known, the sum of activity partial fractions for any combination of the radionuclides for each neutron shielded canister must be less than or equal to unity, or:

$$\sum_{i=1}^{n} \frac{a_i}{A_{GN_i}} \leq 1.0$$

where, for a particular payload container mix, a_i is the actual curie content of radionuclide "i" and A_{GN_i} is the limiting curie content of radionuclide "i".

The neutron source was computed in ED-042[10] for the isotopes of interest; the total neutron spectrum was taken from Table 3 and Table 5 of ED-042, and each spectrum was entered into MCNP as a histogram distribution. Note that the lower energy bound was conservatively set at 0.1 MeV in MCNP, although the lower energy bound was 0 MeV in ED-042.

To minimize self-shielding, no fissile material is included in the neutron shielding models. Because no fissile material is included, no subcritical neutron multiplication is performed by MCNP. A factor of 2.7 may be conservatively used to account for subcritical neutron multiplication, as determined in conjunction with Section 5.5.2 of the RH-TRU 72-B SAR.[1] This subcritical multiplication factor was determined by surrounding a point source with a sphere comprised of 325 grams Pu-239 and a 30% polyethylene/70% water mixture. The U-238 spectrum, which has the lowest average energy of the isotopes under consideration and hence highest subcritical multiplication factor, was conservatively utilized for the point source in that analysis. This subcritical neutron multiplication factor is conservatively applicable to this analysis.

Gamma energy and intensity data was taken from Kinsey.[11] All gamma energies less than 0.100 MeV were conservatively rounded to 0.100 MeV. Mass attenuation coefficients for each element as a function of gamma energy and isotropic point-source buildup factors using the geometric progression method are taken from ANSI/ANS-6.4.3-1991[12]. Gamma-ray isotropic

---

[10] *Neutron Source Rates for TRU Waste*, ED-042, Rev. 2, Packaging Technology, Inc., Tacoma, Washington, November 2000.

[11] R. R. Kinsey, et al., *The NUDAT/PCNUDAT Program for Nuclear Data, paper submitted to the 9th International Symposium of Capture Gamma-Ray Spectroscopy and Related Topics*, Budapest, Hungary, October 1996; data extracted from the NUDAT database, version September 7, 2000, CD-ROM.

[12] ANSI/ANS-6.4.3-1991, *Gamma-Ray Attenuation Coefficients and Buildup Factors for Engineering Materials*, American Nuclear Society (ANS), La Grange Park, Illinois, 1991.

point-source buildup factors are determined by conservatively assuming iron as the dominant shielding material. Although the actual buildup factors will lie somewhere between iron (atomic number, $Z = 26$) and lead ($Z = 82$), use of iron as the buildup factor conservatively bounds the maximum isotopic quantity (curies) allowed for transport because the buildup factor increases as the atomic number decreases.

ANSI/ANS-6.1.1-1977[13] flux-to-dose rate conversion factors are used in both the neutron and gamma shielding calculations. Table 5.1-7 presents a summary of activity limits for HAC.

[13] ANSI/ANS-6.1.1-1977, *American National Standard Neutron and Gamma-Ray Flux-to-Dose-Rate Factors*, American Nuclear Society (ANS), La Grange Park, Illinois, 1977.

Table 5.1-7 – Summary of HAC Activity Limits per Neutron Shielded Canister

Radio-nuclide	Gamma Emitter	Neutron Emitter	NS30 Maximum Allowable Activity (Ci), A_{GN}①	NS15 Maximum Allowable Activity (Ci), A_{GN}①	Radio-nuclide	Gamma Emitter	Neutron Emitter	NS30 Maximum Allowable Activity (Ci), A_{GN}①	NS15 Maximum Allowable Activity (Ci), A_{GN}①
^{3}H	–	–	unlimited	unlimited	^{91}Y	✖	–	3.369E+04	3.649E+04
^{10}Be	–	–	unlimited	unlimited	^{88}Zr	✖	–	2.320E+05	2.513E+05
^{14}C	–	–	unlimited	unlimited	^{90}Zr	–	–	unlimited	unlimited
^{22}Na	✖	–	7.410E+01	8.026E+01	^{90m}Zr	–	–	unlimited	unlimited
^{32}P	–	–	unlimited	unlimited	^{93}Zr	✖	–	unlimited	unlimited
^{33}P	–	–	unlimited	unlimited	^{95}Zr	✖	–	5.867E+02	6.355E+02
^{35}S	–	–	unlimited	unlimited	^{93m}Nb	✖	–	unlimited	unlimited
^{45}Ca	✖	–	unlimited	unlimited	^{94}Nb	✖	–	1.986E+02	2.151E+02
^{46}Sc	✖	–	7.429E+01	8.047E+01	^{95}Nb	✖	–	4.819E+02	5.220E+02
^{49}V	–	–	unlimited	unlimited	^{95m}Nb	✖	–	1.600E+06	1.733E+06
^{51}Cr	–	–	unlimited	unlimited	^{99}Tc	✖	–	unlimited	unlimited
^{54}Mn	–	–	3.093E+02	3.350E+02	^{99m}Tc	✖	–	unlimited	unlimited
^{55}Fe	–	–	unlimited	unlimited	^{103}Ru	✖	–	7.537E+03	8.164E+03
^{59}Fe	✖	–	9.029E+01	9.780E+01	^{106}Ru	–	–	unlimited	unlimited
^{57}Co	✖	–	5.521E+05	5.980E+05	^{103m}Rh	✖	–	unlimited	unlimited
^{58}Co	✖	–	3.286E+02	3.559E+02	^{106}Rh	✖	–	2.294E+03	2.485E+03
^{60}Co	✖	–	3.835E+01	4.154E+01	^{107}Pd	–	–	unlimited	unlimited
^{59}Ni	–	–	unlimited	unlimited	^{108}Ag	✖	–	6.243E+04	6.762E+04
^{63}Ni	–	–	unlimited	unlimited	^{108m}Ag	✖	–	5.330E+02	5.774E+02
^{64}Cu	✖	–	1.321E+04	1.431E+04	^{109m}Ag	✖	–	unlimited	unlimited
^{65}Zn	✖	–	2.151E+02	2.330E+02	^{110}Ag	✖	–	2.075E+04	2.247E+04
^{73}As	✖	–	unlimited	unlimited	^{110m}Ag	✖	–	6.633E+01	7.184E+01
^{79}Se	–	–	unlimited	unlimited	^{109}Cd	✖	–	unlimited	unlimited
^{85}Kr	✖	–	1.614E+06	1.748E+06	^{113m}Cd	✖	–	unlimited	unlimited
^{86}Rb	✖	–	1.385E+03	1.501E+03	^{115m}Cd	✖	–	4.145E+03	4.490E+03
^{87}Rb	–	–	unlimited	unlimited	^{114}In	✖	–	4.990E+04	5.405E+04
^{89}Sr	✖	–	2.295E+06	2.486E+06	^{114m}In	✖	–	1.762E+04	1.908E+04
^{90}Sr	–	–	unlimited	unlimited	^{115m}In	✖	–	9.785E+06	1.060E+07
^{88}Y	✖	–	2.616E+01	2.833E+01	^{119m}Sn	✖	–	unlimited	unlimited
^{90}Y	✖	–	unlimited	unlimited	^{121m}Sn	✖	–	unlimited	unlimited
^{90m}Y	✖	–	1.574E+04	1.705E+04	^{123}Sn	✖	–	1.844E+04	1.998E+04

Radio-nuclide	Gamma Emitter	Neutron Emitter	NS30 Maximum Allowable Activity (Ci), A_{GN}①	NS15 Maximum Allowable Activity (Ci), A_{GN}①	Radio-nuclide	Gamma Emitter	Neutron Emitter	NS30 Maximum Allowable Activity (Ci), A_{GN}①	NS15 Maximum Allowable Activity (Ci), A_{GN}①
^{126}Sn	✗	–	unlimited	unlimited	^{151}Sm	✗	–	unlimited	unlimited
^{124}Sb	✗	–	5.266E+01	5.704E+01	^{150}Eu	✗	–	2.894E+02	3.135E+02
^{125}Sb	✗	–	4.385E+03	4.750E+03	^{152}Eu	✗	–	1.209E+02	1.309E+02
^{126}Sb	✗	–	2.007E+02	2.174E+02	^{154}Eu	✗	–	1.166E+02	1.263E+02
^{126m}Sb	✗	–	4.830E+02	5.232E+02	^{155}Eu	✗	–	unlimited	unlimited
^{123}Te	–	–	unlimited	unlimited	^{152}Gd	–	–	unlimited	unlimited
^{123m}Te	✗	–	unlimited	unlimited	^{153}Gd	✗	–	unlimited	unlimited
^{125m}Te	✗	–	unlimited	unlimited	^{160}Tb	✗	–	1.451E+02	1.572E+02
^{127}Te	✗	–	8.607E+06	9.322E+06	^{166m}Ho	✗	–	2.699E+02	2.924E+02
^{127m}Te	✗	–	8.364E+06	9.059E+06	^{168}Tm	✗	–	3.229E+02	3.497E+02
^{129}Te	✗	–	1.295E+04	1.403E+04	^{182}Ta	✗	–	9.435E+01	1.022E+02
^{129m}Te	✗	–	1.784E+04	1.932E+04	^{198}Au	✗	–	3.235E+04	3.504E+04
^{125}I	✗	–	unlimited	unlimited	^{207}Tl	✗	–	8.879E+04	9.618E+04
^{129}I	✗	–	unlimited	unlimited	^{208}Tl	✗	–	1.702E+01	1.843E+01
^{131}I	✗	–	1.252E+04	1.356E+04	^{209}Tl	✗	–	4.020E+01	4.354E+01
^{134}Cs	✗	–	2.573E+02	2.786E+02	^{209}Pb	–	–	unlimited	unlimited
^{135}Cs	–	–	unlimited	unlimited	^{210}Pb	✗	–	unlimited	unlimited
^{137}Cs	✗	–	1.335E+03	1.446E+03	^{211}Pb	✗	–	6.723E+03	7.282E+03
^{133}Ba	✗	–	2.071E+06	2.243E+06	^{212}Pb	✗	–	6.384E+07	6.915E+07
^{137}Ba	–	–	unlimited	unlimited	^{214}Pb	✗	–	2.070E+04	2.242E+04
^{137m}Ba	✗	–	1.260E+03	1.365E+03	^{207}Bi	✗	–	1.170E+02	1.267E+02
^{141}Ce	✗	–	unlimited	unlimited	^{210}Bi	–	–	unlimited	unlimited
^{142}Ce	–	–	unlimited	unlimited	^{211}Bi	✗	–	2.575E+07	2.789E+07
^{144}Ce	✗	–	unlimited	unlimited	^{212}Bi	✗	–	1.412E+03	1.529E+03
^{143}Pr	✗	–	unlimited	unlimited	^{213}Bi	✗	–	1.986E+04	2.152E+04
^{144}Pr	✗	–	2.518E+03	2.728E+03	^{214}Bi	✗	–	5.869E+01	6.357E+01
^{144m}Pr	✗	–	7.758E+04	8.403E+04	^{209}Po	✗	–	4.941E+04	5.352E+04
^{146}Pm	✗	–	9.887E+02	1.071E+03	^{210}Po	✗	–	2.967E+07	3.214E+07
^{147}Pm	✗	–	unlimited	unlimited	^{211}Po	✗	–	3.830E+04	4.149E+04
^{148}Pm	✗	–	1.853E+02	2.007E+02	^{212}Po	–	–	unlimited	unlimited
^{148m}Pm	✗	–	2.712E+02	2.937E+02	^{213}Po	✗	–	9.015E+06	9.765E+06
^{146}Sm	–	–	unlimited	unlimited	^{214}Po	–	–	unlimited	unlimited
^{147}Sm	–	–	unlimited	unlimited	^{215}Po	✗	–	unlimited	unlimited

Radio-nuclide	Gamma Emitter	Neutron Emitter	NS30 Maximum Allowable Activity (Ci), A_{GN}①	NS15 Maximum Allowable Activity (Ci), A_{GN}①	Radio-nuclide	Gamma Emitter	Neutron Emitter	NS30 Maximum Allowable Activity (Ci), A_{GN}①	NS15 Maximum Allowable Activity (Ci), A_{GN}①
^{216}Po	✗	–	1.874E+07	2.030E+07	^{237}U	✗	–	unlimited	unlimited
^{218}Po	–	–	unlimited	unlimited	^{238}U	✗	✗	3.118E+04	9.407E+04
^{211}At	✗	–	3.463E+05	3.751E+05	^{239}U	✗	–	3.271E+04	3.543E+04
^{217}At	✗	–	1.761E+07	1.908E+07	^{240}U	✗	–	unlimited	unlimited
^{219}Rn	✗	–	1.073E+06	1.162E+06	^{237}Np	✗	✗	2.037E+06	5.942E+06
^{220}Rn	✗	–	3.551E+06	3.846E+06	^{238}Np	✗	–	2.327E+02	2.521E+02
^{222}Rn	✗	–	9.805E+06	1.062E+07	^{239}Np	✗	–	5.248E+07	5.684E+07
^{221}Fr	✗	–	7.038E+07	7.623E+07	^{240}Np	✗	–	2.642E+02	2.862E+02
^{223}Fr	✗	–	4.316E+04	4.675E+04	^{240m}Np	✗	–	8.578E+02	9.291E+02
^{223}Ra	✗	–	7.889E+05	8.545E+05	^{236}Pu	✗	✗	9.390E+05	2.558E+06
^{224}Ra	✗	–	2.376E+07	2.573E+07	^{238}Pu	✗	✗	1.027E+06	2.869E+06
^{225}Ra	✗	–	unlimited	unlimited	^{239}Pu	✗	✗	1.562E+06	4.437E+06
^{226}Ra	✗	–	unlimited	unlimited	^{240}Pu	✗	✗	2.247E+05	6.406E+05
^{228}Ra	✗	–	unlimited	unlimited	^{241}Pu	✗	✗	unlimited	unlimited
^{225}Ac	✗	–	3.079E+06	3.335E+06	^{242}Pu	✗	✗	2.609E+03	7.434E+03
^{227}Ac	✗	–	unlimited	unlimited	^{243}Pu	✗	–	6.709E+07	7.266E+07
^{228}Ac	✗	–	1.821E+02	1.973E+02	^{244}Pu	–	✗	1.161E+01	3.433E+01
^{227}Th	✗	–	1.695E+06	1.836E+06	^{241}Am	✗	✗	1.188E+06	3.260E+06
^{228}Th	✗	–	unlimited	unlimited	^{242}Am	✗	–	unlimited	unlimited
^{229}Th	✗	–	unlimited	unlimited	^{242m}Am	✗	✗	6.559E+07	unlimited
^{230}Th	✗	✗	2.268E+06	6.635E+06	^{243}Am	✗	✗	1.365E+06	3.768E+06
^{231}Th	✗	–	unlimited	unlimited	^{245}Am	✗	–	unlimited	unlimited
^{232}Th	✗	✗	4.995E+06	1.577E+07	^{240}Cm	–	✗	2.111E+05	5.552E+05
^{234}Th	✗	–	unlimited	unlimited	^{242}Cm	✗	✗	1.431E+05	3.947E+05
^{231}Pa	✗	✗	1.526E+06	3.644E+06	^{243}Cm	✗	✗	1.343E+05	3.602E+05
^{233}Pa	✗	–	3.281E+06	3.554E+06	^{244}Cm	✗	✗	8.250E+03	2.262E+04
^{234}Pa	✗	–	1.442E+02	1.562E+02	^{245}Cm	✗	✗	4.935E+04	1.368E+05
^{234m}Pa	✗	–	8.910E+03	9.651E+03	^{246}Cm	–	✗	3.579E+01	9.941E+01
^{232}U	✗	✗	1.417E+06	3.981E+06	^{247}Cm	✗	–	1.867E+05	2.022E+05
^{233}U	✗	✗	1.978E+06	5.745E+06	^{248}Cm	–	✗	1.209E-01	3.427E-01
^{234}U	✗	✗	2.017E+06	5.904E+06	^{250}Cm	–	✗	1.494E-02	4.400E-02
^{235}U	✗	✗	2.250E+06	6.613E+06	^{247}Bk	✗	–	unlimited	unlimited
^{236}U	✗	✗	2.266E+06	6.748E+06	^{249}Bk	✗	✗	1.176E+07	3.436E+07

Radio-nuclide	Gamma Emitter	Neutron Emitter	NS30 Maximum Allowable Activity (Ci), A_{GN}①	NS15 Maximum Allowable Activity (Ci), A_{GN}①	Radio-nuclide	Gamma Emitter	Neutron Emitter	NS30 Maximum Allowable Activity (Ci), A_{GN}①	NS15 Maximum Allowable Activity (Ci), A_{GN}①
^{250}Bk	✘	–	1.628E+02	1.763E+02	^{254}Cf	–	✘	8.066E-03	2.044E-02
^{249}Cf	✘	✘	2.541E+05	3.614E+05	^{252}Es	✘	–	1.744E+03	1.889E+03
^{250}Cf	✘	✘	1.040E+01	2.675E+01	^{253}Es	✘	✘	7.928E+04	2.022E+05
^{251}Cf	✘	✘	9.861E+05	2.684E+06	^{254}Es	✘	✘	1.965E+05	5.065E+05
^{252}Cf	✘	✘	2.643E-01	6.745E-01	^{254m}Es	✘	✘	1.594E+01	3.995E+01

Notes:

① The designation of "unlimited" is made for any radionuclide whose limiting activity is greater than 1×10^8 curies (Ci).

5.1.6 Criticality Evaluation

The designs of the NS15 and NS30 neutron shielded canisters are an augmentation of the existing removable lid canister design that include the internal addition of an HDPE neutron shield in the form of a body pipe and two end caps. The addition of the HDPE materials could increase the system reactivity over that evaluation in the RH-TRU 72-B SAR under Case A – General Payload. [1] However, the Case C – Machine-Compacted Waste criticality evaluation models an optimally moderated fissile sphere with 100% polyethylene surrounded by a 99% polyethylene/1% beryllium reflector inside the canister metallic shell. The system reactivity increase due to the presence of the NS15 and/or NS30 neutron shield components is conservatively bounded by the Case C evaluation as the full polyethylene moderation and polyethylene/beryllium reflector represent a thicker and more reactive reflector than the 5-inch thick end caps or 3.387-inch thick NS15 body pipe.

Therefore, both machine-compacted and manually-compacted waste containing up to 1 wt% special reflector materials can be safely shipped in an NS15 or NS30 neutron shielded canister with up to 245 fissile gram equivalent ^{239}Pu (FGE).   The Case C analysis demonstrates that the NS15 and NS30 payload configurations comply with the requirements of 10 CFR §71.55 and §71.59. The criticality safety index, per 10 CFR §71.59, is 0.

5.1.7 Authorized Payload Contents for the Neutron Shielded Canister

As demonstrated in Section 5.1.5, *Shielding Evaluation*, when loaded with gamma and/or neutron emitting isotopes with maximum activity limits summarized in Table 5.1-7, the NS15 or NS30 neutron shielded canister payload meets HAC dose rate limits. As demonstrated in Section 5.1.6, *Criticality Evaluation*, when loaded with machine- or manually-compacted waste with less than 1 wt% special reflector materials and a maximum mass limit of 245 FGE, the neutron shielded canister payload meets the calculated reactivity limit and is safely subcritical.

5.1.8 Conclusion

The neutron shielded canister design consists of a vented removable lid canister fitted with internal HDPE shielding. The internal shield consists of a body pipe and top and bottom end caps that utilize an open-cell urethane foam gasket attached with a carbon steel retaining ring to provide gross particulate confinement in the shield. The neutron shielded canister encompasses two designs, the thinner wall NS30 and the thicker wall NS15, that are to be used for shipment of specific transuranic waste forms contained in approximately 30- and 15-gallon drums, respectively, in the RH-TRU 72-B package.

The analyses summarized in this appendix demonstrate the ability of the neutron shielded canister to safely transport limited quantities of gamma and/or neutron emitting isotopes and fissile isotopes. Using geometries consistent with, or conservative with respect to, the structural and thermal analyses, the shielding evaluation showed that the dose rate limits for NCT and HAC (including appropriate shielding damage assumptions in each case) are met with the maximum authorized contents. In addition, the criticality evaluation showed that the reactivity limit is met for manually- or machine-compacted wastes under the machine-compacted waste mass limit.